Development of chemical probes for intracellular nucleotide delivery, profiling of the metabolic fate(s) of nucleoside monoester phosphoramidates, and a nucleotide mimetic inhibitor of eIF4E

A DISSERTATION
SUBMITTED TO THE FACULTY OF THE
UNIVERSITY OF MINNESOTA
BY

Aniekan Matthew Okon

IN PARTIAL FULFILMENT OF THE REQUIREMENTS
FOR THE DEGREE OF
DOCTOR OF PHILOSOPHY

Dr. Carston Rick Wagner, Advisor

July 2018

Acknowledgements

I would like to express my sincere gratitude to my advisor, Dr. Carston R. Wagner, for giving me the opportunity to be a member of his research group. He has been a tremendous source of inspiration and has helped me develop the temperament for research. Above all, I thank him for his patience throughout the years.

I also would like to Dr. Courtney C. Aldrich, Dr. William Pomerantz, and Dr. Rodney Johnson for serving on the thesis committee and for their advice/guidance whenever I came knocking. A special thanks to our collaborators Dr. Mamta Gupta and Dr. Luciana Jesus da Costa and their lab members for their contributions towards the success of our research. I would also like to thank Dr. Yingchun Zhao, Xun Ming, and Emily Boldry for their help with mass spectrometry and proteomics.

A special thanks to members of the Wagner Lab that I have had the opportunity to meet over the years. I truly enjoyed our time together! Finally, I would like to express my sincerest gratitude to my family and all my friends for providing the much-needed emotional balance outside of the lab.

Dedication

To Leti……. and the Wu-Tang.

Abstract

Significant progress has been made towards the development of phosphate prodrugs for intracellular delivery of monophosphates. Such efforts led to the successful application of the aryloxy amino acid phosphoramidate (ProTide) strategy for development of sofosbuvir. Although widely successful, several drawbacks of the ProTide strategy limit its utility for delivery of significant levels of nucleotide analogs in tissues other than the liver. In order to broaden the utility of phosphate prodrugs, we have developed pronucleotide strategies that address the inefficiencies of the ProTide system.

Chapter 2 describes the design and development of an anchimerically activated pronucleotide strategy, incorporating 2-(methylthio)ethyl and tryptamine as phosphate protecting moieties. The prodrug is activated by a sulfur mediated intramolecular cyclo-de-esterification reaction to yield a monoester phosphoramidate, which gets hydrolyzed by HINT1 to release a monophosphate. In a proof-of-concept application, we applied the pronucleotide strategy towards intracellular delivery of 7-Chlorophenoxyethyl guanosine monophosphate, as a chemical tool for translational control of protein synthesis. Furthermore, in **Chapter 3** we provide another proof-of-concept application of the new pronucleotide strategy for intracellular delivery of 2′-C-β-Methyl guanosine monophosphate as an anti-Dengue virus (DENV) agent.

In a related project, we sought to profile the protein interacting partners of nucleoside monoester phosphoramidates. Mapping the small molecule-protein interactome of nucleoside monoester phosphoramidates should help us decipher the mode

of cellular uptake and identify other metabolizing enzymes of nucleoside monoester phosphoramidates (excluding HINT1). **Chapter 4** outlines the design and synthesis of phosphoramidate-based photoaffinity probes as chemical tools for profiling the protein binding partners of nucleoside monoester phosphoramidates. The synthesized probes were utilized for *in vitro* proteomics studies in whole cell extracts (lysates) and in live cells.

Finally, we describe the design and development of a nucleotide mimetic inhibitor of eIF4E in **Chapter 5**. As a proof-of-concept application, we employed a sulfamido alkyl moiety as a substitute for 5′-phosphate in the design of 5′-mRNA cap analog antagonists of eIF4E. We successfully synthesized a mimetic of 7-Chlorophenoxyethyl guanosine monophosphate and demonstrated that its binding potency to eIF4E is comparable to that of the parent nucleotide, with only a modest loss in binding potency.

Table of Contents

List of Tables

List of Schemes

List of Figures

Chapter 1

1.1. Introduction

1.1.0. Nucleoside and Nucleotide Analogs

The genetic information of every organism is encoded in the organism's DNA (2′-deoxyadenosine, 2′-deoxyguanosine, thymidine, and 2′-deoxycytidine), which upon transcription into mRNAs carry the appropriate information needed for gene expression. As an organism goes through cellular division, the genome (DNA) must be duplicated/copied as the organism divides into two separate cells. The process of DNA replication is a highly delicate event and requires the highest degree of fidelity and accuracy in order to ensure that mutations are not introduced to the next generation of cells. As a result of the need for accurate replication of DNA, DNA polymerases also possess proofreading functionalities (3′ – 5′ exonuclease activity).

Similar to DNA replication, transcription of DNA into RNA requires a high level of accuracy since incorporation of an incorrect base could lead to non-coding RNA or coding of a mutant protein(s) with defective function(s). RNA polymerase II (pol II) has been shown to utilize both high NTP selectivity and proofreading (3′ – 5′ exonuclease activity) to ensure proper synthesis of RNA transcripts. A comprehensive review of eukaryotic DNA replication and transcription has been presented.[1, 2]

Much like eukaryotes, viruses must replicate and transcribe their genome during viral replication. Depending on the genomic classification, the task of genome replication and transcription is performed by each genome-specific polymerase (i.e. RNA-dependent

RNA polymerase is responsible for genome replication and transcription in RNA viruses). Unlike the replication and transcription events in eukaryotes, the corresponding viral events are error-prone because viral polymerases generally lack proofreading capabilities. For example, error frequencies in RNA viruses are usually 10^{-3} to 10^{-5} for every nucleotide extension.[3, 4] Consequently, viral genome is likely to contain mutations, which could be beneficial to the virus since mutations could provide the evolutionary diversity for evasion of antiviral therapeutics. However, the propensity for incorrect incorporation of nucleotides during replication and/or transcription could also be exploited for antiviral therapeutic benefits. Indeed, the propensity for incorporation of incorrect nucleotide forms the basis of nucleoside analog-based antiviral therapy.[5]

Ever since the US Food and Drug Administration (FDA) approval of idoxuridine (IDU) for treatment of herpetic keratitis, there has been tremendous interest in the development of nucleoside analogs as antivirals and anticancer agents. Such efforts have led to the approval of numerous nucleoside analogs and their prodrug derivatives for the treatment of viral and malignant diseases. Depending on the mechanism of action, nucleoside analogs are classified as either mutagenic agents, obligate chain terminators, non-obligate chain terminators (**Figure 1-1**). Mutagenic agents such as ribavirin and 5-fluorouridine can mimic the hydrogen bonding patterns of purines (A or G) when incorporated into a nascent oligonucleotide, thus leading to transition mutations when they base-pair with uridine and cytidine. The introduction of mutations into the viral genome of a *quasispecies* such as a virus, can engender an *error catastrophe* since

subsequent replicative events can produce a viral population with severely compromised fitness, leading to a potentially lethal outcome.[3, 4, 6, 7]

Unlike mutagenic nucleosides that target the viral genome, chain terminators exert their antiviral activity by targeting viral polymerases. Chain terminating nucleosides usually have a modified ribose whereby their incorporation into a newly synthesized oligonucleotide leads to the termination of elongation. This class of nucleoside analogs typically lacks a reactive 3′-hydroxyl group (obligate chain terminators) or contain a ribose modification that either blocks subsequent binding of the next nucleotide or interferes with post-polymerization translocation of the polymerase (non-obligate chain terminators) (**Figure 1-1**).[8-10]

Non-obligate chain terminators have a reactive 3′-hydroxyl moiety but also contain modifications appended to their ribose, which interfere with the polymerization event. Examples of this class of nucleoside analogs are molecules bearing a 2′-methyl substituent (**Figure 1-1**). Termination of chain elongation leads to fragmented nucleic acid chains and leads to inhibition of viral replication.

Irrespective of the mechanism of activity, all nucleoside analog inhibitors depend on metabolic activation into the respective mono-, di-, or tri-phosphorylated forms before exhibiting antiviral or anticancer activity (**Figure 1-2**). Considered as prodrugs, nucleoside analogs are activated exclusively by host cellular kinases or in combination with virally encoded kinases. A close look at the kinases involved in nucleoside analog metabolism is presented below.

Figure 1-1. Examples of nucleoside analogs and their classification based on their mechanism of action.

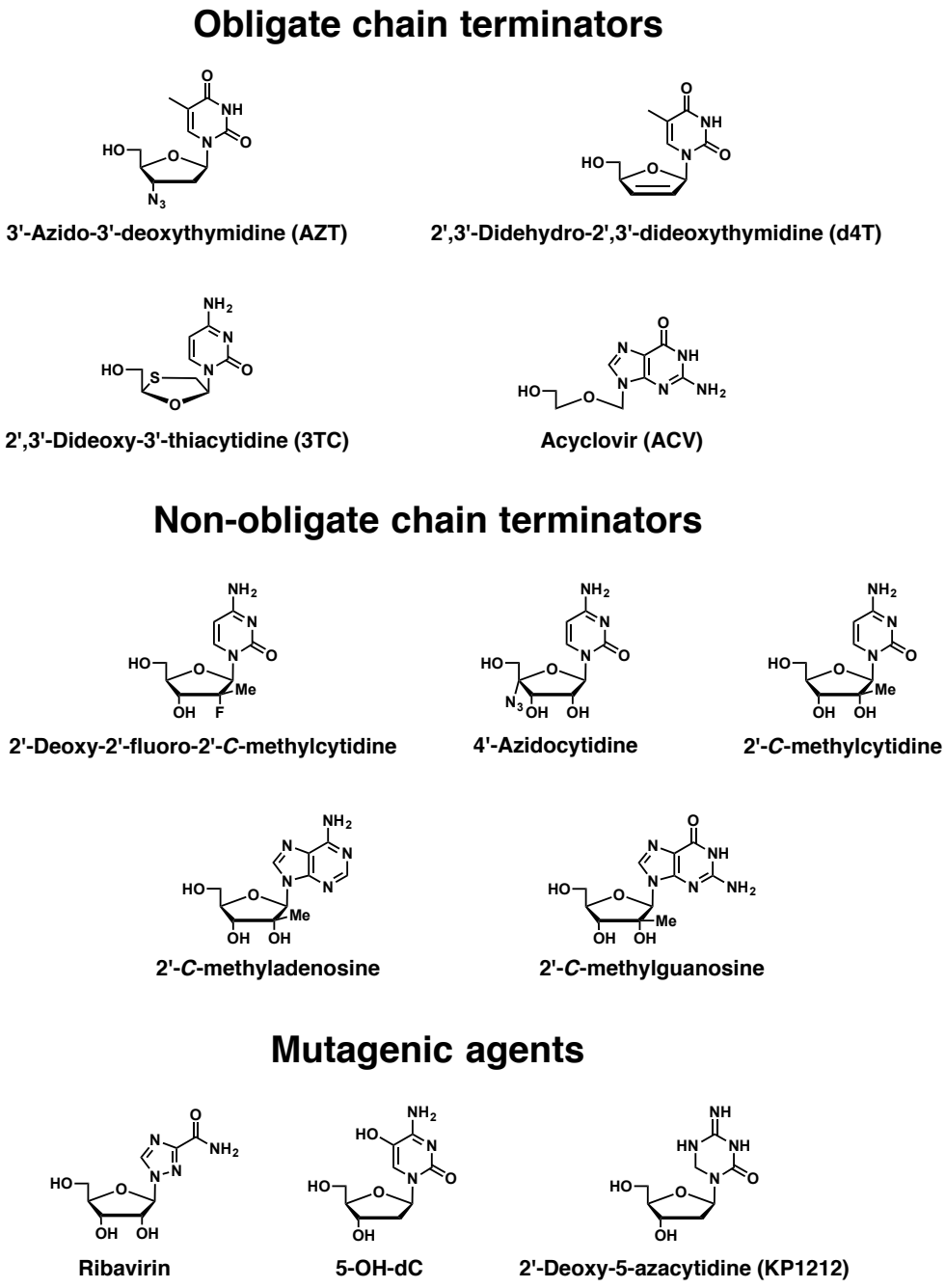

1.1.1. Deoxynucleoside Kinases (dNKs)

Initial phosphorylation of most nucleoside analogs is catalyzed by enzymes/kinases involved in the salvage pathway of deoxyribonucleoside biosynthesis. Deoxythymidine kinase (dTK) 1 and 2, deoxycytidine kinase (dCK), and deoxyguanosine kinase (dGK) are the primary mammalian kinases involved in the monophosphorylation of nucleoside analogs.[11-13] Human deoxynucleoside kinases belong to two classes. The first class of kinase includes human cytosolic dCK, dGK, and the human mitochondrial dTK2. Kinases in this class exist solely as homodimers and have about 40% sequence identity.[12] In addition, these kinases are characterized by low enantioselectivity as they have been shown to phosphorylate D- and L-enantiomers of nucleoside analogs, as well as, being able to phosphorylate some acyclic nucleoside analogs, for example dGK phosphorylation of ganciclovir.[12] The second class of human dNKs is comprised of the cytosolic thymidine kinase (TK1). TK1 possess a strict enantioselectivity for D-enantiomers of thymidine and its analogs. Thymidine analogs with small C-5 modifications have been shown to be substrates of TK1, while analogs with bulky C-5 substitutions (e.g. brivudin) are not recognized by the kinase.[12]

A relevant virus encoded nucleoside kinase is herpes simplex virus 1 (HSV1) TK, which displays broader substrate specificity than the human variant. HSV1 TK can phosphorylate all naturally occurring D- nucleoside, L- enantiomers of deoxythymidine, thymidine analogs with bulky C-5 substitution, as well as, acyclic nucleoside analogs such as acyclovir and ganciclovir. The ability to monophosphorylate acyclic nucleoside analogs forms the basis for the success of these nucleosides as antiherpes agents, since

kinases in uninfected cells are unable to efficiently catalyze the initial phosphorylation step.[12] Unlike other kinases mentioned thus far, HSV1 TK utilizes other nucleoside triphosphates (NTPs) other than ATP as phosphate donors and has been shown to also catalyze conversion of dTMP to dTDP.[12]

1.1.2. Nucleoside Monophosphate Kinases (NMPKs)

The second phosphorylation step in the activation of nucleoside analogs is catalyzed by nucleoside monophosphate kinases. In human tissues, there are broadly four NMPKs: uridylate-cytidylate kinase (UMP-CMPK), thymidylate kinase (dTMPK), adenylate kinase (AMPK, six isoforms), and guanylate kinase (GMPK).[12, 13] Humans have two isoforms of UMP-CMPK, which is characterized by loose enantioselectivity, a preference for dCMP over dUMP as substrates, as well as, a preference for deoxynucleoside monophosphates over ribonucleoside monophosphates.[12] In addition, human UMP-CMPK is inactive for dTMP phosphorylation.[12] Furthermore, UMP-CMPK is inhibited by excess D-nucleotide analogs and is responsible for phosphorylation of the acyclic nucleoside phosphonate, cidofovir.[12] Similar to UMP-CMPK, the major human AMPK isoforms 1 and 2 can phosphorylate acyclic phosphonates. However, AMPK1 and AMPK2 have strict enantioselectivity and only accept D-(d)AMP and acyclic mimics of dAMP as substrates.[12, 13] The soluble form of human GMPK (also called GUK) also accepts acyclic nucleotides in addition to (d)GMP as substrates. Notably, phosphorylation of monophosphates of acyclovir and ganciclovir in virus-infected cells is catalyzed by GMPK.[14]

In contrast to the nucleoside monophosphate kinases mentioned thus far, only the expression of dTMPK is cell cycle regulated. While other NMKs are constitutively expressed as cells progress through the cell cycle, expression of dTMPK is restricted to only proliferating cells. Notably, dTMPK activity is nonexistent in nonproliferating tissues (e.g. adult liver) compared to rapidly proliferating cells such as lung carcinomas and neonatal liver. Such distinct expression pattern is the basis for the observed low toxicity of thymidine analogs.[12, 13] In terms of the substrate specificity, dTMPK phosphorylates dUMP, dTMP, and is enantioselective for D-enantiomers of dUMP analogs. In addition, only C5-halogen-substituted analogs are effectively phosphorylated while analogs bearing bulky substituents at the C5-position are not accepted for phosphorylation.[12]

1.1.3. Nucleoside Diphosphate Kinases (NDPKs)

The final step in the activation cascade of nucleosides and their analogs is catalyzed by NDPK. There are two major human isoforms of NDPK: NDPK A and NDPK B. The phosphorylation step catalyzed by the enzymes involves the transfer of the γ-phosphate of a donor nucleotide (ATP or GTP) onto the nucleoside diphosphate acceptor molecule.[12] Transfer of the γ-phosphate onto the substrate goes through two "ping-pong" steps dependent on formation of a phosphohistidine enzyme intermediate.[15] In terms of substrate specificity, NDPK accepts any nucleoside or deoxynucleoside diphosphate but is enantioselective for D-enantiomers.[12, 16] However, the nature of the sugar severely impacts the activity of the enzyme. In fact, substrates lacking a 3′-hydroxyl group are processed less efficiently compared to the 2′-deoxy counterparts.[12]

Apart from NDPK, human phosphoglycerate kinase (hPGK) and human creatine kinase (hCK) have been shown as other kinases involved in phosphorylation of (d)NDPs.[16] In particular, hPGK was found to preferentially phosphorylate L-nucleoside diphosphates compared to the D-enantiomers.[16] Furthermore, substrates lacking a 3′-hydroxyl group are also phosphorylated by hPGK and hCK.[16]

Figure 1-2. (A) Nucleotide salvage pathway for metabolism of naturally occurring ribonucleosides. (B) Nucleoside analogs are activated by enzymes of the nucleotide salvage pathway into the respective mono-, di-, and tri-phosphate metabolites in order to be active in cells.

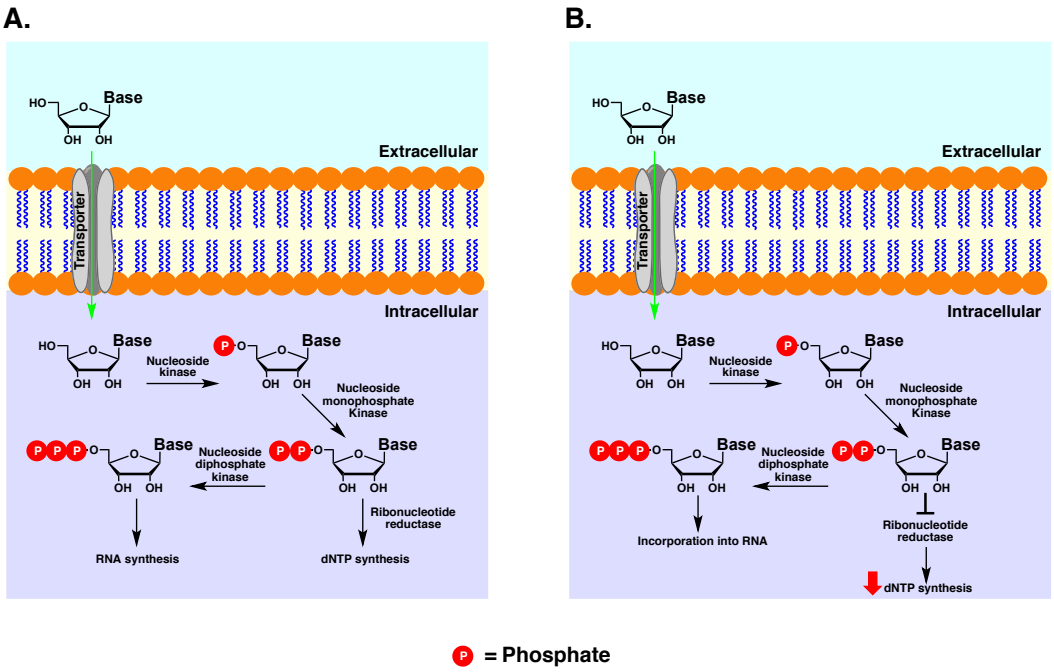

1.2.0. Cellular Resistance to Nucleoside Analogs

The application/utility of nucleoside analogs as anticancer and antiviral therapeutics can be hampered by the development of drug resistance. Mechanisms of resistance to nucleoside analog based therapies can be broadly categorized into three groups. The foremost mechanism of resistance to nucleoside analogs relates to alterations in the genes and expression of proteins responsible for their cellular uptake and metabolism into the active nucleotide metabolites. Insufficient cellular accumulation of the active nucleotides could be a result of, 1) inefficient transport of a nucleoside analog by nucleoside transporters, 2) inefficient kinase activation, 3) elevated deaminase activity in the case of cytidine-based nucleoside analogs, and 4) elevated degradation of nucleoside analogs monophosphate by catabolizing enzymes such as 5′-nucleotidases (**Figure 1-3**). The second category of resistance mechanisms can be attributed to mutations in viral or cancer cells to nucleoside analog target proteins such as DNA or RNA polymerases, ribonucleotide reductase, and CTP synthase.[17, 18] Lastly, the third category of resistance mechanism involves the cellular response to counteract nucleoside analog induced stress, such as increased activity of DNA repair enzymes. The current work will only address mechanisms of resistance outlined in the first category (**Figure 1-3**).

Figure 1-3. Mechanisms of cellular resistance to nucleoside analogs. Inefficient transport by nucleoside transporter (A), inefficient or lack of phosphorylation by nucleoside kinases (B), deamination of cytidine and adenosine analogs (C), and dephosphorylation by 5´-nucleotidases (D) are some of the mechanisms by which cells develop resistance to nucleoside analogs.

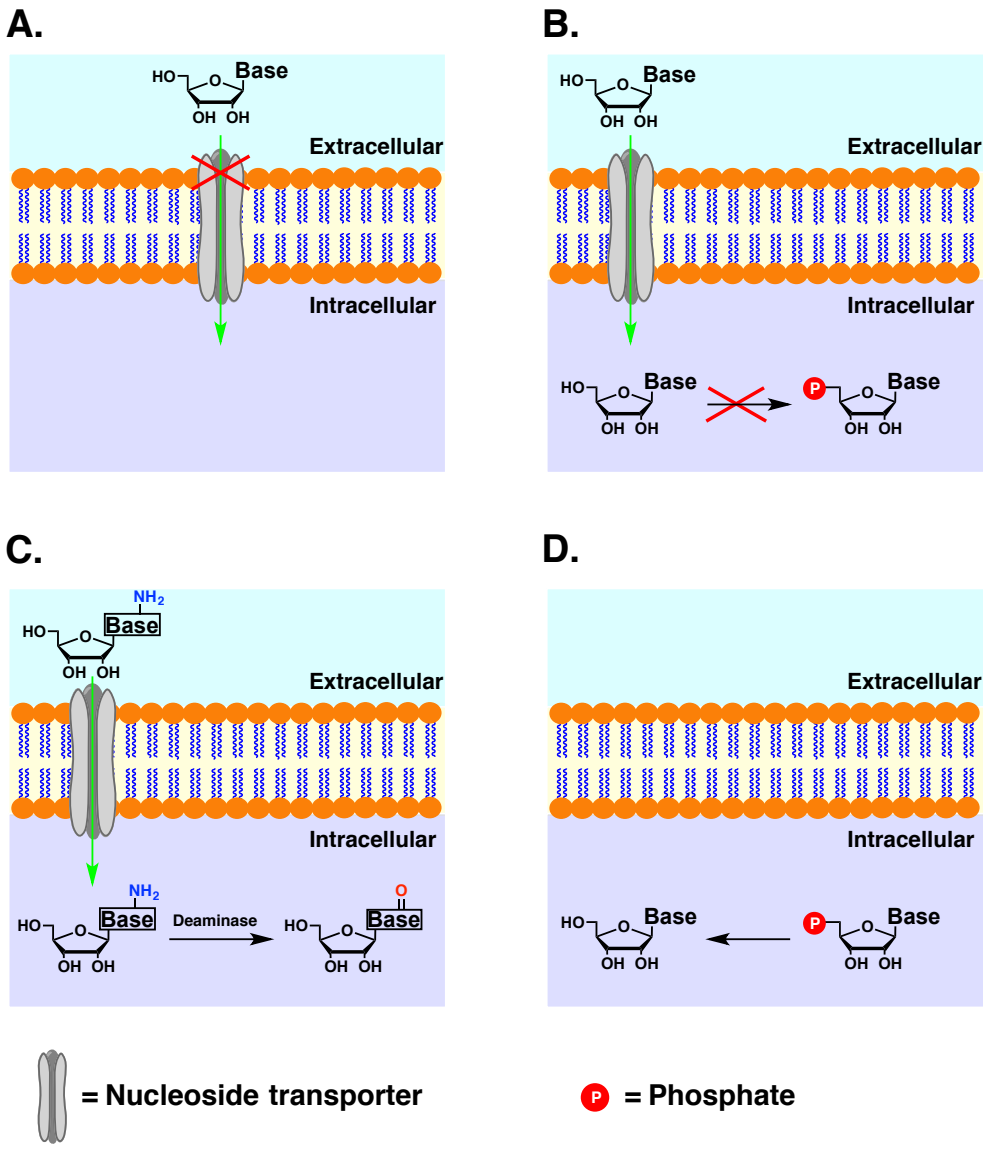

1.2.1. Plasma Membrane Transporters Contribution to Drug Resistance

Nucleoside analogs are hydrophilic molecules and are dependent on specific nucleoside transporters (NTs) for cellular uptake (**Figure 1-2**). Human nucleoside transporters are classified into two families, equilibrative nucleoside transporters (ENT) and concentrative nucleoside transporters (CNT). There are two well-characterized isoforms of human ENT responsible for transport of natural nucleosides, which are encoded for by solute carrier family 29 (SLC29).[18-22] Human ENT1, which is sensitive to inhibition by nitrobenzylmercaptopurine ribonucleoside (NBMPR) and ENT2, which is resistant to NBMPR. Each of these transporters mediate transport of nucleosides down a concentration gradient and have similar selectivity towards purines and pyrimidines, albeit with a lower affinity when compared to other membrane transporters. In terms of tissue distribution, hENT1 is ubiquitously expressed in human tissues, while hENT2 is predominantly expressed in skeletal muscle and brain tissues.

Encoded by the SLC28 family of genes, the three well-characterized human CNT proteins (hCNT1, hCNT2, and hCNT3) are abundantly expressed in highly differentiated tissues such as the liver and kidneys. Human CNTs transport nucleosides against a concentration gradient by coupled transport of sodium ions and are insensitive to transport inhibition by NBMPR.[20, 23] In addition, the stoichiometry of sodium/nucleoside ratio is 1:1 for hCNT1 and 2, while that for hCNT3 is 2:1. Unlike hENTs which has broad substrate selectivity, hCNTs display preferences for nucleosides with hCNT1 preferring pyrimidines while hCNT2 prefers purines. hCNT3 appears to have broad substrate selectivity for purines and pyrimidines.

Other membrane transporters implicated in the transport of nucleoside analogs are the SLC22 gene family encoded organic anion and organic cation transporters. Organic anion transporters (OAT1-4) are the best characterized so far and are encoded for by SLC6-8 and 11.[23] OATs are mainly expressed in the kidneys, however the brain, placenta, and liver have been reported to express OAT1/3, OAT1, and OAT2, respectively. Transport by OATs is by anion exchange or via facilitated transport of anions, with broad substrate selectivity for amphiphilic organic ions, uncharged compounds, and even cyclic nucleotides. In terms of nucleoside analogs transported by OATs, AZT is the only nucleoside analog transported by OAT1-4, while other nucleoside analogs are selectively transported by OAT1-3.

The three well-characterized organic cation transporters (OCT) 1- 3 are encoded by SLC22A1-3. Transport by OCTs is electrogenic, independent of sodium ion, with transport largely driven by the electrochemical gradient of the transported organic cation. Similar to the OATs mentioned above, OCT 1-3 are expressed in select tissues such as kidneys (OCT2), liver, (OCT1). OCT3 is expressed by liver, placenta, skeletal muscle, and heart tissues. Substrate selectivity of OCTs is reported to be broad and have been reported to transport antiviral and some anticancer nucleoside analogs.

Several *in vitro* studies with cultured cell lines and *ex vivo* studies on human clinical samples have revealed a relationship between NT expression and resistance to nucleoside analog-based anticancer and antiviral therapies. In particular, tumors from patients who were resistant to gemcitabine showed an overall decrease in hENT1 expression.[24-26] In fact, better survival outcomes were observed in pancreatic

adenocarcinoma patients on gemcitabine therapy who displayed detectable hENT1 expression when compared to patients who were negative for hENT1 protein.[24-26] Similarly, sensitivity to cytarabine (ara-C) in children with AML was shown to correlate with mRNA expression levels of hENT1.[27]

Apart from the down regulation of NT expression, the structural requirements for NT recognition of nucleoside analogs could also contribute towards resistance to nucleoside analog chemotherapies. Specifically, the presence of a 3′-hydroxyl moiety, for hydrogen bonding interaction, is critical for transport by all NTs.[21] Moreover, transport by CNT1 – 3 is sensitive to 2′-C, 5′-C, and N-3 modifications on pyrimidines, while hENTs are sensitive to modifications at 2′-C and 5′-C of pyrimidines.[21, 28-30] Since nucleoside analogs usually have modifications to their sugars and nucleobases, it is possible that such modifications could reduce the transportability of certain nucleoside analogs.[21]

1.2.2. Nucleoside Kinases Contribution to Drug Resistance

Deoxycytidine kinase is generally recognized as the critical rate-limiting enzyme for initial phosphorylation of nucleoside analogs. Down-regulation or the absence of dCK activity has been identified as a source of resistance to nucleoside analogs in a variety of cell lines.[31-34] In addition, cancer cell lines deficient in dCK have been shown to exhibit cross-resistance between purine and pyrimidine analogs *in vitro*.[33, 34] In fact, supplementation of dCK activity through transfection of dCK gene into dCK-deficient cells was shown to sensitize dCK-deficient cells to nucleoside analogs.[35, 36] The likely cause of reduced/nonexistent dCK activity *in vitro* could be due to mutations in the dCK

gene and the presence of alternative splice variants.[37, 38] Although, *in vitro* studies on the contribution of dCK activity to resistance to nucleoside analogs have been sharply defined, there is considerable controversy as to its clinical significance in patients resistant to nucleoside analog therapies. Several studies on patients with hematological cancers such as ALL, AML, and CLL reported a correlation between either dCK mRNA expression or low dCK activity with drug resistance.[39, 40] On the other hand, studies on these class of patients have indicated that neither dCK activity nor its mRNA expression are responsible for resistance to nucleoside analogs.[41, 42] This discordance in association of dCK activity with the clinical response to nucleoside analogs could point to the involvement of other metabolic enzymes in the development of drug resistance.[41]

Tyrosine kinase (TK) is required for phosphorylation of antivirals targeted towards DNA viruses. Nucleoside analogs such as acyclovir and BVDU have been shown to be ineffective against cytomegalovirus (CMV) and Epstein-Barr virus, which are devoid of TK activity. In addition, TK deficient mutants of HSV and varicella zoster virus (VZV) are also insensitive towards these nucleoside analogs.[43, 44]

1.2.3. Deaminases and 5´-Nucleotidase Contribution to Drug Resistance

Cytidine deaminase (CDA) and dCMP deaminase are responsible for the conversion of cytidine, deoxycytidine, and their monophosphate metabolites to uridine derivatives.[45-48] Cellular resistance to cytidine analogs has been shown to be the result of deamination by both deaminases. In particular, several nucleoside analogs such as gemcitabine, ara-C, decitabine, and 5-azacytidine have been shown to be substrates of CDA, which could explain the reason why these compounds are inactive against

hepatotropic cancers due to high CDA expression levels in the liver.[46, 49] In fact, hematologic cancer patients with elevated CDA activity and mRNA expression display resistance to cytidine analog therapy with an overall worse disease outcome compared to patients who responded to cytidine analog therapy.[50-52] Administration of the CDA inhibitor, tetrahydrouridine (THU), was shown to reverse resistance to cytidine analogs both *in vitro* and in patients with hematologic cancers; thus, combination treatment of THP and cytidine analogs has been recommended.[49, 53-56] Certain single nucleotide polymorphisms of CDA gene have been identified in patients with poor response to cytidine analogs. However, the contributions of other factors such as transcriptional regulation and post-translational regulation cannot be ruled out as the molecular basis for the observed disparity in responders and non-responders to cytidine analogs.[18, 50]

Another contributing factor towards cellular resistance to nucleoside analogs is the action of 5′-nucleotidases (5′-NT). These enzymes catalyze the dephosphorylation of nucleoside monophosphates, thereby reducing the intracellular concentration of other downstream phosphate metabolites of nucleoside analogs.[17, 18] Consequently, hematologic patients displaying resistance to nucleoside analog chemotherapy were shown to have high levels of 5′-NT mRNA expression and protein activity.[40, 57] For example, the activity of 5′-NTs have been associated with cellular resistance to the antiviral AZT.[58] There is considerable dephosphorylation of AZT monophosphate back to AZT by 5′-NTs in CEM cell extracts exposed to a AZTMP.[58] In fact, AZTMP has been shown to be a better substrate for 5′-NTs when compared to deoxythymidine monophosphate (dTMP).[58] Such catabolic processes results in an increase in the

intracellular pool of the nucleoside with low accumulation of the triphosphorylated metabolites.[58]

1.3.0. Circumventing Cellular Resistance to Nucleoside Analogs

The first phosphorylation step by cellular kinases is generally recognized as the limiting step during metabolism of nucleoside analogs. Consequently, lack of phosphorylation is considered the most important contributor towards drug resistance. In principle, inefficient phosphorylation could be remedied via direct administration of nucleoside monophosphates to cells. However, such a strategy has been shown to be ineffective with the nucleotides displaying a reduced potency as the parent nucleoside analog.[59, 60] The failure of direct administration of nucleotide to cells stems from the inability of nucleotides to permeate cell membranes due to the highly charged and polar phosphate moiety (at physiological pH), leading to little or no accumulation of the desired nucleotide in cells (**Figure 1-4A**).[59] In addition, nucleotides are metabolically unstable and are easily dephosphorylated by 5′-NTs and phosphatases to yield the parent nucleosides.[61] Consequently, efforts at delivering nucleotides in cells have centered on the development of nucleotide analogs such as nucleoside phosphonates, as well as the development of nucleotide prodrugs.

Figure 1-4. Pronucleotides strategy for delivery of nucleotides in cells. Direct delivery of nucleotides to cells (A) is inefficient but lipophilic pronucleotides (B) can effectively deliver nucleotides in cells upon cellular metabolism to remove the phosphate protecting groups.

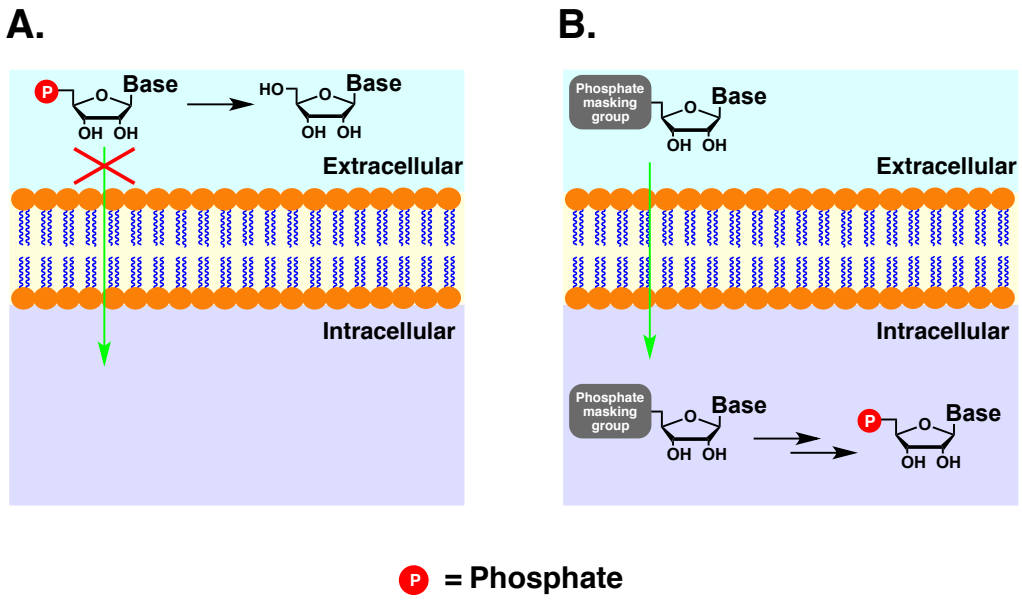

1.3.1. Nucleoside Phosphonates as Nucleotide Analogs

Phosphonates are bioisosteres of phosphates with a CH_2-P-bond replacing the O-P-bond linking the phosphate group to the rest of the molecule (**Figure 1-5**).[62] Although ionized at physiological pH, phosphonates such as *p*-nitrobenzylphosphonic acid and phosphonoacetic acid were shown to possess antiviral activity in cells.[63, 64] The observed cellular activity could be explained by the relative improved lipophilicity inherent to phosphonates when compared to phosphates. Phosphonates are mostly singly ionized at physiological pH since the pKa for deprotonation of the second hydroxyl is usually above 7.4 for a methyl phosphonate (**Figure 1-5**).[62]

Although less acidic and potentially less bioactive than the corresponding phosphates, phosphonates are metabolically resistant to chemical and enzymatic degradation as a result of the phosphonic acid CH_2-P-bond.[65] Following the development of 5′-deoxyuridine 5′-phosphoric acid by Holý,[66] substantial efforts have been employed in developing nucleoside phosphonates and their derivatives as nucleotide analogs. Such efforts have led to the development of acyclic nucleoside phosphonates (ANPs) and cyclic nucleoside phosphonates (CNPs) as antiviral therapeutic agents (**Figure 1-5**).

ANPs such as cidofovir, adefovir, and tenofovir are FDA approved antivirals and have been shown to undergo two intracellular phosphorylation steps to their yield mono- and di-phosphate metabolites. Despite the well-documented clinical efficacy of nucleoside phosphonates, the scope of their clinical utility is somewhat limited as a result of their generally poor oral bioavailability. The poor oral bioavailability exhibited by nucleoside phosphonates can be attributed to the charged phosphonic acid moiety.[67]

Figure 1-5. (A) Ionization pKa of methyl phosphate and methyl phosphonate. (B) Mechanism of activation of nucleoside phosphonates. (C) Examples of acyclic and cyclic nucleoside phosphonates.

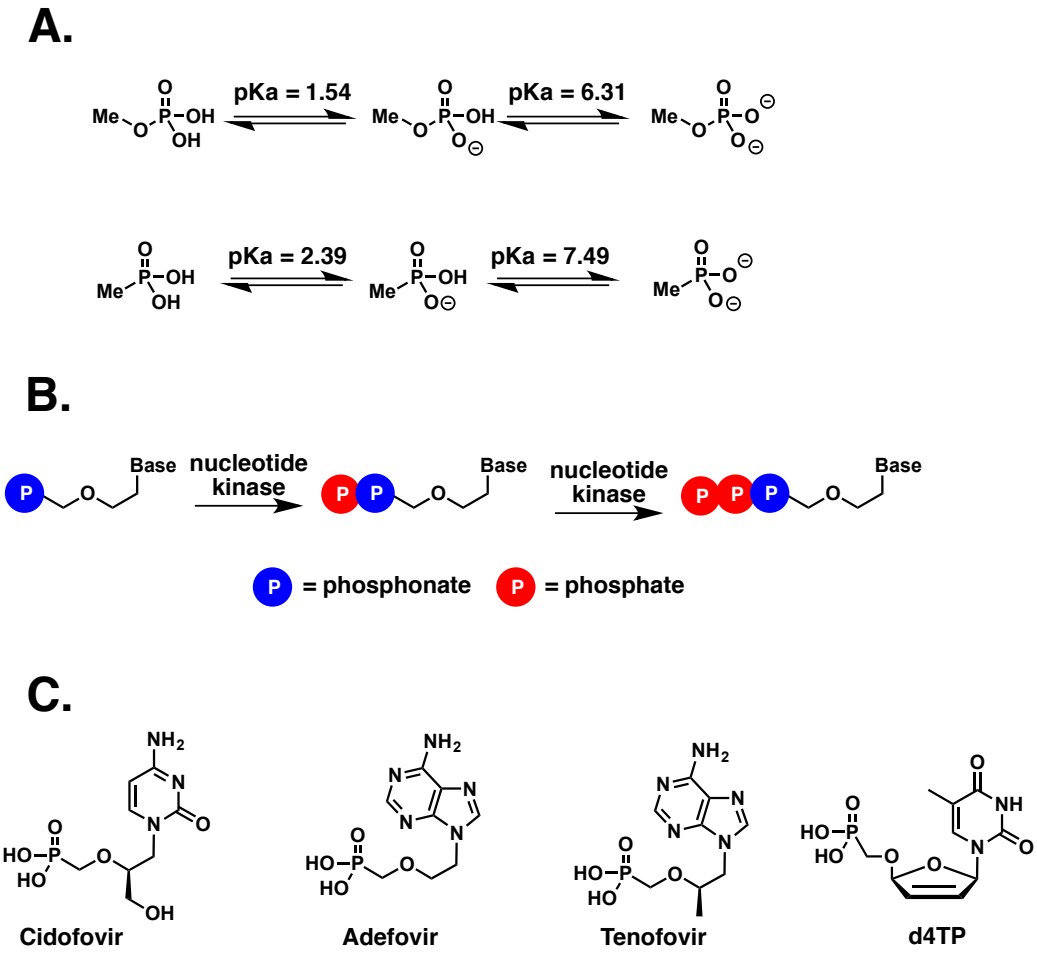

1.3.2. Nucleoside Monophosphate Prodrugs

Prodrugs provide a means to overcome physiochemical challenges to drug delivery such as poor aqueous solubility, metabolic instability, and poor oral bioavailability. Also referred to as pronucleotides, phosphate prodrugs have mostly been developed as a means to circumvent/bypass the inefficiency inherent in the first phosphorylation step during the metabolism nucleoside analogs.[59, 61, 65] Furthermore, phosphate prodrug strategies can also prevent metabolic inactivation of nucleoside/nucleotide analogs by nucleoside and nucleotide deaminases.[68, 69]

Typically, the design of pronucleotides involves the use of phosphate protecting groups as a means to mask or reduce the highly anionic property of phosphates, thus generating a nonionizable and highly lipophilic derivative of the intended nucleotide at physiological pH (**Figure 1-4B**).[61, 65, 70,71] Generally, improved lipophilicity engenders improved cellular uptake and in principle leads to an improved delivery of the intended nucleotide, upon metabolism of the pronucleotide.[59] Furthermore, the intracellular release of the phosphate protecting groups should ideally generate nontoxic metabolites.

Over the years, several pronucleotide strategies have been developed, which have greatly leveraged known chemical and enzymatic processes in cells as a means for activation of pronucleotides and release of the intended nucleotides. The pronucleotide strategies reported to date can be broadly classified either as *phosphoester*- or *amidate*-based systems (**Figure 1-6**).[72]

Figure 1-6. Examples of nucleoside monophosphate prodrug strategies. These strategies can be broadly classified as phosphoesters or amidate-based systems.

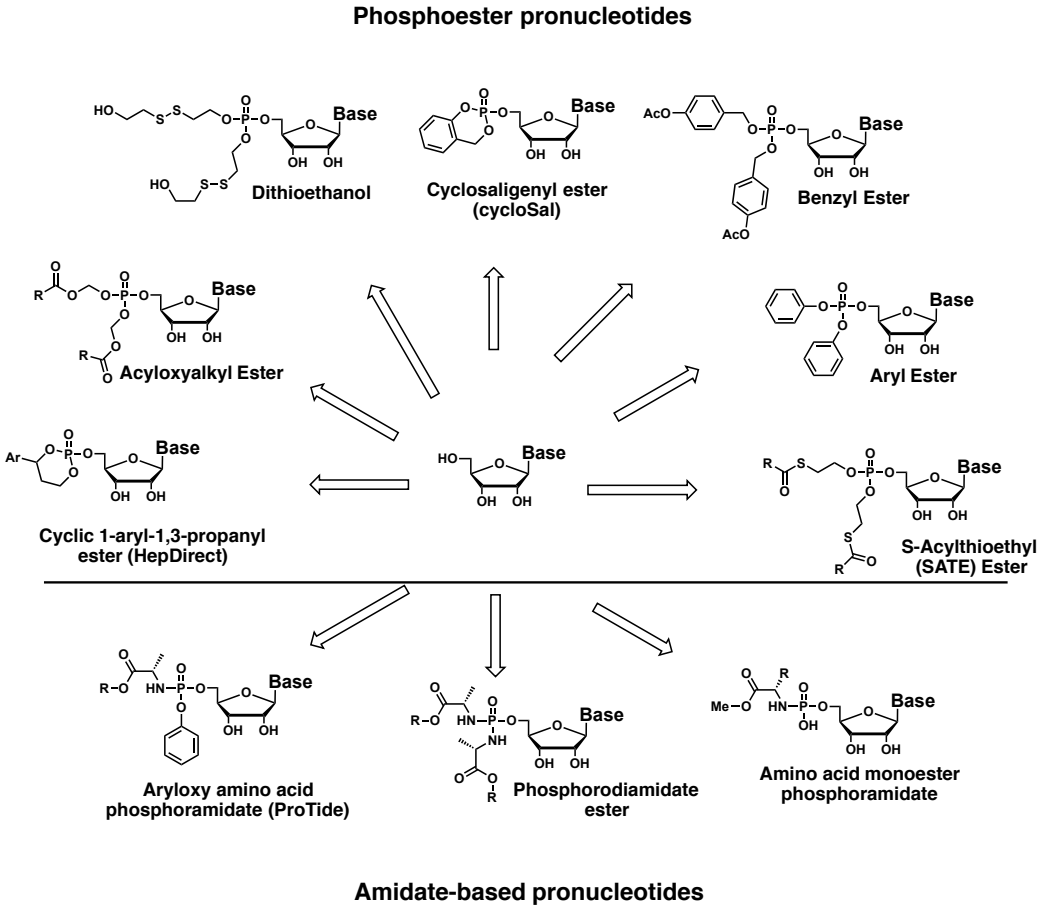

1.3.2a. Phosphoester Pronucleotides

i. *Acyloxyalkyl and Alkyloxycarbonyloxyalkyl Esters*

First reported by Farquhar and cowrkers,[73] acyloxyalkyl phosphate prodrugs such as the bis(pivaloyloxymethyl) [bis(POM)] require enzymatic activation through hydrolysis of the pivaloyl group by a carboxyesterase. The resulting hydroxymethyl compound spontaneously decays to yield formaldehyde and a mono-POM intermediate. The ensuing mono-POM intermediate can proceed through another round of deprotection initiated by a carboxyesterase or could be directly cleaved by a phosphodiesterase to release the desired nucleotide (**Scheme 1-1**). The bis-POM pronucleotide strategy was later applied for cellular delivery of monophosphates of 2′-deoxy-5-fluorouridine, and 2′,3′-dideoxyuridine.[74, 75] These pronucleotides demonstrated significant antitumor and antiviral activities when compared to the otherwise inactive nucleosides. In fact, the bis-POM prodrug of 2′,3′-dideoxyuridine was shown to protect CEM/TK$^-$ cells from HIV-1 infection while the parent nucleoside was inactive in these cells.[74]

Although bis-POM pronucleotides exhibit impressive aqueous stability, they are rapidly degraded in rat plasma ($t_{½}$ < 5 min)[75] due to the high concentration of carboxyesterases in rodent plasma, and as such the utility of bis-POM containing phosphate prodrugs has been limited to *in vitro* applications.[78] The most successful application of the bis-POM prodrug strategy has been in the development of phosphonate prodrugs such as the FDA approved adefovir dipivoxil for treatment of hepatitis B and tenofovir disoproxil for treatment of HIV.[78]

The application of bis-POM prodrug strategy is further curtailed by the toxicity concerns attributed to the released pivalate.[65] Pivalic acid is eliminated as pivaloylcarnitine and this mode of elimination has been shown to alter carnitine homestasis.[76, 77] Consequently, the development of the bis(isopropyloxycarbonyloxymethyl) [bis(POC)] ester prodrugs was an attempt at addressing the toxicity issues related to the release of pivalic acid in the bis-POM strategy. First reported by Arimilli and coworkers, bis(POC) pronucleotides incorporate a carbonate diester in its design, which upon enzymatic activation by a carboxyesterase leads to the release of isopropanol.[76] The resulting carbonate intermediate spontaneously decays to liberate carbon dioxide, formaldehyde, and a mono-POC intermediate. The ensuing mono-POC intermediate can undergo another carboxyesterase-catalyzed deprotection or could be cleaved by a phosphodiesterase to release the desired nucleotide (**Scheme 1-1**). The bis(POC) pronucleotide strategy was successfully applied for developing prodrugs of 9-[2-(phosphonomethoxy)propyl]adenine (PMPA). These prodrugs displayed significantly improved antiretroviral activities when compared to the parent phosphonate, and ultimately led to the FDA approval of tenofovir disoproxil as an anti-HIV agent.[76, 78]

Scheme 1-1. Mechanism of activation of acyloxyalkyl (A) and alkyloxycarbonyloxyalkyl ester pronucleotides (B).

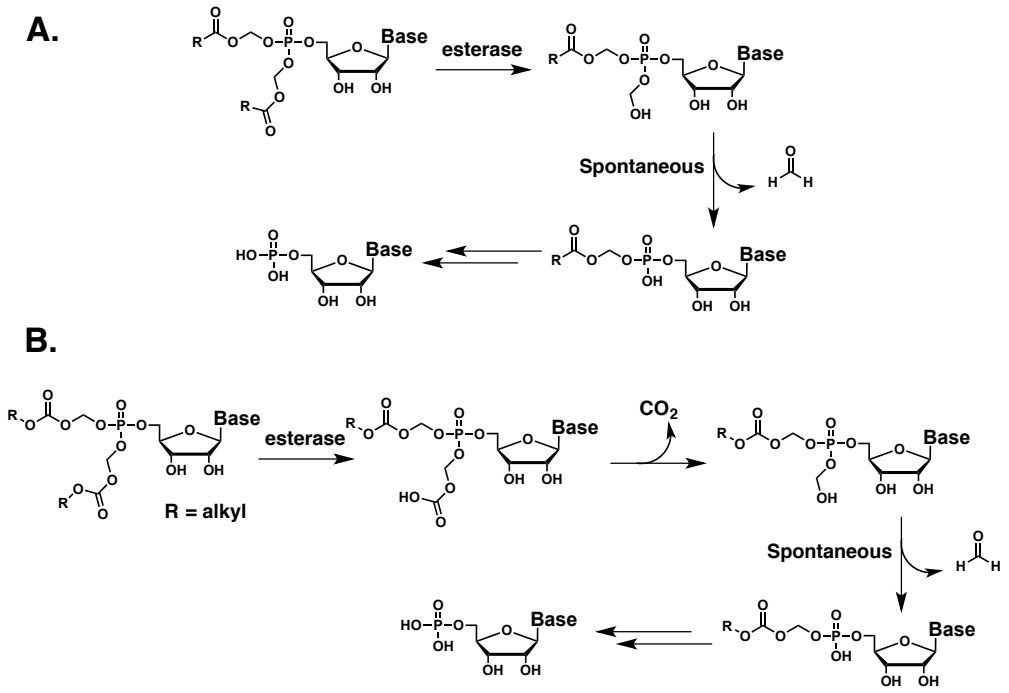

ii. *Aryl and Benzyl Esters*

McGuigan and coworkers first demonstrated the application of aryl esters as phosphate protecting groups.[79] Although less active than the parent nucleoside, the diphenyl ester prodrug of AZT monophosphate was found to possess superior anti-HIV activity when compared to the simple dialkyl ester prodrugs.[68, 79] In addition, a bis(p-nitrophenyl) ester derivative showed superior anti-HIV activity when compared with AZT, albeit with an increase in cytotoxicity.[79]

Further examples of aryl ester phosphate prodrugs are scant. However, application of this prodrug strategy has been reported for the development of phosphonate prodrugs.[80, 81] The diphenyl ester phosphonate prodrugs of neutral endopeptidase (NEP) inhibitors have been prepared and evaluated for their pharmacokinetic properties. The diphenyl ester prodrugs exhibited superior *in vivo* activity and oral bioavailability when compared to the parent *N*-phosphonomethyl dipeptide.[80, 81] In another example, diphenyl ester derivatives of 9-[2-(phosphonomethoxy)ethoxy]adenine (PMEA) were prepared and evaluated for oral bioavailability in mice.[82] The unsubstituted diphenyl derivative demonstrated a superior oral bioavailability (F = 50% as a hydrochloride salt) when compared to the parent phosphonate (F = 0%).[82] Intracellular metabolism to release the desired phosphonate is thought to proceed via initial aqueous hydrolysis to generate a monophenyl intermediate, which is subsequently hydrolyzed by an (as yet to be identified) enzyme to release the desired phosphonate. [82, 83]

The use of unsubstituted benzyl groups as phosphate protecting groups failed to undergo productive deprotection to yield the desired phosphonates.[84] However, 4-acyloxy

substituted benzyl protecting group was effectively metabolized to yield the intended phosphonate metabolites.[84] The use of 4-acyloxybenzyl groups was originally intended as a means to separate the site of esterase activity from the monoionic phospho group during activation of the second acyloxymethyl moiety of bis(POM) prodrugs.[85]

Metabolism of bis(4-acyloxybenzyl) ester prodrugs is initiated by carboxyesterase hydrolysis of the acyloxy moiety to yield a 4-hydroxybenzyl intermediate, which subsequently leads to elimination of a quinone methide metabolite and a monoionic diester metabolite.[85, 86] Removal of the second 4-acyloxybenzyl moiety proceeds in the same manner to yield the desired phospho metabolite. The liberated quinone methide was shown to react with water to form 4-hydroxybenzyl alcohol (**Scheme 1-2**).

Initial application of 4-acyloxybenzyl esters was demonstrated with methylphosphonic acid, where the prodrug was shown to be stable to aqueous hydrolysis, while displaying efficient conversion to the desired phosphonate in the presence of porcine liver carboxyesterase (PLCE).[86] Subsequent application in the development of prodrugs of AZT showed successful *in vitro* conversion to the monophosphorylated metabolite in the presence of PLCE.[87] In addition, these prodrugs were shown to display equipotent anti-HIV activities when compared to AZT in C8166 cells. An increase in toxicity in uninfected cells was also observed, which could be a result of the released quinone methide. Except for the *tert*-butyl derivative, the bis(4-acyloxybenzyl) ester prodrugs exhibited a nearly five-fold superior anti-HIV activity when compared to the unsubstituted dibenzyl AZT prodrug. The antiviral activity of this prodrug could result from the intracellular degradation of all tested prodrugs to AZT. Further application of

bis(4-acyloxybenzyl) esters as phosphonate protecting groups only yielded compounds with modest improvement in *in vivo* oral bioavailability.[82]

Scheme 1-2. Mechanism of activation of aryl ester pronucleotides.

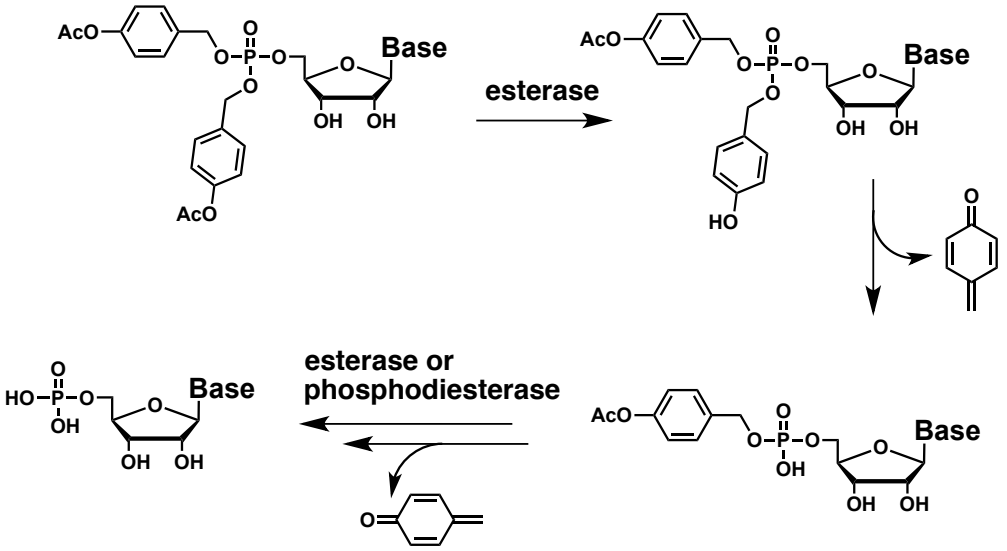

iii. *S-acylthioethyl (SATE) and Dithioethanol Esters*

Similar to the acyloxyalkyl ester prodrugs, the activation of SATE ester prodrugs such as in the bis(SATE) ester pronucleotides is mediated by carboxyesterase hydrolysis of the acyl portion of such compounds.[88-90] The resulting thioethyl ester intermediate decomposes to release ethylene sulfide and a mono(SATE) ester pronucleotide, which undergoes a similar deprotection sequence as the first SATE moiety (**Scheme 1-3A**).[88-90] Sensitivity towards enzymatic activation of SATE prodrugs is influenced by modification to the acyl portion of such compounds. More lipophilic variants such as bis(*t*-ButylSATE) where more stable to carboxyesterase activation compared to the bis(MeSATE) variants.[90] Furthermore, hydroxylation of the acyl group such as with bis(hydroxy *t*BuSATE) ester was shown to reduce the rate of prodrug activation when compared to the bis(*t*-BuSATE) derivatives.[91, 92] Such a reduction in the rate of activation of bis(hydroxyl *t*-BuSATE) ester AZT prodrug was identified as the reason for its reduced potency in TK deficient cells when compared to the more lipophilic bis(*t*-BuSATE) AZT derivative.[92]

SATE phosphate protecting groups have been applied for the intracellular delivery of monophosphates of AZT,[90] ddU,[89] and β-L-ddA[93] as anti-HIV and anti-HBV agents. These studies consistently demonstrated that bis(SATE) ester pronucleotides displayed superior antiviral activities in cells where the parent nucleoside was inactive. The improved antiviral activity was attributed to the release of monophosphates in the viral infected cells.[89, 90, 93] The SATE pronucleotide approach has also been applied for the delivery of phosphonates in cells. Bis(*t*-BuSATE) ester prodrug of PMEA displayed

superior anti-HIV when compared to PMEA and the bis(POM) ester pronucleotide. In addition, bis(*t*-BuSATE)PMEA was considerably more stable in human serum and gastric juice when compared with bis(POM)PMEA (5 h vs <5 min in human gastric juice).[94] Although such stability in human gastric juice was hypothesized to be indicative for potential improved oral bioavailability, there has not been any study, to date, to verify such claims.[78]

Application of the SATE prodrug approach has also been extended towards the development of SATE-aryl mixed pronucleotides. Such pronucleotides were envisioned to utilize initial enzymatic processing by carboxyesterase to yield an aryl phosphodiester intermediate, which is subsequently hydrolyzed by a phosphodiesterase to yield the desired nucleotide (**Scheme 1-3A)**.[91, 95] The involvement of a phosphodiesterase in the second activation step was intended as a means of improving the rate of release of the nucleotide, which is rate-limiting in the bis(SATE) ester approach.[91] Although sometimes more toxic to uninfected cells, mixed SATE-aryl pronucleotides of AZT displayed anti-HIV activities that were comparable to that of AZT in TK^+ cells. In addition, the anti-HIV activity in TK deficient cells was superior to that of AZT, which was inactive in these cells.[91, 95]

Development of bis(dithioethyl) [bis(DTE)] ester pronucleotides was first reported for ddU, AZT, and PMEA.[96] Similar to bis(SATE) pronucleotide approach, bis(DTE) ester pronucleotides rely on reductase-mediated cleavage of a disulfide bond to generate an *O*-2-mercaptoethyl intermediate, which upon nucleophilic attack at the α-methylene of the phosphate leads to the formation of a monoDTE intermediate and

ethylene sulfide (**Scheme 1-3B**). Removal of the second DTE moiety can either proceed via the same reductase-mediated cascade or through phosphodiesterase mediated hydrolysis to yield the desired nucleotide. Bis(DTE) pronucleotides of AZT and ddU were shown to possess superior anti-HIV activities in TK deficient cells when compared to their otherwise inactive parent nucleosides.[96, 97] Similarly, bis(DTE)PMEA also displayed a higher anti-HIV activity in different cell lines when compared to PMEA, which was attributed to the enhanced cellular uptake and release of the desired phosphonate (PMEA).[96] Compared to the related bis(SATE) pronucleotides of AZT, AZT bis(DTE) pronucleotides generally display reduced cellular anti-HIV activities.[89, 90]

A major concern relating to the application of SATE and DTE in the design of pronucleotides is the potential toxicity of the released ethylene sulfide.[65, 70, 78] While there have been no known studies to address this issue in humans, intracellular release of ethylene sulfide does not seem to induce additional toxicity in cells treated with SATE or DTE ester pronucleotides.[97]

Scheme 1-3. Mechanism of activation of S-acylthioethyl (SATE) (A) and dithioethanol (DTE) ester (B) pronucleotides.

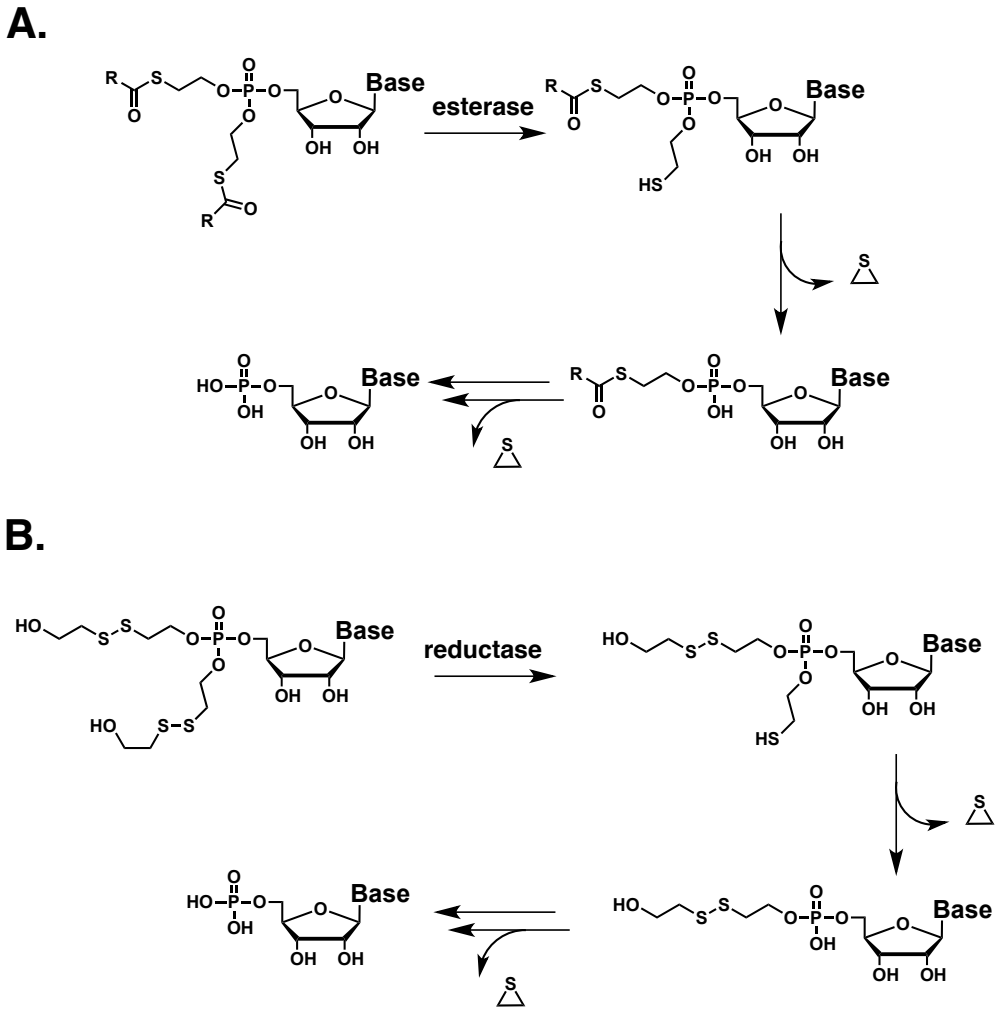

iv. *Cyclosaligenyl (cycloSal) Ester*

Unlike most pronucleotide strategies that utilize enzymes as a means of intracellular activation/release of nucleotides, the cycloSal pronucleotide strategy was designed to strictly undergo chemical processing/hydrolysis for intracellular delivery of nucleotides.[98] The cycloSal strategy takes advantage of the difference in rate of chemical hydrolysis between phenyl (more reactive) and benzyl (less reactive) esters of phosphates in aqueous environments. By employing salicyl alcohol as a protecting group, a cycloSal ester possesses both benzyl ester and phenyl ester characteristics. Hydrolysis of cycloSal ester pronucleotides is initiated by nucleophilic attack (S_NP) at the phosphate, which hydrolyzes the phenolic phosphate ester to form a 2-hydroxybenzyl phosphate diester intermediate (**Scheme 1-4A**). The strongly electron donating 2-hydroxyl induces cleavage of the benzyl ester intermediate to release the desired nucleotide and 2-quinone methide, which is quenched by water to generate a nontoxic salicyl alcohol.[99, 100]

CycloSal esters are stabilized by electron-donating substitutions at the 3- and/or 5-positions, while electron-withdrawing substitutions at the 5- or 6 positions lead to a more chemically reactive trimester.[98] The combination of both activating and stabilizing substitutions identified 3,5-di-*tert*-butyl-6-fluoro-cycloSal as an optimal configuration for effective release of nucleotides in cells. This optimized cycloSal scaffold also has the added benefit of being non-inhibitory to human acetylcholine esterase (AChE) and butyrylcholine esterase (BChE).[101] The rate of hydrolysis of cycloSal ester pronucleotides has also been observed to vary for a pair of phosphate diastereomers. Such differences in

the rate of activation usually translate to differences in the cellular antiviral activity, where the more stable diastereomer typically displays superior cellular activity.[99, 102]

The cycloSal pronucleotide strategy has been applied for intracellular delivery of nucleotides such as d4TMP, ddAMP, and AZTMP. CycloSal-d4TMPs displayed similar anti-HIV activities as d4T in wild-type CEM cells and were about 180-fold more potent than d4T against HIV replication in CEM/TK$^-$ cells.[99] More impressive was the over 1000-fold enhancement in anti-HIV activity in TK deficient cells of these cycloSal-d4TMPs when compared with AZT. Application of cycloSal for intracellular delivery of ddAMP yielded chemical entities with over 100-fold improvement in anti-HIV activity with concomitant improvements in selectivity indices when compared to ddA.[100] Further application for delivery of 2′-F-*ara*-ddAMP produced pronucleotides with about ten-fold higher anti-HIV activity than the parent nucleoside.[103] Moreover, cycloSal-F-*ribo*-ddAMPs were shown to confer anti-HIV activity to an otherwise inactive 2′-F-*ribo*-ddA.[103] Extension of the cycloSal strategy for cellular AZTMP delivery yielded compounds that were nearly equipotent to AZT in HIV-infected wild-type CEM cells.[104] However, these cycloSal pronucleotides were mostly inactive in HIV-2 infected CEM/TK$^-$ cells (EC_{50} was between 7 μM and >100 μM).[104] This loss of activity in TK deficient cells was reasoned to be as a result of the inefficient metabolism of AZTMP to AZTDP. When applied for delivery of phosphonates such as PMEA, cycloSal-PMEA showed modest improvements in antiviral activity compared to PMEA (3.0 – 5.0 μM vs 10.0 μM).[105]

Although initially developed to be strictly dependent on chemical activation, later generations of cycloSal pronucleotides were developed to incorporate a "lock-in" functionality.[98] The "lock-in" feature incorporates (carboxy)esterase-labile substitutions, which upon hydrolysis generates an anionic intermediate which becomes trapped inside cells and facilitates better accumulation of pronucleotides inside cells (**Scheme 1-4B**). Subsequent cleavage of the cycloSal releases the intended nucleotides intracellularly. As a proof-of-concept, the intracellular delivery of d4TMP resulted in over a 100-fold superior anti-HIV potency in TK deficient CEM cells compared to the parent nucleoside.[106] In addition, these "lock-in" cycloSal pronucleotides also retained anti-HIV activity in wild-type CEM cells.[106]

Another application of the "lock-in" functionality has been reported for third-generation cycloSal, whereby a highly unstable aldehyde-substituted cycloSal intermediate is generated upon esterase hydrolysis of lipophilic ester protecting groups.[107] The highly unstable intermediate leads to rapid intracellular release of a charged phosphodiester intermediate (**Scheme 1-4C**).[107] Application of this concept for delivery of d4T in HIV-infected cells yielded compounds that were equipotent against HIV-1 and HIV-2 in CEM/0 cells, while also displaying improved anti-HIV activity in CEM/TK$^-$ cells when compared to the parent nucleoside (EC_{50} were between 3.0 – 10.5 μM vs 47.5 μM).[107] Nevertheless, despite the numerous examples of cycloSal pronucleotides described in the literature for *in vitro* delivery of nucleotides, examples of their application for *in vivo* nucleotide delivery have yet to be reported.

Scheme 1-4. Mechanism of activation of cyclosaligenyl (cycloSal) ester pronucleotide and its "lock-in" derivatives.

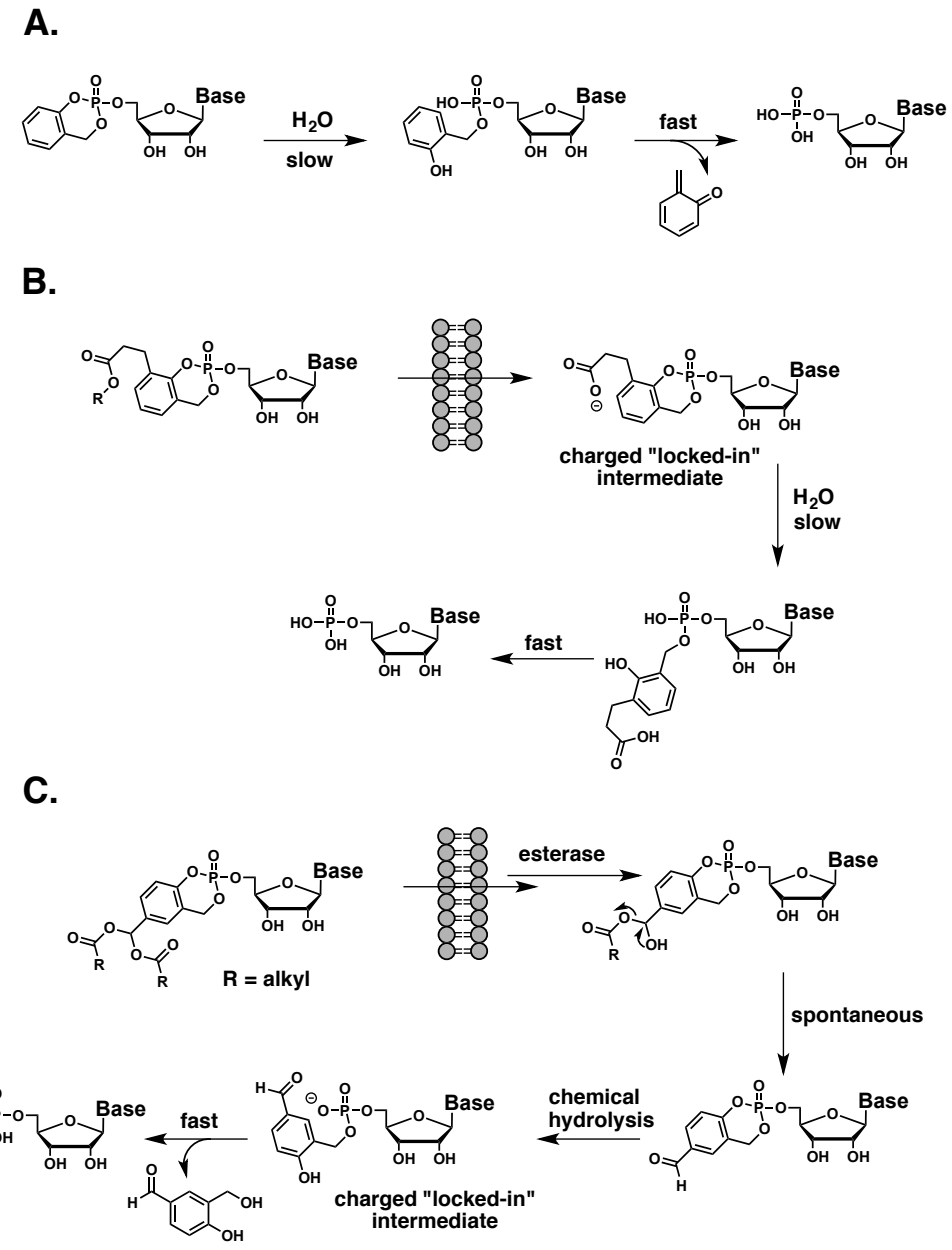

v. *Cyclic 1-Aryl-1-3-propanyl Ester (HepDirect)*

Extracellular enzymatic activation of pronucleotides reduces the levels of circulating intact pronucleotides in the blood, which reduces the delivery and accumulation of intended nucleotides in tissues. In order to improve delivery of nucleotides to the liver, the HepDirect pronucleotide strategy was developed as a means to achieve exclusive metabolism of a pronucleotide in the liver.[108] The HepDirect pronucleotide strategy relies on CYP3A4-mediated hydroxylation at the C4 position to generate a chemically unstable intermediate, which undergoes a ring opening reaction to generate a phosphodiester intermediate (**Scheme 1-5)**. Subsequent β-elimination releases the intended nucleotide and an aryl vinyl ketone, which gets trapped by glutathione (**Scheme 1-5**). The HepDirect prodrug strategy was applied to araC and was shown to deliver araCTP primarily to the liver, with an approximately 120-fold difference in araCTP levels when compared to araC treated mice.[109] Application for delivery of PMEA in rats produced 15-fold more PMEA levels in the liver when compared to rats that were treated with adefovir dipivoxil.[110] Further evaluation in a phase 2 clinical trial showed superior targeted delivery to the liver of hepatitis B patients, when compared to patients who received adefovir dipivoxil.[111]

Scheme 1-5. Mechanism of activation of cyclic 1-Aryl-1-3-propanyl ester (HepDirect) pronucleotide.

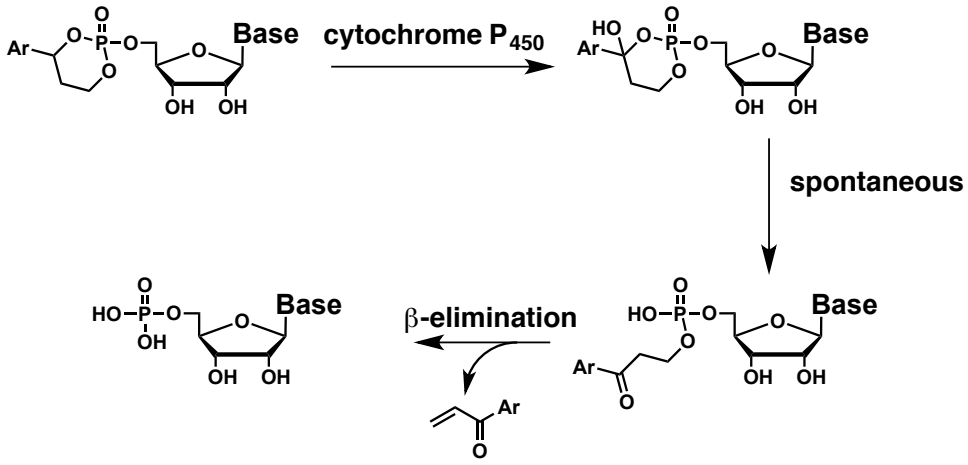

1.3.2b. Amidate-based Ester Pronucleotides

i. *Aryloxy Amino Acid Phosphoramidate (ProTide)*

Pioneered by C. McGuigan, the "ProTide" strategy utilizes ester- protected amino acids and *O*-aryl moieties as phosphate protecting groups. Activation of ProTides is initiated by esterase-catalyzed hydrolysis of the ester within the amino acid moiety (**Scheme 1-6A)**. The generated carboxylate then engages in an intramolecular nucleophilic attack at the phosphate, leading to elimination of the aryl group and generation of a 5-membered cyclic intermediate (**Scheme 1-6A**). Spontaneous hydrolysis of the 5-membered cyclic intermediate by water forms an amino acyl phosphoramidate. The amino acyl intermediate is hydrolyzed by a phosphoramidase, later discovered to be histidine triad nucleotide binding protein 1 (HINT1),[136] to release the desired nucleoside monophosphate.[112-114]

A crucial component of this activation cascade is the use of an α-amino acid, since proTides with simple amines are resistant to metabolic activation.[115] Only an α-amino acid can form the requisite 5-membered intermediate. SAR studies identified L-alanine as a preferred amino acid scaffold, while glycine was a surprisingly poor choice as a phosphate protecting group.[116] Cyclic intermediates larger than 5-membered systems (even as small as a 6-membered ring) are disfavored and only generate ester hydrolyzed intermediates, which cannot undergo further metabolism to release the intended nucleotide.[117, 118]

Aryl protecting groups have mostly been limited to phenyl and naphthyl groups whereby naphthyl-containing proTides are generally more active *in vitro* than phenyl-

containing analogs. This is presumably a result of their higher lipophilicity, hence better cellular permeation by naphthyl-containing proTides.[119] Of particular concern is the intracellular release of phenol and naphthanol, which could have associated toxicity.[120, 121] Recent use of *o*-methylbenzyl alcohol as a phosphate protecting moiety avoids release of such potentially toxic aryl by-products.[122] Activation of the *o*-methylbenzyl ProTide analog is initiated by esterase-catalyzed hydrolysis of the amino acid carboxylic ester to generate a stable amino acyl proTide intermediate. Subsequent hydroxylation at the benzylic position by liver P450 enzyme and hydrolysis generates the amino acyl monoester phosphoramidate and 2-methylbenzaldehyde (**Scheme 1-6B**). The phosphoramidate intermediate is hydrolyzed by HINT1 to release the intended nucleotide.[122] The liberated 2-methylbenzaldehyde is further metabolized to innocuous 2-methylbenzoic acid, which upon conjugation with glycine can be excreted as *o*-methylhippuric acid.[122]

Since its first description by McGuigan and co-workers for intracellular delivery of AZTMP,[79, 123] application of the proTide technology has been widely adapted for intracellular delivery of monophosphates of other anti-HIV nucleotides such as d4T,[124] abacavir,[125] and carbocyclic L-d4A derivatives.[126] Consistently, these examples demonstrated improved cellular activities when compared to the parent nucleosides. In particular, the AZT and d4T series were shown to retained anti-HIV activity in TK-deficient cells, whereas the parent nucleosides were inactive.[123, 124] In addition, proTide derivatives of acyclovir (ACV) have been prepared and were shown to be very potent agents against HIV-1 and 2 replication when compared to the otherwise inactive ACV.[127]

Further application for development of intracellular delivery of anti-HCV nucleotides has been excellently reviewed.[128]

Recently, such efforts have led to the development of PSI-7977 (sofosbuvir) (**Figure 1-7**),[129] which gained approval by the US Food and Drug Administration (FDA) for use in the clinic as a curative anti-HCV agent. Most importantly, evaluation of anti-HCV proTides in preclinical *in vivo* models consistently demonstrated the ability for liver targeted delivery of the desired nucleotide metabolites.[129] Another significant application of proTide technology has been in the development of GS-5734 as an anti-Ebola virus (EBOV) agent (**Figure 1-7**). GS-5734 was shown to have anti-EBOV activity in a rhesus monkey EBOV model after parenteral treatment.[130] Furthermore, the same report also reported that GS-5734 was approved for compassionate use in two cases of human Ebola virus disease (EVD), resulting in a complete cure of both patients.[130] GS-5734 is currently in phase 2 clinical trials.

Although less explored, application of the proTide technology towards delivery of antitumor compounds have been reported. Such examples have shown proTides derivatives of gemcitabine,[69] FUdR,[131] and BVDU[132] to be potent antitumor agents that still retain activity in cancer cells resistant to the respective parent nucleosides.

Application towards intracellular delivery of phosphonates have been reported for adefovir (PMEA) and tenofovir (PMPA).[133] The phosphonamidate proTides were shown to be activated in the same manner as phosphoramidate proTides.[133] Similarly, SAR around the amino acid moiety confirmed L-alanine methyl ester containing proTides to be the most active against HIV replication in various cell lines.[133] Further development of

the tenofovir derivative led to the discovery of GS-7340.[134] GS-7340 is a single diastereomer proTide with L-alanine isopropylester as a phosphonate protecting group (**Figure 1-7**). *In vitro* anti-HIV activity of GS-7340 in MT-2 cells was shown to be 1000-fold greater than tenofovir. Moreover, in an *in vivo* pharmacokinetic evaluation in dogs, GS-7340 had an oral bioavailability of 17% relative to intravenously administered tenofovir. Furthermore, GS-7340 produced superior tissue distribution when compared to the already FDA approved tenofovir disoproxil fumarate (tenofovir DF).[134] More recently, GS-7340 received regulatory approval and is administered as a tenofovir alafenamide fumarate (TAF) as an anti-HIV agent (**Figure 1-7**).[135]

Scheme 1-6. Mechanism of activation of aryloxy amino acid phosphoramidate (ProTide) (A) and its *o*-methylbenzyl derivative (B).

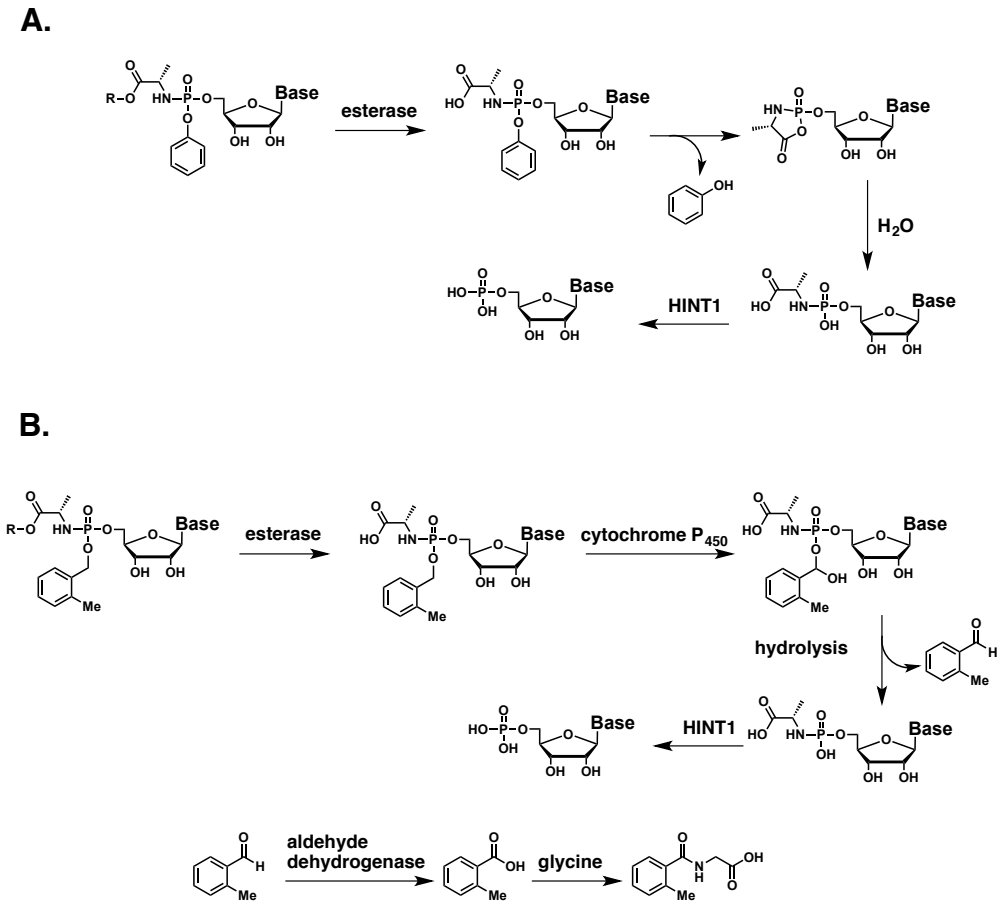

Figure 1-7. Chemical structures of antiviral ProTide-based pronucleotides.

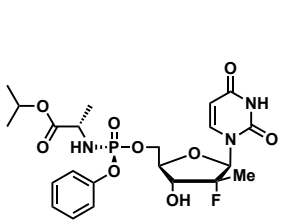

Sofosbuvir

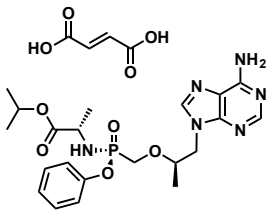

Tenofovir alafenamide fumarate

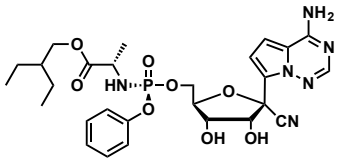

GS-5734

ii. *Amino Acid Monoester Phosphoramidate*

First described by Wagner and coworkers as a water soluble alternative to aryloxy amino acid phosphoramidates, monoester phosphoramidates lack an aryl phosphate protecting moiety and undergo P-N bond cleavage to release the intended monophosphate (**Figure 1-8**).[136-138] Subsequent work by Wagner and coworkers demonstrated for the first time that the intracellular hydrolysis of nucleoside monoester phosphoramidates P-N bond is catalyzed by HINT1.[137] Initial applications for intracellular delivery of monophosphates of AZT,[136, 139-141] FUdR,[142] and 3′-fluoro-3′-deoxythymidine (FLT)[141] established L-aromatic amino acid methyl ester phosphoramidate derivatives as potent and non-toxic anticancer and anti-HIV agents. Further SAR studies have shown that aromatic amine such as tryptamine is a tolerable substitute for L-aromatic amino acids.[138] In terms of their effectiveness as tools for intracellular delivery of nucleotides, the anionic nature of monoester phosphoramidates results in slow cellular uptake, with concomitant lower intracellular delivery of nucleotides compared to a phosphoramidate triester.[143] Moreover, monoester phosphoramidates have poor oral bioavailability due to their anionic nature.[143] However, parenteral administrations of monoester phosphoramidates have proved to be effective means for nucleotide delivery *in vivo*.[144, 145]

L-tryptophan methyl ester and phenylalanine methyl ester phosphoramidate monoesters of AZT were reported to be potent inhibitors of HIV-1 replication in CEM cell (EC_{50} = 3.5 nM and 1 nM, respectively).[140] This compared favorably to parent nucleoside AZT (EC_{50} <1 nM). Most importantly, the pronucleotides were far less toxic

when compared to AZT (>100 μM for both pronucleotides vs 14.2 μM for AZT). Furthermore, both phosphoramidate monoesters were shown to also be potent anticancer agents. When evaluated for anticancer activity, the most potent compound was the L-tryptophan methyl ester AZT phosphoramidate, which was cytotoxic to MCF-7 cells at 59 nM, while AZT was cytotoxic at 8 nM.[139] Such selective cytotoxic towards MCF-7 cells was reasoned to be a result of the over two-fold more intracellular levels of phosphorylated metabolites observed in MCF-7 cells compared to CEM cells.[139]

An L-alanine 2-propylpentyl ester monoester phosphoramidate of 2′-methylcytidine has also been prepared and shown to effectively deliver 2′-MeCTP in rat, dog, rabbit, human, hamster, and rhesus monkey hepatocytes.[145] Although not orally bioavailable, the compound was shown to deliver 2′-MeCTP in hamster rabbits after subcutaneous administration.[145]

Recently, tryptamine monoester phosphoramidates of 5′-mRNA cap analogs have been prepared and shown to be effective chemical tools for delivery of nucleotide inhibitors of eukaryotic translation initiation factor 4E (eIF4E).[146-148] Inhibition of eIF4E was shown to restore chemo-sensitivity in mesothelioma cells,[146] breast cancer cells,[147] as well as, reverse mesenchymal to epithelial transition (EMT) in TGF-β transformed mouse lung epithelial (MLE) cells.[148] These applications are a testament to the utility of this class of pronucleotides for *in vitro* and *in vivo* delivery of nucleoside monophosphates to cells and tissues.

Figure 1-8. Mechanism of activation of amino acid monoester phosphoramidate and structure of eIF4E pronucleotide inhibitor 4Ei-1.

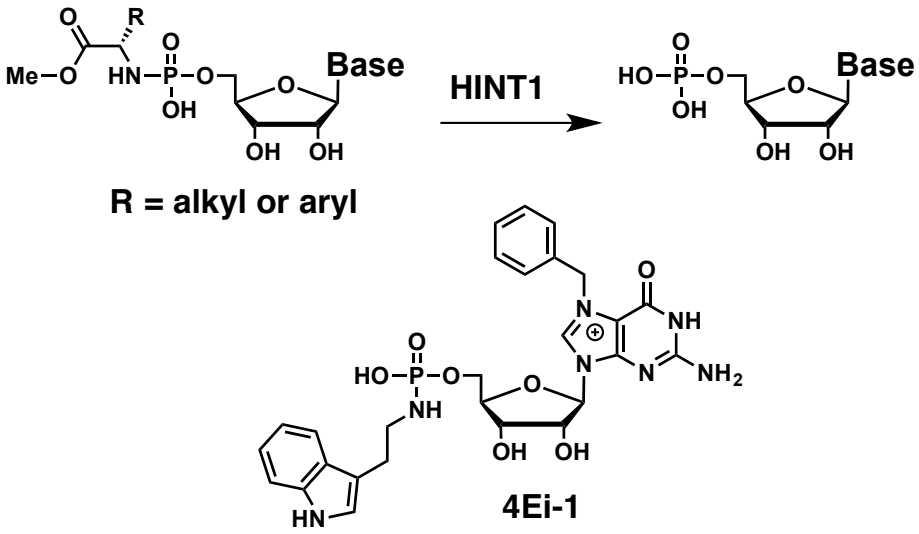

iii. *Phosphorodiamidate and Phosphonate diamidate*

This class of pronucleotides, pioneered by C. McGuigan, employs two amino acids esters as phosphate/phosphonate protecting moieties.[149] Compared to the proTide strategy, diamidate ester prodrugs are achiral at the phosphorus atom since the same amino acid serves as phosphate/phosphonate protecting groups. In addition, the release of nontoxic amino acids during prodrug activation/metabolism makes this class of pronucleotides an attractive alternative to pronucleotide systems such as the proTide and the POM/POC esters, which liberate potentially toxic byproducts during their activation/metabolism. Bioactivation of diamidate pronucleotides is initiated by an enzyme-catalyzed hydrolysis of the carboxyl ester of the amino acid moieties. The resulting carboxylate undergoes intramolecular nucleophilic attack at the phosphorus to hydrolyze one amino acid ester. The resulting five-membered cyclic intermediate becomes hydrolyzed by water to generate a monoester phosphoramidate intermediate. Subsequent hydrolysis of the monoester phosphoramidate by HINT1 leads to release of the desired nucleotide (**Scheme 1-7**).[150, 151]

Scheme 1-7. Mechanism of activation of phosphorodiamidate pronucleotide.

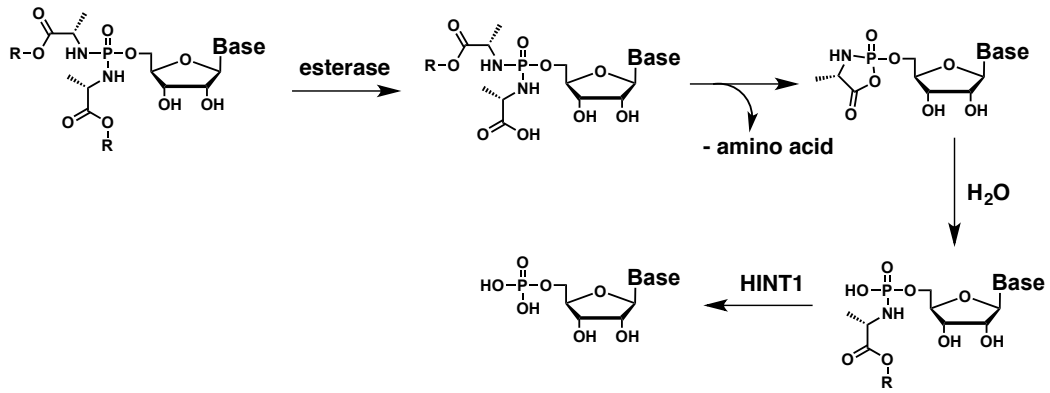

A series of diamidate ester prodrugs of AZT have been described. Although generally less active than AZT, these prodrugs were shown to be active against HIV-1 replication, with the bis(phenylalanine methyl ester) derivative showing the best antiviral activity (EC_{50} = 0.05 μM vs EC_{50} = 0.004 μM for AZT).[149] Application for delivery of monophosphorylated 2′-*C*-methyl-6-*O*-guanosine identified over 50 diamidate derivatives that were active in replicon assays against HCV replication, of which eight derivatives with EC_{50} values between 0.03 – 0.58 μM were selected for *in vivo* PK studies in rats.[150] Following oral administration in rats, the selected derivatives were shown to effectively deliver substantial levels of 2′-C-methylguanosine triphosphate in the liver, which was on par with liver triphosphate levels achieved with the proTide INX-189 (**Figure 1-9**).

Phosphonate diamidate prodrugs of PMEA have been prepared as inhibitors of orthopoxvirus replication. In this series of prodrugs, bis(butyl L-alaninyl PME-N6-(cyclopropyl)DAP (GS-8361) and bis(butyl L-alaninyl) PMEA (GS-8357) (**Figure 1-9**) were shown to be potent inhibitors of viral replication *in vitro*, with modest toxicity observed for GS-8361.[152] The antiviral activities of both prodrugs were comparable to that of adefovir dipivoxil and were far superior to their respective parent phosphonates.[152] A phosphonate diamidate prodrug of (phosphonomethoxyethyl)guanosine (PMEG), GS-9191 (**Figure 1-9**) was also reported to effectively deliver PMEG-DP in HPV infected cells.[153] Upon cellular uptake, GS-9191 is metabolized to 9-(2-phosphonylmethoxyethyl)-N^6-cyclopropyl-2-6-diaminopurine (crPMEDAP), which is deaminated to form PMEG.[153] The released PMEG undergoes two phosphorylation events to form the active metabolite,

PMEG-DP. Proof-of-concept studies with a rabbit model for HPV-induced lesions showed that as a topically applied agent, GS-9191 was curative and was superior to cidofovir.[153] GS-9191 has been reported to be undergoing clinical trials for treatment of lesions in HPV patients.[154]

Figure 1-9. Chemical structures of antiviral phosphonate diamidates pronucleotides.

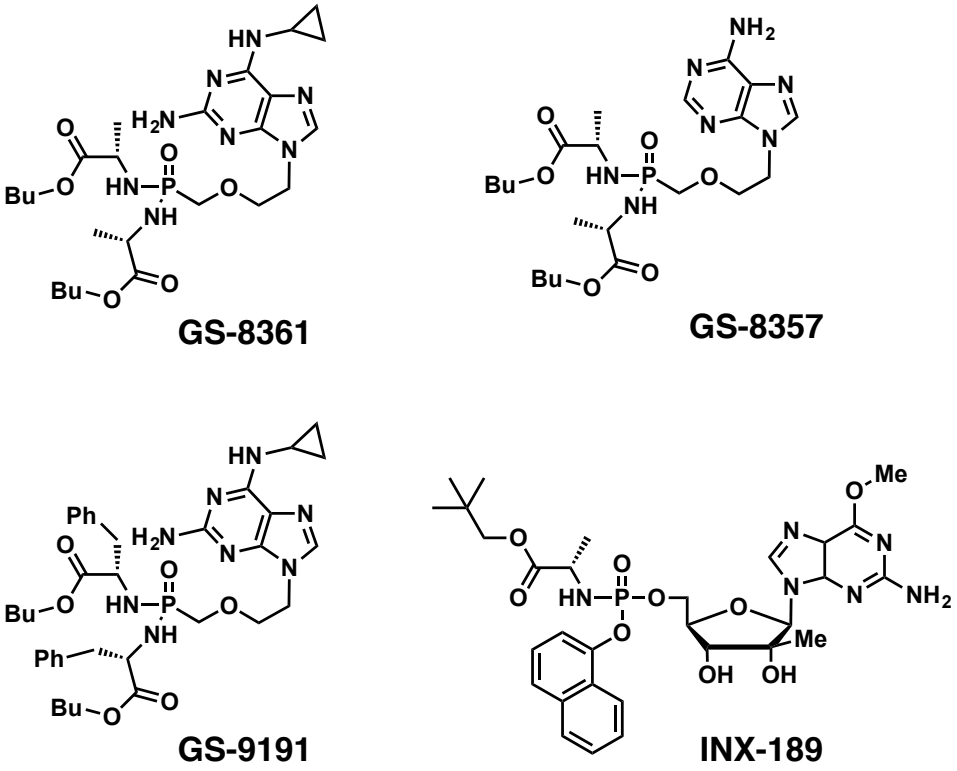

iv. *MonoSATE Phosphoramidate Ester*

The monoSATE phosphoramidate pronucleotide strategy incorporates design elements from both SATE and proTide systems (**Figure 1-10)**. Bioactivation of this class of pronucleotide involves initial enzyme-catalyzed ester hydrolysis to yield a thioethanol intermediate, which undergoes intramolecular nucleophilic attack at the α-methylene to release a monoester phosphoramidate intermediate. Hydrolysis of the ensuing monoester phosphoramidate by a phosphoramidase (likely HINT1) leads to formation of the desired nucleoside monophosphate (**Figure 1-10**).

First reported by Beltran and coworkers, application of monoSATE phosphoramidate for delivery of AZTMP was shown to be feasible.[155] In fact, a series of aliphatic amine derivatives were shown to be active against HIV replication in CEM/TK$^-$ cells whereas AZT was inactive in these cells.[155] Although examples of monoSATE phosphoramidate pronucleotides are scant in the literature, this prodrug class was successfully employed to develop a pronucleotide inhibitor of HCV replication. Developed by researchers at Idenix Pharmaceuticals Inc., IDX184 was shown to deliver levels of 2′-MeGTP in primary hepatocytes that was 30-40 fold greater than those formed by clinically relevant nucleosides such as 2′-methyl-2′-fluorocytidine, 2′-methylcytidine, and 4′-methyl-azido-cytidine.[156] IDX184 was also shown to produce high levels of 2′-MeGTP in the liver of HCV-infected chimpanzees upon oral administration.[157] Further evaluation in a phase 2 clinical trial was discontinued as a result of concerns about possible cardiovascular toxicity.[158]

Figure 1-10. Mechanism of activation of monoSATE pronucleotide and structure of antiviral pronucleotide IDX184.

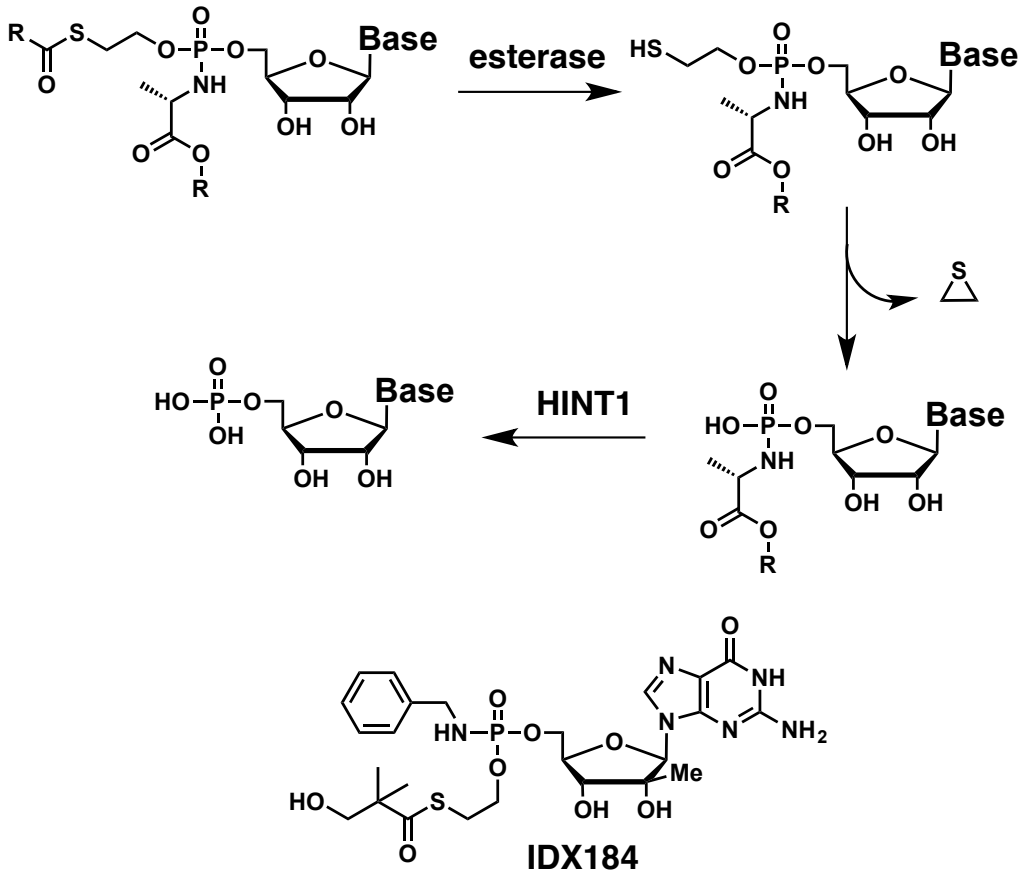

1.4. Thesis Statement

Over the decades, efforts at developing phosphate prodrug strategies have greatly expanded the utility of nucleoside analogs, both as chemical tools for basic research and as clinically relevant molecules for the treatment of diseases. Applications of various pronucleotide strategies as a means to improve the therapeutic indices of antiviral and anticancer nucleoside analogs are well documented in the literature. The recent FDA approval of sofosbuvir (ProTide of 2′-deoxy-2′-fluoro-2′-C-methyluridine) as the first curative antiviral is a testament to the immense impact this area of research has had on improving the quality of life of patients in the clinic. Such a high-profile success, however, can mask some of the shortcomings of the proTide strategy.

Drawbacks to the application of proTide technology includes excessive hepatic extraction during first pass metabolism, which can hamper efforts to deliver significant levels of monophosphates to tissues other than the liver. Furthermore, the requirement for initial bioactivation of proTides by carboxyesterases makes it challenging to define meaningful PK parameters in rodents (rats and mice) since these animals have high levels of circulating esterases in their blood. Moreover, the generation of a stereogenic phosphorus, in some cases, necessitates stereospecific synthesis of proTides, due to the discriminating substrate specificity by activating esterases for diastereomers.

These shortcomings can be directly attributed to the esterase-lability of proTides. Hence, as a means to further expand the utility of phosphate prodrugs, a major research focus of my research has been to develop pronucleotide strategies that address some, if not all, of the deficiencies inherent to the proTide system.

This thesis will detail our efforts at developing a new pronucleotide strategy that incorporates an initial chemical activation, followed by an enzymatic P-N bond hydrolysis. Chapter 2 describes the design principles of the proposed anchimerically activated pronucleotides and proof-of-concept application towards intracellular delivery of nucleotide inhibitor of eIF4E (a 5′-mRNA cap analog) as a chemical tool for translational control of protein synthesis. In chapter 3, I offer further proof-of-concept of the utility of this approach by developing an anchimerically activated pronucleotide of 2′MeG and demonstrate its utility for intracellular delivery of 2′-MeGMP as an anti-Dengue virus (DENV) agent.

Nucleoside monoester phosphoramidates have been shown to deliver nucleoside monophosphates in cells, albeit with slower uptake kinetics. The slow uptake kinetics is likely a result of the anionic nature of monoester phosphoramidates at physiological pH. To our knowledge, there has been no definitive investigation into the mode of intracellular uptake of nucleoside monoester phosphoramidates. To fill this gap in our knowledge about monoester phosphoramidate metabolism, I have set out to map the small molecule-protein *interactome* of nucleoside monoester phosphoramidates. Chapter 4 describes our work at developing phosphoramidate-based photo-affinity probes as chemical probes to define protein-binding partners of nucleotide monoester phosphoramidates. We envision that information obtained from this research will provide clues as to what protein, other than HINT1, are needed for cellular uptake and metabolic processing of nucleoside monoester phosphoramidates.

Finally, a description of our research at developing a nucleotide mimetic inhibitor of eIF4E will be presented in chapter 5. Nucleotide inhibitors of eIF4E could be subject to dephosphorylation by phosphatases such as 5′-nucleotidases. Such metabolic deactivation could diminish the cellular activity of the nucleotide inhibitors. As a proof-of-concept application, I have explored substituting the 5′-phosphate of a nucleotide inhibitor of eIF4E with a sulfamino alkyl diacid moiety, as a phosphate mimic. Chapter 5 will outline the design, synthesis, and biological evaluation of such a nucleotide-mimetic.

Chapter 2.

The following chapter contains published work from Okon, A.; Han, J. J.; Dawadi, S.; Demosthenous, C.; Aldrich, C. C.; Gupta, M.; Wagner, C. R. *J. Med. Chem.* **2017**, *60* (19), 8131-8144.

Anchimerically activated pronucleotides as inhibitors of cap-dependent translation and inducers of chemosensitization in mantle cell lymphoma

2.1. Introduction

Nucleoside and nucleoside analogs have proven to be important antiviral and anti-cancer agents. As antiviral and anti-cancer agents, nucleoside and nucleoside analogs rely on conversion by cellular kinases into the respective mono-, di-, and tri-phosphate nucleoside metabolites, which could then interdict viral replication or cancer proliferation.[152] A major drawback for nucleoside/nucleotide-based therapies lies in the activation pathway into the respective functional nucleotide metabolite(s). Specifically, the first phosphorylation step by a nucleoside kinase has been shown to be inefficient for many nucleoside analogs, because of the strict substrate specificity of nucleoside kinases.[152]

One could propose a direct administration of nucleoside analog monophosphates as a means to bypass the inefficient first phosphorylation step. However, such a strategy is impractical because of the highly polar nature of a nucleotide, which renders it impermeable to the cell membrane. In addition, nucleotides are metabolically unstable and are susceptible to dephosphorylation by cellular and plasma phosphatases. To bypass

the inefficient initial phosphorylation step, prodrugs of nucleoside monophosphates, referred to as ProTides have been developed.[152, 153]

Pronucleotides serve to mask the negatively charged phosphate backbone, thus ensuring passage though the cell membrane. Once internalized, the nucleoside monophosphate is typically released by enzymatic and/or chemical processes.[61, 70] The unveiled monophosphate can ultimately undergo multiple phosphorylation steps by cellular kinases to form the therapeutically active nucleotide(s). Kinase bypass strategies have been validated with a wide range of antiviral and anticancer nucleosides.[159, 160] Currently, the most clinically successful pronucleotide strategy involves nucleoside prodrugs containing the aryloxy amino acid phosphoramidate (ProTide) moiety (**Figure. 2-1A**).[123] Activation of ProTides are initiated by esterase hydrolysis of the amino acid ester, followed by spontaneous intramolecular nucleophilic attack at the phosphorus center to eliminate the aryl moiety.[112] The resulting cyclic intermediate is hydrolyzed by water to form the amino acid monoester phosphoramidate, which is ultimately enzymatically hydrolyzed by the intracellular nucleoside phosphoramidase, Histidine Triad Nucleotide Binding Protein 1 (Hint1) to yield the corresponding nucleoside monophosphate (**Figure 2-1A**).[107, 109]

Figure 2-1. Activation pathways for aryloxy amino acid phosphoramidate (ProTide) (A) and amino acid monoester phosphoramidate (B). (C) Proposed anchimerically activated pronucleotide strategy.

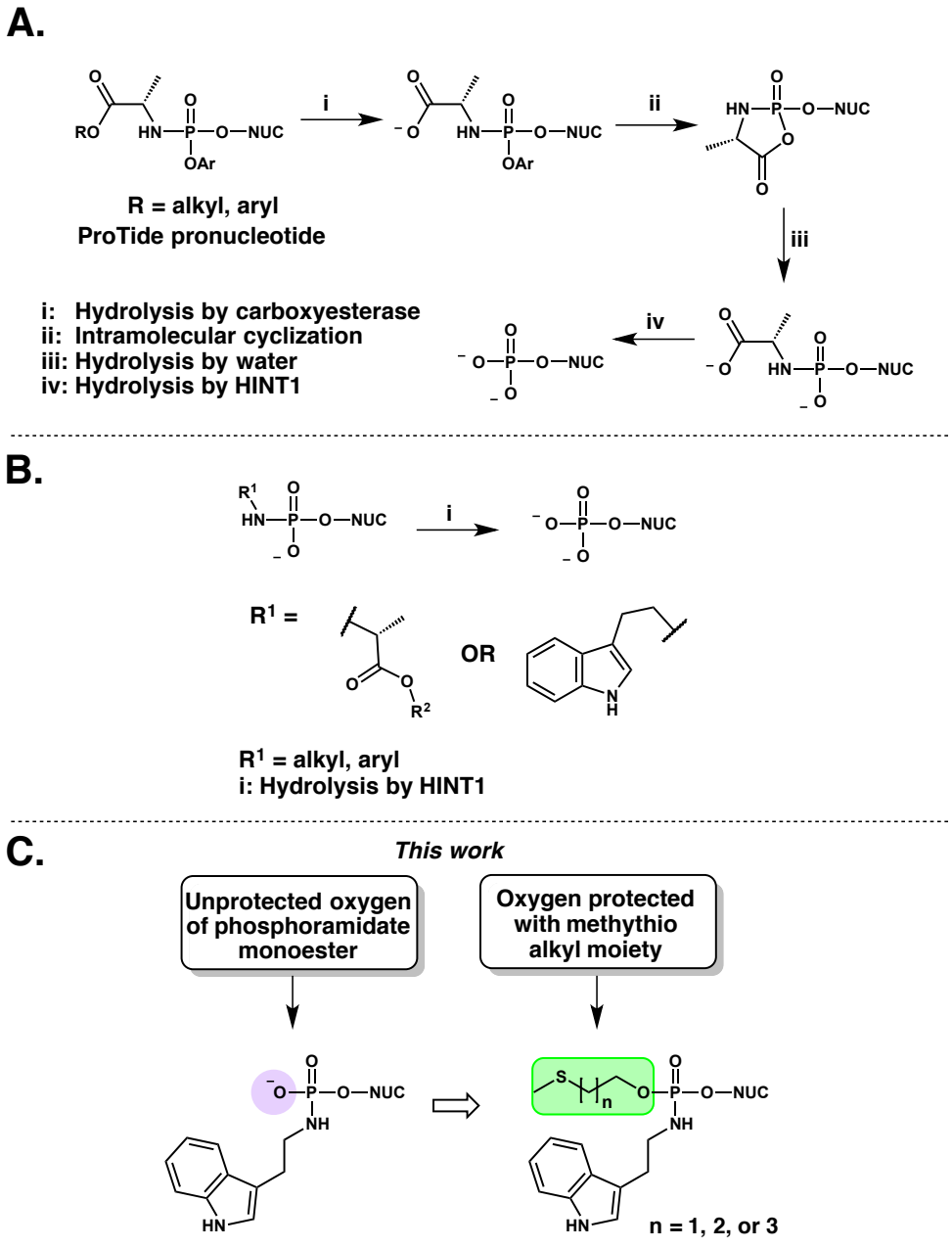

Although the ProTide technology has been widely adapted for delivery of nucleotides in cells, the first step of the activation of ProTides depends on the expression levels and stereospecific preference of intracellular esterases. Typically, one of the phosphorous stereoisomers of a ProTide displays significantly more potent biological activity than the other, thus requiring the development of a stereospecific synthesis of the preferred isomer.[129, 161, 162] In addition, ProTides have been viewed as liver targeting because the initial esterase hydrolysis occurs rapidly during first pass metabolism after oral dosing.[114, 163] Consequently, ProTides may not be that effective for delivery of significant amounts of monophosphate to tissues other than the liver. To further expand the utility of ProTides, we explored the development of a new prodrug approach that incorporates a chemically releasable thiomethyl ethanol moiety and Hint1 cleavable tryptamine phosphoramidate (**Figure 2-1C**). This approach offers an alternative to the ProTide approach, since the first activation step does not require enzymatic activation or carboxylate attack at the chiral phosphorous. The resulting monoester phosphoramidate can then undergo P-N bond hydrolysis by Hint1.

Amino acid nucleoside monoester phosphoramidates (**Figure 2-1B**) have been shown to undergo intracellular uptake and to deliver antiviral and anticancer nucleoside monophosphates.[164-169] These monoester phosphoramidates were shown to be water soluble, non-toxic and cell permeable *in vitro*.[167, 170] In particular, we have demonstrated that the monoester phosphoramidate, 4Ei-1 (**Figure 2-2**) is capable of undergoing cellular uptake to deliver the eIF4E selective antagonist, 7-BnGMP.[166] Treatment of tumor cells with 4Ei-1 has demonstrated that eIF4E is critical in epithelial to mesenchymal transition

(EMT).[148, 168] In addition, enhanced chemosensitization to gemcitabine and pemetrexed in mesothelioma, lung, and breast cancer cells has been shown to be dependent on eIF4E after treatment with 4Ei-1.[166, 169] Furthermore, 4Ei-1 has been used to demonstrate that eIF4E is necessary for the induced proliferation and expansion of both $CD4^+Foxp3^+$ and $CD4^+Foxp3^-$ T-cells, as well as T-cell subset identity.[171] While 4Ei-1 has been shown to be a useful probe of eIF4E function in cells, its low potency has hindered it from being used *in vivo*. The low potency of 4Ei-1 is likely due to the low affinity of 7-BnGMP for eIF4E (K_d = 0.8 μM)[168] and likely lower than expected cellular uptake of the zwitterionic monoester phosphoramidate. Consequently, we hypothesized that the development of a pronucleotide with greater membrane permeability and incorporating a more potent eIF4E antagonist would afford an enhanced chemical agonist of eIF4E.

Figure 2-2. (A) Chemical structures of nucleotide inhibitors of eIF4E and pronucleotide 4Ei-1. (B) Sulfur-mediated cyclo-deesterification of 4-(methylthio)-1-butyl protected oligonucleotide.

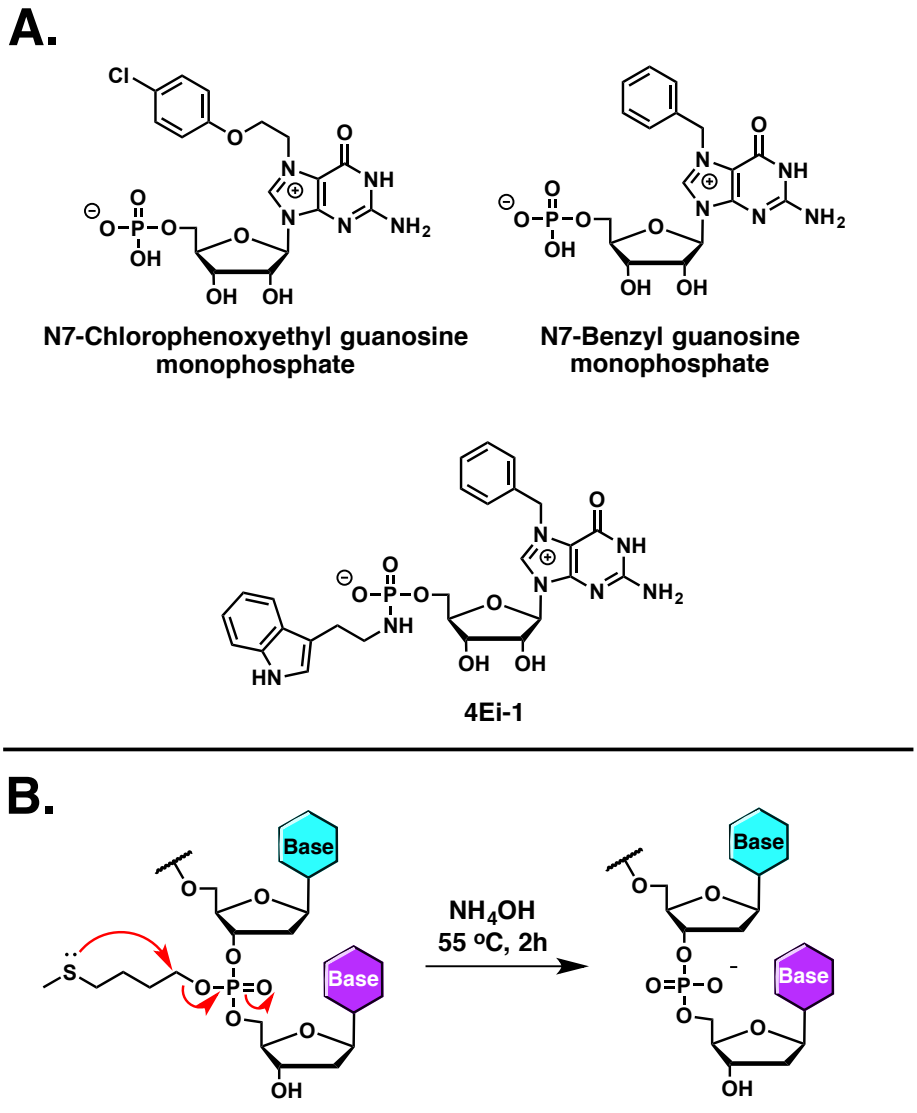

2.2. Results and Discussion

2.2.1. Design strategy for the proposed pronucleotide.

In an effort to improve the membrane permeability of nucleoside phosphoramidate monoesters, we chose to prepare nucleoside phosphoramidate diesters containing a methylthio alkyl moiety conjugated to the phosphoramidate oxygen (**Figure 2-1C**). Cieślak and coworkers had previously reported the use of methylthio alkyl protecting groups for the synthesis of oligonucleotides.[172] Unmasking of the phosphate oxygen is thought to proceed according to a sulfur-mediated intramolecular cyclo-de-esterification reaction (**Figure 2-2B**). Although the half-life for the deprotection reactions were fast at high temperatures (~ 115 s^{-1} – 225 s^{-1} at 55 °C), we reasoned that the half-life for deprotection of the methylthio alkyl moieties would be considerably slower under physiological conditions and thus sufficient to facilitate membrane permeability and intracellular uptake.

The recent discovery of N^7-(*p*-chlorophenoxyethyl)guanosine-5′-monophosphate (7-Cl-Ph-Ethyl-GMP)[173] (**Figure 2-2A**) as an inhibitor of eIF4E, presents an attractive substrate to develop a more potent eIF4E pronucleotide inhibitor compared to 4Ei-1. 7-Cl-Ph-Ethyl-GMP was found to have a greater than 200-fold affinity for eIF4E compared to 7-BnGMP.[173] Nevertheless, 7-Cl-Ph-Ethyl-GMP, was found to possess no cellular activity, likely due to its low cellular permeability.[173] Therefore, we chose to prepare tryptamine methylthio alkyl 7-Cl-Ph-Ethyl-GMP phosphoramidate pronucleotides to enhance the cellular potency of 7-Cl-Ph-Ethyl-GMP. This pronucleotide strategy adds to our previous work, which demonstrated that tryptamine nucleoside phosphoramidates are

excellent substrates for Hint1 and facilitates intracellular release of a nucleoside monophosphate.[132]

Aberrant eIF4E activity has been shown to cause malignant transformations in a variety of cells, and has been found to be a driver of tumorigenesis, disease progression, and poor survival rates in certain carcinomas of the breast, head and neck, acute and chronic myelogenous leukemias, colon, and non-Hodgkin's lymphomas.[174, 175] Consistent with these findings, several studies have shown that interdiction of eIF4E activity reduces tumorigenesis and resistance to apoptosis in certain carcinomas.[175, 176] eIF4E is highly expressed in 76% of diffuse large B cell lymphomas, which correlates with poor prognosis. In particular, patients with recurrent/refractory mantle cell lymphoma (MCL) have been shown to have significant failure-free survival (FFS) and overall survival (OS) upon modulation of eIF4E activity.[177, 178] These results were consistent with the finding that shRNA targeted eIF4E expression resulted in an ~80% reduction in colony formation in cancer cells.[179] Given the dependence of MCL on eIF4E, we chose to determine the uptake and biological activity of our new anti-eIF4E pronucleotide approach in MCL cells.

2.2.2. Chemistry

For preparation of our target compounds **6a-c**, we envisioned introduction of the methylthio alkyl moieties via 5′–*O* phosphonation using phosphonating agents such as **1a-c** (**Scheme 2-1A**). Such phosphonating agents were synthesized by treating the appropriate methylthio alcohol with diphenyl phosphite followed by aqueous workup and dichloromethane (DCM) washes. The phosphonating agents were then used without

further purification, after being judged to be of sufficient purity by ^{1}H NMR and ^{31}P NMR. The alkylating agent **2** was prepared by alkylation of *p*-chlorophenol with dibromoethane in the presence of sodium hydroxide. Alkylation of 2′,3′-*O*-TBS guanosine with **2** provided the N^{7}- alkylated product **4** in 30% yield. With the guanosine derivative **4** in hand, phosphonation of 5′-*O* was performed by treatment with phosphonating agents (**1a-c**) in the presence of pivaloyl chloride. The resulting *H*-phosphonate product was not isolated due to its propensity to degrade during silica column chromatography. Hence, we attempted a one-pot approach to install the tryptamine by employing Atherton-Todd[180] oxidation conditions. Reaction of the *H*-phosphonate intermediate with five equivalents of tryptamine under stringent anhydrous conditions gave only a 1:1 mixture of the desired tryptamine phosphoramidates **5a-c** and the phosphodiester side product (**Scheme 2-1B**). We reasoned that the oxygen source likely resulted from formation of a pivaloyl acyl-phospho mixed anhydride, formed during the Atherton-Todd oxidation in the presence of pivalic acid, followed by nucleophilic attack at the carbonyl center (**Scheme 2-1B**). Removal of pivalic acid by aqueous workup prior to Atherton-Todd oxidation was found to be beneficial and afforded the desired phosphoramidate **5a-c**, without significant amounts of the phosphodiester side products. Subsequent 2′,3′-*O* desilylation afforded the tryptamine phosphoramidate diester **6a-c**.

Scheme 2-1. (A) Preparation of *O*-(thiomethyl)alkyl-containing phosphoramidate pronucleotides (**6a-c**). (B) Putative mechanism for formation of phosphodiester side-product. (C) Synthesis of monoester phosphoramidate **7**.

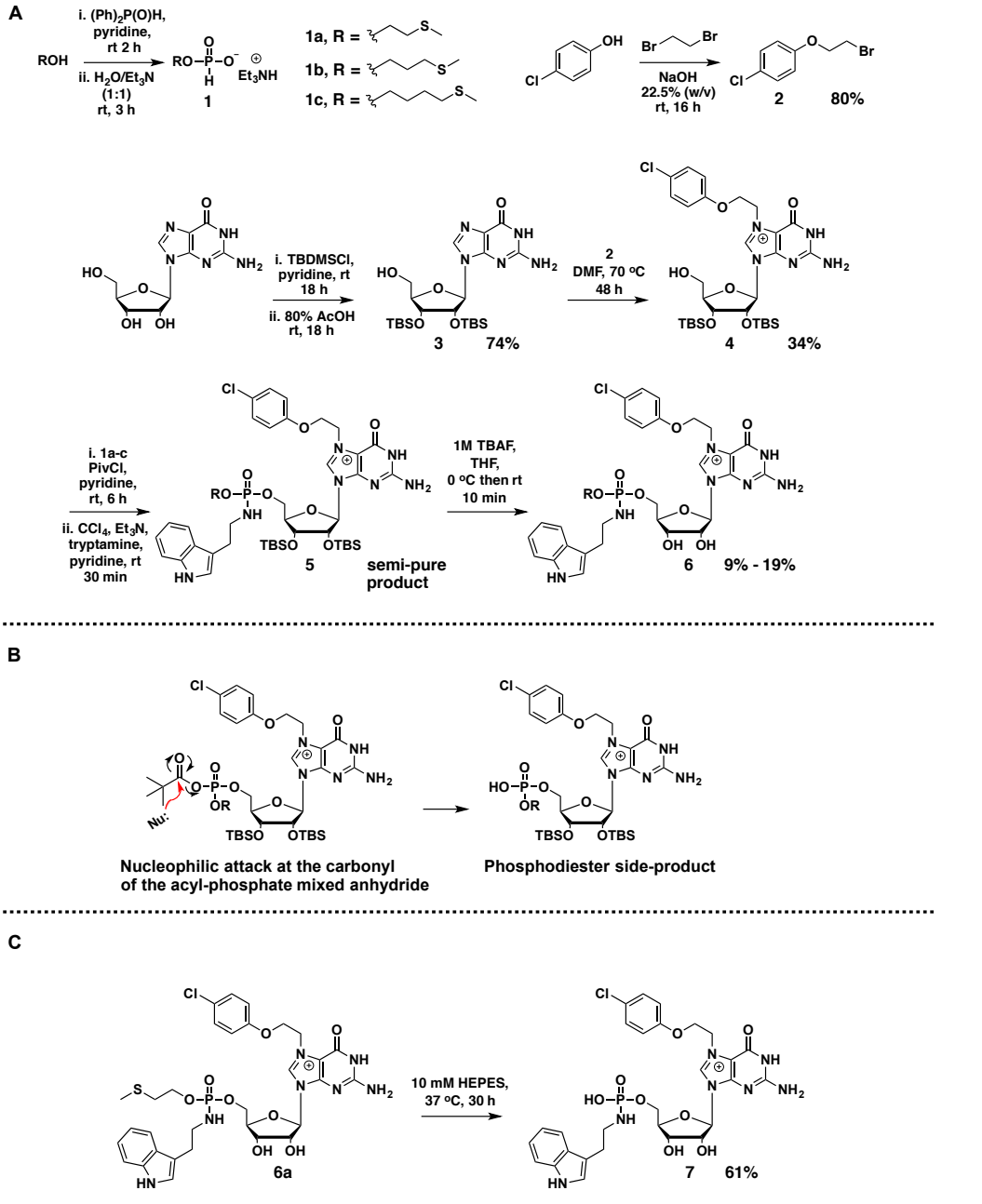

2.2.3. *In vitro* stability of methylthio alkyl pronucleotides

With the synthesized compounds in hand, we next examined the deprotection kinetics of the methylthio alkyl moieties in an aqueous environment. The compounds **6a-c** were incubated in HEPES buffer (pH 7.4, 37 °C) and the progress of the deprotection monitored by reverse phase high performance liquid chromatography (RP-HPLC) (**Figure 2-3**). The ethyl and butyl derivatives, **6a** and **6c** underwent significant deprotection under neutral conditions with half-lives ($t_{½}$) of 8.5 ± 0.9 h and 10.4 ±1.1 h, respectively (**Table 2-1**). In contrast, deprotection of the propyl derivative, **6b**, was found to have a half-life of greater than 60 h. The slow deprotection observed for **6b** under neutral aqueous conditions is likely due to the highly unfavorable ability of the 3-(methylthio)propyl moiety to form the necessary four-membered cyclic sulfonium species.[181, 182] Given the stability of the protecting groups under neutral conditions, we then assessed the kinetics of deprotection under acidic condition (HEPES buffer pH 2, 37 °C). Similar to neutral conditions, compounds **6a** and **6c** exhibited deprotection half-lives of 5.0 ± 0.4 h and 13.0 ± 2.5 h, respectively (**Table 2-1**).

Figure 2-3. Deprotection of methylthioalkyl protecting groups in 20 mM HEPES buffer (pH 7.2, 37 °C).

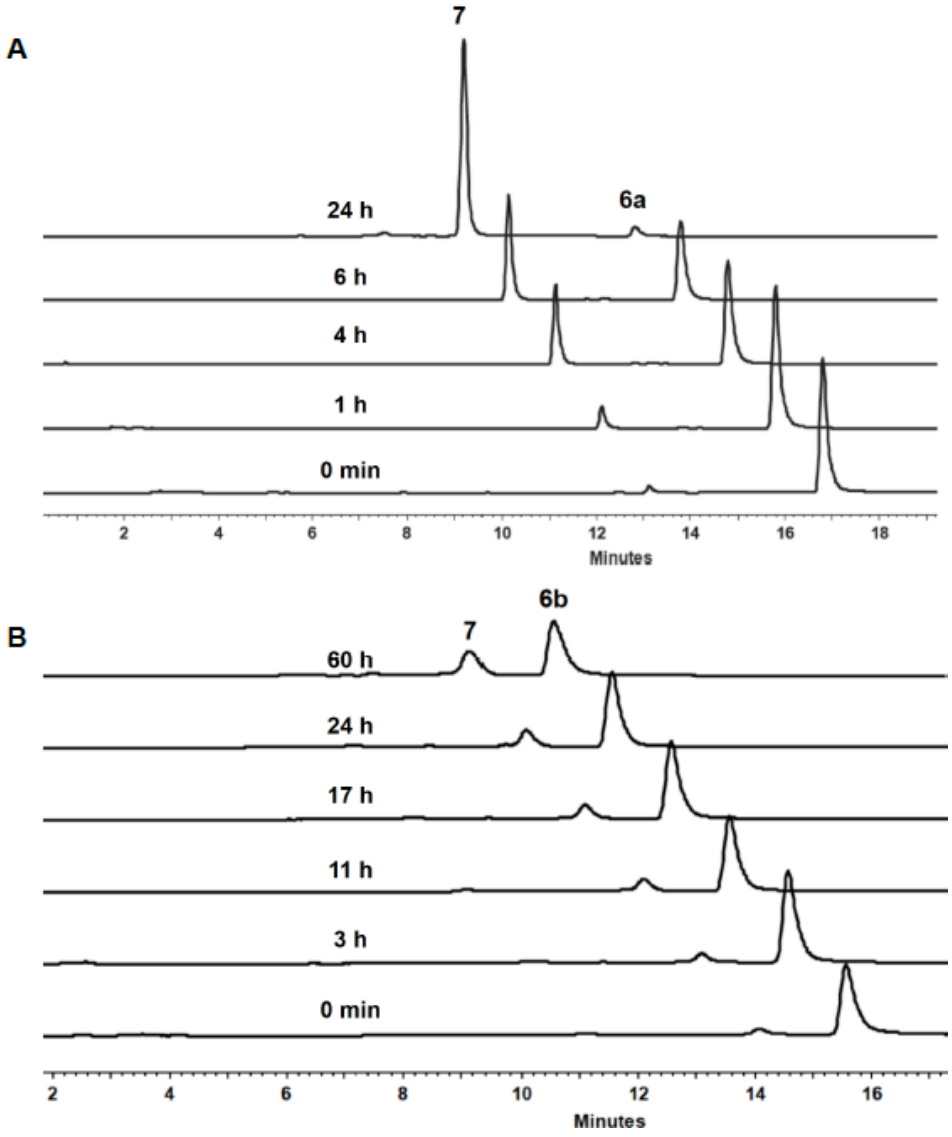

Table 2-1. Deprotection of thiomethylalkyl moiety from pronucleotides **6a-c**[a]

	$t_{1/2}$ (h)		
compd	HEPES (pH = 7.2)	HEPES (pH = 2.0)	Rat plasma (pH = 7.4)
6a	8.5 ± 0.9	5.0 ± 0.4	7.3 ± 1.5
6b	>60	ND	ND
6c	10.5 ± 1.1	13.0 ± 2.5	ND

[a]All data represent the mean (±SD) of triplicate experiments. ND, not determined.

Given the reasonably moderate stability of **6a** under both neutral and acid conditions, we further evaluated its half-life in rat plasma. Incubation of **6a** with rat plasma at physiological pH and 37 °C produced reasonable deprotection of the 2-(methylthio)ethyl moiety, with a half-life of 7.2 ± 1.2 h, which is similar to the 8.5 h ± 0.9 h half-life observed at pH 7.2. (**Table 2-1**) Consequently, we chose to determine the ability of **6a** to undergo cellular uptake and delivery of 7-Cl-Ph-Ethyl-GMP.

2.2.4. Cellular uptake and metabolism of 6a

Mantle cell lymphoma cells Granta 519, Mino, and Z138 were treated with **6a** and assessed after 12 hours for cellular uptake and formation of the corresponding monophosphate metabolite, using tandem liquid chromatography/mass spectrometry (LC-MS/MS). Upon cellular uptake of **6a**, we found that **6a** undergoes chemical deprotection to form the corresponding monoester phosphoramidate metabolite **7**, which is ultimately hydrolyzed by cellular HINT1 to form the monophosphate metabolite (**Figure 2-4**). LC-MS/MS analyses showed substantial accumulation of 7-Cl-Phe-Ethyl GMP in Mino cells (217.7 ± 29.6 pmol per 5 million cells) and Z138 cells (272 ± 14.2 pmol per 5 million cells). The observed amount of monophosphate metabolite in these cells was significantly greater than that observed after exposure to monoester phosphoramidate derivative **7** (**Table 2-2**). Furthermore, the observed amount of monophosphate (per 5 million cells) was significantly lower in Granta 519 cells - 10.3 ± 0.92 pmol (**Table 2-2**). Consistent with the significantly higher accumulation of monophosphate metabolite in Mino and Z138, we observed that these cell lines also had significantly higher intracellular amounts of monoester phosphoramidate **7** (**Table 2-2**). Taken together, **6a** increased the amount

of 7-Cl-Phe-Ethyl GMP in MCL cells relative to the corresponding phosphoramidate monoester **7**, from 520-fold (Z138 cells) to 1.9-fold (Granta 519 cells) (**Table 2-2**). It is not clear why within this set of MCL cells the delivery efficiency for 7-Cl-Phe-Ethyl GMP varies by over 250-fold. In relation to the mechanism of cellular uptake and release of the nucleotide, it is likely that intracellular release of 7-Cl-Phe-Ethyl GMP proceeds via Route A (**Figure 2-5**). Although, we cannot rule out some degree of uptake via extracellular activation, followed by uptake of the corresponding phosphoramidate monoester (**7**) (Route B in **Figure 2-5**), the low intracellular amounts of 7-Cl-Phe-Ethyl GMP observed in all the cell lines after incubation with monoester phosphoramidate **7**, suggests that the cellular uptake is dominated by Route A and not Route B (**Figure 2-5**).

Figure 2-4. Quantitation of intracellular amounts of 7-Cl-Phe-Ethyl-GMP and monoester phosphoramidate **7**.

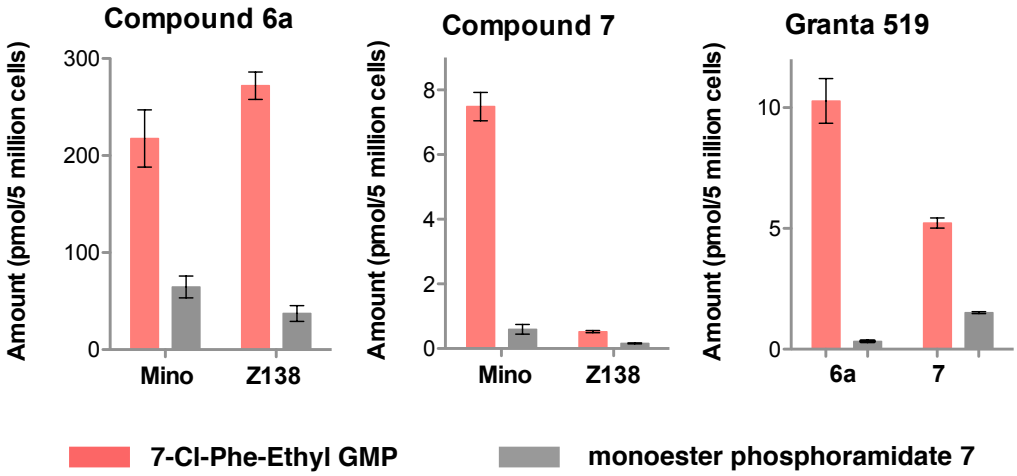

Table 2-2. Intracellular quantification of **7** and 7-Cl-Phe-Ethyl-GMP in MCL cells after exposure to **6a** and **7**[a]

compd	MCL cell line	**7**[b]	7-Cl-Phe-Ethyl-GMP[b]
6a	Mino	64.6 ± 11.3	218 ± 29.6
	Z138	37.3 ± 8.20	272 ± 14.2
	Granta 519	0.328 ± 0.02	10.3 ± 0.92
7	Mino	0.593 ± 0.15	7.49 ± 0.44
	Z138	0.163 ± 0.02	0.523 ± 0.03
	Granta 519	1.52 ± 0.04	5.23 ± 0.21

[a]All data represent the mean (±SD) of triplicate experiments.
[b]Intracellular amounts of metabolites is in pmol/5 million cells.

Figure 2-5. Proposed mechanism for cellular uptake and activation of **6a**.

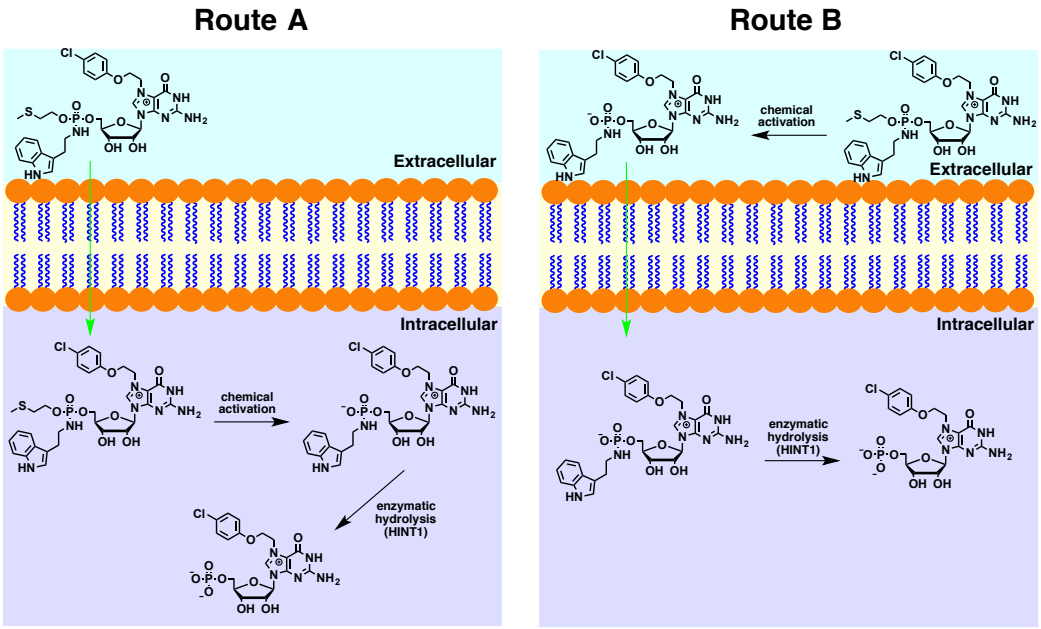

2.2.5. Biological activity of 6a.

With the confirmed enhanced intracellular delivery of 7-Cl-Phe-Ethyl-GMP by **6a** over **7**, we set out to assess the inhibition of eIF4E activity in MCL cells treated with **6a**. First, disruption of the interaction between mRNA 5′ cap and eIF4E was assessed by a 7-methylguanosine 5′-triphosphate (m^7 GTP) pull-down assay on lysates generated from MCL cells exposed to **6a**. The binding of free eIF4E was clearly blocked for cells treated with **6a**, compared to untreated MCL cells (**Figure 2-6**). These results are consistent with the results of our cellular uptake and metabolism studies demonstrating delivery of 7-Cl-Phe-Ethyl-GMP.

Due to the implication of eIF4E hyperactivation as a driver of lymphomagenesis,[183] we then assessed if **6a** was able to inhibit proliferation and reduce survival in MCL cells. MCL proliferation, as a measure of thymidine incorporation, was significantly reduced in a dose dependent manner by **6a** (IC_{50} = 50 μM, **Figure 2-6B**), with complete inhibition of proliferation observed at 200 μM. Surprisingly, with the exception of Z138 cells, survival of MCL cells was not significantly affected by **6a** (IC_{50} > 200 μM) when compared to untreated control (**Figure 2-6C**). The observed decrease in cellular proliferation after exposure to **6a** may result from reduced translation of pro-proliferative mRNA transcripts.

The transcription factor c-Myc is a known promoter of cell proliferation[184, 185] and its overexpression correlates with a negative prognosis in a variety of lymphomas.[186] Specifically, previous studies have shown that overexpression of c-Myc positively cooperates with eIF4E and other components of the eIF4F complex to drive translation in

lymphomas.[187-189] eIF4F is a protein complex consisting of eIF4E, eIF4G and RNA helicase eIF4A, of which eIF4E is the limiting component. To assess if translation of c-Myc in MCL was governed by eIF4E, we determined if eIF4E physically associates with c-Myc mRNA. RNA immunoprecipitation with eIF4E suggests that eIF4E does physically associate with c-Myc transcripts in MCL and that such association is much higher when compared to eIF4E association with the pro-survival Bcl-2 transcript (**Figure 2-7A**). This result suggests that eIF4E might be directly regulating translation of c-Myc in MCL. Indeed, MCL cell lines Mino and Granta, showed a dose dependent reduction in the expression levels of c-Myc and a dose dependent increase in p27 levels upon exposure to **6a**, with only a negligible effect on expression of Bcl-2 and Mcl-1 (**Figure 2-6D**). Furthermore, the observed reduction in the expression levels of c-Myc appears to be strictly due to reduced translation since the levels of c-Myc mRNA remain unchanged in Mino cells exposed to **6a**, compared to untreated control (**Figure 2-7B**). The observed dose dependent build-up of p27 in response to **6a** is interesting since it suggests protection against proteasomal degradation of p27, which is a hallmark in MCL. Reduced p27 expression correlates with poor overall survival rates and prognoses in MCL patients.[190] p27 is an inhibitor of cyclin-dependent kinase (CDK) and cyclin D1 is overexpressed in MCL.[190-192] Thus, the result suggests that **6a** causes an accumulation of p27, which could counter the abnormally high levels of cyclin D1 and elicit an anti-proliferative phenotype in MCL cells.

Figure 2-6. (A) m^7GTP pull-down assay of lysates generated from MCL cells treated with **6a**. Anti-proliferative (B) and anti-survival (C) activity of **6a** in MCL cells. (D) Effect of **6a** on expression of pro-proliferative and pro-survival proteins c-Myc and Bcl-2 in MCL cells.

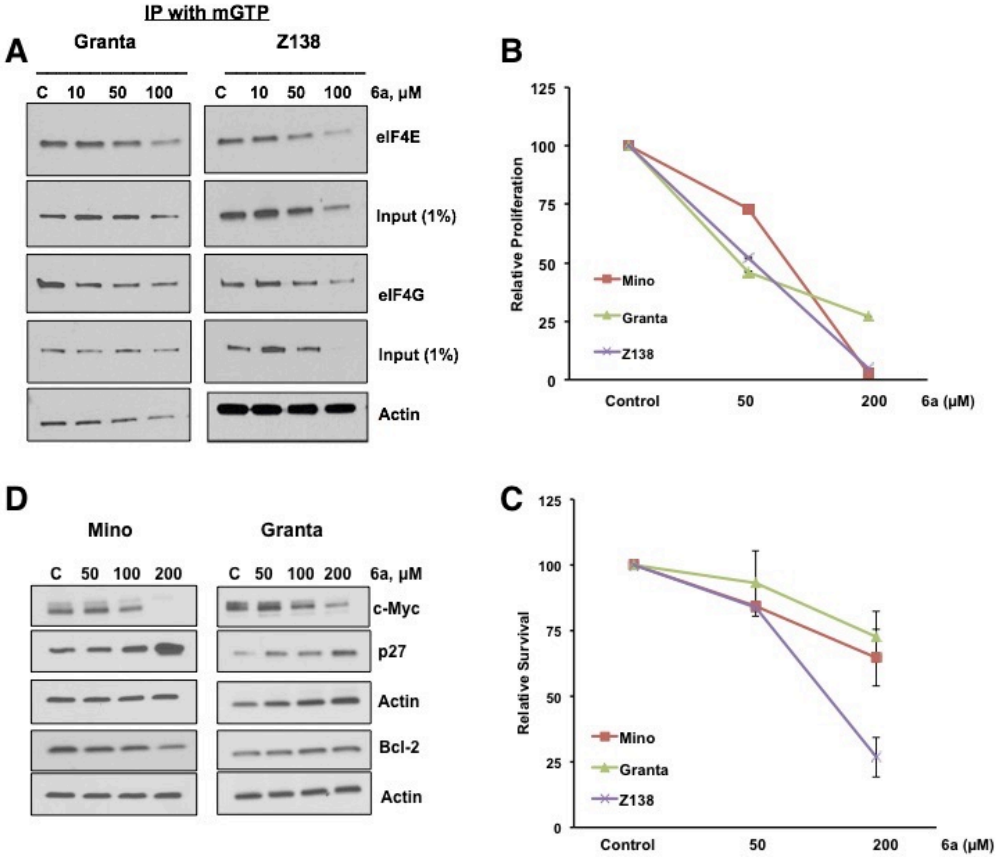

Figure 2-7. (A) RNA immunoprecipitation with eIF4E, c-Myc, Mcl-1, and Bcl-2 antibodies in Mino and Granta 519 cells. (B) Quantification of c-Myc, Mcl-1, and GAPDH mRNAs in Mino cells treated with 100 μM of **6a** (4Ei-10).

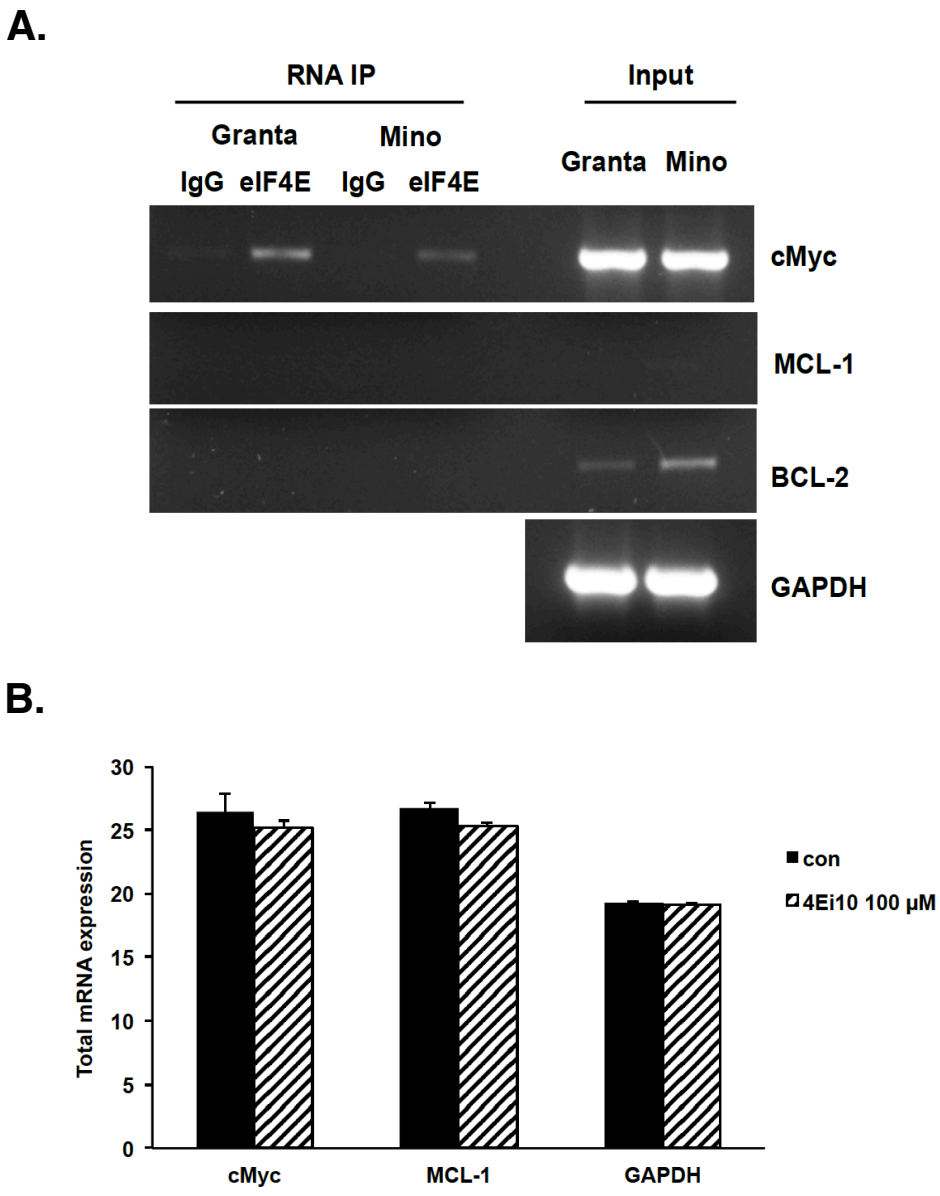

Mantle cell lymphoma is an aggressive B-cell lymphoma, largely resistant to traditional chemotherapy. Consistent with the effect of eIF4E antagonism on c-Myc, previous studies have reported that *Eμ-Myc/eIF4E* lymphomas are resistant to doxorubicin as a single anticancer therapy.[193] However, the observed chemoresistance in *Eμ-Myc/eIF4E* lymphoma mice was reversed when doxorubicin therapy was coupled with attenuated eIF4F activity.[193] Thus, we next assessed if chemoresistance in MCL cells can be reversed upon treatment with **6a**. Mino cells showed no reduction in proliferation when treated with doxorubicin alone compared to untreated control cells (**Figure 2-8A**). However, treatment with **6a** alone showed significant reduction in proliferation, which was further reduced when Mino cells were exposed to both doxorubicin and **6a**. The observed chemosensitization was significant ($p = 0.05$) when compared to untreated control cells, doxorubicin treated cells, or cells treated with **6a** alone (**Figure 2-8A**). Surprisingly, there was no significant impact on survival of Mino cells with the doxorubicin/**6a** combination treatment compared to untreated control cells, doxorubicin treated cells, or **6a** treated cells. We speculate that the observed resistance to apoptosis could possibly be a result of pro-survival signaling by Bcl-2, whose levels were relatively unchanged in Mino cells treated with **6a** (**Figure 2-6D**).

To assess if concomitant inhibition of eIF4E and downregulation of Bcl-2 is advantageous for reducing survival in Mino cells, we treated Mino cells with **6a** and dexamethasone. A previous study had shown that dexamethasone induced down regulation of Bcl-2 expression in acute lymphoblastic leukemia.[194] Combination treatment of Mino cells with **6a** and dexamethasone produced results that were similar to

that observed in doxorubicin/**6a** treated cells ($p = 0.05$). We observed an enhanced anti-proliferative response with dexamethasone/**6a** combination treatment when compared to untreated control, dexamethasone alone, or **6a** alone in Mino cells (**Figure 2-8B**). However, survival of Mino cells was little changed when compared to cells treated with **6a** alone or dexamethasone alone (**Figure 2-8B**). This result suggests the involvement of other molecular processes as drivers of Mino cell survival. However, we do not rule out the possibility that Mino cells are resistant to dexamethasone induced apoptosis or that dexamethasone does not induce down regulation of pro-survival Bcl-2 protein in Mino cells.

Figure 2-8. Chemosensitization of Mino cells treated with either a combination of (A) **6a** and doxorubicin, (B) **6a** and dexamethasone, or (C) **6a** and ibrutinib.

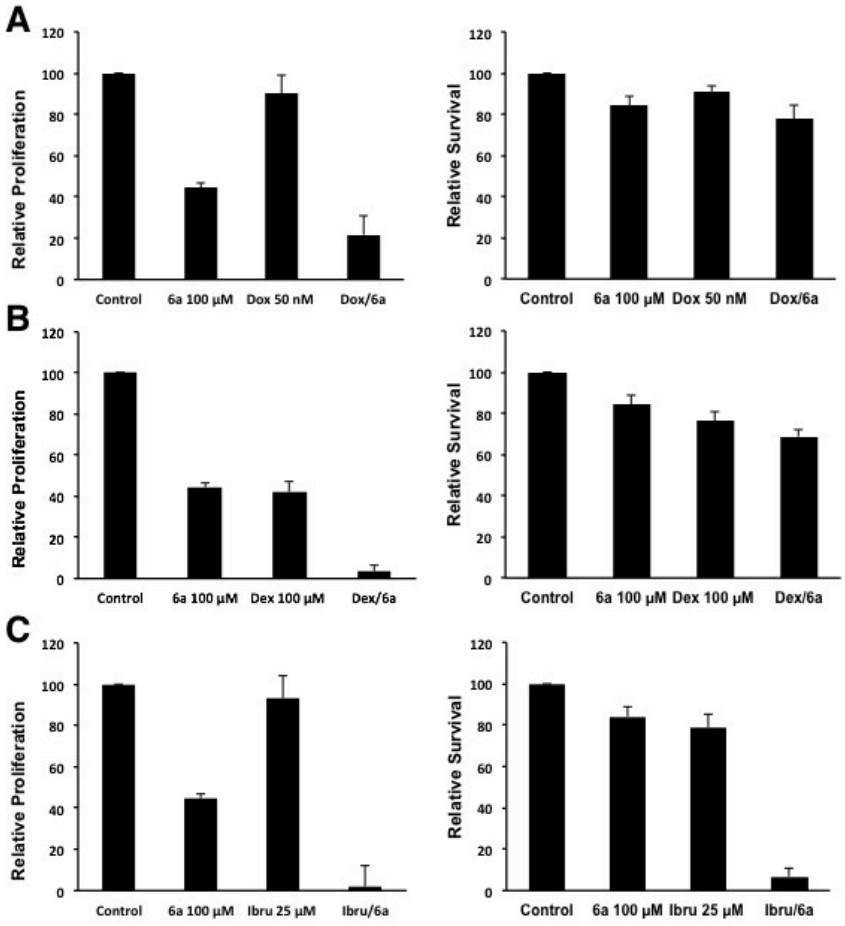

To further probe if downregulation of Bcl-2 and inhibition of eIF4E are sufficient to reduce survival in Mino cells, we elected to disrupt B-cell receptor (BCR) signaling through inactivation of Bruton tyrosine kinase (BTK). BCR signaling has been shown to be involved in activation of NF-κB pathway in MCL.[195, 196] NF-κB is a transcription factor that regulates expression of Bcl-2[197], which is overexpressed in MCL cells and primary tumors.[196] Recently, therapeutic inhibition of BCR/BTK pathway has entered the clinic for treatment of patients with recurrent MCL. Ibrutinib is a potent inhibitor of BTK and despite its approval as a single agent; many patients still acquire resistance to ibrutinib.[198] We next assessed if combination treatment of **6a** and ibrutinib could reverse chemoresistance in MCL cells. Mino cells were treated with ibrutinib (25 μM) in the presence or absence of **6a**, and proliferation and survival were analyzed. Mino cells showed no reduction in proliferation or survival when treated with ibrutinib alone compared to untreated control cells (**Figure 2-8C**). However, treatment with **6a** alone showed significant reduction in proliferation ($p = 0.05$), which was further reduced when cells were exposed to both ibrutinib and **6a**. Interestingly, the combination treatment also had a significant effect ($p=0.05$) on the survival of Mino cells (**Figure 2-8C**). We also evaluated the effect of ibrutinib alone or in combination with **6a** on c-Myc protein by western blotting. Interestingly both ibrutinib and **6a** reduced the level of c-Myc, but the combination treatment had a much more profound effect on the downregulation of c-Myc (**Figure 2-9**). Altogether, these results suggest that chemoresistance in MCL cells could be reversed through a combination of eIF4E inhibition and attenuation of BCR signaling. This is consistent with the previous report by Wu and coworkers, who showed that

simultaneous inhibition of BTK activity and MNK mediated phosphorylation of eIF4E elicited a strong apoptotic response in hematologic malignancies.[199]

Cap dependent translation initiation complex is negatively regulated by hypophosphorylated 4EBP1 protein. Several studies have shown that 4EBP1 is hyperphosphorylated in lymphoma patient samples and correlates with poor prognosis.[200, 201] Next, we sought to determine if the combination of **6a** and ibrutinib could reduce phosphorylation of 4EBP1 at both serine (Ser 65) and threonine sites (Thr 37/46).[202] Phosphorylation of 4EBP1 at Thr37/46 is regulated by mTOR and does not prevent its binding to eIF4E, but primes 4EBP1 for subsequent phosphorylation at Ser 65.[203] Compound **6a** alone did not have much effect on 4EBP1 phosphorylation at either site. However, ibrutinib alone was able to decrease 4EBP1 phosphorylation at Ser 65 without any change in phosphorylation at Thr 37/46. Interestingly the combination treatment reduced 4EPBP1 phosphorylation at only the Ser 65 site (**Figure 2-9**).

Figure 2-9. Effect on 4EBP1 phosphorylation in Mino cells treated with **6a**.

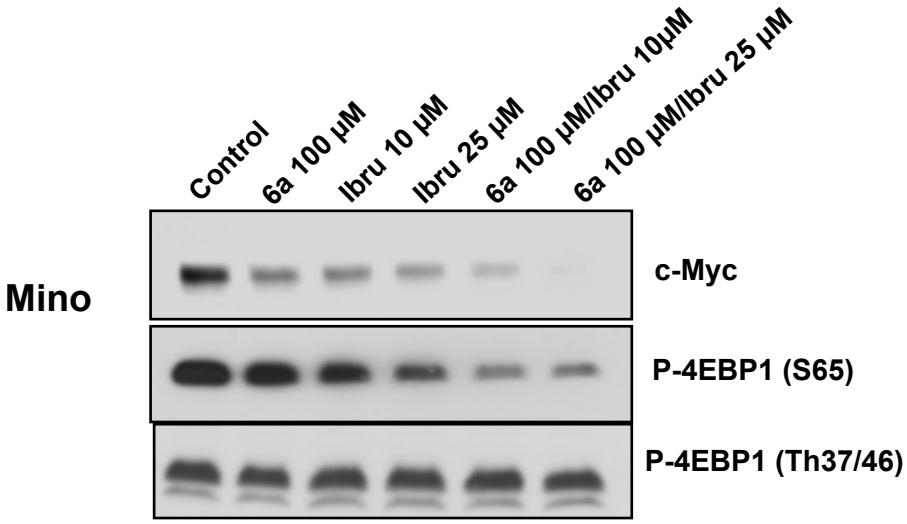

2.2.6. *In vivo* pharmacokinetic properties of 6a.

To assess the potential of our pronucleotide approach to enhance the bioavailability of the parent nucleoside phosphoramidate, we carried out pharmacokinetic (PK) studies of **6a** and **7** in female Sprague-Dawley rats (pharmacokinetic parameters of **6a** and **7** are summarized in **Table 2-3**). Quantitation of all metabolites was LC-MS/MS using N^7-(*m*-fluorobenzyl) guanosine-containing internal standards (**Scheme 2-2, Table 2-4**). After intravenous (*i.v.*) administration (2.5 mg/kg), **6a** exhibited biexponential kinetics with a rapid distribution phase followed by a slow terminal elimination phase resulting in an extremely large steady state volume of distribution (V_d = 205 ± 45 $L \cdot kg^{-1}$) (**Figure 2-10**). The high clearance of **6a** (1.8 ± 0.2 $L \cdot min^{-1} \cdot kg^{-1}$) indicates extra-hepatic metabolism since the clearance vastly exceeds rat hepatic blood flow (0.055 $L \cdot min^{-1}$) and is consistent with nonenzymatic cleavage of the methylthio-alkyl-protecting group to release **7**. The extensive tissue distribution of **6a** compensates for the rapid clearance resulting in a respectable half-life ($t_{½}$) of 79 minutes. The C_{max} of **6a** and **7** following oral (*p.o.*) dosing (25 mg/kg) of **6a** were 5.0 ng/mL and 6.0 ng/mL, respectively, which were achieved at 30 minutes. The oral bioavailability (*F*) of **6a** was 23% based on the combined $AUC_{0\text{-}8h}$ values of **6a** and **7**, which underestimates *F* since the levels of **6a** and **7** remained steady and did not decline at 8 hours. The parent nucleotide 7-Cl-Phe-Ethyl-GMP was not detected in the plasma after both oral and *i.v.* doses of **6a**, which further confirms the pronucleotide design strategy as phosphoramidate cleavage of **7** by Hint1 is expected to primarily occur in tissues. Given the highly polar (cationic) nature of the nucleoside, it is probable that a higher level of oral bioavailability and enhanced *in vivo*

life time will be observed with more nonpolar nucleosides.[204] To evaluate the impact of the methylthioalkyl protecting group in **6a**, we also performed analogous PK studies with phosphoramidate monoester **7**, which exhibited substantially lower oral bioavailability (F = <1%) affirming the importance of the methylthio-alkyl-protecting group. The volume of distribution and clearance of **7** were 3- and 6-fold lower than **6a**, respectively resulting in nearly a 2-fold reduced terminal elimination rate constant and corresponding 2-fold longer half-life. The oral exposure of **7** ($AUC_{0\text{-}8h}$ = 1.9 $\mu g \cdot min \cdot mL^{-1}$) was nearly identical to **6a** ($AUC_{0\text{-}8h}$ = 1.7 $\mu g \cdot min \cdot mL^{-1}$) because the 6-fold reduced clearance of **7** relative to **6a** was nearly perfectly offset by the 6-fold lower bioavailability of **7**. Direct *i.v* administration of **7** to rats provided substantially higher levels of this compound enabling detection of the parent drug 7-Cl-Phe-Ethyl-GMP ($AUC_{0\text{-}8h}$ = 13.1 $\mu g \cdot min \cdot mL^{-1}$, C_{5min} = 583 ng/mL) in plasma. Collectively, these results suggest that the pronucleotide strategy might offer sufficient protection from first pass hepatic extraction, thus making it possible to achieve systemic circulation of 2-(methylthio)ethyl and phosphoramidate monoester containing pronucleotides. Such feasibility could be especially attractive for the delivery of both pronucleotides to organs other than the liver.

Table 2-3. *In vivo* pharmacokinetic parameters **6a** and **7**, and AUCs of their metabolites after dosing **6a** and **7** in female Sprague Dawley rats (n = 3, mean ±SD).

Pharmacokinetic indices	7		6a		
	7	7-Cl-Phe-Ethyl GMP	6a	7	7-Cl-Phe-Ethyl GMP
Dose *i.v.*, *p.o.* (mg/kg)	2.5, 25		2.5, 25		
$AUC_{0\text{-}8h}$ (*p.o.*, $\mu g \cdot min \cdot mL^{-1}$)	1.9 ± 0.2	<LOQ	1.7 ± 0.3	2.6 ± 0.1	<LOD
$AUC_{0\text{-}8h}$ (*i.v.*, $\mu g \cdot min \cdot mL^{-1}$)	8.8 ± 2.2	13.1 ± 10.1	1.4 ± 0.2	0.5 ± 0.1	<LOQ
V_d (*i.v.*, $L \cdot kg^{-1}$)	70 ± 19		205 ± 45		
Cl (*i.v.*, $L \cdot min^{-1} \cdot kg^{-1}$)	0.3 ± 0.1		1.8 ± 0.2		
$t_{1/2}$ (*i.v.*, min)	163 ± 29		79 ± 14		
F (%)	<1		23 ± 4		

Figure 2-10. Plasma concentration of compounds **6a** and **7** after *i.v.* administration of **6a** (A), plasma concentration of compounds **6a** and **7** after *p.o.* administration of **6a** (B), plasma concentration of compounds **7** and **7-Cl-Phe-Ethyl GMP** after *i.v.* administration of **7** (C), and plasma concentration of compounds **7** after *p.o.* administration of **7** (D) in female Sprague-Dawley rats.

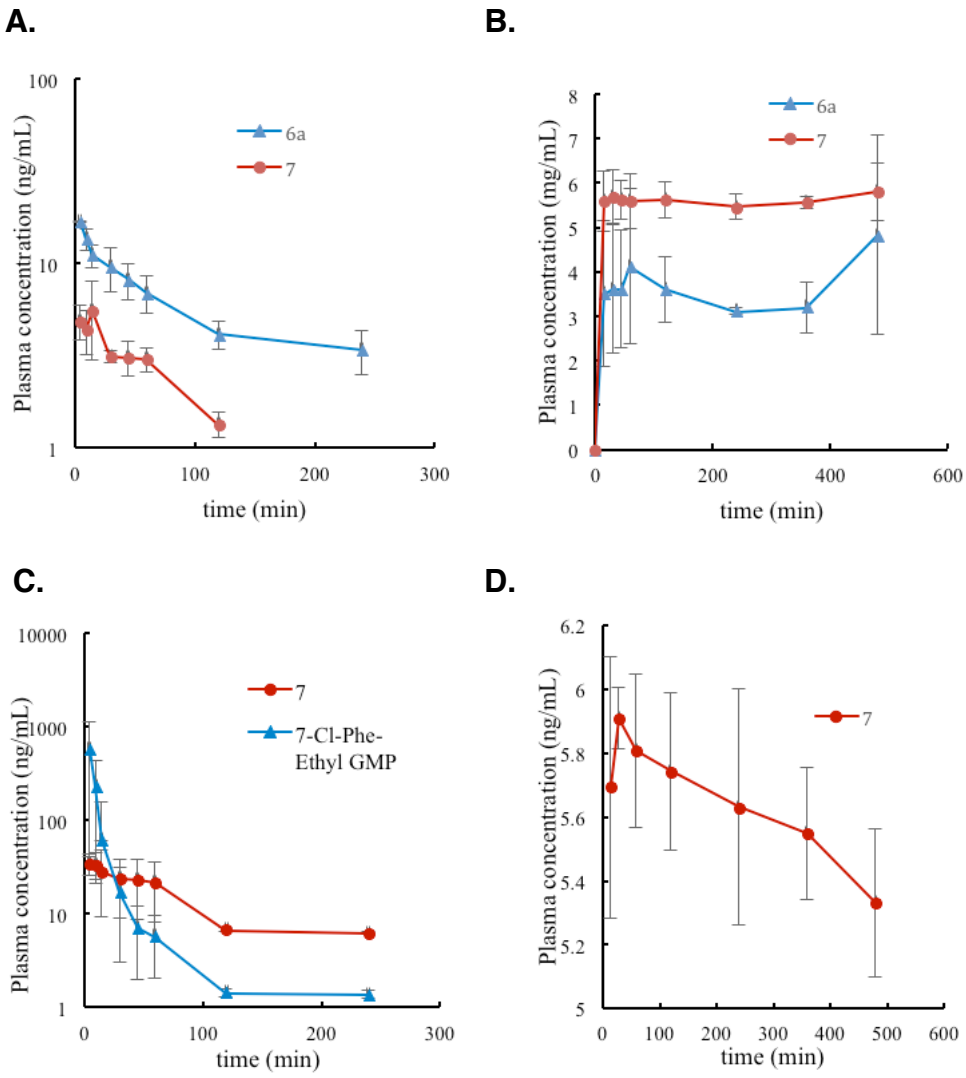

Scheme 2-2. Preparation of N^7-(*m*-fluorobenzyl) guanosine-containing internal standards

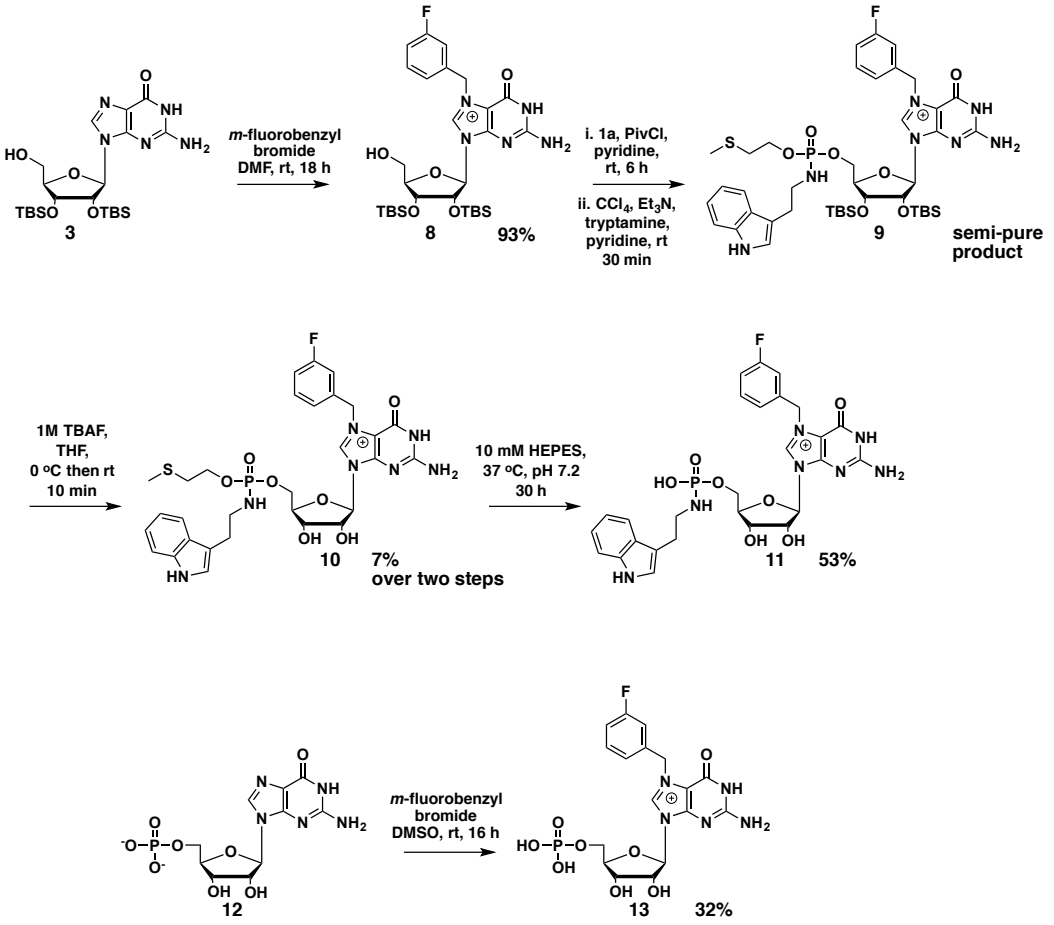

Table 2-4. Key fragmentation used for multiple reaction monitoring and retention times.

Compound	Precursor ion (m/z)	Product ion (m/z)	Retention time (min)	LOQ[a] (ng/mL)
6a	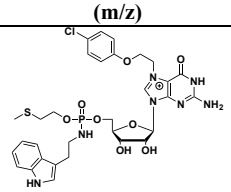 m/z = 734.2	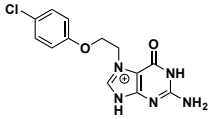 m/z = 306.1	3.36	2.9
7	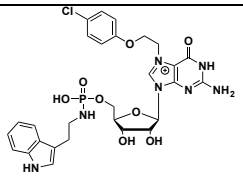 m/z = 660.2	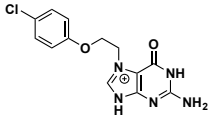 m/z = 306.1	3.11	1.3[b]
7-Cl-Phe-Ethyl GMP	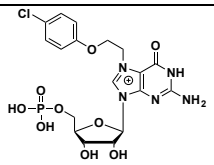 m/z = 518.1	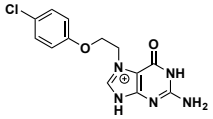 m/z = 306.1	2.48	1.4
Internal Standard-1	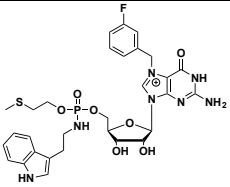 m/z = 688.2	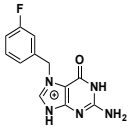 m/z = 260.1	3.20	
Internal Standard-2	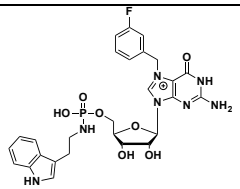 m/z = 614.2	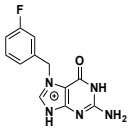 m/z = 260.1	2.81	
Internal Standard-3	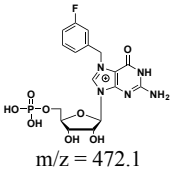 m/z = 472.1	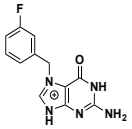 m/z = 260.1	2.00	

Declaustering potential (DP) = 35 V, Collision energy (CE) = 33 V.

[a]LOQ = (10 × stdev of lowest conc)/slope of calibration line.

[b]LOQ calculated based on signal to noise ratio (S/N) method.

2.3. Conclusions

Kinase bypass strategies have proven to be an effective means for delivering otherwise charged nucleotides in cells.[160, 205] The US Food and Drug Administration (FDA) approval of the phosphoramidate ProTide, sofosbuvir, for the curative treatment of HCV is a testament to the effectiveness/utility of bypass strategies to deliver clinically relevant nucleotide analogs into cells. Phosphoramidate diester ProTides, such as in sofosbuvir, mask the negative charge of the intermediate phosphoramidate monoester, thus enhancing their cellular uptake and potential for monophosphate delivery. Here, we have described the design and development of a pronucleotide strategy, which incorporates a chemically cleaved 2-(methylthio)ethyl moiety and an enzymatically cleaved tryptamine phosphoramidate as phosphate protecting groups. The incorporation of 2-(methylthio)ethyl as a phosphate protecting group eliminates the need for carboxyesterase-dependent activation. Furthermore, the new strategy was successfully utilized to generate **6a**, which exhibited efficient *in vitro* and in-cell activation to produce the parental nucleotide, 7-Cl-Ph-Ethyl-GMP, a potent inhibitor of eIF4E in cap-dependent translation. *In vitro*, **6a** was found to inhibit MCL cellular proliferation, without significantly affecting cell survival. It is possible that the inhibition of eIF4E activity induces cell cycle arrest similar to the effect observed with mTOR inhibitors rapamycin and PP242 in lymphoma.[183, 206] Work on this hypothesis is ongoing in our laboratory and will be reported in due time. The combination of doxorubicin, dexamethasone, or ibrutinib with **6a** demonstrated the ability to reverse chemoresistance observed in Mino cells that were treated with doxorubicin, dexamethasone, or ibrutinib

alone. Taken together, these results demonstrate that 2-(methylthio)ethyl phosphoramidate pronucleotides are capable of enhancing cellular delivery of monoester nucleoside phosphoramidates and the delivery of the corresponding nucleoside monophosphate. In addition, we have demonstrated that pharmacological abrogation of eIF4E:mRNA 5′-cap interaction could be an attractive anticancer strategy in mantle cell lymphomas. Most importantly, this work has established **6a** as a chemical tool, which is specific to eIF4E, for use in studying translational control in biological systems where aberrant cap-dependent protein translation leads to a disease phenotype.

2.4. Materials and Methods

General Methods and Materials

All chemicals and reagents were obtained from commercial sources and were used without further purification. Anhydrous *N*,*N*-Dimethylformamide (DMF) was obtained from a dry solvent purification system (MBraun) and dispensed under argon. Dexamethasone, doxorubicin, and ibrutinib were purchased from Sigma Pharmaceuticals. Antibodies for eIF4E, eIF4G, c-Myc, p27, p4EBP1, and Bcl-2 were purchased from Cell Signaling Technologies. Antibody to Actin was purchased from Santa Cruz (Dallas, TX, USA). All reactions were performed under an atmosphere of dry nitrogen unless otherwise noted. All silica gel chromatography and preparative reverse phase purification was performed on a Teledyne Isco CombiFlash Rf system, using Redisep Rf high performance gold silica gel columns (for normal phase purifications) and Redisep Rf high performance gold C18 columns (for reverse phase purifications). Reverse phase purifications were with water and acetonitrile. Lyophilization of compounds after reverse

phase purification was performed on a FreeZone 12 Plus freeze dry system (Labconco). All analytical HPLC analyses were performed on a Beckman Coulter System Gold instrument using a Haisil 100 C18 column (4.6 mm X 250 mm, 5 μm, Higgins Analytical Inc.); eluting with a gradient of 10% acetonitrile in phosphate buffer (50 mM, pH 7.4) to 90% acetonitrile in phosphate buffer over 24 minutes at a flow rate of 1.0 mL/min. The purity of all test compounds was determined with RP-HPLC and all test compounds were ≥95 % pure. All Nuclear Magnetic Resonance spectra were obtained on a Brucker Avance III HD 500 MHz spectrometer or on an Agilent/Varian 600 MHz spectrometer at ambient temperature. Chemical shifts were recorded in parts per million using the solvent peaks as internal references. All high-resolution mass spectroscopy (HRMS) were performed on an LTQ Orbitrap Velos instrument (Thermo Scientific) in positive-ion mode.

General Procedure for the Synthesis of Methylthio Alkyl H-Phosphonates Triethylammonium Salts 1a-c. Diphenyl phosphite (1 equiv) and anhydrous pyridine (10 mL) were added to an oven-dried round bottom flask and purged/evacuated extensively with N_2 under vacuum. To the mixture was added the appropriate methylthio alcohol and stirred for two hours at ambient temperature. Triethylamine/water (1:1, 6 mL) was added and the reaction was stirred for three hours at ambient temperature. The reaction was concentrated in vacuo at ambient temperature. The resulting oily residue was dissolved with water (10 mL) and washed with DCM (5 X 10 mL). The aqueous layer was concentrated in vacuo without heating, dried overnight on high vacuum, and used without further purification after being judged to be of sufficient purity by NMR spectroscopy (^{1}HNMR and ^{31}PNMR).

Triethylammonium 2-(methylthio)ethyl phosphonate (**1a**). The title compound was prepared from 2-(Methylthio)ethanol (0.76 mL, 8.74 mmol) using the general procedure for synthesis of methylthioalkyl *H*-phosphonate triethylammonium salts. The compound was obtained as a clear oil. ^{1}H NMR (500 MHz, DMSO-d_6) δ 1.18 (t, J = 7.5 Hz, 6H), 2.08 (s, 3H), 2.66 (t, J = 7.0 Hz, 2H), 3.04 (q, J = 7.0 Hz, 4H), 3.87 (q, J = 7.0 Hz, 2H), 6.64 (d, J_{PH} = 619.5 Hz, 1H), 10.32 (br s, 1H). ^{13}C NMR (125 MHz, DMSO-d_6) δ 8.4, 14.9, 33.7 (d, $J_{C\text{-}P}$ = 6.3 Hz), 45.3, 62.2 (d, $J_{C\text{-}P}$ = 4.6). ^{31}P NMR (202 MHz, DMSO-d_6) δ 2.28.

Triethylammonium 3-(methylthio)propyl phosphonate (**1b**). The title compound was prepared from 3-(methylthio)-1-propanol (0.90 mL, 8.75 mmol) using the general procedure for synthesis of methylthioalkyl *H*-phosphonate triethylammonium salts. The compound was obtained as a clear oil. ^{1}H NMR (500 MHz, DMSO-d_6) δ 1.17 (t, J = 7.5 Hz, 5H), 1.79 (quint, J = 7.0, 2H), 2.04 (s, 3H), ~2.50 (obscured by solvent peak), 3.04 (m, 4H), 3.83 (q, J = 6.5 Hz, 2H), 6.61 (d, J_{PH} = 625.0 Hz, 1H), 10.2 (br s, 1H). ^{13}C NMR (125 MHz, DMSO-d_6) δ 8.4, 14.6, 29.5, 29.7 (d, $J_{C\text{-}P}$ = 6.4 Hz), 45.4, 61.9 (d, $J_{C\text{-}P}$ = 4.6 Hz). ^{31}P NMR (202 MHz, DMSO-d_6) δ 2.69.

Triethylammonium 4-(methylthio)butyl phosphonate (1c). The title compound was prepared from 4-(Methylthio)-1-butanol (1.06 mL, 8.74 mmol) using the general procedure for synthesis of methylthioalkyl *H*-phosphonate triethylammonium salts. The compound was obtained as a clear oil. ^{1}H NMR (500 MHz, DMSO-d_6) δ 1.18 (t, J = 7.5 Hz, 5H), 1.59 (m, 4H), 2.03 (s, 3H), 2.47 (t, J = 7.0 Hz, 2H), 3.04 (q, J = 7.0 Hz, 4H), 3.74 (q, J = 6.0 Hz, 2H), 6.59 (d, J_{PH} = 614.5 Hz, 1H), 10.23 (br s, 1H). ^{13}C NMR (125

MHz, DMSO-d_6) δ 8.5, 14.6, 25.0, 29.3 (d, $J_{C\text{-}P}$ = 6.8 Hz), 32.8, 45.4, 62.6 (d, J = 5.0 Hz). ^{31}P NMR (202 MHz, DMSO-d_6) δ 2.58.

1-(2-bromoethoxy)-4-chlorobenzene (2). 4-chlorophenol (6.43 g, 50 mmol) and 22.5% (w/v) NaOH solution (18.5 mL) were added to a round bottom flask at ambient temperature. To the mixture was added 1,2-dibromoethane (17.2 mL, 200 mmol) and the reaction was refluxed overnight. The reaction was extracted with DCM (3X) and the organic extract was washed with H_2O, dried over Na_2SO_4, filtered and concentrated in vacuo. The crude product was purified by silica gel flash column chromatography, eluting with petroleum ether/EtOAc (0 – 5% pet. ether) to give **2** as a clear oil (9.47 g, 80% yield). ^{1}H NMR (500 MHz, $CDCl_3$) δ 3.64 (t, J = 6.0 Hz, 2H), 4.28 (t, J = 6.0 Hz, 2H), 6.87 (d, J = 9.0 Hz, 2H), 7.27 (d, J = 9.0 Hz, 2H). ^{13}C NMR (125 MHz, $CDCl_3$) δ 29.0, 68.3, 116.2, 126.5, 129.6, 156.8. HRMS-ESI$^+$ (*m/z*) calcd $[M + H]^+$ for C_8H_8BrClO: 234.9520. Found: 234.9526.

2′,3′-O-bis[(tert-butyldimethylsilyl)oxy]guanosine (**3**). To an oven-dried round-bottom flask was added guanosine (3.0 g, 10.6 mmol), imidazole (5.8 g, 84.7 mmol), and DMF (57.0 mL). The reaction vessel was purged/evacuated extensively with N_2, TBDMSCl (6.40 g, 42.4 mmol) was added and the reaction was stirred overnight at room temperature. The reaction was quenched/diluted with water (30 mL) and extracted with DCM (3X). The organic extract was washed with sat. aq. NH_4Cl (1X), water (2X), brine (1X), dried over $MgSO_4$, filtered, and concentrated in vacuo. To the resulting residue was added 80% AcOH (86.0 mL) and stirred at 60 °C for 12 hours. Acetic acid was removed under vacuum and coevaporated with EtOH. The resulting residue was purified by silica

gel flash chromatography, eluting $CHCl_3$/MeOH (0 – 20% MeOH) to give the title compound as a white solid (4.01 g, 74% yield over two steps). ^{1}H NMR (500 MHz, DMSO-d_6) δ -0.31 (s, 3H), -0.09 (s, 3H), 0.10 (s, 3H), 0.11 (s, 3H), 0.73 (s, 9H), 0.91 (s, 9H), 3.53 – 3.57 (m, 1H), 3.64 – 3.68 (m, 1H), 3.91 (t, J = 4.0 Hz, 1H), 4.23 (d, J = 4.5 Hz, 1H), 4.68 (dd, J = 4.5 Hz and 7.0 Hz, 1H), 5.21 (t, J = 5.5 Hz, 1H), 5.73 (d, J = 7.0 Hz, 1H), 6.44 (s, 2H), 7.97 (s, 1H), 10.6 (br s, 1H). ^{13}C NMR (125 MHz, DMSO-d_6) δ -5.5, -4.78, -4.76, -4.7, 17.6, 17.8, 25.5, 25.7, 61.2, 73.1, 75.0, 85.7, 86.7, 116.7, 135.7, 151.4, 153.6, 156.6. HRMS-ESI$^+$ (*m/z*) calcd $[M + H]^+$ for $C_{22}H_{41}N_5O_5Si_2$: 512.2719. Found: 512.2725.

2-Amino-9-((2R,3R,4R,5R)-3,4-bis((tert-butyldimethylsilyl)oxy)-5-(hydroxymethyl)tetrahydrofuran-2-yl)-7-(2-(4-chlorophenoxy)ethyl)-6-oxo-6,9-dihydro-1H-purin-7-ium (4). To an oven-dried round-bottom flask was added **3** (1 g, 1.95 mmol) and dry DMF (20 mL). The solution was purged/evacuated extensively with N_2 under vacuum. To the solution was added 2 (2.02 g, 8.60 mmol) and the reaction was stirred for 72 h at 70 °C. The mixture was concentrated in vacuo and the resulting residue was purified by silica gel flash column chromatography, eluting with $CHCl_3$/MeOH (+10% NH_4OH) – gradient 0 – 20% to give 4 as slight yellow solid (0.444 g, 34% yield). ^{1}H NMR (500 MHz, DMSO-d_6) δ -0.26 (s, 3H), -0.09 (s, 3H), 0.08 (s, 3H), 0.11 (s, 3H), 0.75 (s, 9H), 0.90 (s, 9H), 3.59 – 3.61 (m, 1H), 3.76 – 3.79 (m, 1H), 4.03 (d, J = 3.0 Hz, 1H), 4.27 (m, 1H), 4.37 – 4.44 (m, 2H), 4.81 (t, J = 5.0 Hz, 2H), 4.85 (t, J = 5.5 Hz, 1H), 5.55 (s, 2H), 5.82 (d, J = 6.0 Hz, 1H), 5.90 (br s, 1H), 6.95 (d, J = 9.0 Hz, 2H), 7.31 (d, J = 9.0 Hz, 2H), 9.21 (s, 1H). ^{13}C NMR (125 MHz, DMSO-d_6) δ -5.4, -5.1, -4.9, -4.6, 17.5,

17.7, 25.5, 25.7, 47.7, 60.6, 65.9, 72.1, 74.4, 87.1, 88.9, 107.9, 116.3, 124.8, 129.2, 133.2, 149.4, 156.6. HRMS-ESI$^+$ (m/z) calcd [M]$^+$ for $C_{30}H_{49}ClN_5O_6Si_2^+$: 666.2904. Found: 666.2885.

General Procedure for Preparation of Methylthio Alkyl Tryptamine Nucleoside Diester Phosphoramidates. Compound **4** (1 equiv) and the appropriate *H*-phosphonate **1a-c** (1.5 equiv) were added to an oven-dried round-bottom flask and dried overnight on the high vacuum. To the flask was added anhydrous pyridine and the mixture was purged/evacuated extensively with N_2 under vacuum. To the mixture was added PivCl (2.75 equiv) in a dropwise manner and the reaction was stirred for seven hours at ambient temperature. The reaction was quenched over sat. aq. $NaHCO_3$ and extracted three times with DCM. The organic extract was dried over Na_2SO_4, filtered, and concentrated in vacuo at ambient temperature and dried for an hour on the high vacuum. The dried residue was dissolved with anhydrous pyridine and the reaction vessel was purged/evacuated extensively with N_2 under vacuum. To the solution was added Et_3N (2 equiv). Tryptamine (4.0 equiv, dissolve in dry pyridine) and CCl_4 (1.5 equiv) were added simultaneously to the reaction mixture and stirred for 25 min at ambient temperature. The reaction was diluted with MeOH and concentrated in vacuo at ambient temperature. The resulting residue was purified by silica gel flash column chromatography, eluting with $CHCl_3$/MeOH (+10% NH_4OH) – gradient 0 – 20% to give semi-purified products **5a-c** as off-white solids. The products tend to coelute with unreacted nucleoside **4**, hence all fractions with product were pooled and advanced to the desilylation step.

General Procedure for Desilylation. To a solution of semi-purified **5** (1.0 equiv) in dry THF at 0 °C was added 1 M TBAF (3.0 equiv) dropwise until reaction became cloudy. The reaction was removed from the ice bath and stirred for five minutes at ambient temperature. The reaction was diluted with MeOH and concentrated in vacuo at ambient temperature. The resulting residue was purified by silica gel flash column chromatography, eluting with $CHCl_3$/MeOH (+10% NH_4OH) – gradient 0 – 20% to give **6** as slight yellow solid. Reverse phase flash column purification afforded the products as white powders after lyophilization.

9-((2R,3R,4R,5R)-5-(((((2-(1H-indol-3-yl)ethyl)amino)(2-(methylthio)ethoxy)phosphoryl)oxy)methyl)-3,4-bis((tert-butyldimethylsilyl)oxy)tetrahydrofuran-2-yl)-2-amino-7-(2-(4-chlorophenoxy)ethyl)-6-oxo-6,9-dihydro-1H-purin-7-ium (5a). The title compound was prepared from **4** (734 mg, 1.10 mmol), PivCl (373 µL, 3.02 mmol), and **1a** (424 mg, 1.65 mmol) in anhydrous pyridine (17.4 mL). The second step of the synthesis was performed with CCl_4 (160 µL, 1.65 mmol), tryptamine (705 mg, 4.40 mmol), Et_3N (0.31 mL, 2.20 mmol), and anhydrous pyridine (46 mL). The title compound was obtained as an off-white solid after silica gel flash column chromatography. The semi-purified product was advanced to the next step.

9-((2R,3R,4R,5R)-5-(((((2-(1H-indol-3-yl)ethyl)amino)(3-(methylthio)propoxy)phosphoryl)oxy)methyl)-3,4-bis((tert-butyldimethylsilyl)oxy)tetrahydrofuran-2-yl)-2-amino-7-(2-(4-chlorophenoxy)ethyl)-6-oxo-6,9-dihydro-1H-purin-7-ium (5b). The title compound was prepared from **4** (101

mg, 0.151 mmol), PivCl (52 μL, 0.416 mmol), and **1b** (62 mg, 0.227 mmol) in anhydrous pyridine (2.3 mL). The second step of the synthesis was performed with CCl_4 (22 μL, 0.227 mmol), tryptamine (97 mg, 0.604 mmol), Et_3N (42 μL, 0.302 mmol), and anhydrous pyridine (6.5 mL). The title compound was obtained as an off-white solid after silica gel flash column chromatography and the semi-purified product was advanced to the next step.

9-((2R,3R,4R,5R)-5-(((((2-(1H-indol-3-yl)ethyl)amino)(4-(methylthio)butoxy)phosphoryl)oxy)methyl)-3,4-bis((tert-butyldimethylsilyl)oxy)tetrahydrofuran-2-yl)-2-amino-7-(2-(4-chlorophenoxy)ethyl)-6-oxo-6,9-dihydro-1H-purin-7-ium (5c). The title compound was prepared from **4** (150 mg, 0.225 mmol), PivCl (76 μL, 0.619 mmol), and **1c** (91.5 mg, 0.337 mmol) in anhydrous pyridine (3.6 mL). The second step of the synthesis was performed with CCl_4 (52 μL, 0.337 mmol), tryptamine (144 mg, 0.900 mmol), Et_3N (63 μL, 0.450 mmol), and anhydrous pyridine (9.5 mL). The title compound was obtained as an off-white solid after silica gel flash column chromatography and the semi-purified product was advanced to the next step.

9-((2R,3R,4S,5R)-5-(((((2-(1H-indol-3-yl)ethyl)amino)(2-(methylthio)ethoxy)phosphoryl)oxy)methyl)-3,4-dihydroxytetrahydrofuran-2-yl)-2-amino-7-(2-(4-chlorophenoxy)ethyl)-6-oxo-6,9-dihydro-1H-purin-7-ium (6a). The title compound was prepared using **5a** (402.8 mg, 0.418 mmol), 1 M TBAF (1.25 mL, 1.25 mmol), and dry THF (22 mL). The product was obtained as a white powder after reverse phase flash column chromatography (0.152 g, 19% yield over two steps). ^1H

NMR (500 MHz, DMSO-d_6) δ 2.02 (d, J = 17.5 Hz, 3H), 2.65 (q, J = 6.5 Hz, 2H), 2.83 (q, J = 6.0 Hz, 2H), 3.05 (m, 2H), 3.88 – 3.99 (m, 2H), 4.05 – 4.29 (m, 4H), 4.40 – 4.44 (m, 2H), 4.55 (br s, 1H), 4.66 – 4.77 (m, 2H), 5.19 (dq, J = 13.5, 7.0 Hz, 1H), 5.46 (br s, 1H), 5.81 (br s, 2H), 5.86 (d, J = 4.5 Hz, 1H), 6.91 – 6.96 (m, 3H), 7.02 – 7.06 (m, 1H), 7.13 (d, J = 11.0 Hz, 1H), 7.26 – 7.33 (m, 3H), 7.45 – 7.49 (m, 1H), 9.09 (d, J = 7.0 Hz, 1H), 10.8 (s, 1H). ^{13}C NMR (125 MHz, DMSO-d_6) δ 14.8, 14.9, 27.6, 33.1, 41.7, 47.5, 64.2, 65.9, 69.9, 73.2, 83.2, 88.7, 107.8, 111.4, 111.5, 116.4, 118.1 (d, J = 3.9 Hz), 118.2 (d, J = 3.4 Hz), 120.9, 122.7, 124.8, 127.1, 129.3, 132.5, 136.2, 149.8, 156.6, 162.7, 163.7. ^{31}P NMR (202 MHz, DMSO-d_6) δ 10.45 and 10.31. HRMS-ESI$^+$ (m/z) calcd $[M]^+$ for $C_{31}H_{38}ClN_7O_8PS^+$: 734.1923. Found: 734.1908.

9-((2R,3R,4S,5R)-5-(((((2-(1H-indol-3-yl)ethyl)amino)(3-(methylthio)propoxy)phosphoryl)oxy)methyl)-3,4-dihydroxytetrahydrofuran-2-yl)-2-amino-7-(2-(4-chlorophenoxy)ethyl)-6-oxo-6,9-dihydro-1H-purin-7-ium (6b). The title compound was prepared using **5b** (66.1 mg, 0.058 mmol), 1 M TBAF (203 μL, 0.203 mmol), and dry THF (3.7 mL). The product was obtained as a white powder after reverse phase flash column chromatography (15.3 mg, 9% yield over two steps). ^{1}H NMR (500 MHz, DMSO-d_6) δ 1.77 (sex, J = 14.5, 6.5 Hz, 2H), 1.98 (d, J = 11.5 Hz, 3H), 2.45 (dt, J = 12.0, 7.5 Hz, 2H), 2.82 (q, J = 7.0 Hz, 2H), 2.97 – 3.06 (m, 2H), 3.84 – 3.94 (m, 2H), 4.04 – 4.28 (m, 4H), 4.37 – 4.44 (m, 2H), 4.54 (d, J = 4.0 Hz, 1H), 4.66 – 4.77 (m, 2H), 5.15 (dq, J = 14.0, 7.0 Hz, 1H), 5.44 (t, J = 4.5 Hz, 1H), 5.75 (d, J = 5.0 Hz, 1H), 5.81 (br s, 1H), 5.86 (d, J = 4.5 Hz, 1H), 6.94 (m, 3H), 7.04 (m, 1H), 7.12 (dd, J = 10.0, 1.5 Hz, 1H), 7.27 (dd, J = 9.0, 6.0 Hz, 2H), 7.32 (dd, J = 8.0, 3.5 Hz, 1H), 7.46 (dd, J = 12.5, 8.0

Hz, 1H), 9.09 (d, J = 6.0 Hz, 1H), 10.79 (br s, 1H). ^{13}C NMR (150 MHz, DMSO-d_6) δ 14.5, 27.7, 29.3 (d, J = 2.9 Hz), 29.35 (d, J = 6.6 Hz), 41.7 (d, J = 4.4 Hz), 47.5, 64.1, 65.2, 65.8, 69.9, 73.2, 83.2, 88.7, 107.8, 111.4, 111.5, 116.4 (d, J = 3.5 Hz), 118.1, 118.2 (d, J = 4.2 Hz), 120.9, 122.7, 124.8, 127.1 (d, J = 3.3 Hz), 129.3, 132.5, 136.2, (d, J = 1.8 Hz), 149.9, 156.6 (d, J = 2.4 Hz), 162.4, 163.4. ^{31}P NMR (202 MHz, DMSO-d_6) δ 10.55 and 10.39. HRMS-ESI$^+$ (m/z) calcd $[M]^+$ for $C_{32}H_{40}ClN_7O_8PS^+$: 748.2080. Found: 748.2058.

9-((2R,3R,4S,5R)-5-(((((2-(1H-indol-3-yl)ethyl)amino)(4-(methylthio)butoxy)phosphoryl)oxy)methyl)-3,4-dihydroxytetrahydrofuran-2-yl)-2-amino-7-(2-(4-chlorophenoxy)ethyl)-6-oxo-6,9-dihydro-1H-purin-7-ium (6c). The title compound was prepared using **5c** (15.2 mg, 0.0153 mmol), 1 M TBAF (46 μL, 0.046 mmol), and dry THF (1 mL). The product was obtained as a white powder after reverse phase flash column chromatography (8.2 mg, 10% yield over two steps). ^{1}H NMR (600 MHz, DMSO-d_6) δ 1.50 -1.60 (m, 4H), 1.94 – 1.99 (m, 3H), 2.35 – 2.43 (m, 2H), 2.77 – 2.84 (m, 2H), 3.01 – 3.03 (m, 2H), 3.78 – 3.83 (m, 3H), 4.03 – 4.24 (m, 3H), 4.35 – 4.43 (m, 3H), 4.54 (m, 1H), 4.68 – 4.76 (m, 2H), 5.71(br s, 2H), 5.86 (s, 1H), 6.90 – 6.96 (m, 2H), 7.01 – 7.05 (m, 1H), 7.11 – 7.14 (m, 1H), 7.24 – 7.33 (m, 2H), 7.42 – 7.48 (m, 2H), 9.08 (d, J = 7.8 Hz, 1H), 10.80 (br s, 1H). ^{13}C NMR (151 MHz, DMSO-d_6) δ 14.5, 24.6, 27.6, 28.9, 32.7, 41.7, 47.4, 64.9, 65.0, 65.9, 73.3, 107.9, 111.3, 111.5, 116.4, 118.1, 120.8, 122.7, 124.8, 127.1, 129.3, 132.1, 136.16, 136.17, 149.9, 156.6, 162.7, 163.7. ^{31}P NMR (202 MHz, CD_3OD) δ 10.89 and 10.77. HRMS-ESI$^+$ (m/z) calcd $[M]^+$ for $C_{33}H_{42}ClN_7O_8PS^+$: 762.2236. Found: 762.2220.

9-((2R,3R,4S,5R)-5-(((((2-(1H-indol-3-yl)ethyl)amino)(hydroxy)phosphoryl)oxy)methyl)-3,4-dihydroxytetrahydrofuran-2-yl)-2-amino-7-(2-(4-chlorophenoxy)ethyl)-6-oxo-6,9-dihydro-1H-purin-7-ium (7). Compound **6a** (74.2 mg, 0.101 mmol) was dissolved with a mixture of MeOH/MeCN (1:1, 15 mL) and to the mixture was added 10 mM HEPES buffer (340 mL, pH 7.2). The resulting suspension was incubated for 30 hours at 37 °C. Water was removed in vacuo and the resulting residue was purified by silica gel flash column chromatography, eluting first with solvent A (20% MeOH in $CHCl_3$) and then with solvent B ($CHCl_3$/MeOH/H_2O/NH_4OH – 5:3:0.5:0.005). The fractions containing the title compound were pooled and concentrated in vacuo and the resulting residue was purified by reverse phase C18 flash column chromatography to give product as a white fluffy solid (40.6 mg, 61% yield). ^{1}H NMR (500 MHz, DMSO-d_6) δ 2.73 - 2.77 (m, 2H), 2.97 - 2.99 (m, 2H), 3.80 (m, 1H), 3.97 (m, 1H), 4.08 (br s, 1H), 4.25 (br s, 1H), 4.40 – 4.44 (m, 3H), 4.76 (br s, 2H), 5.75 (br s, 1H), 5.88 (d, J = 3.5 Hz, 1H), 5.93 – 5.99 (m, 1H), 6.10 (br, 1H), 6.85 – 6.88 (m, 3H), 6.98 – 7.01 (m, 1H), 7.06 (br s, 1H), 7.18 (d, J = 8.5 Hz), 7.28 – 7.30 (m, 1H), 7.42 (d, J = 8.0 Hz, 1H), 9.99 (br s, 1H), 10.79 (br s, 1H). ^{13}C NMR (151 MHz, DMSO-d_6) δ 28.0, 42.7, 47.2, 62.5, 65.9, 70.4, 75.1, 84.7, 88.5, 107.3, 111.2, 112.6, 116.27, 116.31, 116.36, 117.9, 118.2, 120.6, 122.4, 124.6, 127.3, 129.1, 136.2, 150.0, 156.7, 189.3. ^{31}P NMR (202 MHz, DMSO-d_6) δ 6.30. HRMS-ESI$^+$ (m/z) calcd $[M]^+$ for $C_{28}H_{32}ClN_7O_8P^+$: 660.1733. Found: 660.1724.

Synthesis of internal standards (see Scheme 2-2)

2-amino-9-((2R,3R,4R,5R)-3,4-bis((tert-butyldimethylsilyl)oxy)-5-(hydroxymethyl)tetrahydrofuran-2-yl)-7-(3-fluorobenzyl)-6-oxo-6,9-dihydro-1H-purin-7-ium (8). To an oven-dried round bottom flask was added **3** (200 mg, 0.391 mmol) and anhydrous DMSO (1.7 mL). The solution was purged/evacuated extensively with N_2 under vacuum. To the solution was added 3-fluorobenzyl bromide (216 μL, 1.76 mmol) dropwise and the reaction was stirred overnight at room temperature. The reaction was diluted with water (10 mL) and the organic layer was extracted with EtOAc (3X). The combined organic extract was dried over Na_2SO_4, filtered, and concentrated in vacuo. The resulting residue was purified by silica gel flash column chromatography, eluting with $CHCl_3$/MeOH (+10% NH_4OH) – gradient 0 – 20% to give **8** as an off-white solid (225.3 mg, 93% yield). ^{1}H NMR (500 MHz, DMSO-d_6) δ -0.23 (s, 3H), -0.05 (s, 3H), 0.07 (s, 3H), 0.09 (s, 3H), 0.73 (s, 9H), 0.88 (s, 9H), 3.58 – 3.60 (m, 1H), 3.77 – 3.79 (m, 1H), 4.01 – 4.03 (m, 1H), 4.24 (t, J = 3.5 Hz, 1H), 4.72 (t, J = 5.0 Hz 2H), 5.60 (br, 1H), 5.67 (q, J = 14.5 Hz, 2H), 5.79 (d, J = 5.0 Hz 2H), 6.48 (s, 2H), 7.20 (t, J = 7.5 Hz, 1H), 7.33 (d, J = 7.5 Hz, 2H), 7.43 (q, J = 7.5 Hz, 1H), 9.43 (s, 1H). ^{13}C NMR (125 MHz, DMSO-d_6) δ -5.3, -5.0, -4.9, -4.6, 17.5, 17.7, 25.5, 25.7, 50.4, 60.1, 71.3, 74.6, 86.5, 88.9, 107.3, 115.3 (d, $J_{C\text{-}F}$ = 22.3 Hz), 115.5 (d, $J_{C\text{-}F}$ = 20.6 Hz), 124.6 (d, $J_{C\text{-}F}$ = 2.5 Hz), 130.9 (d, $J_{C\text{-}F}$ = 8.3 Hz), 134.2, 137.6 (d, $J_{C\text{-}F}$ = 7.9 Hz), 149.6, 158.9, 159.9, 162.1 (d, $J_{C\text{-}F}$ = 243 Hz). ^{19}F NMR (471 MHz, DMSO-d_6) δ -112.5. HRMS-ESI$^+$ (m/z) calcd $[M]^+$ for $C_{29}H_{47}FN_5O_5Si_2^+$: 620.3094. Found: 620.3074.

9-((2R,3R,4S,5R)-5-(((((2-(1H-indol-3-yl)ethyl)amino)(2-(methylthio)ethoxy)phosphoryl)oxy)methyl)-3,4-dihydroxytetrahydrofuran-2-yl)-2-

amino-7-(3-fluorobenzyl)-6-oxo-6,9-dihydro-1H-purin-7-ium (10). Using the general procedure for Preparation of Methylthio Alkyl Tryptamine Nucleoside Diester Phosphoramidates, the title compound was prepared from **8** (150 mg, 0.242 mmol), PivCl (82 μL, 0.666 mmol), and **1a** (93.3 mg, 0.362 mmol) in anhydrous pyridine (3.8mL). The second step of the synthesis was performed with CCl_4 (47 μL, 0.484 mmol), tryptamine (116.3 mg, 0.726 mmol), Et_3N (67.2 μL, 0.484 mmol) in 10 mL anhydrous pyridine. The title compound was obtained as an off-white solid after silica gel flash column chromatography. Semi-pure product was advanced to the desilylation step. Using the general procedure for desilylation, removal of TBS groups was performed with semi pure compound **9** (88.7 mg), dry THF (5.0 mL) and 1 M TBAF (290 μL, 0.290 mmol). The title compound was obtained as a white solid powder after reverse phase C18 flash column chromatography (11 mg, 7% yield over two steps). ^{1}H NMR (500 MHz, DMSO-d_6): δ 2.01 (d, J = 21.5 Hz, 3H), 2.64 (q, J = 7.0 Hz, 2H), 2.82 (q, J = 6.5 Hz, 2H), 3.00 – 3.09 (m, 2H), 3.86 – 3.99 (m, 3H), 4.04 – 4.27 (m, 4H), 4.54 (q, J = 4.0 Hz, 1H), 5.19 (sex, J = 13.5, 6.5 Hz, 1H), 5.45 (br, 1H), 5.56 – 5.64 (m, 2H), 5.72 (s, 2H), 5.83 (d, J = 3.0 Hz, 1H), 6.94 (q, J = 8.0 Hz, 1H), 7.01 – 7.06 (m, 1H), 7.12 – 7.17 (m, 2H), 7.29 – 7.39 (m, 3H), 7.41 – 7.49 (m, 2H), 9.19 (d, J = 9.5 Hz, 1H), 10.79 (s, 1H). ^{13}C NMR (151 MHz, DMSO-d_6) δ 14.8, 27.6, 33.1, 41.7, 49.8, 64.3, 69.9, 73.2, 83.2, 88.9, 91.5, 107.7 (d, J = 24.4 Hz), 109.6, 111.3 (d, $J_{C\text{-}F}$ = 12.0 Hz), 111.5, 115.1, 115.4 (d, $J_{C\text{-}F}$ = 29.8 Hz), 118.2, 120.9, 122.8, 124.5, 127.1, 130.7, 131.5, 136.2, 138.5, 149.7, 161.2, 163.1 (d, $J_{C\text{-}F}$ = 136 Hz), 163.6. ^{31}P NMR (202 MHz, DMSO-d_6) δ 10.47 and 10.31. ^{19}F NMR (471

MHz, DMSO-d_6) δ -112.6. HRMS-ESI$^+$ (*m/z*) calcd [M]$^+$ for $C_{30}H_{36}FN_7O_7PS^+$: 688.2113. Found: 688.2095.

((2R,3S,4R,5R)-5-(2-amino-7-(3-fluorobenzyl)-6-oxo-1,6-dihydro-9H-purin-7-ium-9-yl)-3,4-dihydroxytetrahydrofuran-2-yl)methyl (2-(1H-indol-3-yl)ethyl)phosphoramidate (11). Compound **10** (47.7.2 mg, 0.0693 mmol) was dissolved with a mixture of MeOH/MeCN (1:1, 2 mL) and to the mixture was added 10 mM HEPES buffer (70 mL, pH 7.2). The resulting suspension was incubated for 30 hours at 37 °C. Water was removed in vacuo and the resulting residue was purified by silica gel flash column chromatography, eluting first with solvent A (20% MeOH in $CHCl_3$) then with solvent B ($CHCl_3$/MeOH/H_2O/NH_4OH – 5:3:0.5:0.005). The fractions containing the title compound were pooled and concentrated in vacuo and the resulting residue was purified by reverse phase C18 flash column chromatography, to give product as a white fluffy solid (22.6 mg, 53% yield). ^{1}H NMR (500 MHz, D_2O) δ 2.79 (t, J = 7.5 Hz, 2H), 3.00 – 3.11 (m, 2H), 3.96 – 3.99 (m, 1H), 4.11 – 4.13 (m, 1H), 4.35 – 4.38 (m, 2H), 4.47 (t, J = 4.5 Hz, 1H), 5.14 (s, 2H), 5.86 (d, J = 4.0 Hz, 1H), 6.78 (t, J = 7.0 Hz, 1H), 6.98 (t, J = 7.5 Hz, 1H), 7.01 – 7.06 (m, 3H), 7.09 (s, 1H), 7.25 (d, J = 7.5 Hz, 1H), 7.29 (q, J = 7.5 Hz, 2H). ^{13}C NMR (125 MHz, DMSO-d_6) δ 28.3 (d, J = 7.0 Hz), 43.3, 52.5, 64.4, 70.9, 75.9, 85.7 (d, J = 9.1 Hz), 90.3, 109.5, 113.1, 113.8, 116.4 (d, $J_{C\text{-}F}$ = 22.5 Hz), 117.2 (d, $J_{C\text{-}F}$ = 20.9 Hz), 119.4, 119.9, 122.9, 123.9, 125.3, 128.2, 132.4 (d, J = 8.0 Hz), 137.5, 137.9, 138.0, 151.1, 162.6 (d, J = 11.8), 162.9, 164.9. ^{31}P NMR (202 MHz, D_2O) δ 9.23. ^{19}F NMR (471 MHz, DMSO-d_6) δ -112.5. HRMS-ESI$^+$ (m/z) calcd [M]$^+$ for $C_{27}H_{30}FN_7O_7P^+$: 614.1923. Found: 614.1914.

((2R,3S,4R,5R)-5-(2-amino-7-(3-fluorobenzyl)-6-oxo-1,6-dihydro-9H-purin-7-ium-9-yl)-3,4-dihydroxytetrahydrofuran-2-yl)methyl hydrogen phosphate (13).[207] To an oven-dried round bottom flask was added guanosine monophosphate disodium salt (203.6 mg, 0.50 mmol) and anhydrous DMSO (2.5 mL). The solution was purged/evacuated extensively with N_2 under vacuum. To the solution was added 3-fluorobenzyl bromide (307 μL, 2.50 mmol) dropwise and the reaction was stirred overnight at room temperature. The reaction was diluted with water (5 mL) and washed with Et_2O (5X). The aqueous layer was purified on a DEAE Sephadex A-25 column, eluting with 1 M triethylammonium bicarbonate buffer (pH 7.2) on a gradient of 0 – 60%. The relevant fractions were pooled, lyophilized, and the resulting residue was subjected to ion exchange using a Dowex 50WX8 ion-exchange column (mesh size: 200 - 400, hydrogen form). The relevant fractions were pooled, concentrated in vacuo, and purified by reverse phase C18 flash column chromatography to give 75 mg of product after lyophilization – 32% yield. ^{1}H NMR (500 MHz, D_2O) δ 4.02 – 4.06 (m, 1H), 4.14 – 4.19 (m, 1H), 4.40 – 4.41 (m, 1H), 4.52 (t, J = 4.5 Hz, 1H), 4.71 (t, J = 4.5 Hz, 1H), 5.70 (d, J = 2.0 Hz, 2H), 6.10 (d, J = 4.0 Hz, 1H), 7.10 (td, J = 2.0, 8.5 Hz, 1H), 7.16 (d, J = 9.5 Hz, 1H), 7.21 (d, J = 7.5 Hz, 1H), 7.39 (q, J = 8.0 Hz, 1H). ^{13}C NMR (125 MHz, D_2O) δ 51.8, 62.6, 69.7, 75.1, 84.9 (d, J = 8.6 Hz), 89.3, 107.9, 114.4 (d, $J_{C\text{-}F}$ = 22.5 Hz), 115.4 (d, $J_{C\text{-}F}$ = 20.9 Hz), 123.4, 130.7 (d, $J_{C\text{-}F}$ = 8.4 Hz), 136.56, 136.6, 150.1, 158.1, 158.6, 162.5 (d, $J_{C\text{-}F}$ = 243 Hz). ^{31}P NMR (202 MHz, D_2O) δ 3.67. ^{19}F NMR (471 MHz, D_2O) δ -112.8. HRMS-ESI$^+$ (*m/z*) calcd $[M]^+$ for $C_{17}H_{20}FN_5O_8P^+$: 472.1028. Found: 472.1020.

Methylthioalkyl deprotection studies.

An aliquot (400 μL) of either ProTides **6a** or **6c** (80 μM in 20 mM HEPES buffer, pH 7.2 or 2.0) was subjected to RP-HPLC (t = 0) and the remaining solution was incubated at 37 °C. Subsequent RP-HPLC analyses on aliquots of the solution was performed at t = 1, 4, 6,12, 18, and 24 hours. The same analyses were performed for compound **6b** at t = 1, 3, 6, 11, 17, 24, and 60 hours. The half-life of deprotection was determined by plotting the area under the curve (AUC) against time.

Plasma Stability Study with 6a.[208]

Stability of ProTide **6a** in plasma was performed with pooled female Sprague Dawley rat plasma (BioChemed, Winchester, VA) in triplicates. Briefly, rat plasma (500 μL) was pre-incubated at 37 °C for two minutes. The plasma was then spiked with **6a** so that the final concentration was 150 μM. Aliquots (100 μL) of the reaction were drawn at different time points (t = 1, 2, 4, 6, and 9 hours) for RP-HPLC analysis. To the aliquots were added MeCN (100 μL) and the mixture was spun at 13,300g for 10 minutes to separate the precipitated proteins. The supernatant was removed and filtered through a 0.2 μm nylon filter and then subjected to RP-HPLC analysis. The stability of **6a** was determined by calculating the half-live from curves generated by plotting AUCs of remaining parent compound against time.

In vitro **cellular uptake**.

Human Mantle cell lymphoma cell lines Mino, Granta, and Z138 were purchased from ATCC (Manassas, VA, USA). The cells were cultured in Roswell Park Memorial Institute medium (RPMI) supplemented with 10% fetal bovine serum (FBS), 100 U mL^{-1}

penicillin, 100 μg mL^{-1} streptomycin, and L-glutamine at 37 °C and 5% CO_2. MCL cells (five million) were incubated with either **6a** (150 μM) or **7** (150 μM) for 12 hours at 37 °C. Cells were rinsed with ice-cold phosphate–buffered saline (PBS) upon removal of pronucleotide–containing media. Cells were harvested, and cell pellet was obtained by centrifugation. The resulting cell pellet was resuspended in MeOH/NH_4OAc (v/v = 60:40), spiked with 80 fmol each of internal standards **11** and **13** (**Table 2-4**), and subjected to three freeze – thaw cycles in liquid nitrogen. The resulting mixture was centrifuged at max speed (17,200g, 4 °C) and the supernatant was removed. The supernatant was filtered through a 0.2 μm nylon filter and the filtrate was dried in a speed-vac. The resulting residue was resuspended with 100 μL HEPES buffer (20 mM, pH 7.2) and analyzed by LC-MS/MS. LC-MS/MS method: Analytical Agilent Zorbax SB-C18 5 μm column 5.0 mm X 150 mm. Buffer A – water (+0.1% formic acid); Buffer B: MeCN (+0.1% formic acid). Analysis was performed on a gradient of 98% Buffer A (0 to 2 min), then to 82% Buffer A (2 to 18 min), then to 5% Buffer A (18 to 20 min), and isocratic 5% Buffer A (20 to 23 min), followed by a linear gradient to 98% Buffer A (23 to 25 min), and finally isocratic 98% Buffer A (25 to 40 min). All LC-MS/MS analyses were performed at a flow rate of 15.0 μL/min. Standards for 7-Cl-Ph-Ethyl-GMP[209] (see notes for synthesis) and phosphoramidate **7** were prepared and spiked with 80 fmol of either internal standard **11** (for phosphoramidate **7** standards) or internal standard **13** (for 7-Cl-Ph-Ethyl_GMP standards). All standards were prepared so that the ratio of analyte to internal standard (in fmol) was 1:50, 1:10, 1:2, 1:1, and 2:1. A standard curve was generated by plotting the observed internal standard to analyte ratios against the expected

internal standard to analyte ratios. The amount of analyte in each sample was determined from the following equation.

$$\frac{\text{slope x AUC}_{\text{analyte}}}{\text{AUC}_{\text{internal standard}}} = \frac{\text{Analyte amount}}{\text{Amount}_{\text{internal standard}}}$$

Cap affinity assay.

7-Methyl guanosine triphosphate-Sepharose 4B (m7GTP) beads were purchased from GE Healthcare (Buckinghamshire, HP7 9NA UK). Briefly eight to ten million MCL cells treated with **6a** were washed with ice-cold 1X PBS followed by lysis with cap binding buffer, and cap affinity assay was performed as described before.[179]

***In vivo* pharmacokinetics properties of 6a and 7 in Sprague-Dawley rats**.

All animal care, housing, and laboratory procedures were approved by the University of Minnesota Institutional Animal Care and Use Committee (IACUC, protocol #1509A33023). The animal care and housing was maintained by University of Minnesota Research Animal Resources (RAR) and veterinarian staff.

The single dose pharmacokinetic studies were performed with rats by monitoring plasma time course of **7** and **6a** after administration via oral (*p.o.*) and intravenous (*i.v.*) routes. A group of three female Sprague-Dawley rats (250-274 g, Envigo, Indianapolis, IN) was used first in a *p.o.* study followed by an *i.v.* study after a three-day washout period. All rats were received with in-dwelling dual femoral/jugular vein catheters, which were used for blood withdrawing and *i.v.* dosing, respectively. 10 mg/mL solutions of compounds were prepared in 0.5% aqueous sodium carboxymethylcellulose (CMC) with 5% DMSO and rats were given a single *p.o.* or *i.v.* dose of 25 or 2.5 mg/kg by oral

gavage or injection respectively. Blood samples (0.15 mL) were drawn at various times post dose (*p.o.*: 0, 15, 30, 45, 60, 120, 240, 360, and 480 min; *i.v.*: 0, 5, 10, 15, 30, 45, 60, 120, 240, and 480 min) and collected in vacutainer tubes containing 3.6 mg K_2EDTA. They were centrifuged at 3000g for 5 min and plasma was harvested and stored at –80 ºC until analyzed. Plasma (20 µL) was protein-precipitated with acetonitrile (20 µL) containing a mixture of corresponding internal standards (100 nM each, **Table 2-4**), centrifuged, and the supernatant was analyzed by LC-MS/MS (Shimadzu-AB Sciex Qtrap 5500).

Reverse-phase LC was performed on a Kinetix C18 column (50 mm × 2.1 mm, 2.6 µm particle size; Phenomenex, Torrance, CA). Mobile phase A was 0.1% aqueous formic acid while mobile phase B was 0.1% formic acid in acetonitrile. Initial conditions were 5% B from 0 to 0.5 min, after which the %B was increased to 95% from 0.5 to 3 min. The column was washed in 95% B for 2 min, returned to 5% over 0.2 min, and allowed to re-equilibrate for 2.8 min in 5% B to provide a total run time of 8 min. The flow rate was 0.5 mL/min and the column oven was maintained at 40 °C. The injection volume was 10 µL. All analytes were analyzed by mass spectrometry in positive ionization mode by Multiple Reaction Monitoring (MRM). To determine the optimum MRM settings (**Table 2-4),** each analyte was infused at a concentration of 10 µM (in 1:1 water: acetonitrile containing 0.1% formic acid) onto the MS by a syringe pump at a flow of 10 µL/min.

Analyte and internal standard peak areas were calculated (MultiQuant, version 2.0.2). Analyte peak areas were normalized to the corresponding internal standard peak

areas and the analyte concentrations were determined using an appropriate standard curve for each compound. The standard solutions were prepared by serial dilution in rat plasma and treated similarly as for samples described above. PK parameters were calculated from concentration-time profiles by non-compartamental analysis (Phoenix WinNonLin, version 6.3, Pharsight Corporation). Oral bioavailability (%*F*) was calculated individually for each rat using the dose normalized *p.o.* and *i.v.* area under the curve (AUC).

Thymidine incorporation assay.

MCL lymphoma cell lines were treated with **6a** for 48 hours and then thymidine was added for another 16 hours. Proliferation was assessed by thymidine incorporation assay as described earlier.[210] Pronucleotide **6a** was added daily.

Annexin V/PI flow cytometry assay for survival.

MCL cell lines were treated with **6a** for 48 hours and inhibition of survival was assessed by AnnexinV/PI staining using flow cytometry, as described before.[210] Pronucleotide **6a** was added daily.

RNA-Immunoprecipitation (RNA-IP).

RNA-IP was performed on Granta and Mino cells with Magna RIP RNA-Binding Protein Immuno-precipitation Kit (Millipore, Billerica, MA, USA) as described earlier.[211]

Western blotting.

MCL cell lines were treated with **6a** for 48 hours and protein quantification was performed. Western blotting was performed as described before using eIF4E, eIF4G, actin, c-Myc, and Bcl-2 antibodies.[211]

Notes: aReagents and conditions: (a) diphenyl phosphite, pyridine, rt for 2 h, then H2O/Et3N (1:1), rt for 3 h; (b) 1,2-dibromoethane, 22.5% (w/v) NaOH, rt, 16 h, 80%; (c) TBDMSCl, pyridine, rt, 18 h, then 80% AcOH, rt, 18 h, 74%; (d) 2, DMF, rt, 48 h, 34%; (e) 1a-c, PivCl, pyridine, rt, 6 h, then tryptamine, CCl4, NEt3, rt, 30 min; (f) TBAF, THF, 0 °C then rt for 10 min, 9 – 19%; (g) 10 mM HEPES, 37 °C, 30 h, 61%.

7-Cl-Ph-Ethyl-GMP was synthesized according to ref 22; purified by ion exchanged with Dowex50X8 to remove triethylammonium salt, and finally, by reverse phase C18 column chromatography.

Chapter 3

The following chapter contains published work from Okon, A.; Matos de Souza, M. R.; Shah, R.; Amorim, R.; da Costa, L. J.; Wagner, C. R. *ACS Med. Chem. Lett.* **2017***, 8* (9), 958-962.

Anchimerically Activated Antiviral Pronucleotides

3.1. Introduction

Nucleoside/nucleotide analogs have over the years emerged as powerful tools for combating viral infections.[159] Specifically, nucleoside analogs require conversion by cellular kinases to their active nucleotide metabolites, which can directly inhibit intracellular enzymes or get incorporated into newly synthesized DNA or RNA.[159,212] The tight substrate specificity of human kinases compared to viral kinases provides a basis for selectivity of nucleoside/nucleotide analogs as antiviral therapies.[212, 213] Incorporation of a nucleoside analog triphosphate during viral DNA/RNA synthesis may lead to termination of chain elongation, accumulation of mutations during viral replication, or initiation of apoptosis by viral infected cells.[159, 214]

Dengue virus (DENV) is a positive-stranded RNA virus belonging to the family *Flaviviridae*. Transmission of DENV is mostly through *Aedes* mosquitoes and manifestation of the disease ranges from mild dengue fever to potentially fatal forms of dengue fever such as dengue shock syndrome (DSS) and dengue hemorrhagic fever. Treatment of the disease is mostly supportive. A lot of the efforts at developing curative

interventions of DENV have focused on developing small molecules to target vial and host factors.[215]

As a well-studied drug target, significant efforts have been made at developing nucleoside analogs that target viral polymerases. Non-structural protein 5 (NS5) is highly conserved in flaviviruses. For example, the NS5 protein of DENV has about 67 – 82% conserved amino acids between all four DENV serotypes (DENV1 – 4).[216] DENV NS5 is comprised of an N-terminal RNA methyltransferase domain (MTase) and a C-terminal RNA-dependent RNA polymerase domain (RdRp). The RdRp domain is responsible for *de novo* RNA synthesis, which enables the virus to convert its positive-sense RNA template to a negative-sense viral RNA. The negative-sense viral RNA then serves as a template for synthesis of more positive-sense viral RNA, which could be packaged into infective virions or used as templates for synthesis of viral proteins (**Figure 3-1**).[208] Thus, the RdRp of flaviviruses has emerged as an attractive drug target because of its pivotal role in the synthesis/replication of the viral genome of this family of RNA viruses.[159, 214] Several studies have established nucleoside analogs bearing a 2′-*C*- modification as a common pharmacophore in nucleoside analog inhibitors of viral polymerases. Specifically, the 2′-*C*-*β*-Methyl (2′-*C*-*β*-Me) modification has emerged as the preferred pharmacophore in viral nucleoside analog inhibitors. These nucleoside inhibitors, previously developed for hepatitis C virus (HCV), have been shown to be potent inhibitors of DENV due to the phylogenetic similarity between HCV and DENV RdRps.[217, 218] The most potent 2′-*C*-*β*-Me inhibitors of a serotype of DENV (DENV-2) were 2′-*C*-*β*-methyladenosine (2′-*C*-*β*-Me-A) and 2′-*C*-*β*-methylguanosine (2′-*C*-*β*-Me-

G), with antiviral EC_{50} values of 4 μM and 13.6 μM, respectively (**Figure 3-2A**).[219] In addition, 1′-cyano-4-aza-7,9-dideazaadenosine C-nucleotide was shown to have antiviral activity against DENV-2 (EC_{50} = 9.46 μM).[220]

Figure 3-1. Non-structural protein 5 (NS5) RNA-dependent RNA polymerase activity is essential for viral protein synthesis and genome replication in *flaviviridae* viruses.

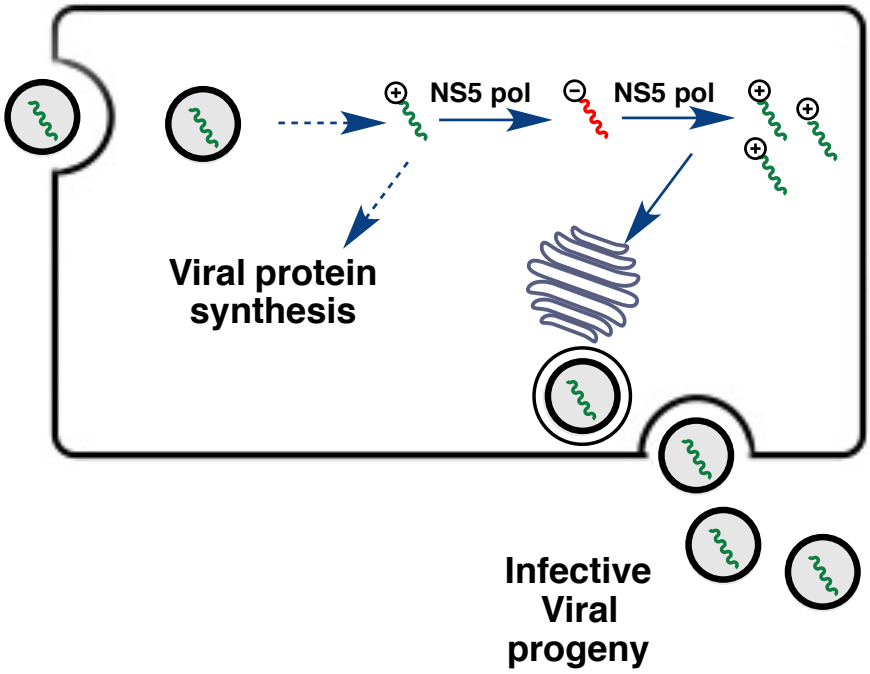

Figure 3-2. Anti-Dengue nucleosides (A) and activation mechanism of 2-(methylthio)ethyl phosphoramidate diester pronucleotide (B).

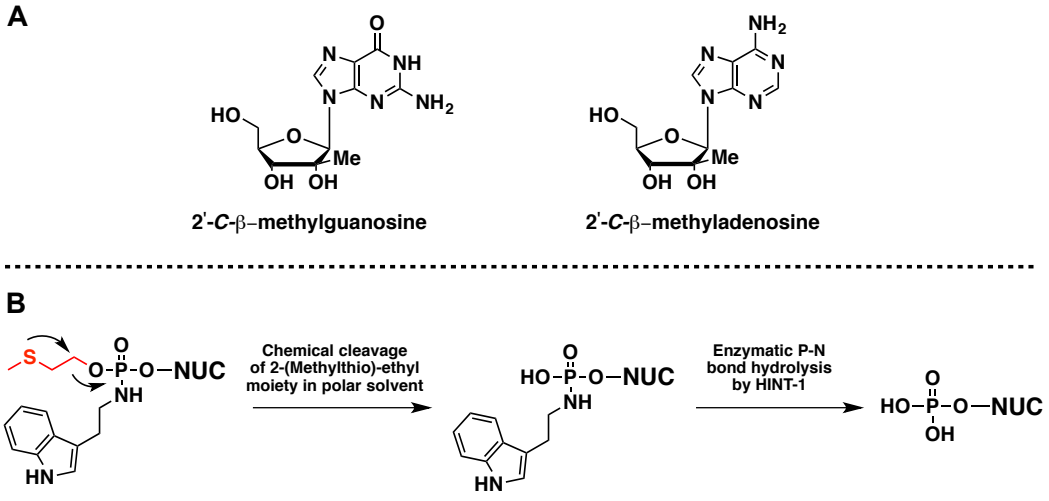

Although nucleoside/nucleotide analogs are an established antiviral therapy, their development as effective therapeutics is faced with several challenges. Since nucleoside analogs are modified derivatives of naturally occurring nucleosides, the efficiency of conversion to sufficient amounts of their respective 5′-triphosphates, by host kinases, can be problematic. In particular, the first phosphorylation event for several nucleosides has been found to be rate limiting. Consequently, several phosphorylation bypass strategies have been developed for the intracellular delivery of monophosphorylated nucleoside analogs.[221-223]Such prodrug strategies have been successfully utilized, as evident in the development of the anti HCV drug sofosbusvir.[224] Sofosbusvir incorporates an aryloxy amino acid (ProTide) phosphoramidate strategy, which utilizes a combination of initial esterase hydrolysis, followed by mixed anhydride chemical hydrolysis, and finally phosphoramidate hydrolysis by hHINT1.[123,225]

Over the last three decades, a variety of pronucleotide approaches have been successfully explored, such as bis-POM[226], SATE[227], cyclophosphamide[228] and cyclo-Sal[229], as well as several others.[221, 230] We and others have investigated the utility of phosphoramidate-based pronucleotide for the delivery of anti-viral and anti-cancer nucleoside monophosphates.[170, 223, 225,167]

Upon investigation of the metabolism of phosphoramidate pronucleotides, we established that P-N bond hydrolysis by HINT1 is responsible for the intracellular release of the nucleoside monophosphate. For example, recently we have shown that 4Ei-1, a monoester phosphoramidate pronucleotide of the eIF4E antagonist *N*7-Benzyl guanosine monophosphate, can serve as a selective inhibitor of the epithelial-mesenchymal

transition (EMT).[148] Building upon our success at developing monoester phosphoramidates, we have focused our efforts at developing phosphoramidate diester prodrugs because of the potential to engender increased lipophilicity and cell permeability compared to monoester phosphoramidates. Nevertheless, to date the conversion of most diester phosphoramidates pronucleotides is typically initiated by esterase dependent hydrolysis of one of the phosphate protecting moieties.[19] Consequently, pre-clinical studies in rodents (rats and mice) have proven to be problematic, since the plasma of mice and rats contains considerably more carboxyesterase activity than in humans.[231, 232,233] In addition, due to the high carboxyesterase activity of the liver and high liver first pass metabolism, accumulation of nucleoside monophosphate after treatment with a diester phosphoramidate ProTide has been reported.[163] Thus, high hepatic extraction can limit the application of ProTides for systemic delivery of nucleotides after oral administration. In order to address some of the drawbacks of currently used ProTide strategy, we propose a diester phosphoramidate strategy that utilizes an initial chemical activation step to liberate the monoester phosphoramidate, which can be hydrolyzed by HINT1 to release the nucleotide.

Cieślak and co-workers had previously reported the use of 2-(methylthio)ethyl protection group for oligonucleotide synthesis.[172] Unmasking of the phosphate oxygen (in a model 4-methylthio-1-butyl system) was shown to be dependent on anchimeric assistance (by sulfur atom) and release of a cyclic sulfonium ion. While the methylthio alkyl protecting groups are stable in organic solvents, intramolecular nucleophilic attack in polar aqueous media has been found to be temperature dependent with a half-life of

approximately 2 – 4 min at 55°C and at pH 7.0.[172] Therefore, we hypothesized that 2-(methylthio)ethyl containing phosphoramidates may have a longer half-life under physiological conditions (37 °C , pH = 7.4) and thus afford a membrane permeable diester phosphoramidate pronucleotide that is able to undergo intracellular release of the monoester phosphoramidate, followed by HINT1 P-N bond cleavage to deliver the nucleoside monophosphate (**Figure 3-2B**). We chose to investigate our hypothesis by preparing a 2-(methylthio)ethyl phosphoramidate diester prodrug of the anti-viral nucleoside, 2′-*C*-*β*-Me-guanosine, followed by characterization of its *in vitro* stability and anti-Dengue biological activity.

3.2. Results and Discussion

The synthesis of 2′-*C*-*β*-Me-G (**1**) was performed according to published procedure.[29] Treatment of **1** with DMTrCl afforded a mixture of 5′-OH mono protected nucleoside (**2a**) as well as a 5′-OH and N^2 –amino bis DMTr protected nucleoside (**2b**). Subsequent treatment of the mixture with Ac_2O afforded a mix of 5′-*O*-DMTr triacetyl-protected nucleoside **3a** and a 5′-*O*-N^2 bis DMTr diacetyl-protected nucleoside **3b**. Subsequent detritylation of the mixture of **3a** and **3b** afforded the triacetyl-protected nucleoside **4**. Since attempts to protect 2′-*C*-*β*-Me-G with DMTrCl yielded a mixture of products, an alternate synthetic route to nucleoside **4** has been developed. 2′-*C*-*β*-Me-G was treated with TBDPSCl in the presence of pyridine to afford a 5′-*O*-silyl protected nucleoside **10**. Subsequent treatment of **10** with Ac_2O under heating afforded the tri-acetylated nucleoside **11**, which was subsequently desilylated to give nucleoside **4** (**Scheme 3-2**).

The *H*-phosphonate monoester intermediate **7** was coupled to nucleoside **4** in the presence of pivaloyl chloride to give the corresponding *H*-phosphonate diester intermediate, which was treated with sat. aq. $NaHCO_3$ and extracted with CH_2Cl_2 to remove excess pivaloyl chloride. Due to the sensitivity of the nucleoside *H*-phosphonate monoester intermediate to hydrolysis during silica gel chromatography, the crude organic extract was subjected to oxidative coupling, to install tryptamine, under standard Atherton-Todd reaction conditions. De-acetylation of the resulting phosphoramidate diester **5**, with methanolic ammonia yielded **6**, as a diastereomeric mixture (7:3).

In addition to preparing the diester phosphoramidate prodrug of 2′-*C*-*β*-Me-G, we also prepared the tryptamine monoester derivative of the nucleoside prodrug. Preparation of the monoester phosphoramidate could be achieved via two routes. Route A involved treatment of nucleoside **1** with $POCl_3$ to give the 5′-*O*- phosphate product **8**, which was subsequently used in an EDC-HCl mediated phosphoramidate-forming reaction to give the desired tryptamine phosphoramidate nucleoside prodrug **9**. Alternatively, phosphoramidate **9** could be accessed via deprotection of the methylthio ethyl moiety in 10 mM HEPES buffer at 37 °C (Route B) (**Scheme 3-1**).

Scheme 3-1. Preparation of pronucleotides **6** and **9**[a]

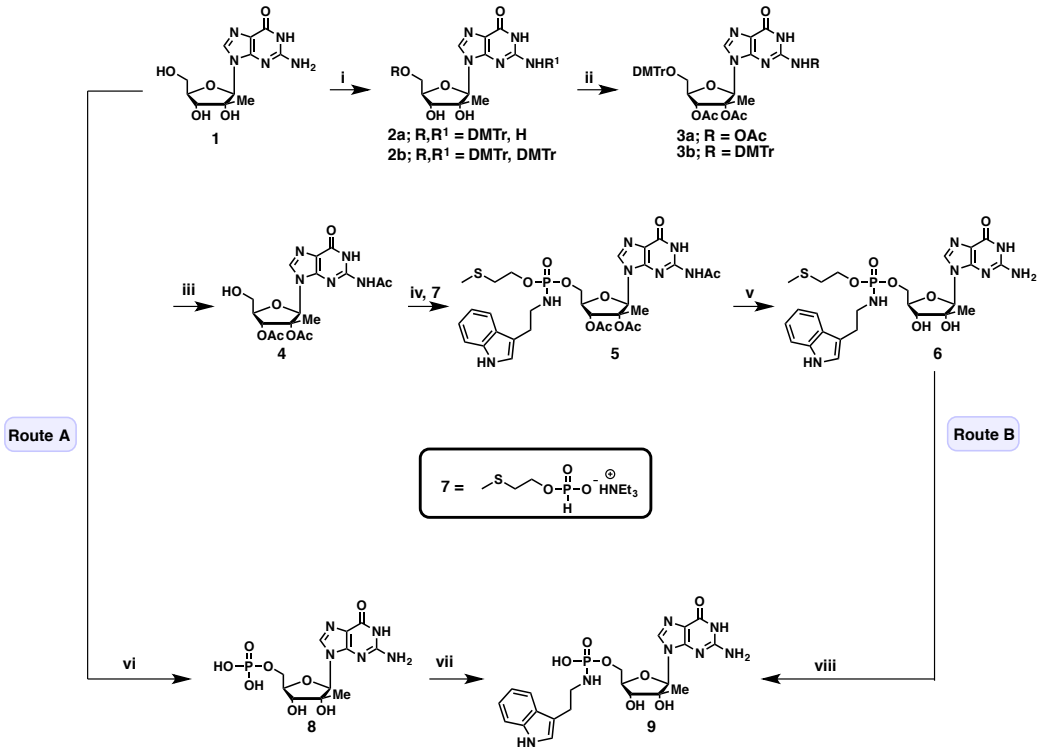

[a]Reagents and conditions: (i) DMTrCl, DMSO, pyridine, rt, overnight; (ii) MeCN, DMAP, Ac_2O, pyridine, rt, overnight; (iii) 80% AcOH, 55 °C, 1.5 h, 27% over 3 steps; (iv) **7**, PivCl, pyridine, rt, 8 h; then tryptamine, CCl_4, NEt_3, pyridine, rt, 30 min, 65%; (v) 7N NH_3/MeOH, rt, 4 h, 64%; (vi) $(EtO)_3PO/POCl_3$ (10:1), 0 °C, 0.75 h, Dowex-50, 74%; (vii) tryptamine, EDC-HCl, H_2O, pH 7, 55 °C, 6 h, Dowex-50WX8, 23%; (viii) 10 mM HEPES, pH 7, 37 °C, 30 h, 84%.

Scheme 3-2. Alternate route for preparation of nucleoside **4**[a]

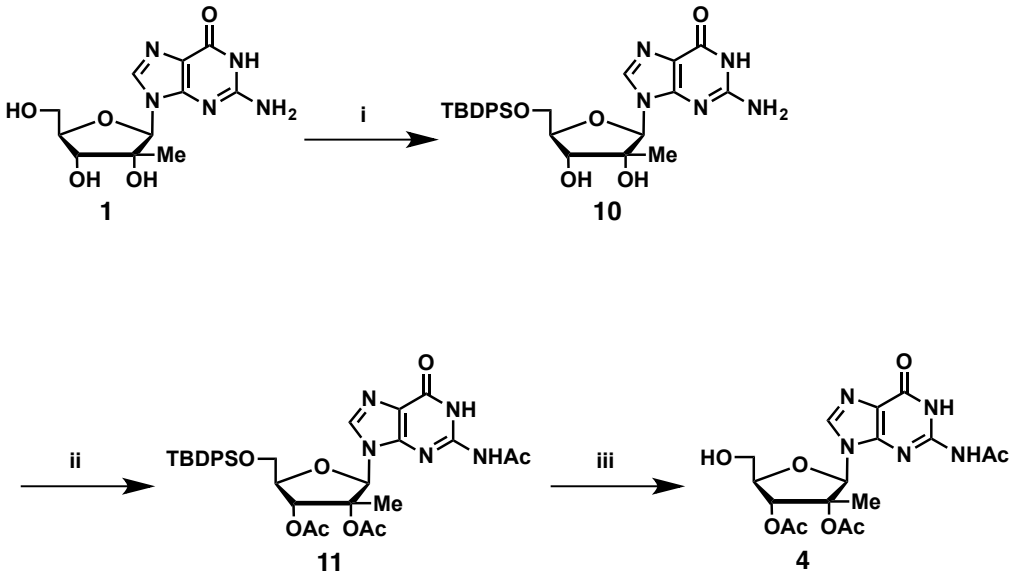

[a]Reagents and conditions: (i) TBDPSCl, pyridine, rt, 24 h, 70%; (ii) DMAP, Ac_2O, pyridine, 90 °C (2 h) then 55 °C, overnight, 74%; (iii) TEA•3HF, THF, 55 °C, 94%.

3.2.1 *In vitro* stability studies with phosphoramidate 6

In order to be effective as therapeutic agents, prodrugs in general should be chemically stable without premature decomposition/release of the active metabolite. Consequently, we evaluated the aqueous stability of the nucleoside phosphoramidate diester **6**.

To determine the half-life for deprotection of the 2-(methylthio)ethyl moiety under physiological conditions, we incubated phosphoramidate diester **6** at 37 °C in 20 mM HEPES buffer (pH 7.4). The deprotection reaction was then monitored by reversed phase high performance liquid chromatography (RP-HPLC). As can be seen in **Figure 3-3**, conversion of both diastereomers of **6** to phosphoramidate **9** proceeded smoothly over the course of 24 h with a half-life of 4.50 ± 0.12 h. When the pH of the reaction mixture was lowered to 2.0, the half-life for the cleavage reaction was 3.78 ± 0.32 h. Overall, the results of the stability studies suggest that prodrug **6** should be sufficiently stable in a biological environment and lipophilic enough to cross cell membranes.

Figure 3-3. Time-course deprotection of 2-(methylthio)ethyl moiety of compound **6** and subsequent formation of compound **9**, as monitored by RP-HPLC.

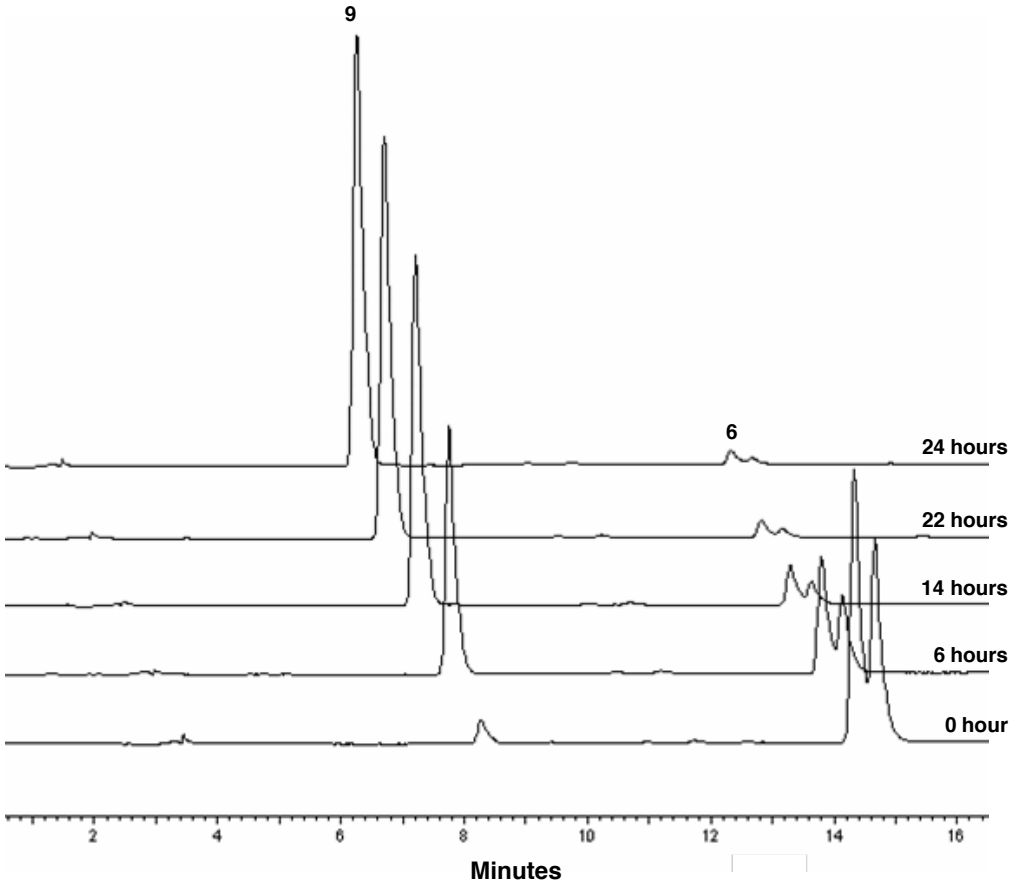

3.2.2. *In vitro* biological activity of 6

The cytotoxicity and anti-viral activities of **1**, **6** and **9** were assessed to determine the impact of our prodrug design on cellular uptake and monophosphate delivery. Firstly, neither compounds **1**, **6,** nor **9** were found to be cytotoxic (IC_{50} > 200 μM) to the host Vero cells (**Figure 3-4**). Secondly, as can been seen in **Table 3-1** and **Figure 3-5**, the ability of diester phosphoramidate **6** to inhibit viral proliferation was five-fold greater than the parent nucleoside **1** and over four-fold greater than monoester phosphoramidate, **9**. Furthermore, nucleoside **1** and monoester phosphoramidate **9** showed no significance difference in their ability to inhibit DENV-2 proliferation. These results suggest that from a biological standpoint, the conversion of 2′-*C*-*β*-Me-G (**1**) to the monophosphate by cellular kinases occurs with similar efficiency as the conversion of monoester phosphoramidate **9** into the nucleotide by HINT1. Most importantly, our findings further suggest that diester phosphoramidate **6** is able to penetrate the cell membrane and deliver 2′-*C*-*β*-Me-G monophosphate more efficiently than **9**, despite the additional anchimeric activation step before HINT1 catalyzed P-N bond cleavage. The necessary role of HINT1 in the activation of phosphoramidates **6** and **9** was confirmed by assessing the antiviral activity of each compound in the presence of HINT1 inhibitor, TrpGc.[234]

Figure 3-4. Cell viability of Vero cells treated with compounds **1**, **6**, and **9**. Vero cells were incubated in the presence of different concentrations of compounds **1**, **6**, and **9** for 72 h. Cell viability was assayed by Neutral Red dye uptake. Results are from six replicates.

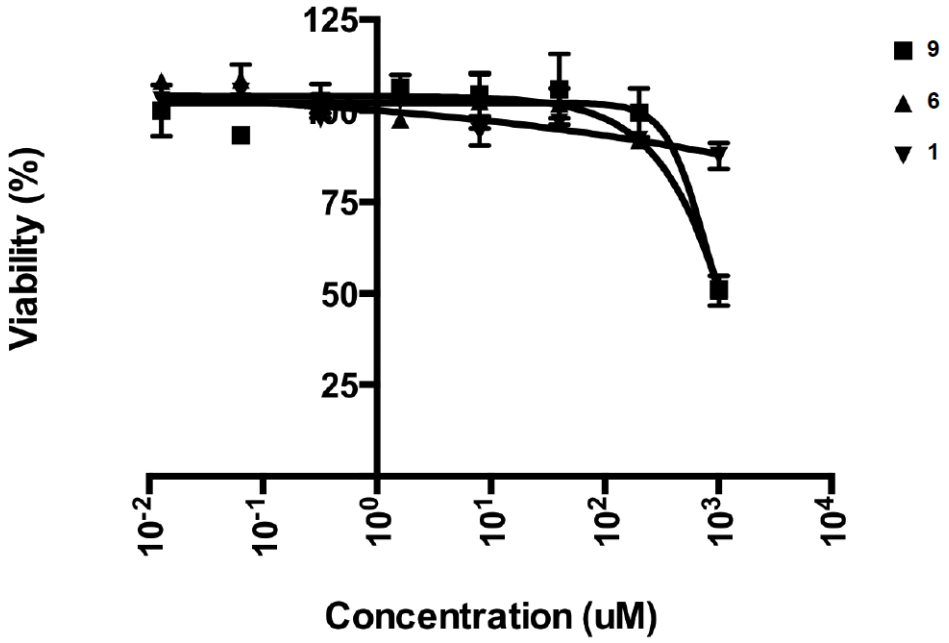

Table 3-1. *In vitro* biological activity of nucleoside **1** and its phosphoramidates **6** and **9**.

compd	IC_{50} (μM)[a]	Observed toxicity (μM)
1	8.14 ± 0.66	>200
6	1.59 ± 0.91	>200
9	6.84 ± 2.36	>200

[a]Experiments were performed in triplicates.

Figure 3-5. Inhibition of DENV-2 replication in Vero cells exposed to compounds **1**, **6**, and **9**.

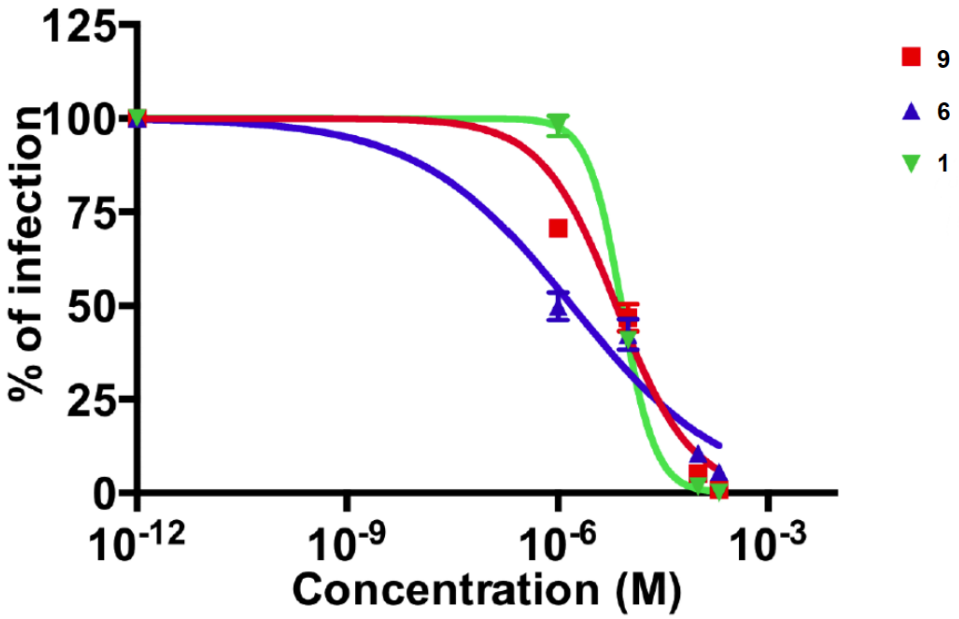

Figure 3-6. Effect of TrpGc on antiviral activity in DENV-2 infected Vero cells treated with compounds **1**, **6**, and **9**. Inhibition of HINT1 reverts the protective effect against DENV-2 replication. Vero cells were infected with DENV-2 (moi = 0.2) and treated with 100 μM of compounds **1**, **6**, and **9** alone or in combination with 100 μM of TrpGc. After 72 hours supernatants were processed for RNA extraction and production of viral progeny was measured by qPCR specific for DENV-2. Results represent the percentage of replication to the untreated DENV-2 infected control. Results are represented as mean of four different experiments. * DENV-2 + (**6**) versus DENV-2 + (**6**) + TrpGc (p = 0.0229). # DENV-2 + (**9**) versus DENV-2 + (**9**) + TrpGc (p = 0.0126). *** DENV-2 versus DENV-2 + (**6**); (**9**); and (**1**) (p = 0.0305; 0.0208; 0.0002, respectively).

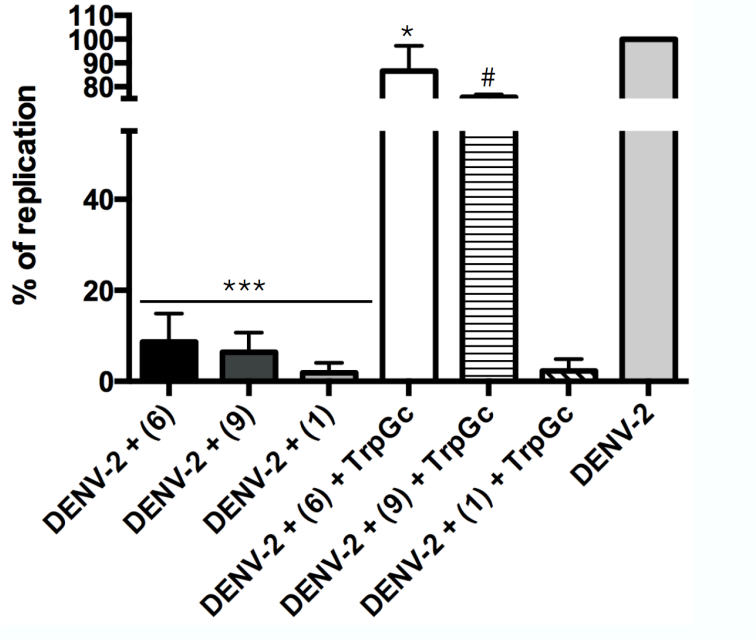

Treatment of DENV-2 infected Vero cells with either compound **6** or **9** in the presence of TpGc resulted in reduced inhibition of viral replication when compared to virus infected cells that were treated with only compound **6** or **9** (**Figure 3-6**). In contrast, DENV-2 infected cells that were treated with nucleoside **1** alone, or in combination with TrpGc did not show significant difference in anti-viral response. This result is expected since the conversion of nucleoside **1** to its monophosphate does not require HINT1. Taken altogether, these results suggest that the phosphoramidase activity of HINT1 is essential for activation of pronucleotides **6** and **9** to 2′-*C*-*β*-Me-G monophosphate.

3.3. Conclusions

Overall, our results demonstrate that the 2-(methylthio)ethyl phosphate masking moiety can be incorporated into a phosphoramidate pronucleotide of an antiviral ribonucleoside, which enhances the anti-viral potency of the parental nucleoside. This approach circumvents the need for an initiating enzymatic activation step, while being dependent on the intracellular liberation of the nucleoside monophosphate from the monoester phosphoramidate metabolite by HINT1. The results of studies addressing the potential for this approach to enhance the oral and systemic delivery of nucleoside monophosphates will be reported in due course.

3.4. Materials and Methods

General Methods and Materials

All chemicals and reagents were obtained from commercial sources and were used without further purification. Anhydrous *N*,*N*-Dimethylformamide (DMF) was obtained from a dry solvent purification system (MBraun) and dispensed under argon. All

reactions were performed under an atmosphere of dry nitrogen unless otherwise noted. All silica gel chromatography and preparative reverse phase purification was performed on a Teledyne Isco CombiFlash Rf system, using Redisep Rf high performance gold silica gel columns (for normal phase purifications) and Redisep Rf high performance gold C18 columns (for reverse phase purifications). Reverse phase purifications were with water and acetonitrile. Lyophilization of compounds after reverse phase purification was performed on a FreeZone 12 Plus freeze dry system (Labconco). All analytical HPLC analyses were performed on a Beckman Coulter System Gold instrument using a Haisil 100 C18 column (4.6 mm X 250 mm, 5 μm, Higgins Analytical Inc.); eluting with a gradient of 10% acetonitrile in phosphate buffer (10 mM or 50 mM, pH 7.4) to 90% acetonitrile in phosphate buffer over 24 minutes at a flow rate of 1.0 mL/min. All Nuclear Magnetic Resonance spectra were obtained on a Brucker Avance III HD 500 MHz spectrometer at ambient temperature. Chemical shifts were recorded in parts per million using the solvent peaks as internal references. All high-resolution mass spectroscopy (HRMS) were performed on an LTQ Orbitrap Velos instrument (Thermo Scientific) in positive-ion mode.

Preparation of compounds 6 and 9

Trityl protection of 5′-*OH and (or)* N^2 *of* 2′-*C-β*-methylguanosine (2a and 2b).[235] To an oven-dried round bottom flask was added 2′-*C-β*-methylguanosine (210 mg, 0.707 mmol), anhydrous DMSO (1.6 mL), and anhydrous pyridine (2.2 mL). The mixture was purged/evacuated extensively under vacuum with N_2. DMTrCl (718 mg, 2.12 mmol) was added to the reaction mixture and stirred overnight at room temperature. The reaction was

diluted with water and extracted with DCM. The organic layer was washed with water, dried over $MgSO_4$, filtered, and concentrated under reduced pressure. The resulting residue was dissolved with DCM and passed through a silica gel plug, eluting first with 1% MeOH in DCM then with 5% MeOH in DCM. The eluted mixture of products was concentrated to dryness under reduced pressure.

5′-*O*-DMTr-2′,3′-*O*-*N*-2 triacetyl 2′-*C*-*β*-methylguanosine (3a) and *N*-2-5′-*O*-DMTr, 2′,3′-*O*-diacetyl 2′-*C*-*β*-methylguanosine (3b). To an oven-dried flask containing 490 mg of the mixed product from the previous step and DMAP (10 mg, 0.150 mmol) was added dry MeCN (7 mL) and anhydrous pyridine (3 mL) and the mixture was purged extensively with N_2. Acetic anhydride (155 μL, 1.63 mmol) was added dropwise and the reaction was stirred overnight at room temperature. The reaction was diluted with water and extracted with DCM (3X) and the organic extract was washed with sat. aq. $NaHCO_3$, water, and brine. The organic layer was dried over $MgSO_4$, filtered and concentrated to dryness. The crude was advanced to the next step.

(2R,3S,4R,5R)-2-(2-acetamido-6-oxo-1,6-dihydro-9H-purin-9-yl)-5-(hydroxymethyl)-3-methyltetrahydrofuran-3,4-diyl diacetate (4). To a round bottom flask containing the crude product from the previous step was added 80% AcOH (2.5 mL) and the reaction was heated for 1.5 h in a pre-warmed oil bath at 55 °C. The reaction was concentrated with co-evaporation with EtOH until the smell of AcOH was not detectable. The resulting residue was purified by flash silica gel chromatography, eluting with $CHCl_3$/MeOH (gradient: 0 – 15%), to give the title compound as a white solid (79.7 mg, 27% yield over three steps). ^{1}H NMR (500 MHz, DMSO-d_6) δ 1.40 (s, 3H), 2.06 (s,

6H), 2.16 (s, 3H), 3.67 (d, J = 12.0 Hz, 1H), 3.78 (d, J = 12.5 Hz, 1H), 4.107 – 4.11 (m, 1H), 5.26 (br s, 1H), 5.35 (d, J = 5.0 Hz, 1H), 6.14 (s, 1H), 8.24 (s, 1H), 11.89 – 12.02 (br, 2H). ^{13}C NMR (125 MHz, $CDCl_3$) δ 18.1, 20.9, 22.0, 24.4, 59.9, 73.2, 80.1, 86.5, 89.9, 122.1, 139.1, 147.5, 147.9, 155.5, 170.46, 170.5, 172.8. HRMS-ESI$^+$ (*m/z*) calcd $[M+H]^+$ for $C_{17}H_{21}N_5O_8$: 424.1463. Found: 424.1447.

Alternate route for synthesis of compound 4

2-amino-9-((2*R*,3*R*,4*R*,5*R*)-5-(((*tert*-butyldiphenylsilyl)oxy)methyl)-3,4-dihydroxy-3-methyltetrahydrofuran-2-yl)-1,9-dihydro-6*H*-purin-6-one (10). Nucleoside **1** (180 mg, 0.606 mmol) was added to an oven-dried round bottom flask, dissolved with anhydrous pyridine (2.6 mL), and purged/evacuated repeatedly under vacuum with N_2. To the solution was added TBDPSCl (0.24 mL, 0.909 mmol) dropwise and the reaction was stirred for 24 h at room temperature. The reaction was diluted with water and the precipitate was filtered under suction. The filtrate was extracted with ethyl acetate (3X), and the combined organic extract was dried over $MgSO_4$, filtered, and concentrated to dryness. The resulting residue was combined with the previously filtered precipitate and recrystallized from MeOH to give 229 mg of product – 70% yield. δ 0.84 (s, 3H), 1.03 (s, 9H), 3.88 – 3.91 (m, 1H), 3.99 (d, J = 11.0 Hz, 2H), 4.07 (t, J = 7.8 Hz, 1H), 5.14 (s, 1H), 5.34 (d, J = 7.0 Hz, 1H), 5.79 (s, 1H), 6.51 (br s, 2H), 7.38 – 7.48 (m, 6H), 7.67 (t, J = 6.0 Hz, 4H), 7.92 (s, 1H), 10.59 (br s, 1H). ^{13}C NMR (125 MHz, $CDCl_3$) δ 18.8, 20.0, 26.7, 63.3, 72.1, 78.3, 81.8, 90.3, 116.5, 127.9, 128.0, 129.9, 132.4, 132.7, 134.7, 135.0, 135.2, 150.8, 153.7, 156.7.

(2*R*,3*R*,4*R*,5*R*)-2-(2-acetamido-6-oxo-1,6-dihydro-9*H*-purin-9-yl)-5-(((*tert*-butyldiphenylsilyl)oxy)methyl)-3-methyltetrahydrofuran-3,4-diyl diacetate (11). To an oven-dried round bottom flask was added compound **10** (189 mg, 0.353 mmol) and DMAP (10 mg, 0.0794 mmol), and dissolved with anhydrous pyridine (2 mL). The mixture was purged/evacuated repeatedly under vacuum with N_2. To the mixture was added acetic anhydride (0.23 mL, 2.47 mmol) dropwise and the reaction was heated at 90 °C for 2 h. The reaction was cooled to 55 °C and was maintained at this temperature overnight with stirring. The reaction was cooled to room temperature, diluted with water, and extracted with DCM (3X). The organic extract was washed with sat. aq. $NaHCO_3$, water, and brine. The organic layer was dried over $MgSO_4$, filtered and concentrated to dryness. The resulting residue was purified by flash silica gel chromatography, eluting with DCM/MeOH (gradient: 0 – 5%), to give 173 mg of product – 74% yield. ^{1}H NMR (500 MHz, $CDCl_3$) δ 1.08 (s, 9H), 1.40 (s, 3H), 2.10 (s, 3H), 2.13 (s, 3H), 2.17 (s, 3H), 3.86 (dd, J = 6.0, 4.0 Hz, 1H), 4.02 (d, J = 11.5 Hz, 1H), 4.21 (m, 1H), 5.81 (d, J = 7.5 Hz, 1H), 6.30 (s, 1H), 7.33 (t, J = 7.5 Hz, 2H), 7.38 – 7.46 (m, 4H), 7.65 (d, J = 7.5 Hz, 2H), 7.69 (d, J = 7.5 Hz, 2H), 8.00 (s, 1H), 8.10 (br s, 1H), 11.87 (br s, 1H). ^{13}C NMR (125 MHz, $CDCl_3$) δ 17.7, 19.3, 20.8, 21.9, 24.5, 27.0, 62.8, 73.6, 81.4, 85.8, 88.2, 122.2, 127.9, 128.1, 130.1, 132.5, 132.9, 135.6, 135.8, 138.1, 147.0, 147.7, 155.5, 169.9, 171.2.

Desilylation of compound **11** (173 mg, 0.261 mmol) was performed with TEA•3HF (85 µL, 0.523 mmol) in dry THF (5 mL) at 55 °C. The reaction was monitored with TLC until completion. Reaction was cooled to room temperature, diluted with MeOH, and concentrated in vacuo. The residue was purified by flash silica gel chromatography,

eluting with $CHCl_3$/MeOH (gradient: 0 – 15%), to give the product – 104.4 mg (94% yield). The ^{1}HNMR and ^{13}CNMR matched those of compound **4**.

(2R,3R,4R,5R)-5-(((((2-(1H-indol-3-yl)ethyl)amino)(2-(methylthio)ethoxy)phosphoryl)oxy)methyl)-2-(2-acetamido-6-oxo-1,6-dihydro-9H-purin-9-yl)-3-methyltetrahydrofuran-3,4-diyl diacetate (5). Nucleoside **4** (79.7 mg, 0.188 mmol) and phosphonating agent 7 (72.7 mg, 0.282 mmol) were added to an oven-dried round-bottom flask and dried overnight on the high vacuum prior to use. Anhydrous pyridine (3.0 mL) was added to the flask and the resulting mixture was purged/evacuated repeatedly under vacuum with N_2. To the mixture was added PivCl (64 μL, 0.517 mmol) over 10 min and the reaction was stirred for eight hours at room temperature. The reaction was quenched over sat. aq. $NaHCO_3$ (5 mL) and extracted with DCM (2X). The organic layer was dried over $MgSO_4$, filtered, concentrated to dryness, and the resulting residue was dried for another hour on the high vacuum. The residue was dissolved with anhydrous pyridine (4 mL) and purged/evacuated repeatedly under vacuum with N_2. Triethylamine (52 μL) was added to the reaction and stirred for a minute at room temperature. Tryptamine (120.5 mg, 0.752 mmol) was dissolved with anhydrous pyridine (1 mL) and was added simultaneously with CCl_4 (27.3 μL, 0.282 mmol) to the reaction. The reaction was stirred for 30 min at room temperature. The reaction was diluted with methanol and concentrated to dryness under reduced pressure. The resulting residue was purified by flash silica gel chromatography, eluting with $CHCl_3$/MeOH (gradient: 0 – 20%), to give a diastereomeric mixture (7:3) of the title compound as a brown solid (88.3 mg, 65% yield). Major diastereomer A: ^{1}H NMR (500 MHz, $CDCl_3$) δ 1.32 (s, 3H), 2.01

(s, 3H), 2.03 (s, 3H), 2.13 (s, 5H, overlaps with proton resonance from diastereomer B), 2.24 (s, 3H), 2.66 (t, J = 7.0 Hz, 2H), 2.98 (t, J = 6.5 Hz, 2H), 3.25 – 3.33 (m, 3H, overlaps with proton resonance from diastereomer B), 3.96 – 4.01 (m, 1H), 4.04 – 4.08 (m, 1H), 4.09 – 4.15 (m, 1H), 4.30 – 4.36 (m, 3H, overlaps with proton resonance from diastereomer B), 4.50 – 4.57 (m, 1H), 5.86 (s, 1H), 6.23 (s, 1H), 7.09 (s, 1H), 7.12 (t, J = 7.5 Hz, 1H), 7.21 (t, J = 7.5 Hz, 1H), 7.39 (d, J = 8.0 Hz, 1H), 7.57 (d, J = 8.0 Hz, 1H), 7.66 (s, 1H), 8.26 (br s, 1H), 11.26 (br s, 1H), 12.25 (br s, 1H). ^{13}C NMR (125 MHz, $CDCl_3$) δ 15.9, 18.0, 20.8, 21.8, 24.1, 27.7 (d, J = 6.75 Hz), 34.1, 34.2, 41.7, 65.3 (d, J = 5.25 Hz), 65.4 (d, J = 5.75 Hz), 75.9, 79.5 (d, J = 10.25 Hz), 86.1, 91.6, 111.6, 112.2, 118.6, 119.7, 122.5 (d, J = 5.13 Hz), 122.9, 127.2, 136.6, 138.6, 147.94, 148.14, 155.8, 169.7, 173.5. ^{31}P NMR (202 MHz, $CDCl_3$) δ 10.79 and 9.15. HRMS-ESI$^+$ (*m/z*) calcd $[M+H]^+$ for $C_{30}H_{38}N_7O_{10}PS$: 720.2211. Found: 720.2192.

((2R,3R,4R,5R)-5-(2-amino-6-oxo-1,6-dihydro-9H-purin-9-yl)-3,4-dihydroxy-4-methyltetrahydrofuran-2-yl)methyl (2-(methylthio)ethyl) (2-(1H-indol-3-yl)ethyl)phosphoramidate (6). To a round-bottom flask containing **5** was added 7N NH_3/MeOH and the resulting mixture was stirred for four hours at room temperature. The reaction was concentrated under reduced pressure and the resulting residue was purified by flash silica gel chromatography, eluting with $CHCl_3$/MeOH (gradient: 0 – 20%), to give the title compound as a white solid. Reverse phase C18 flash column purification with H_2O/MeCN (gradient: 85 – 0% H_2O) and lyophilization gave a diastereomeric mixture (~ 1:1) of title compound as a white powder (46.6 mg, 64% yield). ^{1}H NMR (500 MHz, DMSO-d_6) δ 0.82 (s, 3H), 1.75 (s, 1H), 2.05 (s, 2H), 2.69 (q, J = 7.5 Hz, 2H), 2.82

– 2.85 (m, 2H), 3.00 – 3.10 (m, 2H), 3.89 – 4.08 (m, 4H), 4.14 – 4.17 (m, 1H), 4.23 – 4.30 (m, 1H), 5.12 – 5.22 (m, 2H), 5.42 (dd, *J* = 17.0, 6.5 Hz, 1H), 5.77 (s, 1H), 6.51 (br s, 2H), 6.89 – 6.94 (m, 1H), 7.03 (q, *J* = 7.0 Hz, 1H), 7.11 (d, *J* = 8.0 Hz, 1H), 7.30 (dd, *J* = 5.5, 3.0 Hz, 1H), 7.46 (d, *J* = 7.5 Hz, 1H), 7.81 (d, *J* = 7.0 Hz, 1H), 10.61 (br s, 1H), 10.78 (br s, 1H). ^{13}C NMR (125 MHz, MeOD) δ 15.7, 20.2, 28.7 (d, *J* = 6.13 Hz), 28.8 (d, *J* = 6.0 Hz), 34.66 (d, *J* = 2.38 Hz), 34.73 (d, *J* = 2.38 Hz), 65.8 (d, *J* = 4.63 Hz), 66.4 (d, *J* = 5.13 Hz), 66.46 (d, *J* = 5.5 Hz), 66.55 (d, *J* = 5.63 Hz), 73.9, 74.3, 80.1 (d, *J* = 4.63 Hz), 82.0 (d, *J* = 8.88 Hz), 82.1 (d, *J* = 8.5 Hz), 92.6, 92.9, 112.2 (d, *J* = 5.25 Hz), 113.1 (d, *J* = 2.75 Hz), 117.76, 117.84, 119.31 (d, *J* = 2.75 Hz), 119.6, 122.2 (d, *J* = 4.25 Hz), 123.7 (d, *J* = 1.88 Hz), 128.7 (d, *J* = 1.75 Hz), 137.3, 137.5, 138.1 (d, *J* = 3.0 Hz), 152.7 (d, *J* = 5.75 Hz), 155.3 (d, *J* = 3.75 Hz), 159.4. ^{31}P NMR (202 MHz, MeOD) δ 10.71 and 10.62. HRMS-ESI$^+$ (*m/z*) calcd $[M+H]^+$ for $C_{24}H_{32}N_7O_7PS$: 594.1894. Found: 594.1879.

((2R,3R,4R,5R)-5-(2-amino-6-oxo-1,6-dihydro-9H-purin-9-yl)-3,4-dihydroxy-4-methyltetrahydrofuran-2-yl)methyl phosphate (8).[236] To an oven-dried round-bottom flask was added nucleoside **1** (89.6 mg, 0.301 mmol) and $(EtO)_3PO/POCl_3$ (10:1; 830 μL) at 0 °C. The reaction was stirred at 0 °C for 45 min, quenched with H_2O, and neutralized with conc. ammonium hydroxide. The reaction was purified with a sephadex DEAE column, eluting with 1 M TEAB (pH 7.2; gradient: 0 – 60%). The relevant fractions were pooled and lyophilized to give a white solid. The resulting solid was subjected to ion-exchange through a Dowex50WX8 column. Reverse phase C18 purification and subsequent lyophilization gave the title compound as a white powder – 110 mg, 74%

yield. ^{1}H NMR (500 MHz, D_2O) δ 1.01 (s, 3H), 4.07 – 4.10 (m, 1H), 4.20 – 4.22 (m, 2H), 4.31 (d, J = 9.0 Hz, 1H), 5.98 (s, 1H), 8.22 (s, 1H). ^{13}C NMR (125 MHz, D_2O) δ 18.7, 62.1 (d, J = 4.25 Hz), 72.1, 79.4, 81.4 (d, J = 8.25 Hz), 90.6, 116.3, 137.4, 151.2, 154.9, 160.4. ^{31}P NMR (202 MHz, D_2O) δ 3.98 and 2.62. HRMS-ESI$^+$ (*m/z*) calcd $[M+H]^+$ for $C_{11}H_{16}N_5O_8P$: 378.0809. Found: 378.0814.

((2R,3R,4R,5R)-5-(2-amino-6-oxo-1,6-dihydro-9H-purin-9-yl)-3,4-dihydroxy-4-methyltetrahydrofuran-2-yl)methyl hydrogen (2-(1H-indol-3-yl)ethyl)phosphoramidate (9). Route A: Compound **8** (100 mg, 0.250 mmol) and tryptamine (160 mg, 1.0 mmol) was dissolved with water (1.0 mL) and the pH adjusted to 6.5 with 1N HCl. To the reaction mixture was added EDC (240 mg, 1.25 mmol) and the reaction was stirred at 55 °C. The reaction was concentrated and purified by flash column silica gel chromatography eluting first with 20% MeOH in $CHCl_3$, followed by $CHCl_3$/MeOH/H_2O/NH_4OH (5:3:0.5:0.005). The relevant fractions were pooled and concentrated under vacuum. The resulting residue was ion-exchanged with Dowex50 column. Reverse phase C18 flash column purification with acetonitrile and water and subsequent lyophilization of relevant fractions gave the title compound as a white powder – 15.0 mg, 23% yield.

Route B: Compound **6** (22.0 mg, 0.0371 mmol) was dissolved with MeOH (1 mL) and to the solution was added 10 mM HEPES (240 mL, pH 7.0). The reaction mixture was incubated at 37 °C for 30 h. The reaction was concentrated, and the resulting residue was purified by flash column silica gel chromatography eluting first with 20% MeOH in $CHCl_3$, followed by $CHCl_3$/MeOH/H_2O/NH_4OH (5:3:0.5:0.005). The relevant fractions

were pooled and concentrated to dryness. Reverse phase C18 flash column purification with acetonitrile and water and subsequent lyophilization of relevant fractions gave the title compound as a white powder – 16.2 mg, 84% yield. ^{1}H NMR (500 MHz, D_2O) δ 0.92 (s, 3H), 2.72 – 2.84 (m, 2H), 3.02 – 3.11 (m, 2H), 4.07 – 4.09 (m, 1H), 4.17 – 4.27 (m, 2H), 4.31 (d, J = 9.0 Hz, 1H), 5.77 (s, 1H), 6.93 (t, J = 7.5 Hz, 1H), 7.09 (t, J = 7.0 Hz, 1H), 7.30 (d, J = 8.0 Hz, 1H), 7.36 (d, J = 8.0 Hz, 1H), 7.86 (s, 1H). ^{13}C NMR (125 MHz, D_2O) δ 18.6, 26.7 (d, J = 7.5 Hz), 41.6, 62.6, 72.0, 79.3, 80.6 (d, J = 9.0 Hz), 90.1, 111.2, 112.17, 115.9, 118.1, 118.6, 121.3, 122.3, 126.4, 135.8, 136.5, 150.6, 154.9, 160.4. ^{31}P NMR (202 MHz, D_2O) δ 9.22. HRMS-ESI$^+$ (*m/z*) calcd $[M+H]^+$ for $C_{21}H_{26}N_7O_7P$: 520.1704. Found: 520.1703.

Cells and virus stocks

Vero cells (kidney epithelia from African Green Monkey - CCL81TM) were obtained from ATCC cells and maintained in Dulbecco's Modified Eagle Media, pH 7.2, supplemented with 5% Fetal Calf Serum, 100 U/mL of penicillin and 100µg/mL of streptomycin. Baby hamster kidney cells (BHK), obtained from ATCC, were maintained in Alpha-Minimum Essential Medium supplemented with supplemented with 10% Fetal Calf Serum, 100 U/mL of penicillin and 100µg/mL of streptomycin. All mammalian cells were kept at 37°C in an incubator with a 5% atmosphere of CO_2. C6/36 cells (from *Aedes albopictus* mosquitos), kindly provided by Dr. Andrea T da Poian (IbqM - UFRJ, Brazil) were maintained in Leibovitz medium, pH 7.3, supplemented with 5% Fetal Calf Serum, 3% tryptose phosphate, 7.5% sodium bicarbonate, 2% L-glutamine, essential amino acids 10 mg/mL, and 1% gentamicin. Cells were kept at 28°C in a B.O.D incubator.

Virus isolate used in this work is the DENV-2 prototype 16681 Virus stocks were generated by infecting C6/36 cells at 70% confluence with a multiplicity of infection (m.o.i) of 0.05 in Leibovitz medium with 2% Fetal Calf Serum. Infected cells were incubated at 28 ºC for 9 days and inspected every day until the cytopathic effect was clearly observed. Supernatants were then collected, centrifuged at 1,200 g for 10 min to clear cellular debris and stored at -70°C until use. The titter of viral stocks was measured by Plaque assay in BHK cells.

Cytotoxicity assay

Cell toxicity of all compounds used in this work was tested in Vero by Neutral Red dye exclusion assay. Briefly, cells were cultured with varying concentrations of each compound and incubated for 72 hours at 37°C. After this period, cells were incubated with 0.05% neutral red solution for 3 hours, washed with 1X PBS and fixed with 20% paraformaldehyde for 5 min. Cells were washed again and the incorporated dye was extracted with a 50% methanol and 1% acetic acid solution for 20 min. Plates were read at 490nm in an ELISA reader. Results obtained with the neutral red dye exclusion assay were confirmed using the CellTiter Blue Cell Viability Kit (Promega, Madison - USA) according to manufacturer's instructions.

Virus replication inhibition assay

The antiviral effect of each compound alone (**1**; **6**; and **9**), or in combination with the TrpGc compound (Hint-1 inhibitor) was tested in Vero cells. Monolayers of each cell linage were inoculated with DENV-2 at an m.o.i of 0.2 for 2 hours. After this period, cells were washed with 1X PBS to remove unbound viruses and fresh media was added

with the highest non-cytotoxic concentration of **1**; **6**; and **9**, or the highest concentration of each of these compounds with 100 μM of TrpGc. Infected cells were also cultured with culture medium with 1% DMSO, as negative controls, or with 200 μM of Ribavirin as reference drug for DENV replication inhibition. After 72 h, culture supernatants were collected, and viral RNA was extracted using the QIAamp Viral RNA Mini Kit (Qiagen – Hamburg, Germany), according to manufacturer's instructions. The synthesis of cDNA was performed with random hexamers as primers and the High Capacity cDNA kit (Life Technologies – Carlsbad, USA) according to manufacturer's instructions. The detection and quantification of the cell free viral genomic RNA was performed by qPCR using specific primers and probe hybridizing in the protein E gene region as already described.[237] qPCR conditions were as follow: a reaction mixture consisting of 12.5μL of TaqMan (Invitrogen – Carlsbad, USA), 50 pmol of each primer, 9 pmol of the probe and 7μL of the cDNA reaction to a final volume of 25μL was submitted to 40 cycles of amplification in a ABI PRISM 7000 Detection System (Life Technologies – Carlsbad, USA) using 60C annealing temperature. Amplification results were analyzed using the 7000 SDS software (Life Technologies – Carlsbad, USA) and the threshold parameter was manually adjusted. Percentage of inhibition of DENV replication was calculated by the CT rule. Plaque reduction assay was also performed to confirm the results obtained with qPCR quantification of virus production. All experiments were performed with biological triplicates. The significance of results was tested by unpaired t-test with Welch's correction using GraphPad 5. Differences were considered significant with a $p < 0.05$.

The dose response curve was also performed with the compounds that inhibited DENV replication. For this purpose, DENV-2-infected Vero cells were cultured with the selected compounds at concentrations varying from 0.05 to 100 μM and virus replication was measured by qPCR as above. IC_{50} values were obtained by the Hill's regression curve using Prism 5. Experiments were always performed in triplicates.

Chapter 4

Chemoproteomic Profiling of the Cellular Fate(s) of Nucleotide Monoester Phosphoramidates

4.1. Introduction

Nucleoside analogs are an important class of antiviral and anticancer therapeutics. As a drug class, nucleoside analogs do not have cellular activity on their own but depend on phosphorylation by cellular kinases to the respective mono-, di-, and tri-phosphorylated metabolites. The generated nucleotide metabolites could either directly inhibit cellular proteins/enzymes or could become incorporated into synthesized DNA and RNA, which could ultimately be cytotoxic.[13, 61, 238, 239] Formation of nucleoside monophosphate by nucleoside kinases is generally considered rate limiting during metabolic activation nucleoside analogs.[18, 240]

The utility of this class of compounds can be curtailed due to development of resistance by cells. A primary mechanism of cellular resistance to nucleoside analogs involves inefficient initial phosphorylation by cellular nucleoside kinases. Direct delivery of nucleoside analog monophosphates in cells instead of the parent nucleoside analog, could in theory help circumvent such inefficiencies. However, the highly polar nature of monophosphates, poor membrane permeability, and susceptibility to degradation by phosphatases precludes direct administration of nucleoside monophosphates to cells as a viable strategy for bypassing the inefficient monophosphorylation step. Nevertheless,

several phosphate prodrug strategies have been developed as a means to bypass the inefficient initial phosphorylation of nucleoside analogs in cells.[61, 70, 151]

In general, activation/metabolism of phosphate prodrugs can be achieved through enzymatic, chemical or a combination of both enzymatic and chemical means. For example, the popular aryloxy amino acid phosphoramidates (ProTide) relies on initial (carboxy)esterase catalyzed hydrolysis of an ester within its amino acid moiety. The generated carboxylate undergoes an intramolecular nucleophilic attack at the phosphate to form a five-membered ring intermediate, which is spontaneously hydrolyzed to produce a monoester phosphoramidate intermediate. Subsequent enzymatic hydrolysis of the monoester phosphoramidate by hHINT1 leads to release of the intended nucleoside analog monophosphate (**Figure 4-1A**).[112, 114]

A more streamlined pronucleotide approach developed by Wagner and coworkers is the amino acid monoester phosphoramidate, which upon cellular uptake is directly hydrolyzed by hHINT1 to release the desired monophosphate in one step (**Figure 4-1B**).[136, 142] Notwithstanding its anionic characteristic at physiological pH, the monoester phosphoramidate approach has been shown to be an effective means for intracellular delivery of nucleotides for antiviral and anticancer applications.[145, 148, 241] It is worth noting that several studies have reported the release of a monoester phosphoramidate as a metabolite in the plasma/blood of animals dosed with nucleotide prodrugs employing the ProTide and other amidate-based pronucleotide strategies.[145, 242, 243] As such, monoester phosphoramidates represent an important intermediate necessary for intracellular delivery of nucleotides.

To date, little to no research exists on the mechanism of cellular uptake, intracellular trafficking, and metabolism (apart from HINT1 catalyzed hydrolysis) of nucleoside monoester phosphoramidates. Worthy of note is the observation by Reid and coworkers that multidrug resistant protein 5 (MRP5) was involved in the efflux of alaninyl-d4TMP in cells treated with the ProTide derivative of d4T (**Figure 4-1C**).[244] The potential for active efflux could diminish the cellular activity of nucleoside monoester phosphoramidate prodrugs, highlighting the need to fully define protein interacting partners of such a critical phosphoramidate intermediate.

Figure 4-1. Mechanism of activation for aryloxy amino acid phosphoramidate (ProTide) (A) and amino acid monoester phosphoramidate (B) pronucleotides. (C) Chemical structure of So324, a ProTide derivative of d4T.

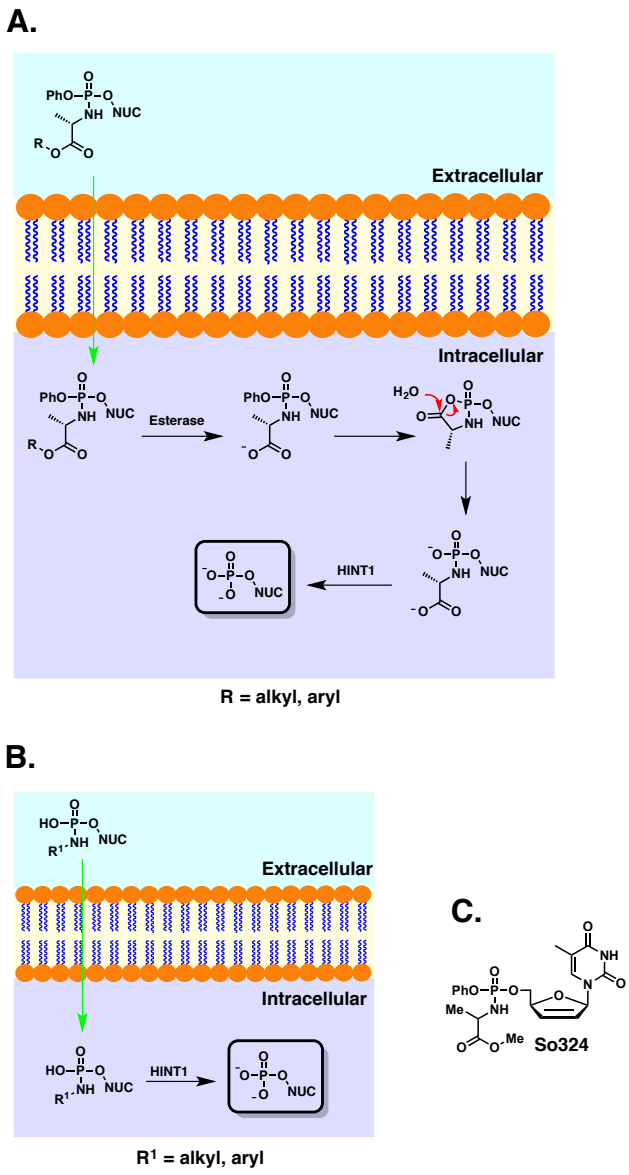

First described by Westheimer and coworkers,[245] photo-affinity labeling (PAL) has emerged as a powerful tool for studying protein-protein, as well as, small molecule-protein interactions. Several strategies for PAL studies have been extensively reviewed.[246-249] Upon binding/interacting with proteins, a small molecule bearing a photocrosslinking moiety can be photoactivated to generate a chemically reactive intermediate, which undergoes covalent conjugation to the bound protein. Typical photoreactive groups used in PAL experiments include benzophenone, diazirines, and aryl azides (**Figure 4-2)**. Coupled with mass spectrometry-based proteomics, protein interacting partners of PAL probes can be identified after avidin-based pulldown/enrichment experiments. Herein, we report the development of monoester phosphoramidate based photo-affinity probes as chemical tools to map the *interactome* of nucleoside monoester phosphoramidates. We envision that information derived from the present study will fill the gap in knowledge as it relates to the cellular uptake and metabolic fate(s) of nucleoside monoester phosphoramidates.

4.2. Results and Discussion

4.2.1. Design and Synthesis of Nucleoside Monoester Phosphoramidate PAL Probes

Owing to our previous work with tryptamine monoester phosphoramidate pronucleotides,[147, 148, 241] we elected to prepare PAL probes incorporating tryptamine as a phosphate-protecting moiety. We limited our choice of photoreactive groups to aryl azide and diazirine due to their relatively small size when compared to benzophenone.[247] Consequently, our initial PAL probe design involved preparation of a 5-azido tryptamine

monoester phosphoramidate of guanosine. For ease of synthesis we envisioned installation of an alkynyl benzyl moiety at the N^7 position as an enrichment arm for use in avidin-based pulldown experiments. Since our PAL probes are monoester phosphoramidates, we sought to reduce or abrogate potential hydrolysis by hHINT1. To achieve this goal, we protected the glycon 2′,3′-hydroxyls with an isopropylidene ketal group. The glycon 2′,3′-hydroxyls of the nucleotide product of hHINT1 catalyzed hydrolysis of nucleoside monoester phosphoramidate have been shown to engage in critical hydrogen-bonding interactions with Asp43 in the active site of hHINT1 (**Figure 4-3**).[250] Hence, nucleoside monoester phosphoramidates lacking this critical interaction could be poor substrates of hHINT1 and should be resistant towards hydrolysis by hHINT1. In addition, due to the low labeling efficiency often associated with aryl azides,[246, 247, 251, 252] we designed another probe bearing a 3-trifluoromethyl-3-aryldiazirine at the N^7 position as a photo-crosslinking arm. A propargyl group was installed at the 2′-OH position, which we envisioned would be sufficient to disrupt the critical H-bond interaction between Asp43 of hHINT1 and the monoester phosphoramidate probe. Moreover, this probe design should ensure the highest level of enrichment in the event of phosphoramidate hydrolysis, since both photo-crosslinking and enrichment moieties are on the nucleoside portion of the probe.

4.2.2. Synthesis of Nucleoside Monoester Phosphoramidate PAL Probes

Probe A (**Scheme 4-1**)

The synthesis of 5-Azido tryptamine (**1**) was performed according to published procedure.[253] 4-Ethynylbenzyl bromide (**2**) was prepared from 4-ethynylbenzyl alcohol as

previously reported.[254] Alkylation of guanosine acetonide with **2** afforded the N^7 alkylated product **3** in 75% yield. In order to install the phosphoramidate moiety, phosphonation of **3** with **Reagent P**[255] was performed in the presence of PivCl and the resulting *H*-phosphonate was subjected to oxidative coupling via standard Atherton-Todd conditions to install 5-azido tryptamine. The methylthio ethyl moiety of the resulting compound **4** was removed in 10 mM HEPES buffer (pH 7.2, 37 °C) to give compound **5** (Probe A) in 16% yield.

Probe B (**Scheme 4-2**)

The synthesis of 4-(trifluoromethyl)diazirine benzyl bromide (**6**) was synthesized from 4-[3-(trifluoromethyl)-3H-diazirin-3-yl]benzyl alcohol according to published procedure.[256] Synthesis of 2′-*O*-propargyl diaminopurine (**8**) was performed with compound **7**[257] according to published procedure,[258] and was subsequently deaminated to give 2′-*O*-propargyl guanosine (**9**). Protection of 5′-OH and N^2-positions of nucleoside **9** with DMTrCl gave compound **10**, which was subsequently treated with TBDMSCl and detritylated with warm AcOH to give nucleoside **11** in 46% yield over two steps. Alkylation of **11** with **6** afforded the N^7 alkylated product **12** in good yield (73% yield). Installation of the tryptamine phosphoramidate moiety was performed in the same manner as previously described for Probe A, and subsequent desilylation gave compound **14** in 8% yield over two steps. Deprotection of the methylthio ethyl moiety in 10 mM HEPES (pH 7.2, 37 °C) afforded **15** (Probe B) in 63% yield.

Figure 4-2. Mechanism of activation and reactive intermediates of benzophenone (A), diazirine (B), and aryl azide (C) photocrosslinkers. Rearrangement of short-lived singlet nitrene into electrophilic benzazirine and dihydroazepine byproducts reduces the labeling efficiency for aryl azide photoaffinity based probes.

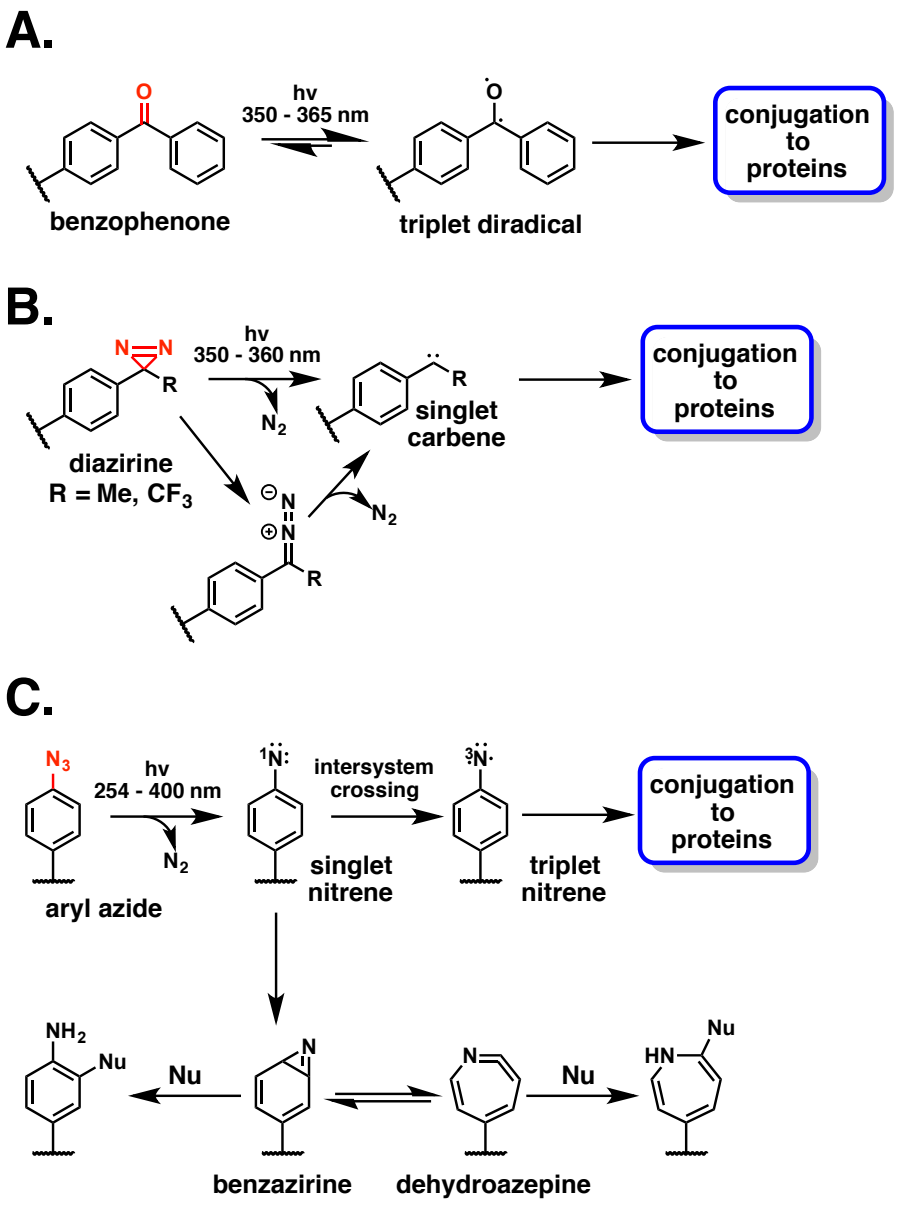

Figure 4-3. High resolution complex of AMP bound to hHINT1 (PDB ID 3TW2). The hydroxyls of the sugar engage in H-bond interactions with Asp43 of hHINT1.

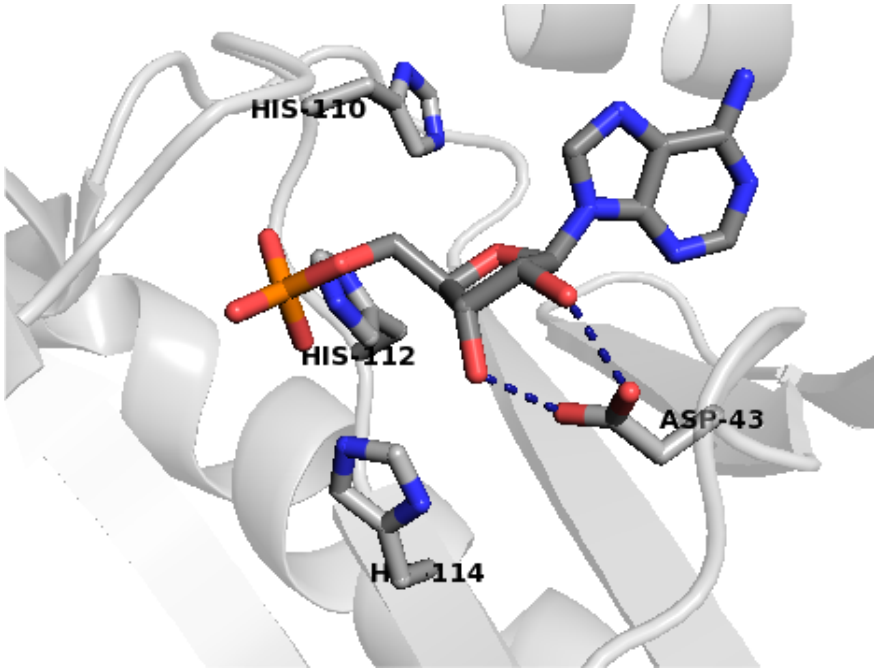

Scheme 4-1. Preparation of PAL Probe A.

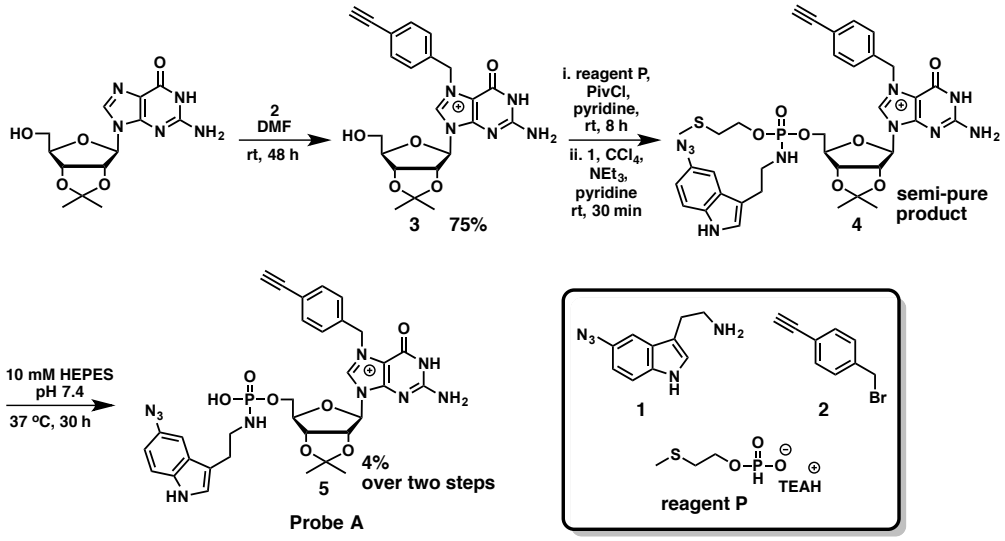

Scheme 4-2. Preparation of PAL Probe B.

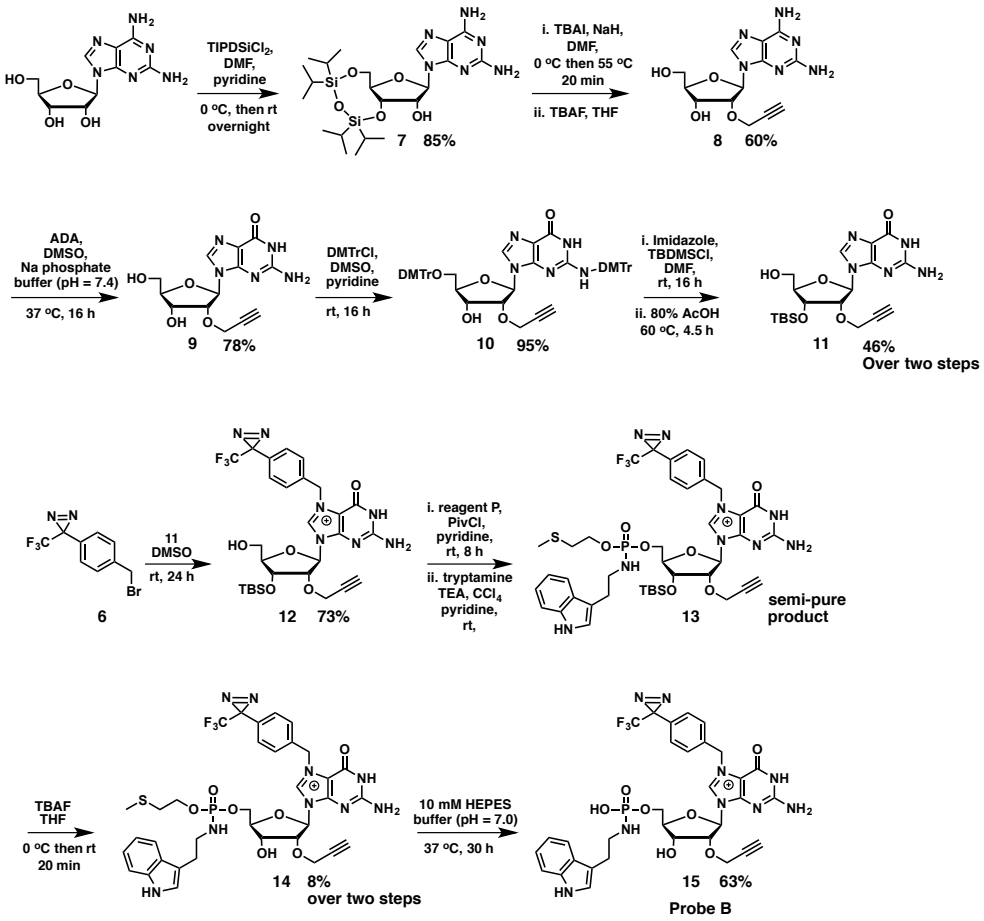

Figure 4-4. (A) Schematic for photoaffinity labeling with PAL probes. (B) Fluorescence spectrum showing that PAL probes are resistant to hHINT1 catalyzed hydrolysis. Fluorescent and total protein loading (Coomassie) gels of photoaffinity labeling with PAL probes (C), and competition experiment with competitor **Y** (D).

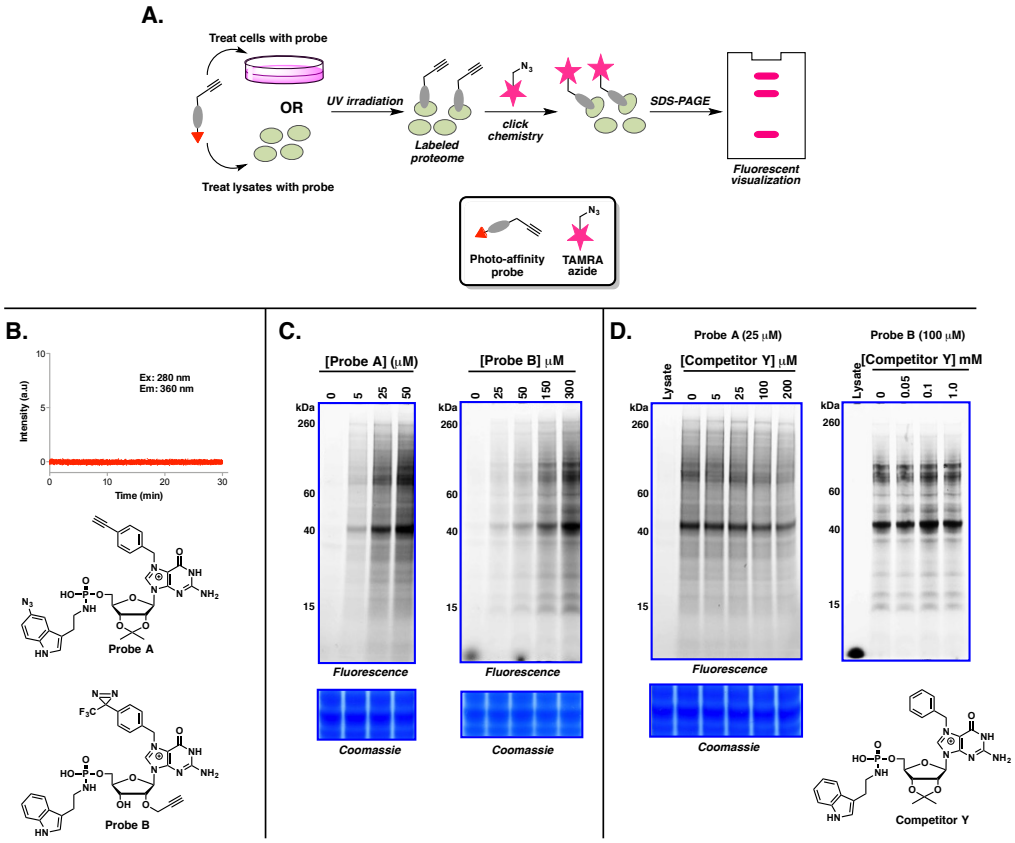

4.2.3. *In vitro* Proteome Labeling with Phosphoramidate PAL Probes.

With the PAL probes in hand, we set out to perform proteome-labeling studies in HEK293T cell lysates (**Figure 4-4A**). Prior to performing these studies, we first determined if our modifications to the glycon 2′,3′-hydroxyls were sufficient to offer protection from hHINT1-catalyzed hydrolysis of our PAL probes. Steady-state hHINT1 catalyzed hydrolysis of PAL probes was evaluated using a continuous fluorescence assay,[138] which showed that both PAL probes were indeed resistant to P-N bond hydrolysis by hHINT1 (**Figure 4-4B)**. Having established the enzymatic stability of our PAL probes, we next performed labeling studies with HEK293T cell lysates. Following incubation with the PAL probes and photoirradiation with a 365 nm UV source, protein labeling was visualized via conjugation of a fluorescent reporter dye, using the copper-catalyzed Huisgen 2,3-dipolar cycloaddition "click" reaction,[259, 260] and the labeled proteome was resolved by SDS-PAGE.

As can be seen in **Figure 4-4C**, both PAL probes showed dose-dependent protein labeling. Notably, the observed protein labeling occurred only after photoirradiation and does not appear to be from nucleophilic conjugation to the cationic centers of the PAL probes (results not shown). Competition studies with competitor **Y**, a non-functionalized derivative of Probe A (**Figure 4-4D**), showed dose-dependent reduction in labeling in lysates treated with Probe A. Unfortunately, no competition for labeling in experiments using Probe B was observed. This result seems to suggest that certain structural feature(s) common to Probe A and the competitor is(are) responsible for the observed protein labeling. We suspected that the isopropylidene moiety could also drive non-specific

hydrophobic interactions between Probe A and the labeled proteins. Such non-specific hydrophobic interactions are most likely absent in the nucleoside monoester phosphoramidates reported in the literature. Furthermore, such non-specific hydrophobic interactions only serve to obfuscate the true small molecule-protein interaction profile of the PAL probe. Therefore, we set out to determine which PAL probe had a higher propensity to engage in non-specific hydrophobic interactions.

If our probes are engaging in meaningful/specific interactions with proteins, we reasoned that such specific interactions would be lost or diminished in denatured lysates. Consequently, any protein labeling observed upon incubation with denatured lysates should be most likely driven by non-specific hydrophobic interactions. Both PAL probes were subjected to labeling experiment using heat-denatured lysates and the labeled proteome was resolved by SDS-PAGE. The result showed that Probe A had a significantly higher level of protein labeling when compared to Probe B (**Figure 4-5**), and as a result, we stopped further evaluation of Probe A and focused only on Probe B.

Figure 4-5. Fluorescence and total protein loading (Coomassie) gels of protein labeling experiment with PAL probes in heat-denatured lysates. High protein labeling by Probe A suggests greater propensity for non-specific hydrophobic interactions compared to Probe B.

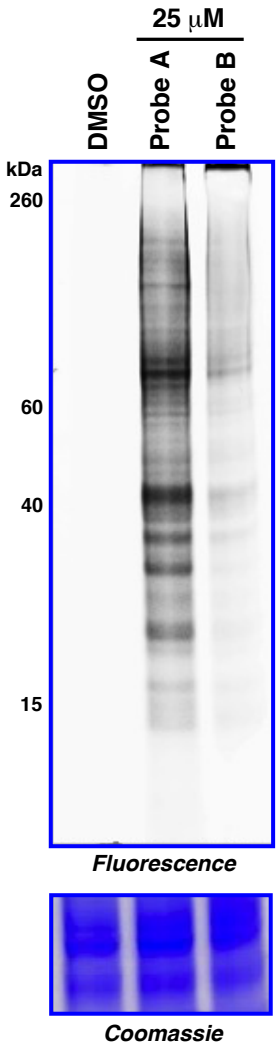

Figure 4-6. (A) Schematic for Chemoproteomics profiling of small molecule-protein interaction with PAL probes. (B) Coomassie stain of enriched proteins following elution from NeutrAvidin resin. Probe A was included in the experiment to assess potential differences in protein enrichment pattern of both PAL probes.

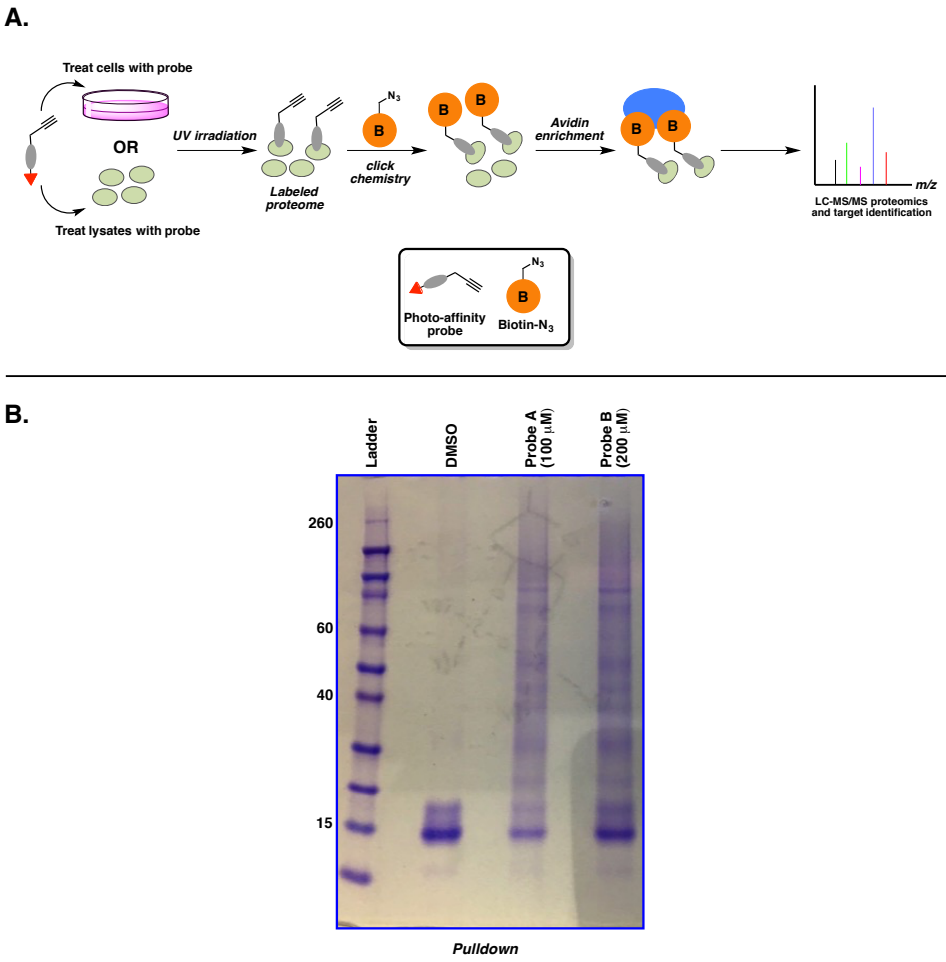

4.2.4. Protein Enrichment and Chemoproteomics with Probe B in HEK293T Lysates

Having demonstrated dose-dependent protein labeling by Probe B, we next evaluated the utility of Probe B for avidin enrichment and pulldown experiments. First, lysates were labeled using Probe B and a biotin reporter was subsequently conjugated to probe-labeled proteins via "click" reaction with biotin-azide (**Figure 4-6A**). The biotinylated proteins were enriched over neutravidin agarose resin, eluted off the neutravidin resin, and resolved by SDS-PAGE. The result showed significant enrichment and pulldown of proteins by Probe B when compared to vehicle (DMSO) treated control (**Figure 4-6B**). We next performed a chemoproteomic study with HEK293T cell lysates, in which probe-labeled proteins were biotinylated, enriched over neutravidin resin, tryptic digested, and subjected to mass spectrometry-based proteomics analysis. Putative proteins were considered relevant hits based on the presence of at least two unique peptides. In addition, the identified proteins were required to be present in at least two out of three replicates. Furthermore, putative proteins were screened against contaminant lists[261, 262] and a database[263] of common protein contaminants before considered as potentially relevant protein hits. In all, we identified 104 putative protein (see **Appendix**) interacting partners of Probe B, thus demonstrating that Probe B is a viable chemical tool for profiling protein interacting partners of nucleoside monoester phosphoramidates.

4.2.5. In-Cell Protein Labeling Studies

With the confirmed utility of Probe B in a protein pulldown experiment, we next assessed the ability of Probe B to label proteins in living cells. Since Probe B could be

potentially metabolized by an unknown process, we first assessed if there was an optimal incubation time for achieving the highest levels of protein labeling. We incubated Probe B with cells for 30, 60, and 120 min and photo-irradiated cells after each time point. Lysates generated from cells at each time point were subjected to "click" chemistry labeling with a fluorescent dye and the labeled proteins were resolved by SDS-PAGE. The result suggested that optimal protein labeling was achieved after a 60 min incubation of cells with Probe B (results not shown).

Next, we carried out a protein labeling study with HEK293T cells with variable concentrations of Probe B. Lysates from the cells were subsequently tagged with a fluorescent reporter and resolved by SDS-PAGE. The result showed that 200 μM of Probe B sufficiently labeled proteins and the observed protein labeling was significantly above the background (**Figure 4-7**). Importantly, no significant protein labeling was observed when cells were treated with 200 μM Probe B without photoirradiation. This result suggests that protein labeling in live cells is mainly due to photoactivation of our probe and not due to nucleophilic conjugation to proteins. Furthermore, the protein labeling pattern was distinct from that observed in lysates. Taken together, our labeling result highlight the importance of the cell membrane as an important exclusionary physiochemical barrier to environmental solutes and suggests that labeling studies performed with lysates potentially obfuscate or overstate the true interactome for any particular small molecule. In fact, we performed a cell-based proteomics experiment with HEK293T cells, in which we identified only 14 putative proteins interacting partners (see

Appendix). The number of identified proteins is significantly lower than that identified with the lysate-based study (104 proteins vs 14 proteins).

Figure 4-7. Fluorescence and total protein loading (Coomassie) gels of in-cell protein labeling experiment with Probe B. HEK293T cells were incubated with Probe B for one hour at 37 °C.

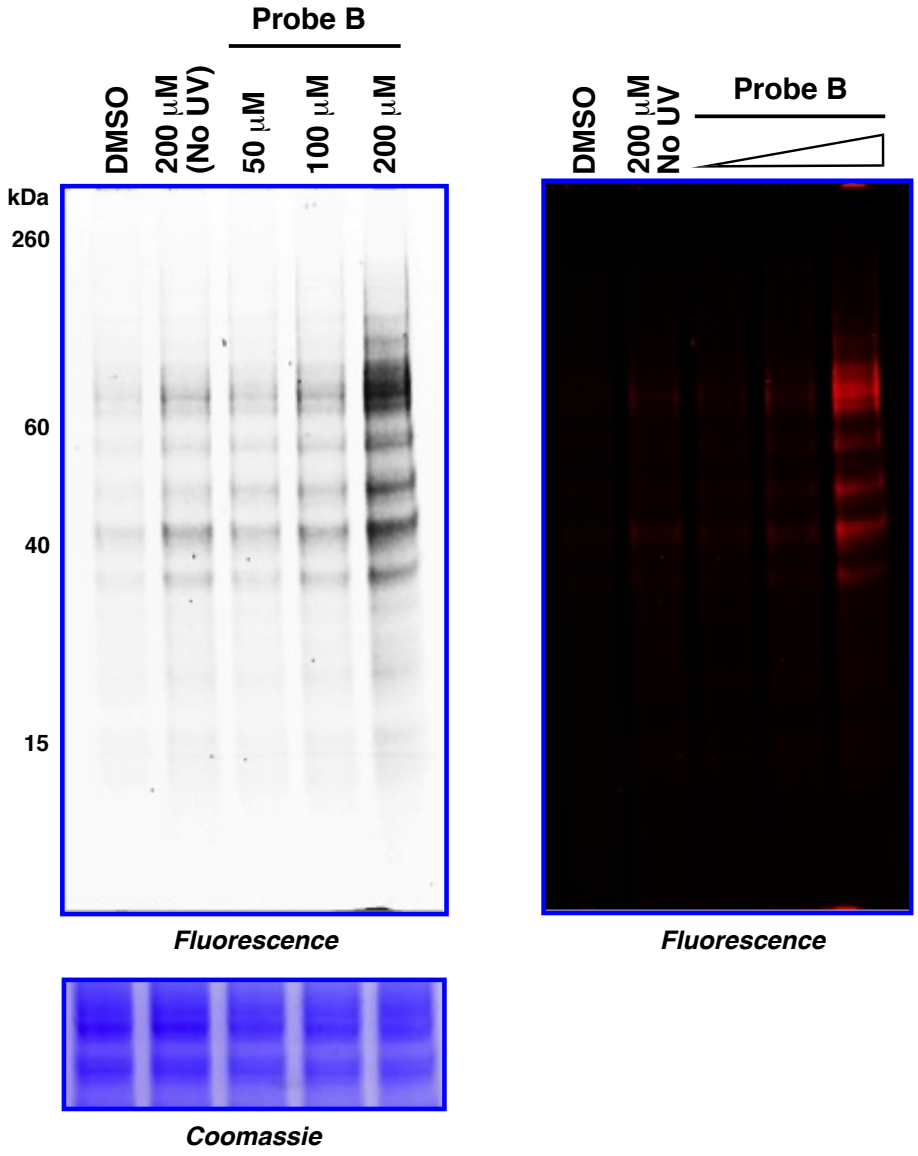

4.2.6. Design and Synthesis of a Nucleoside Monoester Thiophosphoramidate Competitor

Since competitor **Y** (**Figure 4-4D**) was unsuccessful at competing off protein labeling by Probe B, we next set out to identify a suitable nucleoside phosphoramidate that could compete with Probe B for labeling of proteins. For this study, we chose to evaluate non-zwitterionic phosphoramidates since it is probable that proteins identified thus far with Probe B may be specific only to zwitterionic phosphoramidates and might not accurately represent the interactome of nucleoside monoester phosphoramidates. By using a non-zwitterionic phosphoramidate as a competitor, we reasoned that proteins showing a reduction in labeling would likely be true interacting partners of nucleoside monoester phosphoramidates. Competition experiment with TrpAMP and TrpGMP showed that significant competition for protein labeling was observed at a 500-fold molar excess for both compounds, with TrpGMP displaying superior competition for labeling compared to TrpAMP (**Figure 4-8**). The requirement for such a high competitor concentration is probably because both compounds are excellent substrates of hHINT1[138] and undergo rapid hydrolysis, reducing the amount of intact phosphoramidate available to compete off labeling by Probe B. Of particular concern is that such high concentrations could potentially be toxic to cells. Consequently, we set out to identify a phosphoramidate competitor that is either a poor substrate of hHINT1 or is resistant to hHINT1 catalyzed hydrolysis.

While disrupting the interaction between Asp43 and 2′,3′-hydroxyls of nucleoside monoester phosphoramidates is enough to confer protection against hHINT1 hydrolysis,

the presence of the 2′,3′-hydroxyls could also be a critical molecular recognition motif for other cellular proteins/enzymes. Consequently, proteins identified with Probe B may not represent a complete set of nucleoside monoester phosphoramidate-protein interacting partners. With this limitation in mind, we elected to pursue development of competitor(s) that retained 2′,3′-hydroxyls since proteins that are sensitive to competition by such a competitor could be considered to be common interacting partners of nucleoside monoester phosphoramidates containing or lacking a 2′-OH. Furthermore, since Probe B is a purine, it is possible that the putative proteins identified so far are purine-specific. Therefore, we elected to develop a pyrimidine-based competitor, since proteins sensitive to competition would likely be interacting partners of both purine and pyrimidine based phosphoramidates. As a final design element for the competitor, we sought to mitigate hHINT1 hydrolysis of the competitor. To achieve this goal, we elected to develop a nucleoside monoester thiophosphoramidate of uridine. Recently, a thiophosphoramidate monoester of guanosine was shown to undergo slow enzymatic hydrolysis by hHINT1 when compared to the phosphoramidate monoester derivative.[264]

To synthesize our desired competitor, 5′-iodination of uridine was performed in the presence of triphenylphosphine and iodine in 25% yield. Synthesis of uridine thiophosphoramidate monoester was performed according to published procedures using $PSCl_3$, tryptamine, and 5′-iodo-5′-deoxy uridine.[264, 265] The desired thiophosphoramidate **17** was obtained in 57% yield (**Scheme 4-3**).

4.2.7. *In vitro* Competition and Proteomics with HEK293T Lysates

With compound **17** in hand, we first assessed the stability of the nucleoside monoester thiophosphoramidate to hHINT1 catalyzed hydrolysis. The results of the steady state kinetics with hHINT1 demonstrated that **17** has a 140-fold slower turnover rate (k_{cat}) when compared to the analogous TrpUMP. Next, we performed competition experiments with Probe B and probe-labeled proteins were visualized by in-gel fluorescence imaging. The result showed that meaningful competition was obtained with 200-fold excess of the competitor, which is a significant reduction from the 500-fold molar excess required for competition with TrpAMP and TrpGMP

Having demonstrated that **17** competes with Probe B for protein labeling, we next set out to identify those proteins that are common binding partners of Probe B and competitor **17**. To accomplish this, we performed a competition experiment with HEK293T lysates in duplicates and subsequently enriched labeled proteome over neutravidin resin. Proteomics analysis was performed on probe-labeled and competition samples, and label free quantification function of Proteome Discoverer was used to quantify protein abundance (mol %) in all samples. Protein abundance was determined from the exponentially modified protein abundance index (emPAI)[266] values for each protein identified by LC-MS/MS proteomics. Our analyses led to the identification of 57 putative protein interacting partners of nucleoside monoester phosphoramidates. All of the 57 proteins were not enriched for in the competition samples when compared to lysate treated with Probe B only (**Table 4-1**). Identified proteins were considered legitimate hits only if they were enriched in both probe-treated samples and were not enriched in both

competition samples. In addition, only proteins with two or more unique peptides in each sample were considered to be verified hits. Furthermore, we identified another nine proteins that showed a 5-fold enrichment between the probe-treated samples and the competition samples (**Table 4-1**). Gene ontology analyses revealed that Probe B strongly enriched proteins involved in maintenance of cellular redox homeostasis. Subcellular localization analysis showed that a large proportion of identified proteins were classified as cytosolic (28%) or exosome associated (30%), while the remaining identified proteins were classified as nuclear proteins (18%), membrane associated proteins (10%), endoplasmic reticulum proteins (7%), and mitochondrion (7%) (**Figure 4-9**).

The preponderance of exosome associated proteins in our results could suggest a general means of intracellular as well as extracellular trafficking of nucleoside monoester phosphoramidates. For example, the calcium-binding protein Sorcin is involved in vesicle trafficking, regulation of plasma membrane calcium channels and exchangers, and the development of drug resistance to anticancer drugs such as gemcitabine and vincristine.[267-270] Thus, the putative interaction of nucleoside monoester phosphoramidates with sorcin could represent an efflux mechanism in cells exposed to nucleoside monoester phosphoramidates. However, we urge caution when interpreting this result since sorcin is highly expressed in kidney tissues and thus HEK293T cells, which could explain its enrichment in our chemoproteomics studies. Therefore, it is possible that sorcin may not necessarily be an important mediator of small molecule trafficking in those tissues in which its expression levels are low. Efforts to validate sorcin and some of the identified putative proteins with other cell lines, as legitimate

protein binding partners of nucleoside monoester phosphoramidates, are currently underway in our laboratory and will be reported in due course.

Scheme 4-3. Preparation of tryptamine monoester thiophosphoramidate derivative of uridine (A) and preparation of monoester phosphoramidate competitor **Y**(B).

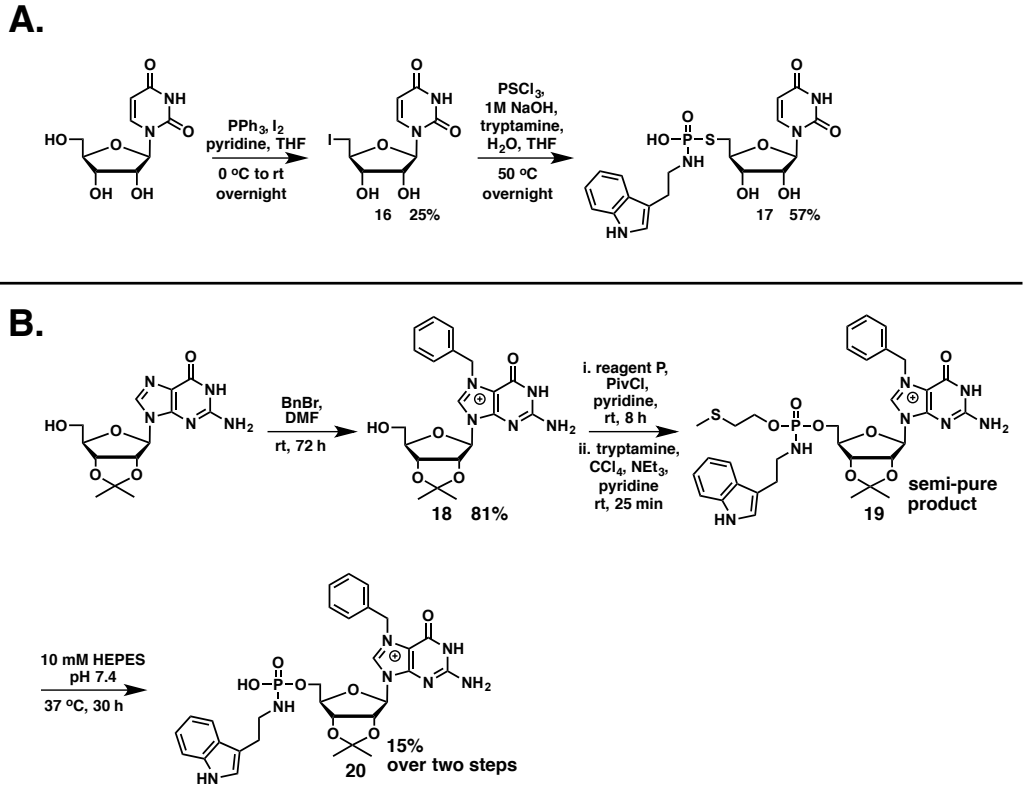

Figure 4-8. Fluorescence and total protein loading (Coomassie) gels for competition experiments with TrpAMP, TrpGMP (A), and thiophosphoramidate **17** (B).

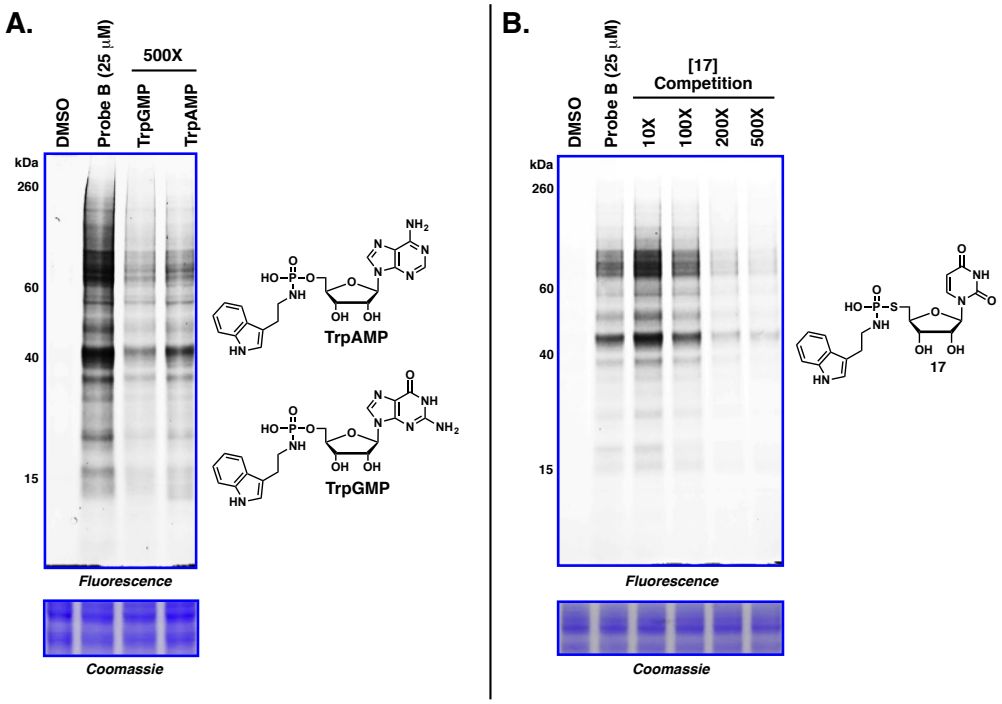

Table 4-1. Putative protein binding partners of nucleoside momoester phosphoramidates identified by chemoproteomics studies with Probe B. Number of unique peptides is the sum of two biological replicates while protein is the average of two biological replicates.

		Protein Abundance (mol%)			
Gene Name	Protein	Probe B	Probe B + 17	Unique Peptides	Probe B/[Probe B + 17]
AKAP12	A-kinase anchor protein 12	0.009	0	5	0
APEH	Acylamino-acid-releasing enzyme	0.028	0	6	0
ARF4	ADP-ribosylation factor 4	0.139	0	5	0
GOT1	Aspartate aminotransferase, cytoplasmic	0.067	0	11	0
ATXN10	Ataxin-10	0.029	0	6	0
BANF1	Barrier-to-autointegration factor	0.250	0	4	0
BID	BH3-interacting domain death agonist	0.141	0	6	0
KCTD12	BTB/POZ domain-containing protein KCTD12	0.059	0	7	0
SPAG9	C-Jun-amino-terminal kinase-interacting protein 4	0.014	0	7	0
CAPNS1	Calpain small subunit 1	0.067	0	5	0
CNN3	Calponin-3	0.070	0	7	0
CALU	Calumenin	0.915	0	21	0
CAPRIN1	Caprin-1	0.022	0	4	0
CCDC43	Coiled-coil domain-containing protein 43	0.124	0	6	0
CSTB	Cystatin-B	0.655	0	7	0
DCTPP1	dCTP pyrophosphatase 1	0.122	0	7	0
DLD	Dihydrolipoyl dehydrogenase, mitochondrial	0.024	0	5	0
DBNL	Drebrin-like protein	0.023	0	4	0
DCTN2	Dynactin subunit 2	0.075	0	10	0
GSR	Glutathione reductase, mitochondrial	0.019	0	4	0
GSTO1	Glutathione S-transferase omega-1	0.038	0	4	0
BAG6	Large proline-rich protein BAG6	0.031	0	9	0
MYL12B	Myosin regulatory light chain 12B	0.079	0	5	0
MTPN	Myotrophin	0.088	0	4	0
MARCKS	Myristoylated alanine-rich C-kinase substrate	0.188	0	9	0
PPIB	Peptidyl-prolyl cis-trans isomerase B	0.098	0	8	0
PEBP1	Phosphatidylethanolamine-binding protein 1	0.053	0	4	0
PAFAH1B2	Platelet-activating factor acetylhydrolase IB subunit beta	0.108	0	6	0
HMBS	Porphobilinogen deaminase	0.036	0	5	0
PFDN2	Prefoldin subunit 2	0.109	0	7	0
PDCD6	Programmed cell death protein 6	0.124	0	7	0
FAM50A	Protein FAM50A	0.048	0	7	0
S100A11	Protein S100-A11	0.105	0	4	0
SET	Protein SET	0.282	0	10	0
SUGT1	Protein SGT1 homolog	0.031	0	4	0
PARK7	Protein DJ-1	0.254	0	10	0
PNP	Purine nucleoside phosphorylase	0.034	0	6	0
RNH1	Ribonuclease inhibitor	0.019	0	4	0
NQO2	Ribosyldihydronicotinamide dehydrogenase [quinone]	0.040	0	4	0
FUS	RNA-binding protein FUS	0.147	0	6	0
SGTA	Small glutamine-rich tetratricopeptide repeat-containing protein alpha	0.098	0	8	0
SRI	Sorcin	0.133	0	8	0
SYAP1	Synapse-associated protein 1	0.063	0	7	0
TXNDC5	Thioredoxin domain-containing protein 5	0.034	0	6	0
TXN	Thioredoxin	0.588	0	8	0
TXNRD1	Thioredoxin reductase 1, cytoplasmic	0.019	0	5	0
TRAPPC3	Trafficking protein particle complex subunit 3	0.103	0	4	0
TSN	Translin	0.063	0	5	0
TNPO3	Transportin-3	0.011	0	4	0
TPM3	Tropomyosin alpha-3 chain	0.155	0	7	0
TPM4	Tropomyosin alpha-4 chain	0.145	0	8	0
UCHL1	Ubiquitin carboxyl-terminal hydrolase isozyme L1	0.058	0	4	0
UCHL3	Ubiquitin carboxyl-terminal hydrolase isozyme L3	0.098	0	6	0
UBE2N	Ubiquitin-conjugating enzyme E2 N	0.059	0	4	0
UBE2V1	Ubiquitin-conjugating enzyme E2 variant 1	0.070	0	5	0
YBX3	Y-box-binding protein 3	0.173	0	5	0
MYL6	Myosin light polypeptide 6	1.045	0.172	13	6
NASP	Nuclear autoantigenic sperm protein	0.273	0.053	31	5
PLIN3	Perilipin-3	0.205	0.042	21	5
PRDX2	Peroxiredoxin-2	1.289	0.188	17	7
P4HB	Protein disulfide-isomerase	0.579	0.109	41	5
RCN1	Reticulocalbin-1	0.229	0.034	12	7
SERPINH1	Serpin H1	0.137	0.019	17	7
TAGLN2	Transgelin-2	1.338	0.251	18	5
RAD23B	UV excision repair protein RAD23 homolog B	0.271	0.032	11	8

Figure 4-9. Subcellular localization of proteins identified from chemoproteomics with Probe B and GO terms enriched in the gene ontology analysis.

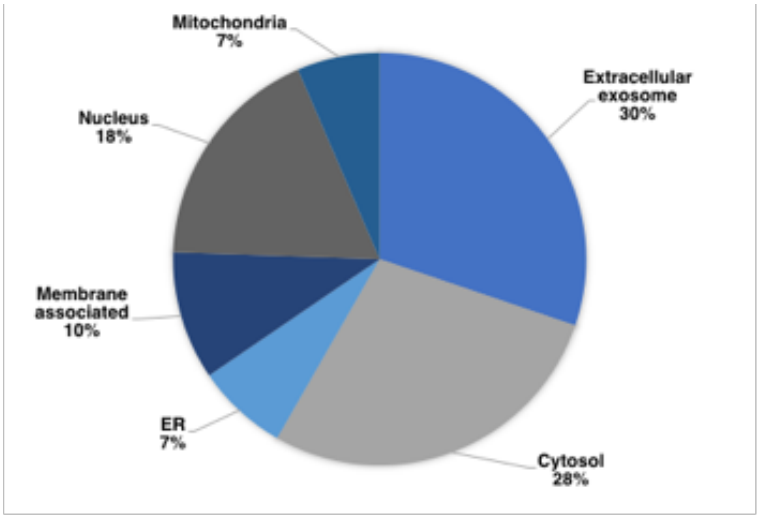

Term	p-value	Category
cell redox homeostasis	3.6E-7	GOTERM_BP_FAT
acetylation	2.0E-21	UP_KEYWORDS
Pyrimidine metabolism	5-0E-2	KEGG_PATHWAY

4.3. Conclusions.

In summary, we have described the development of phosphoramidate based photoaffinity labeling probes for chemoproteomics profiling of the interactome of nucleoside monoester phosphoramidates. Future in-cell chemoproteomics experiments with Probe B could provide more insights regarding the overall means of cellular uptake, intracellular trafficking, and intracellular metabolism of nucleoside monoester phosphoramidates.

4.4. Materials and Methods

General Materials and Methods

All chemicals and reagents were obtained from commercial sources and were used without further purification. Anhydrous *N*,*N*-Dimethylformamide (DMF) and tetrahydrofuran (THF) were obtained from a dry solvent purification system (MBraun) and dispensed under argon. All reactions were performed under an atmosphere of dry nitrogen unless otherwise noted. All silica gel chromatography and preparative reverse phase purification was performed on a Teledyne Isco CombiFlash Rf system, using Redisep Rf high performance gold silica gel columns (for normal phase purifications) and Redisep Rf high performance gold C18 columns (for reverse phase purifications). Reverse phase purifications were with water and acetonitrile. Lyophilization of compounds after reverse phase purification was performed on a FreeZone 12 Plus freeze dry system (Labconco). All Nuclear Magnetic Resonance spectra were obtained on a Brucker Avance III HD 500 MHz spectrometer at ambient temperature and chemical shifts (δ) were recorded in parts per million (ppm) – 500 MHz for ^{1}H, 125 MHz for ^{13}C,

202 MHz for ^{31}P, and 471 MHz for ^{19}F. ^{1}HNMR and ^{13}CNMR spectra were referenced by solvent signal, $CDCl_3$ (δ = 7.26 ppm for ^{1}HNMR and 77.23 ppm for ^{13}CNMR), DMSO-d_6 (δ = 2.50 ppm for ^{1}HNMR and 39.52 ppm for ^{13}CNMR). MeOD (δ = 3.31 ppm for ^{1}HNMR and 49.00 ppm for ^{13}CNMR). D_2O (δ = 4.79 ppm for ^{1}HNMR). All mass spectroscopy was performed with 1100 Series LC/MSD Trap ESI instrument (Agilent) in positive-ion mode.

2-amino-7-(4-ethynylbenzyl)-9-((3aR,4R,6R,6aR)-6-(hydroxymethyl)-2,2-dimethyltetrahydrofuro[3,4-d][1,3]dioxol-4-yl)-6-oxo-6,9-dihydro-1H-purin-7-ium (3). To an oven-dried round bottom flask was added guanosine acetonide (300 mg, 0.928 mmol) and dissolved with anhydrous DMF (9.7 mL). The solution was purged/evacuated extensively with N_2 under vacuum. To the solution was added **2** (797 mg, 4.08 mmol) and the reaction was stirred overnight at room temperature. The reaction was concentrated, and the resulting residue was purified by silica gel flash column chromatography, eluting with $CHCl_3$/MeOH (+10% NH_4OH) – gradient 0 – 20% to give **3** as a white solid (305 mg, 75% yield). ^{1}H NMR (500 MHz, DMSO-d_6) δ 1.33 (s, 3H), 1.51 (s, 3H), 3.60 – 3.67 (m, 2H), 4.24 (s, 1H), 4.44 (s, 1H), 4.96 (d, J = 6.0 Hz, 1H) 5.12 (s, 1H), 5.29 (d, J = 6.0 Hz, 1H), 5.62 (q, J = 15.0 Hz, 2H), 6.07 (s, 1H), 7.28 (br s, 2H), 7.45 (d, J = 8.5 Hz, 2H), 7.49 (d, J = 8.0 Hz, 2H), 9.50 (s, 1H), 11.81 (br s, 1H). ^{13}C NMR (125 MHz, DMSO-d_6) δ 25.0, 26.7, 51.0, 61.2, 81.3, 81.5, 83.0, 84.4, 89.3, 92.7, 106.8, 112.5, 121.9, 128.4, 132.0, 135.3, 136.7, 149.3, 153.8, 156.1. MS [ESI+]: 438.0 [M^+].

2-amino-9-((3aR,4R,6R,6aR)-6-(((((2-(5-azido-1H-indol-3-yl)ethyl)amino)(2-(methylthio)ethoxy)phosphoryl)oxy)methyl)-2,2-dimethyltetrahydrofuro[3,4-d][1,3]dioxol-4-yl)-7-(4-ethynylbenzyl)-6-oxo-6,9-dihydro-1H-purin-7-ium (4). Compound **3** (304.5 mg, 0.694 mmol) and Reagent **P** (268 mg, 1.04 mmol) were added to an oven-dried round bottom flask and dried overnight under high vacuum. To the flask was added anhydrous pyridine (24 mL) and the mixture was purged/evacuated extensively with N_2 under vacuum. To the mixture was added PivCl (235 μL, 1.91 mmol) in a dropwise manner and the reaction was stirred for 12 hours at ambient temperature. The reaction was quenched over sat. aq. $NaHCO_3$ and extracted twice with DCM. The organic extract was dried over $MgSO_4$, filtered, and concentrated in vacuo at ambient temperature and dried for an hour under high vacuum. The resulting residue was dissolved with anhydrous pyridine (30 mL) and the reaction vessel was purged/evacuated extensively with N_2 under vacuum. To the solution was added Et_3N (194 μL, 1.39 mmol). 5-azido tryptamine **1** (489 mg, 2.43 mmol; dissolve in dry pyridine) and CCl_4 (135 μL, 1.39 mmol) were added simultaneously to the reaction mixture and stirred for 25 min at ambient temperature. The reaction was diluted with MeOH and concentrated in vacuo at ambient temperature. The resulting residue was purified by silica gel flash column chromatography, eluting with $CHCl_3$/MeOH (+10% NH_4OH) – gradient 0 – 20% to give semi-pure product **4** as a brown solid, which was carried forward to the next step without further purification.

2-amino-9-((3aR,4R,6R,6aR)-6-(((((2-(5-azido-1H-indol-3-yl)ethyl)amino)(hydroxy)phosphoryl)oxy)methyl)-2,2-dimethyltetrahydrofuro[3,4-d][1,3]dioxol-4-yl)-7-(4-ethynylbenzyl)-6-oxo-6,9-dihydro-1H-purin-7-ium (5). Semi-pure compound **4** (170 mg) was dissolved with a mixture of MeOH/MeCN (1:1; 2 mL) and the mixture was added to 10 mM HEPES buffer (1L, pH 7.2). The resulting suspension was incubated for 30 hours at 37 °C. Water was removed in vacuo and the resulting residue was dried overnight under high vacuum. The residue was purified by silica gel flash column chromatography, eluting first with solvent A (20% MeOH in $CHCl_3$) then with solvent B ($CHCl_3$/MeOH/H_2O/NH_4OH – 5:3:0.5:0.005). The fractions containing the title compound were pooled and concentrated in vacuo and the resulting residue was purified by reverse phase C18 flash column chromatography to give product as a beige solid (20 mg, 4% yield over two steps). ^{1}H NMR (500 MHz, DMSO-d_6) δ 1.27 (s, 3H), 1.49 (s, 3H), 2.75 (t, J = 6.5 Hz, 2H), 2.98 (q, J = 8.5 Hz, 2H), 3.76 – 3.78 (m, 1H), 3.85 – 3.88 (m, 1H), 4.16 (s, 1H), 4.48 (s, 1H), 5.03 (d, J = 5.5 Hz, 1H), 5.21 (d, J = 5.0 Hz, 1H), 5.66 (q, J = 14.5 Hz, 2H), 6.08 (s, 1H), 6.73 (br s, 2H), 6.78 (d, J = 8.5 Hz, 1H), 7.18 (d, J = 13.5 Hz, 2H), 7.36 (t, J = 7.5 Hz, 3H), 7.62 (d, J = 7.5 Hz, 2H), 10.04 (s, 1H), 11.02 (s, 1H). ^{13}C NMR (125 MHz, DMSO-d_6) δ 24.9, 26.8, 27.8 (d, J = 6.1 Hz), 42.6, 50.1, 63.7, 81.2, 81.7, 83.1, 84.8, 88.0, 106.3, 108.0, 112.3, 112.57, 112.65, 112.7, 121.6, 124.3, 128.1, 129.0, 129.6, 131.8, 134.1, 136.5, 149.7. ^{31}P NMR (202 MHz, DMSO-d_6) δ 6.50. MS [ESI+]: 701.2 [M^+].

2-amino-9-((2R,3R,4R,5R)-4-hydroxy-5-(hydroxymethyl)-3-(prop-2-yn-1-yloxy)tetrahydrofuran-2-yl)-1,9-dihydro-6H-purin-6-one (9). To a round bottom flask

was added **7** (233 mg, 0.726 mmol), sodium phosphate buffer (50 mM, pH = 7.4), and DMSO (2 mL) and mixed until solution was clear. Adenosine deaminase (2.5 mg) was added to the reaction mixture and incubated overnight at 37 °C. Reaction was concentrated in vacuo and the resulting oily residue was purified by silica gel flash column chromatography, eluting with $CHCl_3$/MeOH (gradient 0 – 20%) to give 181 mg of product as a white solid – 78% yield. ^{1}H NMR (500 MHz, DMSO-d_6) δ 3.41 (s, 1H), 3.51 – 3.55 (m, 1H), 3.59 – 3.63 (m, 1H), 3.91 (q, J = 3.6 Hz, 1H), 4.20 (dd, J = 2.0 Hz and 16.0 Hz, 1H), 4.25 – 4.29 (m, 2H), 4.44 (t, J = 5.5 Hz, 1H), 5.11 (t, J = 5.5 Hz, 1H), 5.28 (d, J = 5.0 Hz, 1H), 5.81 (d, J = 6.0 Hz, 1H), 6.51 (s, 2H), 7.94 (s, 1H), 10.68 (s, 1H). ^{13}C NMR (125 MHz, DMSO-d_6) δ 56.9, 61.3, 68.8, 77.7, 79.8, 80.1, 84.3, 86.0, 116.6, 135.2, 151.2, 153.8, 156.7. MS [ESI+]: 322.2 [M+H$^+$].

2-amino-9-((2R,3R,4R,5R)-4-hydroxy-5-(hydroxymethyl)-3-(prop-2-yn-1-yloxy)tetrahydrofuran-2-yl)-1,9-dihydro-6H-purin-6-one (10). To an oven-dried round bottom flask was added compound **9** (300 mg, 0.934 mmol) and dissolved with anhydrous DMSO (2 mL) and anhydrous pyridine (2.9 mL). The solution was purged/evacuated extensively with N_2 under vacuum. DMTrCl (950 mg, 2.80 mmol) was added to the mixture and stirred overnight at room temperature. The reaction was diluted with water and extracted with DCM (3X). The combined organic extract was washed with water, dried over $MgSO_4$, filtered, and concentrated under reduced pressure. The resulting residue was dissolved with DCM and passed through a silica gel plug, eluting first with 1% MeOH in DCM then with 5% MeOH in DCM. The eluted product was

concentrated to dryness under reduced pressure and carried forward to the next step without further purification.

2-amino-9-((2R,3R,4R,5R)-4-((tert-butyldimethylsilyl)oxy)-5-(hydroxymethyl)-3-(prop-2-yn-1-yloxy)tetrahydrofuran-2-yl)-1,9-dihydro-6H-purin-6-one (11). To an oven-dried round bottom flask was added compound **10** (815.8 mg, 0.881 mmol), imidazole (180 mg, 2.64 mmol), and anhydrous DMF (4.0 mL). The mixture was purged/evacuated extensively with N_2 under vacuum and TBDMSCl (199 mg, 1.32 mmol) was added. The reaction was stirred overnight at room temperature. The reaction was diluted with water and extracted with DCM (3x). The organic extract was washed with sat. aq. NH_4Cl (1X), water (1X), dried over MgSO4, filtered, and concentrated to dryness. The residue was carried to the next step without further purification – off-white foam. The resulting foam was dissolved with 80% AcOH (7.0 mL) and stirred for 4.5 hours at 60 °C. Acetic acid was removed under reduced pressure with coevaporation with EtOH until no more acid was detected by smell. The resulting residue was purified by flash column chromatography, eluting with $CHCl_3$/MeOH (0 – 20%) to give 176.3 mg of product – 46% yield over two steps. ^{1}H NMR (500 MHz, DMSO-d_6) δ 0.12 (s, 6H), 0.90 (s, 9H), 3.40 (t, J = 2.0 Hz, 1H), 3.51 – 3.55 (m, 1H), 3.59 -3.63 (m, 1H), 3.90 (q, J = 4.0 Hz, 1H), 4.17 (d, J = 2.0 Hz, 2H), 4.45 – 4.46 (m, 1H), 4.50 – 4.52 (m, 1H), 5.19 (t, J = 5.0 Hz, 1H), 5.79 (d, J = 6.5 Hz, 1H), 6.49 (s, 2H), 7.98 (s, 1H), 10.66 (s, 1H). ^{13}C NMR (125 MHz, DMSO-d_6) δ -4.9, -4.8, 17.8, 25.7, 57.2, 60.9, -70.7, 77.6, 79.5, 79.8, 84.1, 86.4, 116.6, 135.2, 151.3, 153.8, 156.7. MS [ESI+]: 458.2 [M+Na^+].

2-amino-9-((2R,3R,4R,5R)-4-((tert-butyldimethylsilyl)oxy)-5-(hydroxymethyl)-3-(prop-2-yn-1-yloxy)tetrahydrofuran-2-yl)-6-oxo-7-(4-(3-(trifluoromethyl)-3H-diazirin-3-yl)benzyl)-6,9-dihydro-1H-purin-7-ium (12). Compound **6** (490 mg, 1.76 mmol) and compound **11** (170 mg, 0.390 mmol) were dried overnight under high vacuum (away from ambient light) prior to use. The compounds were dissolved with anhydrous DMSO (2.0 mL) and stirred for 24 hours at room temperature. The reaction was diluted with water (2 .0 mL) and added dropwise to stirring cold Et_2O at 0 °C. The mixture was kept on ice to ensure precipitation of product. The precipitate was filtered and washed with cold Et_2O. The filtrate was concentrated under reduced pressure to remove Et_2O and the aqueous layer was extracted with DCM until there was no more product visible by TLC (10% MeOH in DCM). The combined organic extract was dried over MgSO4, filtered, and concentrated under reduced pressure. The oily residue and the previously precipitated product was dissolved and purified by flash column chromatography, eluting with DCM/MeOH (0 – 20%) to give 181.4 mg of product – 73% yield. ^{1}H NMR (500 MHz, DMSO-d_6) δ 0.10 (d, J = 2.0 Hz, 6H), 0.88 (s, 9H), 3.34 (t, J = 2.5 Hz, 1H; merged with H_2O peak), 3.57 (dd, J = 12.5 Hz, 2.5 Hz, 1H), 3.74 (dd, J = 12.5 Hz, 3.0 Hz, 1H), 4.00 (q, J = 3.0 Hz, 1H), 4.30 (t, J = 2.5 Hz, 2H), 4.43 (t, J = 4.5 Hz, 1H), 4.52 (t, J = 4.5 Hz, 1H), 5.55 (br s, 1H), 5.72 (s, 1H), 5.94 (d, J = 4.5 Hz, 1H), 6.36 (s, 2H), 7.30 (d, J = 8.0 Hz, 2H), 7.60 (d, J = 8.5 Hz, 2H), 9.32 (s, 1H). ^{13}C NMR (125 MHz, DMSO-d_6) δ -5.1, -4.8, 17.8, 25.7, 26.7 (dd, J = 316.8 Hz, 39.8 Hz), 50.2, 57.7, 60.0, 69.9, 77.5, 79.7, 80.0, 86.4, 87.1, 107.5, 121.8 (q, J = 272.8 Hz), 126.9, 127.6, 129.1, 132.9, 137.7, 149.7, 160.7, 161.6. ^{19}F NMR (471 MHz, DMSO-d_6) δ -64.6. MS [ESI+]: 634.2 [M^+].

9-((2R,3R,4R,5R)-5-(((((2-(1H-indol-3-yl)ethyl)amino)(2-(methylthio)ethoxy)phosphoryl)oxy)methyl)-4-hydroxy-3-(prop-2-yn-1-yloxy)tetrahydrofuran-2-yl)-2-amino-6-oxo-7-(4-(3-(trifluoromethyl)-3H-diazirin-3-yl)benzyl)-6,9-dihydro-1H-purin-7-ium (14). Compound **12** (179 mg, 0.282 mmol) and reagent **P** (109 mg, 0.423 mmol) were added to an oven-dried round bottom flask and dried overnight under high vacuum. To the flask was added anhydrous pyridine (10.0 mL), purged/evacuated extensively with N_2 under vacuum. Pivaloyl chloride (96 μL, 0.776 mmol) was added dropwise over 30 minutes. The reaction mixture was stirred at room temperature for 8 hours. The reaction was poured into sat. aq. $NaHCO_3$ and extracted with DCM (2X). The organic extract was dried over $MgSO_4$, concentrated and placed under high vacuum for an hour. The resulting residue was dissolved with anhydrous pyridine (12.0 mL) and the solution was purged/evacuated extensively with N_2 under vacuum. To the solution was added Et_3N (80 μL). Tryptamine (181 mg, 1.13 mmol) was dissolved with 2.0 mL anhydrous pyridine and was added simultaneously with CCl_4 (55 μL, 0.564 mmol). The reaction was stirred at room temperature for 25 minutes. Reaction was concentrated under reduced pressure with co-evaporation with toluene. The resulting residue was purified by flash column chromatography, eluting with $CHCl_3$/MeOH (+10% NH_4OH) – gradient 0 to 20% to give the phosphoramidate product (52.3 mg), which coelutes with unreacted nucleoside **12**. The impure product was dissolved with anhydrous THF (3.0 mL), cooled to 0 °C, and treated with 1M TBAF (84 μL, 0.0843 mmol). Reaction was brought to room temperature after adding TBAF and allowed to stir for 20 minutes (monitored by TLC). Reaction mixture was concentrated

and purified by flash column chromatography, eluting with $CHCl_3$/MeOH (+10% NH_4OH) – gradient 0 to 20% to give 18.1 mg (8% yield over two steps) of product after reverse phase chromatography (acetonitrile/water) and lyophilization – a mixture of diastereomers. ^{1}H NMR (500 MHz, DMSO-d_6) δ 1.99 (s, 1H), 2.04 (s, 2H), 2.64 (quint, J = 7.0 Hz, 2H), 2.82 (q, J = 7.5 Hz, 2H), 3.00 -3.09 (m, 2H), 3.36 (s, 1H), 3.87 – 3.99 (m, 3H), 4.06 – 4.17 (m, 2H), 4.19 – 4.29 (m, 2H), 4.32 – 4.41 (m, 3H), 4.51 (q, J = 5.0 Hz, 1H), 5.20 (sex, J = 11.5 Hz, 6.5 Hz, 1H), 5.54 (br s, 1H), 5.62 (t, J = 11.5 Hz, 2H), 5.66 – 5.74 (m, 3H), 5.97 (d, J = 3.5 Hz, 1H), 6.93 (q, J = 8.0 Hz, 1H), 7.02 – 7.05 (m, 1H), 7.13 (d, J = 10.5 Hz, 1H), 7.25 (t, J = 8.5 Hz, 2H), 7.32 (d, J = 8.0 Hz, 1H), 7.47 (dd, J = 15.0 Hz, 8.0 Hz, 1H), 7.60 (t, J = 8.5 Hz, 2H), 9.16 – 9.20 (s, 1H, split in half), 10.80 (s, 1H). ^{13}C NMR (125 MHz, DMSO-d_6) δ 14.8, 14.9, 27.6, 27.8, 28.1, 33.1 (t, J = 7.0 Hz), 41.6, 49.9, 57.3, 57.6, 64.3, 65.0, 68.6, 77.6, 79.9, 83.2, 87.0 (d, J = 9.3 Hz), 107.8, 111.4, 111.5 (d, J = 3.5 Hz), 118.1, 118.2, 120.7, 120.9, 122.7, 122.9, 126.8, 127.1 (d, J = 2.9 Hz), 127.5, 129.1 (d, J = 4.4 Hz), 131.2, 136.2, 138.1 (d, J = 2.8 Hz), 149.6, 162.7, 163.7. ^{31}P NMR (202 MHz, DMSO-d_6) δ 10.31 and 10.50. MS [ESI+]: 816.3 [M^+].

9-((2R,3R,4R,5R)-5-(((((2-(1H-indol-3-yl)ethyl)amino)(hydroxy)phosphoryl)oxy)methyl)-4-hydroxy-3-(prop-2-yn-1-yloxy)tetrahydrofuran-2-yl)-2-amino-6-oxo-7-(4-(3-(trifluoromethyl)-3H-diazirin-3-yl)benzyl)-6,9-dihydro-1H-purin-7-ium (15). Compound **14** (13.1 mg, 0.0160 mmol) was dissolved with MeOH (1 mL) and added to 20 mM HEPES/water (1:3, pH 7.0) and placed in an incubator for 30 hours at 37 °C. Water was removed under reduced pressure and the residue dried overnight on the high vacuum. The resulting residue was purified

by flash column chromatography, eluting first with $CHCl_3$/MeOH (20% MeOH) and then with $CHCl_3$:MeOH:H_2O:NH_4OH (5:3:0.5:0.005). Reverse phase purification and lyophilization gave 7.5 mg of product as an off-white powder – 63% yield. ^{1}H NMR (500 MHz, MeOD) δ 2.67 (s, 1H), 2.90 (t, J = 7.0 Hz, 2H), 3.15 (q, J = 7.5 Hz, 2H), 3.94 (dd, J = 11.5 Hz, 3.0 Hz, 1H), 4.11 – 4.14 (m, 1H), 4.19 (s, 1H), 4.40 – 4.47 (m, 3H), 4.49 – 4.50 (m, 1H), 5.60 (dd, J = 42.5 Hz, 14.5 Hz, 2H), 6.12 (d, J = 3.0 Hz, 1H), 6.84 (t, J = 7.5 Hz, 1H), 6.99 (t, J = 7.0 Hz, 1H), 7.03 (s, 1H), 7.09 (d, J = 8.0 Hz, 2H), 7.28 (d, J = 8.0 Hz, 1H), 7.43 (d, J = 8.0 Hz, 1H), 7.56 (d, J = 8.0 Hz, 2H). ^{13}C NMR (125 MHz, MeOD) δ 28.9 (d, J = 7.3 Hz), 29.2, 29.5, 43.6, 52.1, 59.2, 63.7, 70.1, 76.5, 80.2, 83.2, 86.0 (d, J = 8.9 Hz), 88.8, 109.1, 112.2, 113.8, 119.3, 119.4, 122.2, 123.4, 124.6, 128.0, 128.7, 130.1, 130.3, 138.1, 138.7, 151.6, 164.0, 164.3. ^{31}P NMR (202 MHz, MeOD) δ 8.29. ^{19}F NMR (471 MHz, MeOD) δ -67.0. MS [ESI+]: 742.1 [M^+].

1-((2R,3R,4S,5S)-3,4-dihydroxy-5-(iodomethyl)tetrahydrofuran-2-yl)pyrimidine-2,4(1H,3H)-dione (16). Uridine (1.0 g, 4.10 mmol) was added to an oven-dried flask and dried overnight under high vacuum. To the vessel was added PPh_3 (1.3 g, 4.91 mmol), anhydrous THF (6.6 mL), and anhydrous pyridine (3.3 mL). The mixture was purged extensively with N_2 and cooled to 0 °C. Iodine (1.25 g, 4.91 mmol) was dissolved with anhydrous THF (3.3 mL) and was added dropwise to the reaction mixture at 0 °C. The reaction was allowed to warm up to room temperature and was stirred overnight. The reaction was concentrated in vacuo and the residue was taken up EtOAc and washed with sat. aq. Na_2SO_3 (1X). The organic layer was dried over $MgSO_4$, filtered, concentrated, and purified by flash column chromatography, eluting first with DCM/MeOH (0 – 5%

MeOH) to give 369 mg of product – 25% yield. ^{1}H NMR (500 MHz, DMSO-d_6) δ 3.40 (m, 1H), 3.55 (m, 1H), 3.86 (m, 2H), 4.19 (q, J = 5.5 Hz, 1H), 5.35 (d, J = 5.0 Hz, 1H), 5.48 (d, J = 5.5 Hz, 1H), 5.68 (d, J = 8.0 Hz, 1H), 5.80 (d, J = 5.5 Hz, 1H), 7.67 (d, J = 8.0 Hz, 1H), 11.37 (s, 1H). ^{13}C NMR (125 MHz, DMSO-d_6) δ 7.7, 72.3, 72.8, 83.1, 88.2, 102.2, 141.1, 150.7, 163.0. MS [ESI+]: 354.8 [M+H$^+$].

S-(((2S,3S,4R,5R)-5-(2,4-dioxo-3,4-dihydropyrimidin-1(2H)-yl)-3,4-dihydroxytetrahydrofuran-2-yl)methyl) O-hydrogen (2-(1H-indol-3-yl)ethyl)phosphoramidothioate (17).[36,37] To a round bottom flask was added tryptamine (23 mg, 0.141 mmol), 1M NaOH (0.71 mL, 0.705 mmol), H_2O (90 μL), and the mixture was stirred at room temperature. Thiophosphoryl chloride (14 μL, 0.141 mmol) was dissolved with anhydrous THF (0.4 mL) and added dropwise to the mixture with vigorous stirring. To the mixture was added 15 (50 mg, 0.141 mmol) followed by 1 equiv of 1M NaOH. The reaction was stirred overnight at 55 °C. **Note: A cloudy reaction mixture the next day means that the product had degraded due to the pH of the reaction being too acidic**. The reaction was neutralized with 1N HCl and concentrated in vacuo. The resulting residue was dried overnight under high vacuum and later purified by silica gel flash column chromatography, eluting first with solvent A (20% MeOH in $CHCl_3$) then with solvent B ($CHCl_3$/MeOH/H_2O/NH_4OH – 5:3:0.5:0.005). Relevant fractions were pooled, concentrated and subjected to ion exchange with Dowex50 column, eluting with water. The relevant fractions were collected and purified by reverse phase C18 flash column chromatography to give product – 38.6 mg after lyophilization (57% yield). ^{1}H NMR (500 MHz, D_2O) δ 2.73 – 2.79 (m, 1H), 2.84 – 2.90 (m, 1H), 2.92

– 3.02 (m, 2H), 3.16 (q, J = 7.5 Hz, 2H), 3.95 (t, J = 5.5 Hz, 1H), 4.10 – 4.11 (m, 2H), 5.57 (d, J = 8.0 Hz, 1H), 5.68 (d, J = 4.0 Hz, 1H), 7.09 (t, J = 7.5 Hz, 1H), 7.18 – 7.22 (m, 2H), 7.45 (d, J = 8.5 Hz, 1H), 7.55 (d, J = 8.0 Hz, 1H), 7.65 (d, J = 8.0 Hz, 1H). ^{13}C NMR (125 MHz, D_2O) δ 26.2 (d, J = 9.0 Hz), 31.8, 42.1, 71.5, 73.4, 82.5 (d, J = 5.4 Hz), 89.3, 102.1, 111.7, 112.2, 118.6, 118.9, 121.8, 123.3, 126.8, 136.2, 141.1, 152.1, 167.0. ^{31}P NMR (202 MHz, D_2O) δ 24.81. MS [ESI+]: 483.0 [$M+H^+$].

2-amino-7-benzyl-9-((3aR,4R,6R,6aR)-6-(hydroxymethyl)-2,2-dimethyltetrahydrofuro[3,4-d][1,3]dioxol-4-yl)-6-oxo-6,9-dihydro-1H-purin-7-ium (18). To an oven-dried round bottom flask was added guanosine acetonide (200 mg, 0.619 mmol) and dissolved with anhydrous DMF (6.5 mL). The solution was purged/evacuated extensively with N_2 under vacuum. To the solution was added benzyl bromide (0.3 mL, 2.72 mmol) dropwise and the reaction was stirred for 72 hours at room temperature. The diluted with water and added dropwise to a stirring cold toluene to precipitate product. Precipitates were filtered and dried under vacuum. The precipitate was further purified by silica gel flash column chromatography, eluting with $CHCl_3$/MeOH (gradient 0 – 20%) to give product as a white solid (256 mg, 81% yield). ^{1}H NMR (500 MHz, DMSO-d_6) δ 1.32 (s, 3H), 1.51 (s, 3H), 3.60 – 3.68 (m, 2H), 4.44 (s, 1H), 4.97 (d, J = 5.5 Hz, 1H), 5.14 (br s, 1H), 5.29 (d, J = 6.0 Hz, 1H), 5.60 (q, J = 12.0 Hz, 2H), 6.08 (s, 1H), 7.06 – 7.60 (m, 7H), 9.54 (s, 1H), 11.69 (s, 1H). ^{13}C NMR (125 MHz, DMSO-d_6) δ 25.1, 26.8, 51.2, 61.2, 81.3, 84.3, 89.1, 92.4, 106.8, 112.6, 128.2, 128.5, 128.8, 134.7, 135.8, 149.4, 155.9, 157.6. MS [ESI+]: 414.3 [M^+].

9-((3aR,4R,6R,6aR)-6-(((((2-(1H-indol-3-yl)ethyl)amino)(2-(methylthio)ethoxy)phosphoryl)oxy)methyl)-2,2-dimethyltetrahydrofuro[3,4-d][1,3]dioxol-4-yl)-2-amino-7-benzyl-6-oxo-6,9-dihydro-1H-purin-7-ium (19). Compound **18** (100 mg, 0.241 mmol) and Reagent **P** (93 mg, 0.362 mmol) were added to an oven-dried round bottom flask and dried overnight under high vacuum. To the flask was added anhydrous pyridine (3.7 mL) and the mixture was purged/evacuated extensively with N_2 under vacuum. To the mixture was added PivCl (82 μL, 0.664 mmol) in a dropwise manner and the reaction was stirred for 8 hours at ambient temperature. The reaction was quenched over sat. aq. $NaHCO_3$ and extracted twice with DCM. The organic extract was dried over $MgSO_4$, filtered, and concentrated in vacuo at ambient temperature and dried for an hour under high vacuum. The resulting residue was dissolved with anhydrous pyridine (10 mL) and the reaction vessel was purged/evacuated extensively with N_2 under vacuum. To the solution was added Et_3N (67 μL, 0.482 mmol). Tryptamine (154 mg, 0.964 mmol; dissolve in dry pyridine) and CCl_4 (35 μL, 0.362 mmol) were added simultaneously to the reaction mixture and stirred for 25 min at ambient temperature. The reaction was diluted with MeOH and concentrated in vacuo at ambient temperature. The resulting residue was purified by silica gel flash column chromatography, eluting with $CHCl_3$/MeOH (+10% NH_4OH) – gradient 0 – 20% to give semi-pure product **18**, which was carried forward to the next step without further purification.

9-((3aR,4R,6R,6aR)-6-(((((2-(1H-indol-3-yl)ethyl)amino)(hydroxy)phosphoryl)oxy)methyl)-2,2-dimethyltetrahydrofuro[3,4-d][1,3]dioxol-4-yl)-2-amino-7-benzyl-6-oxo-6,9-dihydro-1H-purin-7-ium (20). Semi-pure compound **19** (170 mg) was dissolved with a mixture of MeOH/MeCN (1:1; 2 mL) and the mixture was added to 10 mM HEPES buffer (350, pH 7.2). The resulting suspension was incubated for 30 hours at 37 °C. Water was removed in vacuo and the resulting residue was dried overnight under high vacuum. The residue was purified by silica gel flash column chromatography, eluting first with solvent A (20% MeOH in $CHCl_3$) then with solvent B ($CHCl_3$/MeOH/H_2O/NH_4OH – 5:3:0.5:0.005). The fractions containing the title compound were pooled and concentrated in vacuo and the resulting residue was purified by reverse phase C18 flash column chromatography to give product (23 mg, 15% yield over two steps). ^{1}H NMR (500 MHz, DMSO-d_6) δ 1.29 (s, 3H), 1.48 (s, 3H), 2.79 (br s, 2H), 2.99 – 3.08 (m, 2H), 3.81 (br s, 1H), 3.97 (br s, 1H), 4.52 (s, 1H), 5.08 (s, 1H), 5.32 (s, 1H), 5.65 (q, J = 14.5 Hz, 2H), 6.07 (s, 1H), 6.90 (t, J = 6.5 Hz, 1H), 7.01 (t, J = 7.0 Hz, 1H), 7.10 (s, 1H), 7.27 – 7.31 (m, 5H), 7.49 (br s, 1H), 7.53 (br s, 2H). ^{13}C NMR (125 MHz, DMSO-d_6) δ 25.0, 26.7, 28.0, 42.5, 45.6, 50.8, 60.8, 63.8, 81.6, 84.6, 88.4, 92.0, 106.2, 111.3, 112.3, 112.5, 118.0, 118.3, 120.7, 122.4, 127.3, 128.4, 128.6, 135.3, 136.2, 149.5. ^{31}P NMR (202 MHz, DMSO-d_6) δ 6.74. MS [ESI+]: 636.3 [M^+].

2-(5-azido-1H-indol-3-yl)ethan-1-amine (1).[253] ^{1}H NMR (500 MHz, DMSO-d_6) δ 1.77 (br s, 2H), 2.71 – 2.74 (m, 2H), 2.77 – 2.81 (m, 2H), 6.81 (dd, J = 8.5 Hz, 2.0 Hz, 1H), 7.20 (d, J = 2.5 Hz, 1H), 7.23 (d, J = 2.0 Hz, 1H), 7.37 (d, J = 8.5 Hz, 1H), 10.93 (s, 1H).

^{13}C NMR (125 MHz, DMSO-d_6) δ 29.2, 42.6, 108.0, 112.6, 112.7, 112.8, 124.5, 128.1, 129.7, 134.1.

1-(bromomethyl)-4-ethynylbenzene (2). ^{1}H NMR (500 MHz, $CDCl_3$) δ 3.10 (s, 1H), 4.47 (s, 2H), 7.35 (d, J = 8.0 Hz, 2H), 7.46 (d, J = 8.0 Hz, 2H). ^{13}C NMR (125 MHz, $CDCl_3$) δ 32.9, 78.2, 83.2, 122.4, 129.2, 132.7, 138.5. MS [ESI+]: 196.3 [M+H$^+$].

3-(4-(bromomethyl)phenyl)-3-(trifluoromethyl)-3H-diazirine (6). ^{1}H NMR (500 MHz, DMSO-d_6) δ 4.73 (s, 2H), 7.28 (d, J = 8.0 Hz, 2H), 7.58 (d, J = 8.0 Hz, 2H). ^{13}C NMR (125 MHz, DMSO-d_6) δ 28.0 (q, J = 39.6 Hz), 33.0, 123.3 (q, J = 273.3 Hz), 126.8, 127.4, 130.2, 132.7, 140.5. ^{19}F NMR (471 MHz, DMSO-d_6) δ -64.6. MS [ESI+]: 278.2 [M+H$^+$].

hHINT1 Phosphoramidase assay. Evaluation of hHINT1 hydrolysis of phosphoramidate PAL probes and uridine monoester thiophosphoramidate was performed according to ref **138** on a Cary Variance fluorimeter. The fluorescence from phosphoramidate hydrolysis for PAL probes was monitored for 30 min incubation with hHINT1, while that for thiophosphoramidate competitor was monitored for 2 min. All experiments were performed at ambient temperature. Data from experiments was plotted and analyzed using Prism 5 graphing software.

Cell Culture and Preparation of Whole-Cell Lysates. HEK293T cells were cultured in DMEM supplemented with 10% fetal bovine serum (FBS), 100 U mL^{-1} penicillin, 100 µg mL^{-1} streptomycin, and L-glutamine at 37 °C and 5% CO_2. Cells were grown in a 75 cm^2 (Corning) to 80 – 90% confluency, harvested by repeated pipetting, and settled by centrifugation at 400g x 3 min at ambient temperature. Media was removed, and cell

pellet was washed twice with cold PBS and stored at -80 °C until further use after removing PBS. To lyse cells, the cell pellet was resuspended in cold lysis buffer (1% NP-40, 50 mM HEPES, pH = 7.4) supplemented with 1X – protease inhibitor (Pierce™ EDTA-free) and incubated on ice for 30 min, with vortexing every 10 min. Lysates were clarified by centrifugation (14,000g, 20 min, 4 °C) and total protein was quantified with Pierce® BCA Protein Assay kit (Thermo Scientific) and used immediately for probe labeling applications.

Proteome Labeling and Competition Studies with HEK293T Cell Lysates. Prior to labeling experiments, total protein concentration of lysates was adjusted to 1.0 mg/mL. Lysates were incubated with the respective probe concentration at room temperature (10 min for Probe A and 15 min for Probe B). DMSO control was incubated for the same duration as that of the probe in stand-alone experiments (i.e. 10 min or 15 min) and for 15 min in comparison experiments. After incubation with lysate at room temperature, the crosslinking experiment was performed on ice, in the dark, with a hand-held UV lamp – 365 nm (Spectroline® ENF-240C) as follows: experiment with Probe A was photo-irradiated for 10 min while experiment with Probe B was irradiated on ice for 30 min. DMSO control was placed on ice for either 10 min or 30 min under ambient light for experiments with Probe A and Probe B, respectively. The volume for all reactions was 50.0 μL. After photo-conjugation, lysates were heated for 10 min at 65 °C to denature proteins, allowed to equilibrate to room temperature before Cu(I)-catalyzed [3 + 2] cycloaddition "click" reaction with TAMRA-N_3. $CuSO_4$ (1 μL of 50 mM stock in H_2O) and THPTA (0.5 μL of 200 mM stock in H_2O) were premixed before adding sodium

ascorbate (1 μL of 50 mM stock in H_2O). The premixed "click" agents were added to lysates followed by TAMRA-N_3 (0.5 mM stock in DMSO). The lysates were vortexed briefly and placed on a shaker/mixer for 1 hour at room temperature. Lysates (25 μL) were mixed LDS 4X sample buffer (5 μL, NuPAGE) and 1M DTT (2 μL) and heated at 90 °C for 5 min. After cooling to room temperature, SDS-PAGE resolution of proteins was performed using NuPAGE 4 – 12% polyacrylamide bis-tris gel and 1X MES running buffer. Gels were washed with 50% MeOH in H_2O for 3 – 5 hours to remove excess dye and imaged with a TyphoonFLA700 gel imager (General Electric). Competition studies were performed in a similar manner. Probe and competitor, at the respective concentration, were both to a 0.5 mL Eppendorf tube followed by diluent (lysis buffer). Lysate was added to the mixture so that the final protein concentration was 1.0 mg/mL, and the mixture was incubated at room temperature for 10 min or 15 min for Probe A and Probe B, respectively. Photoirradiation, "click" reaction with TAMRA-N_3, and SDS-PAGE were as already described.

Enrichment of Probe-Labeled Proteins for Proteomics.[271, 272] The total protein concentration of HEK293T lysates were adjusted to 1.5 mg/mL with lysis buffer supplemented with 1X proteases inhibitor. Lysates were incubated at room temperature with the respective probes - 100 μM for Probe A and 200 μM for Probe B at the previously indicated incubation times. Photo-crosslinking at 356 nm was performed in the dark at 0 °C for the previously indicated times for each probe, and photo-irradiated lysates were denatured at 65 °C for 10 min. Lysates were allowed to equilibrate back to

room temperature and subjected to Cu(I)-catalyzed [3 + 2] cycloaddition "click" reaction with biotin-N_3 as already described. The final concentration for click reagents, at I mL reaction volume, was as follows: $CuSO_4$ (1.0 mM), THPTA (0.5 mM), sodium ascorbate (1.0 mM), and biotin-N_3 (0.5 mM). Click reaction with biotin-N_3 was for 1 hour at room temperature, with shaking. To the samples was added water (100 μL), ice-cold methanol (500 μL), and ice-cold chloroform (125 μL). The samples were vortexed vigorously before centrifuging at 2000g for 20 min at 4 °C. The supernatant above the pellet disc was removed first before the organic layer below the pellet disc. The protein pellet was resuspended by sonicating in ice-cold MeOH/$CHCl_3$ (1:1, 1 mL) and centrifuged at 14,000g for 10 min at 4 °C. The supernatant was discarded, and the pellet resuspended in 1 mL ice-cold MeOH, followed by centrifugation at 14,000g (10 min, 4 °C). The supernatant was discarded, and the resulting protein pellet was air dried to remove residual MeOH. To the resulting pellet was added 1% SDS in PBS (1 mL) and resuspended with iterative heating (85 °C, 5 min) and sonication (5 min) until pellet was fully dissolved. Redissolved proteins were allowed to equilibrate to room temperature and any insoluble material was removed by centrifugation (2000g, 1 min, room temperature). The supernatant was removed and placed in a clean 1.5 mL Eppendorf tube. NeutrAvidin agarose resin (Thermo scientific, 50%, 100 μL) was washed/equilibrated with 0.2% SDS in PBS (1 mL, 3X) and settled by centrifugation at 1400g for 3 min at room temperature. To the resin was added PBS (4 mL) followed by dissolved proteins (this dilutes the SDS concentration to 0.2%). The proteins were incubated overnight with the resin at 4 °C with mixing by rotating on an end-over-end

mixer. The next day, the resin was allowed to warm up to room temperature and was washed sequentially with 0.2% SDS in PBS (5 mL, 3X), 5 M Urea (50 mM HEPES, 150 mM NaCl, pH 7.4, 3X), and PBS (3X). Enriched proteins were either eluted off the NeutrAvidin resin for visualization by SDS-PAGE or subjected to on-bead tryptic digest as follows.

Elution of Proteins off NeutrAvidin Agarose Resin. Samples were centrifuged at 1400g for 3 min and the supernatant discarded. Proteins were eluted with 20 µL of 3X LDS sample buffer supplemented with 100 mM DTT by boiling at 95 °C for 5 min. The supernatant was removed after centrifuging at 2000g for 1 min. The protein elution step was repeated once, and the supernatant was combined with that of the first elution. The combined eluents were centrifuged at 2000g for 5 min to settle any residual NeutrAvidin resin. The supernatant was removed and resolved by SDS-PAGE and stained with Coomassie blue.

On-bead Tryptic Digest. Samples were centrifuged at 1400g for 3 min and the supernatant discarded, and the samples were resuspended with 6M urea in PBS (500 µL). To the samples was first added 200 mM TCEP (25 µL) and incubated for 20 min at 65 °C. After Samples equilibrated to ~ 37 °C, 400 mM iodoacetamide (25 µL) was added and incubated in the dark for 30 min at 37 °C. To the samples was added PBS (950 µL) and centrifuged to settle the beads. The supernatant was removed, and the samples were subjected to tryptic digest by adding a 200 µL mixture of urea (2M in PBS), 2 µL of 100 mM Ca_2Cl and 2 µg of mass spectrometry grade trypsin Gold enzyme, transferred to clean 1.5 mL Eppendorf tubes, and placed on a thermomixer and shaken overnight at 37

°C. The next day, samples were pelleted at 1400g for 3 min and the supernatant was removed and placed in clean Eppendorf tubes. The resin was resuspended with water (75 μL), centrifuged, and the supernatant was removed and combined with the previous supernatant. The water wash step was repeated and 17.5 μL of mass spectrometry grade formic acid (Sigma Aldrich) was added to the combined supernatant. The combined supernatant was dried overnight on a speed-vacuum and the dried samples were subjected to desalting by stage-tip.

Desalting by Stage-Tip.[273] Dried samples were redissolved with 60 μL of water/ACN/formic acid (98/2/0.1). Stage-tips were prepared with SDB-XC packing material (Empore™) according to ref. 40 and washed with water/ACN/formic acid (60/40/0.1, 60 μL) by centrifugation at 1000g for 5 min. The prepared stage-tips were then washed twice with water/ACN/formic acid (98/2/0.1, 60 μL, 1000g for 5 min). Dissolved samples were loaded onto the prepared stage-tips and centrifuged at 1000g for 5 min. Samples were then washed twice with water/ACN/formic acid (98/2/0.1, 60 μL, 1000g for 5 min). Peptides were eluted by sequentially washing the stage-tips with ACN/water/formic acid (60/40/0.1, 120 μL), ACN/water/formic acid (80/40/0.1, 60 μL), and ACN/water/formic acid (60/40/0.1, 60 μL). Elution of peptides was by centrifugation at 1000g for 5 min. The peptide solution was concentrated to dryness in a speed-vacuum and stored at -20 °C until LC-MS/MS analyses.

Competition study with HEK293T Cell lysate. Total protein of lysate was adjusted to 1.4 mg/mL and lysates were incubated with either DMSO or Probe B (100 μM) in 500 μL reaction volume for 15 min at room temperature and subsequently photoirradiated Probe

treated samples on ice for 30 min in the dark, while DMSO treated samples were exposed to ambient light on ice for the same duration. For the competition samples, **17** (20 mM) and Probe B (100 μM) were added to diluent (lysis buffer supplemented with 1X protease inhibitor) and mixed properly by pipetting. To the mixture was added lysate so that the final protein concentration was 1.4 mg/mL in a 500 μL reaction volume. The samples were incubated for 15 min at room temperature followed by photoirradiation on ice for 30 min in the dark. All samples were heated for 10 min at 65 °C, allowed to cool to room temperature before being subjected to click chemistry with biotin-N_3 as described previously. Removal of excess biotin-N_3, enrichment over NeutrAvidin resin, peptide digestion, and peptide desalting were performed in the same manner as previously described. Peptides products from each sample group were stored at -20 °C until LC-MS/MS analyses.

Liquid Chromatography-Mass Spectrometry. Analyses of tryptic peptides was performed with an Orbitrap Elite mass spectrometry (Thermo Scientific) in line with a Dionex UltiMate 3000 UHPLC (Thermo Scientific), an RSLCnano pump, and Xcalibur 2.2 software for instrument control. Liquid chromatography was performed with an in-house packed analytical C18 reverse phase column (10 μm emission tip, 75 μm x 200 mm, New Objective, Woburn, MA) using Luna C18 5μm particles (Phenomenex, Torrance, CA). Peptides were eluted with water (0.1% formic acid; Solvent A) and acetonitrile (0.1% formic acid; Solvent A) at flow rate of 0.3 μL/min. Gradient for LC began with 2% B on a linear increase to 10% B in 15 min, then a linear increase to 25% B over 50 min, and another linear increase to 40% B over 29 min. The column was

washed with a linear increase from 40% - 85 % B over 1 min, isocratic at 85% B for 5 min, and the solvent gradient was equilibrated back to 2% B over 1 min and maintained at 2% B for 8 min. Conditions for ESI were – spray voltage was 2.20 kV, capillary temperature was 350 °C, S-lens RF level was 50%. Full scan MS was collected in data-dependent mode in a range of 360-1800 *m*/*z*, and the 12 most intense ion peaks were selected for collision-induced dissociation at 35% normalized collision energy. Intensity threshold was 5000, and the isolation width was 2.0 *m*/*z*. The generated spectral data were searched against SwissProt *H. sapiens* protein database using Proteome Discoverer software (v2.1; Thermo Scientific). Quantitation of proteins in each sample was performed with the quantitation function in Proteome Discoverer whereby the emPAI values were converted to protein abundance (expressed as mol %) using equation (1). Proteins missing in both competition samples but present in both probe-treated samples were identified as possible hits. Also considered as possible hits were proteins with 5-fold reduction in abundance in the competition samples compared to the probe-treated samples. A cutoff of 2 unique peptides was required for all identified proteins. Gene ontology analyses was performed using the functional annotation tool in DAVID (https://david.ncifcrf.gov/).

$$\text{Protein abundance (mol\%)} = \frac{\text{emPAI}}{\sum(\text{emPAI})} \text{ x } 100 \quad \text{.....equation (1)}$$

In-Cell Photoaffinity Labeling with HEK293T Cells. HEK293T cells were grown in 15 mm culture dishes until ~80% confluent. DMEM was removed and the cells were rinsed once with prewarmed serum free F12 (Ham) media supplemented with L-

glutamine (no Pen/Strep, no phenol red, no HEPES). Cells were then treated with the appropriate concentration of Probe B prepared in serum free DMEM/F12 (Ham) media supplemented with L-glutamine (no Pen/Strep, no phenol red, no HEPES) and incubated for one hour at 37 °C. After the incubation period, cells were photo irradiated for 30 min on ice and in the dark. Cells were harvested, settled by centrifugation, washed twice with ice-cold PBS, and lysed as previously described. Click reaction with TAMRA-N_3, SDS-PAGE, and visualization of labeled proteins were performed as previously described.

Chapter 5

Design and Synthesis of Nucleotide Mimetic Inhibitors of Eukaryotic Translation Initiation Factor 4E

5.1. Introduction

Protein synthesis is a highly regulated process, whereby its dysregulation can lead to phenotypic hallmarks of cancer such as excessive cellular proliferation, unchecked growth, metastasis and invasion, and resistance to apoptosis.[274, 275] A key regulatory node during protein synthesis is translation initiation, which is often considered the rate-limiting step in protein synthesis. The initiation of translation in eukaryotes involves several steps required for recruitment of ribosomes to mRNAs, which can be achieved in a cap-dependent or cap-independent manner via internal ribosomal entry sites (IRES).[276-278]

Eukaryotic mRNAs are mostly translated in a cap-dependent manner, which is facilitated by binding of eukaryotic initiation factor (eIF) 4F complex to the 5′-cap structure of mRNAs. eIF4F is comprised of the cap-binding protein eIF4E, the scaffolding protein eIF4G, and the helicase eIF4A, of which binding of 5′-cap mRNA to eIF4E is rate-limiting due to the low abundance of eIF4E relative to the other translation factors.[279, 280] Thus, the availability and interaction of eIF4E with 5′-mRNA cap represents a key molecular event necessary for maintaining the cellular homeostasis of protein production. Regulation of eIF4E is mediated via the PI3K-AKT-mTOR signaling pathway. In resting cells, eIF4E is bound by eIF4E binding proteins (4E-BPs; 4E-BP1 is

the most abundant isoform) which serves to reduce the availability of eIF4E for formation of translation-competent eIF4F complexes. Upon phosphorylation of 4E-BPs by mTOR, eIF4E is released and is then available to associate with eIF4G and eIF4A to form eIF4F (**Figure 5-1B**). Consequently, the levels of phosphorylated 4E-BPs are indicative of eIF4E activity.

Figure 5-1. (A) Cap-dependent translation involves recruitment of formation of translation-competent eIF4F complex and recruitment of mRNA through eIF4E recognition of the m^{7}GTP moiety with the 5′-cap structure. (B) Regulation of eIF4E activity is mediated via the PI3K-AKT-mTOR signaling pathway.

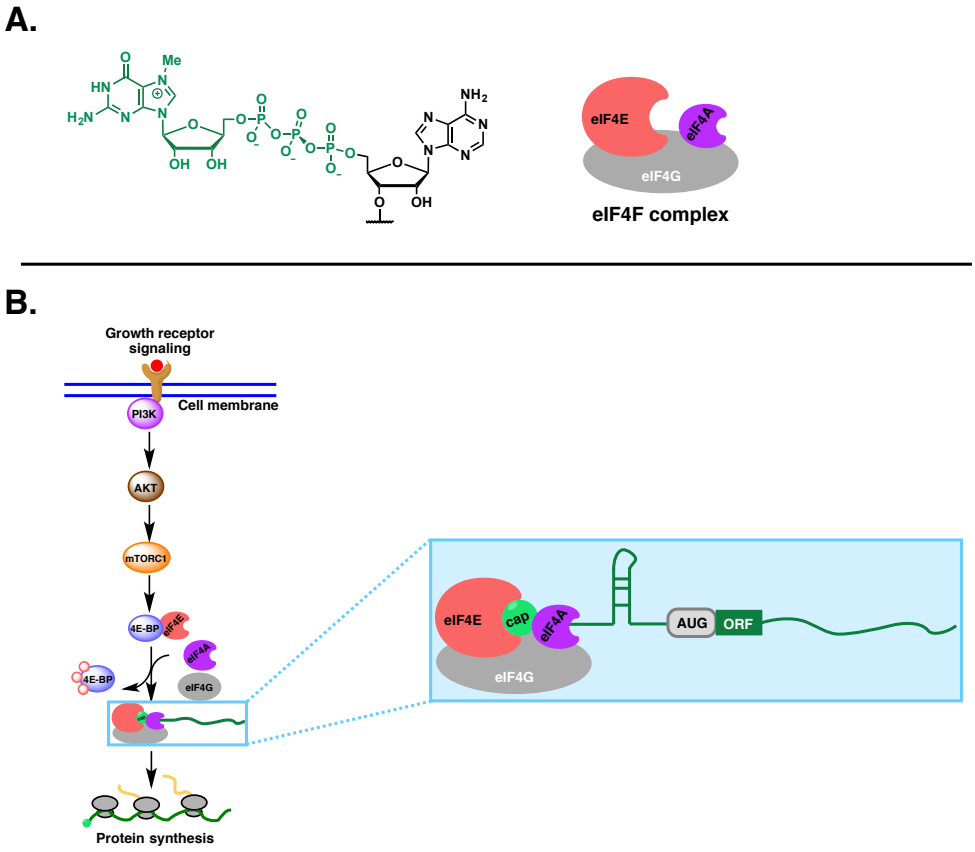

Several studies have shown that aberrant eIF4E activity correlates with increased tumorigenesis and survival of cancer cells. On the other hand, modulation of eIF4E activity has been shown to reduce establishment of tumors, reduce rates of proliferation and growth, as well as reduce metastasis/invasion in several cancers.[174, 175, 281-283] Apart from its role as an oncoprotein, dysregulation of eIF4E activity has been shown to be a significant component during induction of mechanical hypersensitivity[284] and proliferation of lymphocytes during immune response.[285] To this end, pharmacological inhibitors of eIF4E activity could potentially have wide-ranging impacts on the treatment of several human diseases, as well as serve as important chemical tools for studying aberrant cap-dependent protein synthesis in human diseases.

Several small molecules have been shown to disrupt the eIF4E-mRNA 5′-cap interaction of which a vast majority of identified antagonists are mimetics of m^7G nucleotides (**Figure 5-2A**). A few molecular interactions between eIF4E and its nucleotide inhibitors have been identified as essential for maintaining binding potency to the protein.[286] One very important molecular recognition event involves a cation-π interaction between the delocalized positive charge of the imidazolium moiety of 5′-cap analogs and conserved tryptophan residues (Trp56 and Trp102) in the cap-binding pocket of eIF4E (**Figure 5-2B**).

Another critical contributor to the binding potency of 5′-cap analogs to eIF4E involves the interaction of the phosphate group with Arg112, Arg157, and Lys162 in the cap-binding pocket. The phosphate moiety engages in through-water hydrogen-bonding with the positively charged residues. Consequently, truncation of the phosphate moiety

from m^7GTP to m^7GMP leads to a more than 700-fold reduction in the binding affinity to eIF4E.[287]

Finally, the nature of the N^7 modification has been shown to contribute to the binding potency of 5′-cap analogs to eIF4E. In general, bulkier substitutions such as with benzyl substituted 5′-cap analog derivatives engender greater binding affinities when compared to the less bulky methyl substituted derivatives.[287] The basis of the enhanced binding interaction between eIF4E and 5′-cap analogs with bulky N^7 substitutions is mostly due to van der Waals interaction between the N^7 substituent and hydrophobic residues within pocket I or pocket II (**Figure 5-2B**).[286] Increasing the length of the methylene linker between the aromatic group and the N^7 position seems to favor binding of bulky N^7 substituents in the deeper pocket I, which leads to an improvement in the binding potency compared to the benzyl derivative.[286]

Figure 5-2. (A) Examples of 5′-cap analogs and (B) the co-crystal structures of m^7GTP (PDB: 1IPC), Bn^7-GMP (PDB: 2V8X), and 7-Cl-Ph-Ethyl-GMP (PDB: 4DT6) bound to eIF4E. 7-Cl-Ph-Ethyl-GMP binds more potently to eIF4E by accessing the deeper hydrophobic pocket I compared to Bn^7-GMP which can only access the relatively shallow hydrophobic pocket II. Water molecules are shown as magenta spheres.

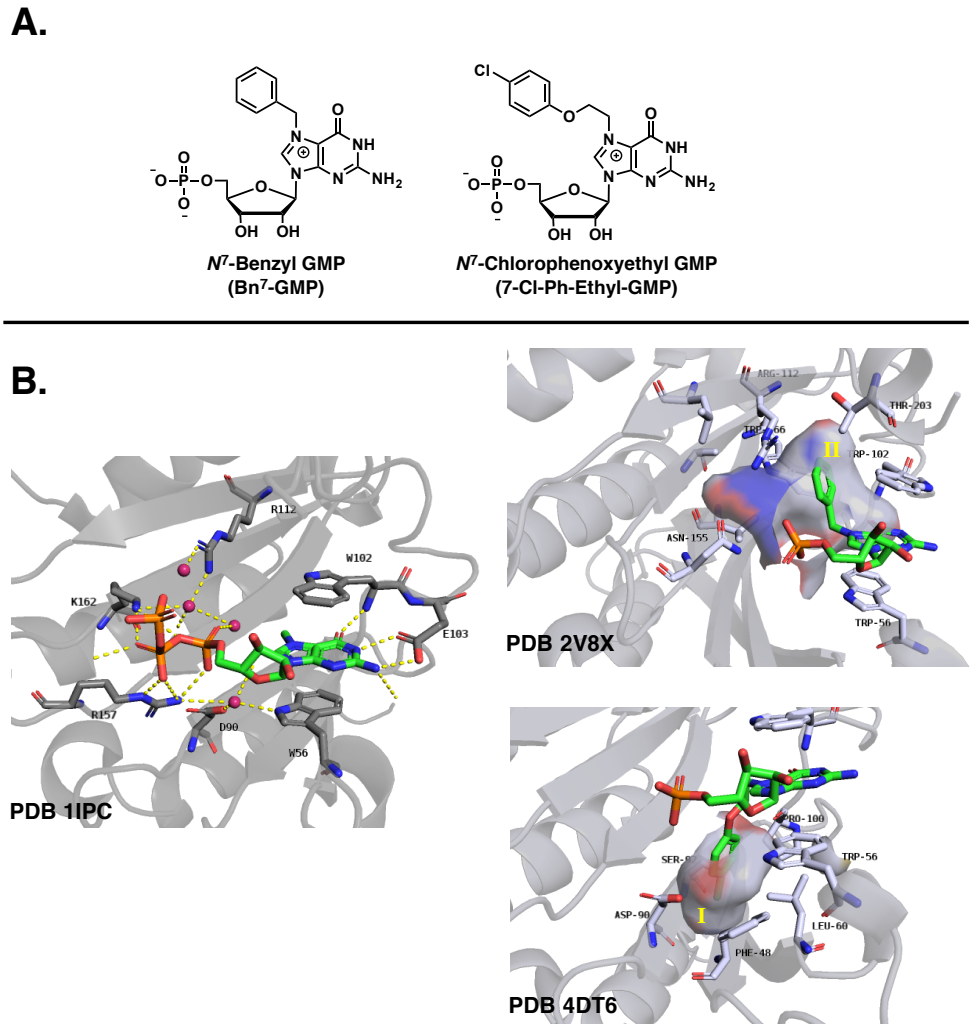

To date, m^7GTP is the most potent antagonist of eIF4E owing to the extensive through-water electrostatic interaction between the 5′-*O*-triphosphate and charged residues in the cap-binding pocket (Arg112, Arg157, and Lys162). This critical molecular interaction is weakened or lost in the monophosphate cap analog derivatives albeit modification to the size of the N^7 substituent has been shown to attenuate such reduction in binding potency. Although cellular delivery of 5′-cap analogs can be facilitated with pronucleotides,[147, 241, 243] the cellular activity of monophosphate cap analogs could be further reduced through possible metabolic dephosphorylation by phosphatases. Consequently, replacing the phosphate moiety could potentially improve the metabolic stability of 5′-cap analogs which in turn should improve their cellular activity. Recent attempts at replacing the 5′-phosphate moiety in m^7- and Bn^7 -GMP cap analogs with phosphate isosteres such as squaramide, sulfamide, and tetrazole yielded compounds with inferior binding potency when compared with Bn^7-GMP (over 14-fold reduction in binding potency) (**Figure 5-3)**.[288] Co-crystal structure of a sulfamide derivative bound to eIF4E suggests that the important electrostatic interaction with the aforementioned basic residues was lacking, which could explain the reduction in binding potency. Of note, the co-crystal structure of the squaramide derivative bound to eIF4E did show electrostatic interactions between the squaramide moiety with the side chain of Arg157, albeit with a suboptimal binding orientation. These results highlight the need for a new design strategy for 5′-cap nucleotide mimetics with the aim of optimizing the electrostatic interaction between the charged residues (Arg112, Arg157, Lys162) and the nucleotide mimetic moiety.

Here, we report the design and synthesis of a 5′-*O*-3-(sulfoamino)pentanedioic acid moiety as a phosphate mimetic. The binding potency of the compound was evaluated using a fluorescence-quenching assay. We also present our efforts at developing a prodrug strategy for cellular delivery of the 5′-cap analog nucleotide mimetic as well as biological evaluation of the 5′-cap nucleotide mimetic as a chemical tool to study cap-dependent protein translation in T cell activation.

5.2. Results and Discussion

5.2.1. Design Strategy

Since proper orientation of a potential phosphate bioisostere moiety is essential for optimal electrostatic interaction with the aforementioned charged residues eIF4E, we chose to incorporate sulfur-based phosphate bioisosteres in our design. Sulfur-containing bioisosteres at full ionization adopt a tetrahedral shape, which is similar to that of a phosphate. In addition, sulfur-based phosphate bioisosteres of phosphate such as methyl sulfate, methyl sulfonate, and methyl sulfamate have p*K*a values of -3.4, -1.9, and 15.6, respectively and thus will be fully ionized at physiological pH with the exception of the sulfamate, which is neutral at physiological pH.[62] However, the mono-anionic state of the sulfates and sulfonates at physiological pH is not sufficient to replicate the electrostatic interactions of a di-anionic phosphate group. The sulfamate is a worse phosphate bioisostere in terms of its charge state at physiological pH (neutral vs -2 charge state).

In order to truly replicate the di-anionic nature of a monophosphate, we envisioned a dicarboxylate moiety as a phosphate mimic for our design. As a phosphate bioisostere, carboxylic acids are easily ionized at physiological pH (p*K*a = 4.0 – 5.0). We

recognized, however, that the trigonal shape of a carboxylate, and its relatively small size might not provide the best option for proper positioning of the phosphate mimic to form meaningful electrostatic interactions with the charged residues (Arg112, Arg157, and Lys162). Nonetheless, we hypothesized that a combination of the tetrahedral shape of a sulfate-based (for proper positioning) and a dicarboxylic acid moiety (to mimic a -2-charge state) might be sufficient to mimic the full electrostatic interactions between eIF4E and the monophosphate of 5′-cap analogs. Consequently, we envisioned installing an alkyl linker between the carboxylic acids and the sulfur moiety as a way to bring the carboxylic acids into close proximity with the charged residues for the needed electrostatic interactions (**Figure 5-3**). In addition, we elected to prepare the sulfamate ester derivative due to possible susceptibility of the sulfate ester derivative to enzymatic or chemical hydrolysis. The nature of the N^7 substituent has been shown to contribute to the binding potency of nucleotide cap analogs, thus we chose to prepare the nucleotide mimetic of N^7-(p-chlorophenoxyethyl)guanosine monophosphate (7-Cl-Ph-Ethyl-GMP) whose N^7 substituent is known to bind in the deeper hydrophobic pocket I leading to higher binding potency to eIF4E.

5.2.2. Synthesis of 5′-Cap Analog Nucleotide Mimetic Inhibitor of eIF4E

Due to ease of synthesis and availability of starting materials, we elected to prepare a symmetric nucleotide mimetic with two carbon spacers between each carboxylic acid and the sulfamate nitrogen. As shown in **Scheme 5-1**, we began our synthesis with reductive amination of dimethyl acetone-1,3-dicarboxylate in the presence of NH_4OAc and sodium cyanoborohydride, which afforded compound **1** in 72% yield.

Protection of the amine with a Boc group and subsequent hydrolysis of the methyl esters afforded compound **3**, which was further esterified with nitrobenzyl bromide to afford compound **4** in 89% yield over two steps. Deprotection of the Boc group gave compound **5** in 98% yield. Treatment of **5** with 4-nitrophenyl chlorosulfate in the presence of excess 4-nitrophenol afforded the 4-nitrophenyl sulfamate **6** in 44% yield. Subsequent treatment of nucleoside **7** with **6** gave sulfamate ester **8** in 56% yield. Desilylation of **8** gave compound **9** in 74% yield, which was subsequently subjected to UV-mediated ester hydrolysis to afford the dicarboxylate **10** in 45% yield.

Figure 5-3. Previous efforts at developing nucleotide mimetic 5′-cap analogs and the proposed design combining a sulfur-based moiety and dicarboxylate moieties as a phosphate mimetic of 5′-cap analogs.

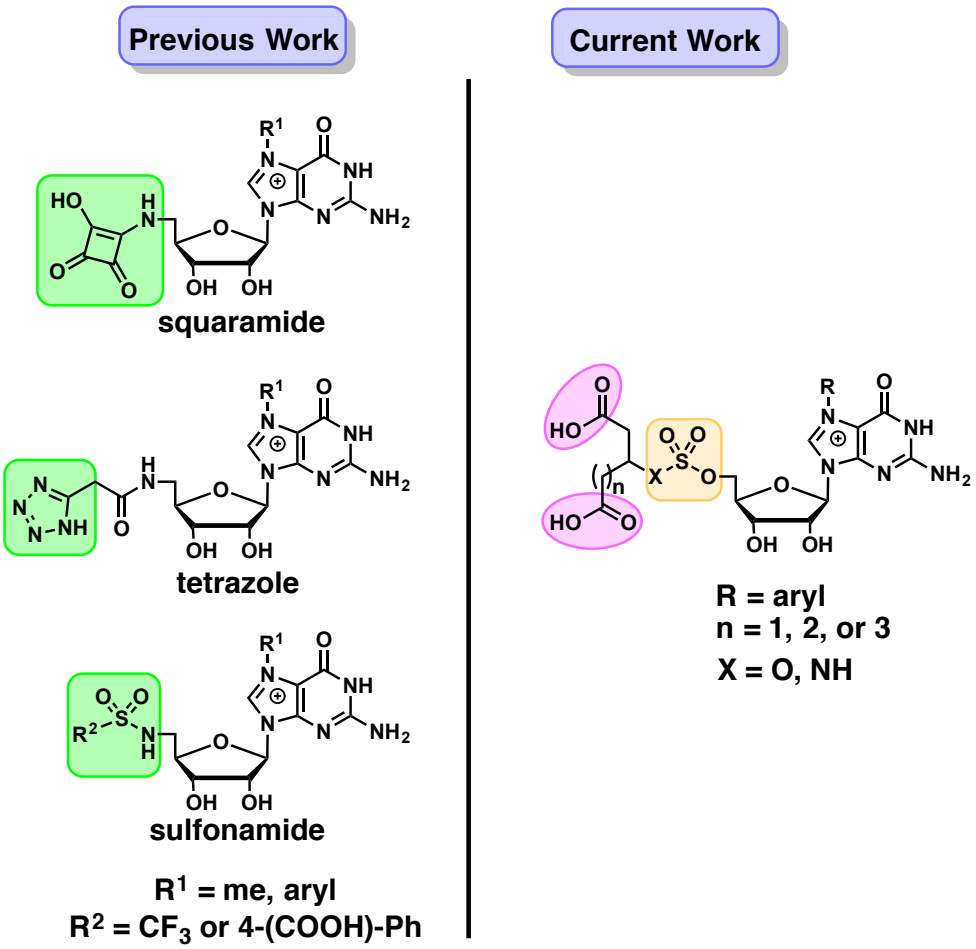

Scheme 5-1. Preparation of nucleotide mimetic **10**.

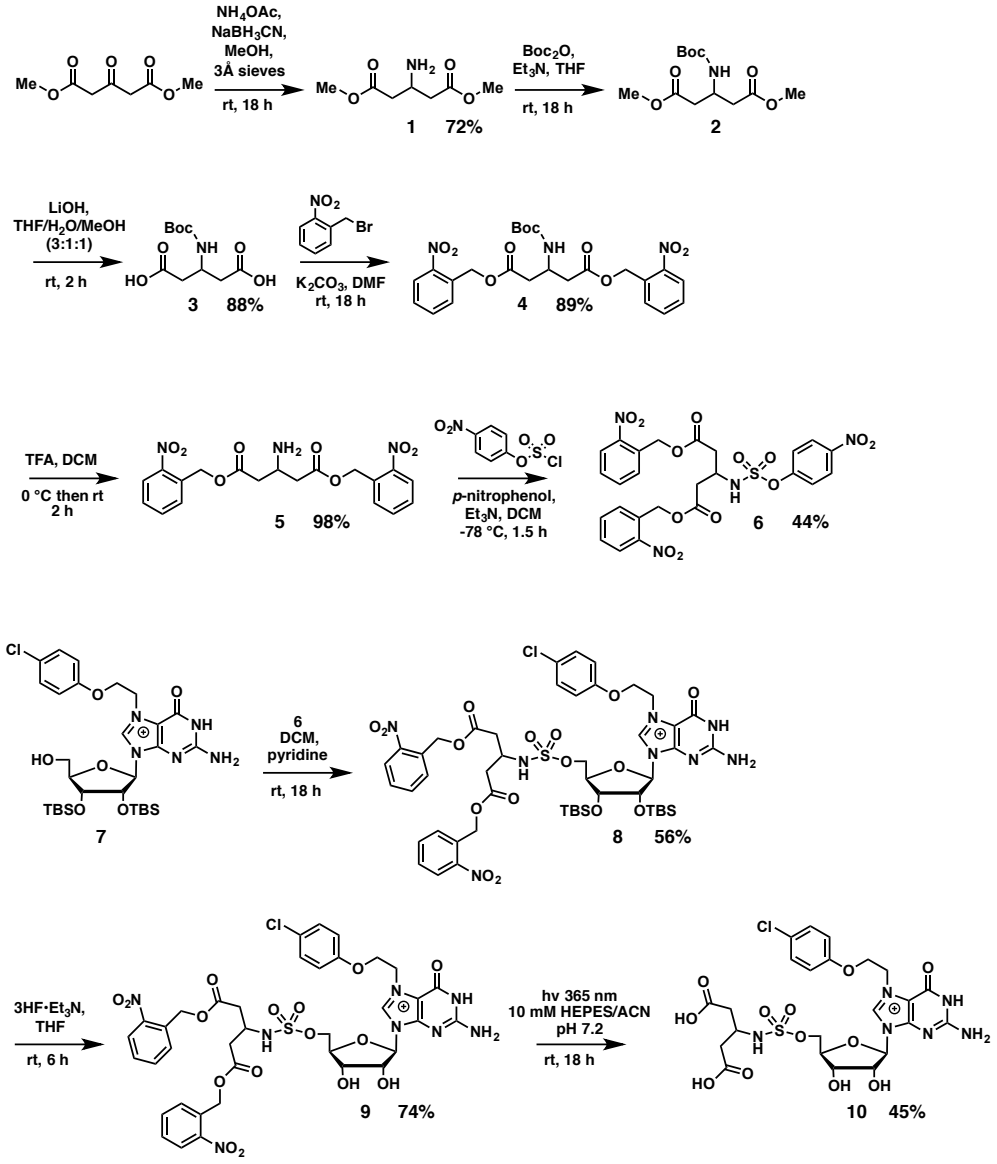

5.2.3. Binding Affinity of Compound 10 to eIF4E

With nucleotide mimetic **10** in hand, we set out to determine its binding affinity to eIF4E in a fluorescence-quenching assay. The assay monitors the fluorescence of four conserved tryptophan residues, which are quenched upon binding of a 5′-cap analog to eIF4E.[289] We also evaluated the binding affinity for 7-Cl-Ph-Ethyl-GMP, for comparison. From our assay, the binding affinity (K_d) of **10** was determined to be 163 ± 0.03 nM while that of 7-Cl-Ph-Ethyl-GMP was found to be 95.3 ± 0.02 nM (see **Appendix**). This result suggests that substituting the 5′-*O*-phosphate of 7-Cl-Ph-Ethyl-GMP with a 5′-*O*-3-(sulfoamino)pentanedioic acid moiety is tolerable with only a modest loss in binding potency, thus validating our nucleotide mimetic design for this particular 5′-cap analog.

To elucidate the basis for the observed binding potency, we sought to determine the binding mode of compound **10** through a molecular modeling study, by docking **10** into the co-crystal structure of 7-Cl-Ph-Ethyl-GMP binding complex with eIF4E (PDB 4DT6). The highest scoring model (docking score = -12.341) had two constraints – hydrogen bonding interactions between guanosine carbonyl to backbone amide of Trp102 and N^2 H-bond interaction with the sidechain of Glu103. This model predicted that the carboxylic acids of **10** engage in H-bond interactions with the sidechains of Arg112 and Lys162, while one of its sulfamate oxygen forms H-bond interactions with the sidechain of Arg157 (**Figure 5-4A**). In addition, compound **10** still maintained the cation-π interaction with Trp56 and Trp102, while the phenyl moiety of its N^7 substituent binds in the hydrophobic pocket I. On the other hand, the lowest scoring model (docking score = -10.763) which was free of constraints predicted that the dicarboxylic acid was bound in a

different orientation and showed only one H-bond interaction with the sidechain of Asn50 (**Figure 5-4B**). This model also showed that compound **10** maintains the cation-π interactions with the conserved tryptophan residues and that the phenyl moiety of its N^7 substituent binds in the hydrophobic pocket I. Similar to the highest scoring model, this model also showed that **10** maintains the same H-bond interaction between the guanosine carbonyl and the backbone amide of Trp102, as well as, the H-bond interactions of N^2 and guanosine amide with the sidechain of Glu103.

It is worth noting that the lowest scoring model and not the highest scoring model could be a more predictive representation of the binding mode of **10** to eIF4E, since there is only one H-bond interaction predicted for its nucleotide mimetic moiety (carboxylic acid and sidechain of Asn50), which could be considered comparable to the single H-bond interaction observed between the phosphate moiety of 7-Cl-Ph-Ethyl-GMP with the sidechain of Arg157. The highest predicted binding mode is unlikely since the predicted H-bond interactions between **10** and eIF4E in that model are comparable to that observed with the triphosphate moiety of m^7GTP, which should in theory lead to a binding potency similar to that of m^7GTP. Overall, the result of our docking studies suggest that our nucleotide mimetic design is at least able to reproduce the molecular recognition events between the phosphate moiety of 7-Cl-Ph-Ethyl-GMP and eIF4E.

Figure 5-4. Predictive binding modes of compound **10** binding to eIF4E showing the highest scoring model (A), lowest scoring model (B), and an overlay of compound **10** (salmon) with 7-Cl-Ph-Ethyl-GMP (green) (C). All models were generated by docking **10** into the co-crystal complex of 7-Cl-Ph-Ethyl-GMP and eIF4E (PDB 4DT6).

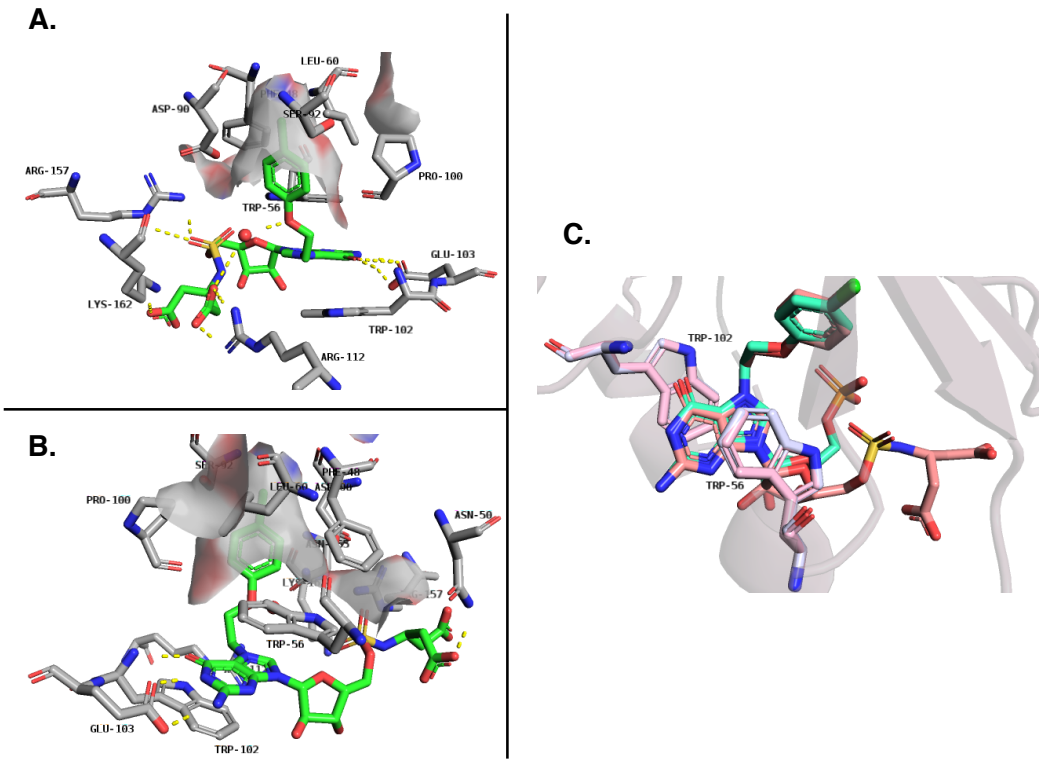

5.2.4. Biological Evaluation of Compound 10

Having established that **10** binds potently to eIF4E, we next assessed the ability of **10** to inhibit eIF4E in cells. We chose to evaluate the effect of **10** on proliferation of $CD4^+$ T cells following antigen-specific activation/stimulation via T cell receptor (TCR) - CD3 complex and costimulatory molecule CD28. T cell activation is an energetically costly process that is marked by increased glucose metabolism, increased glycolysis, increased protein production and a switch from oxidative phosphorylation to oxidative glycolysis akin to the Warburg effect in cancer cells.[290, 291] This increase in glucose metabolism and protein synthesis is necessary as activated cells prepare for proliferation and clonal expansion. Signaling through the TCR-CD3 and costimulatory CD28 serves to activate the PI3K-AKT-mTOR signaling pathway of which eIF4E is a downstream effector.[291] Consequently, the 4E-BP-eIF4E axis has been shown to promote growth and proliferation in lymphocytes and constitutive expression of 4E-BP1 has antiproliferative effect on activated $CD4^+$ T cell.[292] Hence, pharmacological inhibition of eIF4E activity should phenocopy 4E-BP1 mediated impairment of proliferation in activated $CD4^+$ T cells.

Human peripheral blood mononuclear cells (hPBMCs) were activated with CD3/CD28 beads either alone, in the presence of compound **10** (200 μM), or in the presence of eIF4E inhibitor, 4Ei-10 (150 μM) for 72 hours. Since 4Ei-10 is a pronucleotide of 7-Cl-Ph-Ethyl-GMP, hPBMCs were preincubated with the respective compounds (**10** or 4Ei-10) 8 hours prior to activation with CD3/CD28 beads. As can be seen in **Figure 5-5A**, compound **10** did not inhibit proliferation of $CD4^+$ T cells

following stimulation. In contrast, 4Ei-10 showed significant inhibition of $CD4^+$ T cell proliferation (**Figure 5-5**).

We also assessed if inhibition of eIF4E affects expression of T cell activation markers and cytokine production *in vitro*. Activation of hPBMCs in the presence of 4Ei-10 (150 μM) did not produce a significant change in the expression of the late stage T cell activation marker CD25 when compared to vehicle treated, and untreated activated cells (**Figure 5-5F**). However, expression of CD25 was reduced in the cells treated with **10** (**Figure 5-5D**). Overall, the lack of inhibition of proliferation observed for cells treated with **10** suggest that **10** may lack sufficient cell permeability owing to its highly polar nature. On the other hand, these results establish 4Ei-10 as a viable chemical tool for studying the effect of cap-dependent translational control on T cell activation.

5.2.5. Synthesis and Biological Evaluation of Methyl Ester Prodrug of 10

In order to facilitate cellular delivery of **10**, we envisioned a prodrug strategy by esterifying the carboxylic acid moieties. To assess the effect of an ester prodrug, we elected to prepare a bis-methyl ester of **10**. Synthesis of our desired ester prodrug began with treatment of **1** with 4-nitrophenyl chlorosulfate in the presence of excess 4-nitrophenol to afford the 4-nitrophenyl sulfamate **11**. Subsequent treatment of nucleoside **7** with **11** gave sulfamate ester in 73% yield, and desilylation of **12** gave compound **13** in 58% yield (Scheme **5-2**).

With prodrug **13** in hand, we next assessed its inhibition of eIF4E activity in a T cell activation in the same manner as previously described for **10**. Similar to **10**, compound **13** showed no inhibition of $CD4^+$ T cell proliferation when compared to 4Ei-

10 (**Figure 5-5B**). In addition, expression of CD25 was also unaffected upon treatment with **13** (**Figure 5-5E**). This result suggests that there is probably incomplete intracellular ester hydrolysis of the methyl esters, which is not surprising since pig liver esterase was shown to asymmetrically hydrolyze dimethyl β-aminoglutarate to form 2-azetidinone.[293] Thus, other prodrug strategies should be explored for cellular delivery of **10**.

Figure 5-5. $CD4^+$ T-cell proliferation assay with **10** (A), **13** (B), 4Ei-10 (C). 4Ei-10 was used as a positive control in proliferation assays with **10** and **13**. Expression of late activation marker CD25 by $CD4^+$ T cells following treatment with **10** (D), **13** (E), or 4Ei-10 and stimulation for 72 h. Experiment were performed in duplicates due to limitation of test compounds.

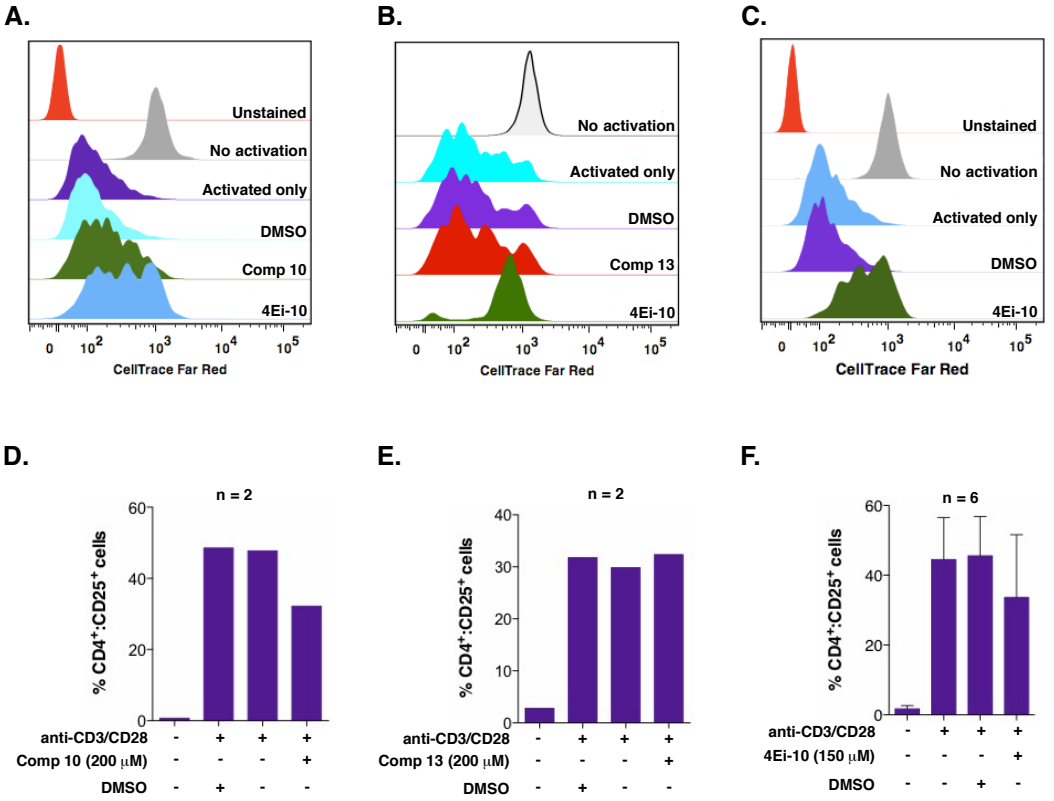

Scheme 5-2. Preparation of bis-methyl ester prodrug **13**.

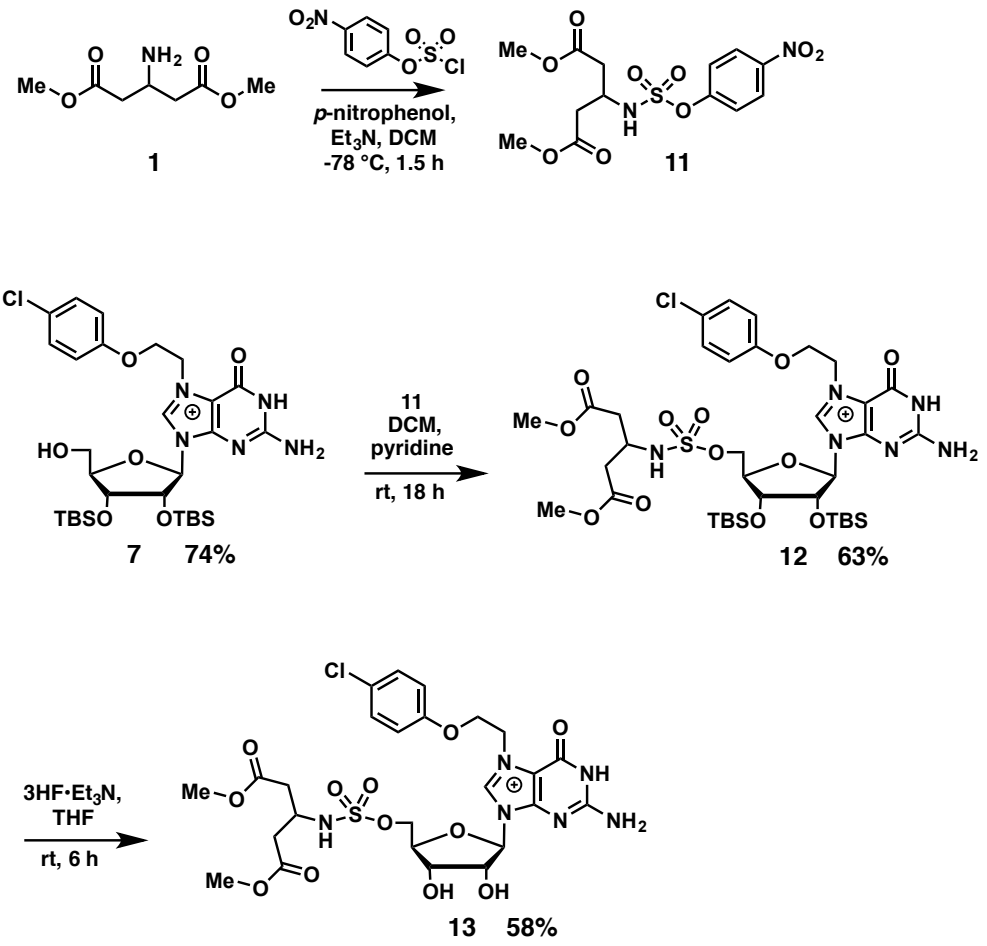

Activation of $CD4^+$ T-cells leads to production of interleukin 2 (IL-2), which is required for proliferation of $CD4^+$ and $CD8^+$ T cells and survival of suppressive regulatory T (T_{reg}) cells ($CD4^+CD25^+Foxp3^+$) .[294, 295] Using an ELISA assay, we observed that the amount of IL-2 in the supernatant of 4Ei-10 treated hPBMCs was unchanged when compared to that of unstimulated control cells (**Figure 5-6B**). Surprisingly, we observed a substantial reduction of IL-2 in the supernatant of vehicle treated and untreated activated hPBMCs. The reduction in the amount of IL-2 could suggest proliferation of T_{regs} in those samples. T_{regs} do not secrete IL-2 and are dependent on IL-2 production by other cells for survival.[294] In addition, consumption of IL-2 by T_{regs} has been proposed as a mechanism for suppression of immune response by T_{regs} *in vitro*.[294] However, we urge caution in interpreting the present data since T_{regs} express low levels of eIF4E and are anergic to signaling via the TCR. However, expression of eIF4E *in vitro* can be induced by a high dose of exogenous IL-2, which in turn induces proliferation of T_{regs}.[296] Since the amount of exogenous IL-2 in these experiments (40 U/mL) is lower than that required for the induction of proliferation in suppressive T_{regs} (1000 U/mL), then proliferation of T_{regs} might not be responsible for the observed reduction in IL-2 levels. Therefore, it is likely that differentiation into T_{regs}, and not their proliferation, is responsible for the observed reduction in IL-2 levels. Overall, these results suggest that pharmacological inhibition of eIF4E activity by 4Ei-10 inhibits or slows down proliferation in activated hPBMCs without substantial changes in the expression of late activation marker CD25.

Figure 5-6. Effects of pharmacological inhibition of eIF4E activity with 4Ei-10 after antiCD3/CD28 stimulation for 60 h. 4Ei-10 slows proliferation of $CD4^+$ T cells, which leads to reduction in the consumption of IL-2 by activated immune cells. Amount of IL-2 after 60 h of stimulation was determined by ELISA.

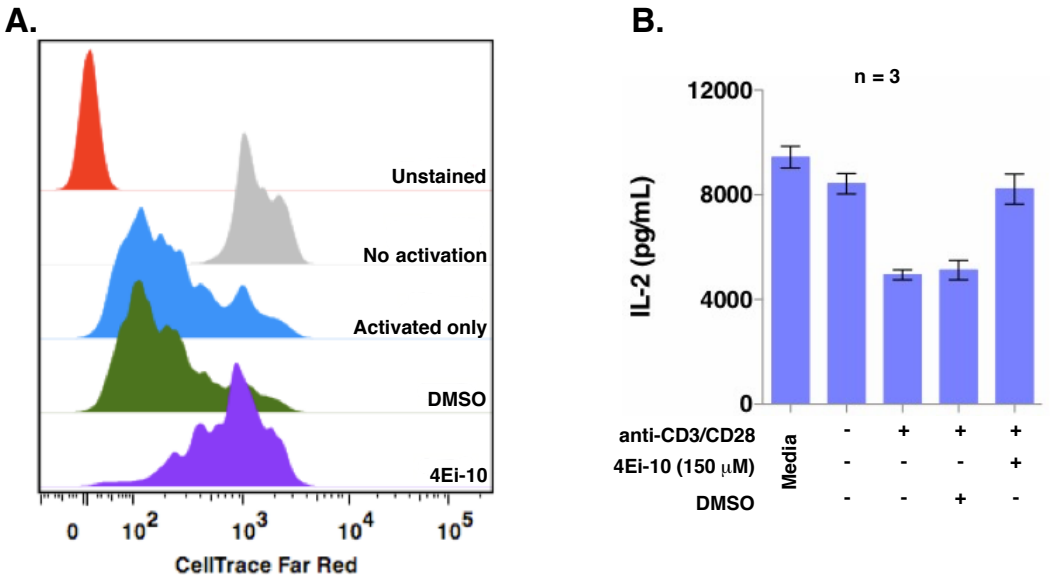

5.3. Conclusions

In summary, we demonstrate here that a 5′-*O*-3-(sulfoamino)pentanedioic acid moiety can serve as a phosphate replacement in the 5′-cap analog 7-Cl-Ph-Ethyl-GMP. Binding potency of compound **10** to eIF4E was less than two-fold lower than that of 7-Cl-Ph-Ethyl-GMP. The modest reduction in binding potency to eIF4E is superior to the over 14-fold reduction in binding potency of the previously reported 5′-cap analog mimetics (sulfamide, tetrazole, and, squaramide). Molecular docking studies suggests that compound **10** binds to eIF4E in a similar pose as 7-Cl-Ph-Ethyl-GMP but with slight differences between the binding modes of the 5′-*O*-3-(sulfoamino)pentanedioic acid moiety of compound **10** and the phosphate moiety of the 5′-cap analog. Although molecular modeling has provided some insight into the binding mode of 10, a co-crystal complex of compound 10 bound to eIF4E should be pursed in order to gain a better insight for future design of 5′-cap analogs in this series.

Although compound **10** lacked cellular activity in a T-cell activation assay, we believe that it is can find some utility as cap-analog in cell free *in vitro* translation assays. Furthermore, pharmacological inhibition of eIF4E activity with 4Ei-10 impeded proliferation of activated $CD4^+$ T cells. Thus, we also have demonstrated that the pronucleotide inhibitor of eIF4E, 4Ei-10 is a viable chemical tool for studying translational control in an eIF4E specific manner.

5.4. Materials and Methods

General Materials and Methods

All chemicals and reagents were obtained from commercial sources and were used without further purification. Anhydrous *N*,*N*-Dimethylformamide (DMF), dichloromethane (DCM), and tetrahydrofuran (THF) were obtained from a dry solvent purification system (MBraun) and dispensed under argon. All reactions were performed under an atmosphere of dry nitrogen unless otherwise noted. All silica gel chromatography and preparative reverse phase purification was performed on a Teledyne Isco CombiFlash Rf system, using Redisep Rf high performance gold silica gel columns (for normal phase purifications) and Redisep Rf high performance gold C18 columns (for reverse phase purifications). Reverse phase purifications were with water and acetonitrile. Lyophilization of compounds after reverse phase purification was performed on a FreeZone 12 Plus freeze dry system (Labconco). All Nuclear Magnetic Resonance spectra were obtained on a Brucker Avance III HD 500 MHz spectrometer unless otherwise noted at ambient temperature. Chemical shifts (δ) were recorded in parts per million (ppm) – 500 MHz for ^{1}H, 125 MHz for ^{13}C. ^{1}HNMR and ^{13}CNMR spectra were referenced by solvent signal, $CDCl_3$ (δ = 7.26 ppm for ^{1}HNMR and 77.23 ppm for ^{13}CNMR), DMSO-d_6 (δ = 2.50 ppm for ^{1}HNMR and 39.52 ppm for ^{13}CNMR), MeOH-d_6 (δ = 3.31 ppm for ^{1}HNMR and 49.00 ppm for ^{13}CNMR), acetone-d_6 (δ = 2.05 ppm for ^{1}HNMR and 29.84 ppm for ^{13}CNMR). All high-resolution mass spectroscopy (HRMS) were performed on an LTQ Orbitrap Velos instrument (Thermo Scientific) in positive-ion mode.

Dimethyl 3-aminopentanedioate (1).[297] To an oven-dried round bottom flask was added dimethyl-3-oxoglutarate (1 mL, 6.93 mmol), ammonium acetate (1.87 g, 24.3 mmol), and

methanol (20 mL). The mixture was purged with N_2 and stirred overnight at room temperature over 3Å molecular sieves (2 g). To the reaction was added sodium cyanoborohydride (566 mg, 9.01 mmol) and acidified with 3M methanolic HCl[297] to pH 3, and the reaction was stirred for another hour at room temperature. The reaction was filtered through celite, concentrated in vacuo, and the resulting residue was dissolved with H_2O (10 mL). The aqueous mix was washed with Et_2O (3X) and the pH was adjusted to about 9 by adding solid potassium carbonate. The basic aqueous layer was extracted with DCM (3X) and the organic extract was washed with brine (1X), dried over $MgSO_4$, filtered, and concentrated in vacuo to give 874 mg of product – 72% yield. ^{1}H NMR (500 MHz, $CDCl_3$) δ 1.66 (br s, 2H), 2.39 (dd, J = 16.0, 8.5 Hz, 2H), 2.50 (dd, J = 16.0, 4.0 Hz, 2H), 3.59 – 3.65 (m, 1H), 3.68 (s, 6H). ^{13}C NMR (125 MHz, $CDCl_3$) δ 41.7, 45.4, 51.8, 172.3. MS [ESI+]: 176.3 [M+H$^+$].

Dimethyl 3-((*tert*-butoxycarbonyl)amino)pentanedioate (2). To an oven-dried round bottom flask was added **1** (200 mg, 1.14 mmol) and anhydrous THF (3.4 mL). The reaction vessel was purged with N_2. Triethylamine (0.16 mL, 1.14 mmol) and Boc_2O (274 mg, 1.26 mmol) were added to the reaction. The reaction was purged with N_2 and stirred overnight at room temperature. The reaction was concentrated in vacuo and the resulting oil was taken up in EtOAc and washed with sat. aq. NH_4Cl (1X), H_2O (2X), and brine (1X). The organic layer was dried over $MgSO_4$, filtered, and concentrated in vacuo. Resulting product was taken forward without further purification.

3-((*tert*-butoxycarbonyl)amino)pentanedioic acid (3). To a round bottom flask was added **2** (350.8 mg, 1.27 mmol), THF/H_2O/MeOH (3:1:1, 6.5 mL), and LiOH (125 mg,

5.21 mmol). The reaction was stirred for two hours at room temperature. The organics were removed in vacuo and the resulting aqueous layer was washed with DCM (1X). The aqueous layer was acidified to ~ pH 2 – 3 with 1N HCl and extracted with EtOAc (5X). The combined organic extract was dried over $MgSO_4$, filtered, and concentrated in vacuo to give 248 mg of product – 88% yield over two steps. ^{1}H NMR (500 MHz, MeOH-d_4) δ 1.43, 2.56 (d, J = 6.5 Hz, 4H), 4.25 (quint, J = 6.5 Hz, 1H). ^{13}C NMR (125 MHz, MeOH-d_4) δ 28.7, 39.5, 46.1, 80.2, 157.4, 174.6. MS [ESI+]: 293.4 [M+2Na$^+$].

Bis(2-nitrobenzyl) 3-((tert-butoxycarbonyl)amino)pentanedioate (4).[298] To an oven-dried round bottom flask was added **3** (245 mg, 0.991 mmol), K_2CO_3 (342 mg, 2.48 mmol), *o*-nitrobenzyl bromide (535 mg, 2,48 mmol), and anhydrous DMF (7.0 mL). The reaction vessel was purged/evacuated extensively with N_2 and the reaction was stirred overnight at room temperature. Reaction was poured over ice-cold water (20 mL) and extracted with EtOAc (3X). The combined organic extract was dried over $MgSO_4$, filtered, and concentrated in vacuo with coevaporation with toluene. The resulting oil was purified by flash column chromatography, eluting with hexanes/EtOAc (5 – 30% EtOAc) to give 455 mg of product – 89% yield. ^{1}H NMR (500 MHz, $CDCl_3$) δ 1.41 (s, 9H), 2.77 (dd, J = 16.0, 6.0 Hz, 2H), 2.85 (dd, J = 16.0, 5.0 Hz, 2H), 4.38 (br s, 1H), 5.32 (d, J = 7.0 Hz, 1H), 5.53 (s, 4H), 7.50 (t, J = 8.0 Hz, 2H), 7.59 (d, J = 7.5 Hz, 2H), 7.65 (t, J = 7.5 Hz, 2H), 8.11 (d, J = 8.5 Hz, 2H). ^{13}C NMR (125 MHz, $CDCl_3$) δ 28.5, 38.0, 44.5, 63.4, 79.9, 125.2, 129.1, 129.3, 131.9, 134.0, 147.7, 155.1, 170.7. MS [ESI+]: 518.3 [M+H$^+$].

Bis(2-nitrobenzyl) 3-aminopentanedioate (5). To an oven-dried round bottom flask was added **4** (453.2 mg, 0.876 mmol), dry DCM (10 mL), and the solution was cooled to 0 °C. Trifluoroacetic acid (1.34 mL, 17.5 mmol) was added dropwise and the reaction was stirred for five minutes at 0 °C. The reaction was removed from the ice bath and allowed to stir for two hours at room temperature. The reaction was cooled to 0 °C, neutralized slowly with sat. aq. $NaHCO_3$ and extracted with DCM (3X). The organic extract was washed with H_2O (1X), dried over $MgSO_4$, filtered, and concentrated in vacuo to give 359 mg of product – 98% yield. ^{1}H NMR (500 MHz, $CDCl_3$) δ 2.82 – 2.92 (m, 4H), 3.94 (quint, J = 6.0 Hz, 1H), 5.52 (s, 4H), 6.55 (br s, 2H), 7.48 (t, J = 8.0 Hz, 2H), 7.58 (d, J = 7.5 Hz, 2H), 7.64 (t, J = 7.5 Hz, 2H), 8.07 (d, J = 8.0 Hz, 2H). ^{13}C NMR (125 MHz, $CDCl_3$) δ 37.7, 45.3, 63.8, 125.2, 129.2, 129.5, 131.4, 134.1, 147.6, 170.7. MS [ESI+]: 418.2 [M+H$^+$].

Bis(2-nitrobenzyl) 3-(((4-nitrophenoxy)sulfonyl)amino)pentanedioate (6). Sulfurochloridate[299] (404 mg, 1.70 mmol) was dissolved with dry DCM (1.2 mL) in an oven-dried flask, purged with N_2, and cooled to -78 °C. To another oven-dried flask was added **5** (355 mg, 0.851 mmol), *p*-nitrophenol (237 mg, 1.70 mmol), triethylamine (0.36 mL, 2.55 mmol), and dry DCM (6 mL). The mixture was purged extensively with N_2 and transferred dropwise to the vessel containing the sulfurochloridate, and stirred for 1.5 hours at -78 °C. The reaction was removed from the -78 °C bath, allowed to warm to room temperature, and concentrated in vacuo. The resulting oil was purified by flash column chromatography eluting with 1% MeOH in DCM. Relevant fractions were pooled and concentrated in vacuo and the resulting residue was dissolved with DCM (100 mL)

and washed with sat. aq. $NaHCO_3$ (5X, 50 mL) to give 230 mg of product – 44% yield. ^{1}H NMR (500 MHz, $CDCl_3$) δ 2.90 – 2.99 (m, 4H), 4.36 (br s, 1H), 5.53 (s, 4H), 6.13 (br s, 1H), 7.43 (d, J = 9.0 Hz, 2H), 7.51 – 7.57 (m, 4H), 7.65 (td, J = 7.5, 1.5 Hz, 2H), 8.10 (dd, J = 8.5, 1.0 Hz, 2H), 8.26 (d, J = 9.0 Hz, 2H). ^{13}C NMR (125 MHz, $CDCl_3$) δ 37.7, 48.8, 64.0, 122.3, 125.4, 125.8, 129.5, 129.9, 131.0, 134.0, 146.1, 147.9, 154.6, 170.3. MS [ESI+]: 641.7 [M+Na^+].

2-amino-9-((2*R*,3*R*,4*R*,5*R*)-5-(((*N*-(1,5-bis((2-nitrobenzyl)oxy)-1,5-dioxopentan-3-yl)sulfamoyl)oxy)methyl)-3,4-bis((*tert*-butyldimethylsilyl)oxy)tetrahydrofuran-2-yl)-7-(2-(4-chlorophenoxy)ethyl)-6-oxo-6,9-dihydro-1*H*-purin-7-ium (8). To an oven-dried round bottom flask was added **7**[243] (40 mg, 0.0595 mmol) and dry pyridine (0.7 mL). The solution was purged/evacuated extensively with N_2 under vacuum. Compound **6** (147 mg, 0.238 mmol) was dissolved with dry DCM (0.3 mL) and added to the reaction vessel containing dissolve **7**. The reaction was purged with N_2 and stirred overnight at room temperature. The reaction was concentrated under reduced pressure with coevaporation with toluene, and the resulting residue was purified by flash column chromatography – eluting with $CHCl_3$/MeOH (0 – 10% MeOH) to give 38 mg of product – 56% yield. *Note: Any p-nitrophenol impurity was removed by washing a DCM solution of product with sat. aq. $NaHCO_3$.* ^{1}H NMR (500 MHz, MeOH-d_4) δ -0.17 (s, 3H), -0.02 (s, 3H), 0.11 (s, 3H), 0.13 (s, 3H), 0.78 (s, 9H), 0.93 (s, 3H), 2.81 – 2.89 (m, 4H), 4.26 (quint, J = 6.5 Hz, 1H), 4.30 – 4.42 (m, 6H), 4.88 (obscured by H_2O resonance), 5.43 – 5.51 (m, 5H), 5.95 (d, J = 5.0 Hz, 1H), 6.89 (d, J = 8.0 Hz, 2H), 7.15 (d, J = 8.0 Hz, 2H), 7.52 (t, J = 7.5 Hz, 2H), 7.64 – 7.69 (m, 4H), 8.06 (t, J = 8.0 Hz, 2H). ^{13}C NMR (125

MHz, MeOH-d_4) δ -4.8, -4.6, -4.2, 18.8 (d, J = 11.3 Hz), 26.3 (d, J = 9.8 Hz), 40.0 (d, J = 15.4 Hz), 64.5 (d, J = 4.9 Hz), 66.9, 69.4, 73.4, 76.4, 85.2, 91.0, 109.3, 117.2, 125.8 (d, J = 27.0 Hz), 127.4, 130.2 (d, J = 4.8 Hz), 130.37, 130.39, 130.5, 132.8 (d, J = 4.5 Hz), 135.0 (d, J = 6.6 Hz), 149.0 (d, J = 13.9 Hz), 151.8, 158.1, 161.3, 162.0, 171.8 (d, J = 23.1 Hz). MS [ESI+]: 1146.1 [M^+].

2-amino-9-((2*R*,3*R*,4*S*,5*R*)-5-(((*N*-(1,5-bis((2-nitrobenzyl)oxy)-1,5-dioxopentan-3-yl)sulfamoyl)oxy)methyl)-3,4-dihydroxytetrahydrofuran-2-yl)-7-(2-(4-chlorophenoxy)ethyl)-6-oxo-6,9-dihydro-1*H*-purin-7-ium (9). Compound **8** (32 mg, 0.0276 mmol) was dissolved with dry THF (0.5 mL), and to the solution was added 3HF•Et_3N (27 μL, 0.165 mmol). The reaction was stirred at room temperature for six hours. The reaction was concentrated under reduced pressure and the resulting residue was purified by flash column chromatography – eluting with $CHCl_3$/MeOH (20% MeOH) to give 18.7 mg of product – 74% yield. ^{1}H NMR (500 MHz, DMSO-d_6) δ 2.70 – 2.79 (m, 4H), 4.07 (quint, J = 6.5 Hz, 1H), 4.15 – 4.20 (m, 2H), 4.22 – 4.28 (m, 1H), 4.30 – 4.37 (m, 1H), 4.42 (t, J = 5.0 Hz, 2H), 4.56 (q, J = 4.0 Hz, 1H), 4.68 – 4.82 (m, 2H), 5.42 (d, J = 3.0 Hz, 4H), 5.48 (d, J = 5.0 Hz, 1H), 5.77 (d, J = 5.5 Hz, 1H), 5.85 (d, J = 4.0 Hz, 1H), 5.90 (br s, 2H), 6.94 (d, J = 8.5 Hz, 2H), 7.27 (d, J = 8.5 Hz, 2H), 7.59 (q, J = 7.0 Hz, 2H), 7.64 – 7.68 (m, 2H), 7.71 – 7.75 (m, 3H), 8.09 (dd, J = 8.0, 4.0 Hz, 2H), 8.45 (br s, 1H), 9.08 (s, 1H). ^{13}C NMR (125 MHz, acetone-d_6) δ 22.5 (d, J = 4.5 Hz), 39.5 (d, J = 14.3 Hz), 49.5, 49.6, 63.8, 66.6, 70.4, 71.2, 75.0, 83.7, 91.5, 108.6, 117.2, 125.6, 126.4, 129.8 (d, J = 3.6 Hz), 130.0, 130.1, 132.7, 132.8, 134.9 (d, J = 3.0 Hz), 148.3 (d, J = 5.9 Hz), 150.8, 157.8, 171.0 (d, J = 6.5 Hz), 172.2. MS [ESI+]: 917.3 [M^+].

2-amino-7-(2-(4-chlorophenoxy)ethyl)-9-((2*R*,3*R*,4*S*,5*R*)-5-(((*N*-(1,3-dicarboxypropan-2-yl)sulfamoyl)oxy)methyl)-3,4-dihydroxytetrahydrofuran-2-yl)-6-oxo-6,9-dihydro-1*H*-purin-7-ium (10). Compound **9** (17.7 mg, 0.0192 mmol) was dissolved with 180 mL of 10 mM HEPES/MeCN (2:8, pH 7.2). The solution was then aliquoted into test tubes and irradiated in a rayonet (365 nm UV) overnight at room temperature in the dark. The aliquots were pooled and concentrated to dryness in vacuo. The resulting residue was purified first by normal phase flash column chromatography (20% MeOH in $CHCl_3$) followed by $CHCl_3$:MeOH:H_2O:NH_4OH (5:3:0.5:0.005). Fraction with the desired product were concentrated to dryness and then purified by reverse phase flash chromatography to give 5.64 mg of product – 45% yield after lyophilization.

Dimethyl 3-(((4-nitrophenoxy)sulfonyl)amino)pentanedioate (11). Sulfurochloridate (1.34 g, 5.83 mmol) was dissolved with dry DCM (4.0 mL) in an oven-dried flask, purged with N_2, and cooled to -78 °C. To another oven-dried flask was added **1** (511 mg, 2.92 mmol), *p*-nitrophenol (811 mg, 5.83 mmol), triethylamine (1.2 mL, 8.76 mmol), and dry DCM (20 mL). The mixture was purged extensively with N_2 and transferred dropwise to the vessel containing the sulfurochloridate, and stirred for 1.5 hours at -78 °C. The reaction was removed from the -78 °C bath, allowed to warm to room temperature, and concentrated in vacuo. The resulting oil was purified by flash column chromatography eluting with 1% MeOH in DCM. Relevant fractions were pooled and concentrated in vacuo and the resulting residue was dissolved with DCM (100 mL) and washed with sat. aq. $NaHCO_3$ (5X, 50 mL) to give 411 mg of product. Product is a bit unstable during the

wash with sat. aq. $NaHCO_3$, and was used immediately in the next step even though it was not pure.

2-amino-9-((2*R*,3*R*,4*R*,5*R*)-3,4-bis((*tert*-butyldimethylsilyl)oxy)-5-(((*N*-(1,5-dimethoxy-1,5-dioxopentan-3-yl)sulfamoyl)oxy)methyl)tetrahydrofuran-2-yl)-7-(2-(4-chlorophenoxy)ethyl)-6-oxo-6,9-dihydro-1*H*-purin-7-ium (12). To an oven-dried round bottom flask was added **7** (154 mg, 0.231 mmol) and dry pyridine (2.6 mL). The solution was purged/evacuated extensively with N_2 under vacuum. Compound **11** (347 mg, 0.923 mmol) was dissolved with dry DCM (1.3 mL) and added dropwise to the reaction vessel containing dissolve **11**. The reaction was purged with N_2 and stirred overnight at room temperature. The reaction was concentrated under reduced pressure with coevaporation with toluene, and the resulting residue was purified by flash column chromatography – eluting with $CHCl_3$/MeOH (0 – 10% MeOH) to give 131.8 mg of product – 63% yield. ^{1}H NMR (500 MHz, $CDCl_3$) δ 0.054, (s, 3H), 0.10 (s, 9H), 0.87 (d, J = 2.0 Hz, 18 H), 2.72 – 2.91 (m, 4H), 3.65 (d, J = 4.5 Hz, 6H), 4.20 (quint, J = 5.5 Hz, 1H), 4.25 – 4.42 (m, 5H), 4.58 – 4.70 (m, 2H), 4.81 (br s, 2H), 5.85 (s, 1H), 6.78 (d, J = 8.5 Hz, 2H), 7.16 (d, J = 8.5 Hz, 2H), 8.86 (br s, 1H). ^{13}C NMR (125 MHz, $CDCl_3$) δ -5.0, -4.7, -4.4, -4.1, 18.1, 25.9, 39.0, 48.8, 49.1, 52.0 (d, J = 5.3 Hz), 66.0, 66.9, 70.4, 75.6, 90.5, 108.4, 116.1, 120.4, 125.2, 126.5, 129.5, 149.9, 156.6, 171.8. MS [ESI+]: 903.3 [M^+].

2-amino-7-(2-(4-chlorophenoxy)ethyl)-9-((2*R*,3*R*,4*S*,5*R*)-5-(((*N*-(1,5-dimethoxy-1,5-dioxopentan-3-yl)sulfamoyl)oxy)methyl)-3,4-dihydroxytetrahydrofuran-2-yl)-6-oxo-6,9-dihydro-1*H*-purin-7-ium (13). Compound **12** (122 mg, 0.135 mmol) was dissolved

with dry THF (2.5 mL), and to the solution was added 3HF•Et_3N (132 μL, 0.810 mmol). The reaction was stirred at room temperature and the reaction progress was monitored by TLC. The reaction was concentrated under reduced pressure and the resulting residue was purified first by flash column chromatography – eluting with $CHCl_3$/MeOH (20% MeOH). Fraction with the desired product were concentrated to dryness and then purified by reverse phase flash chromatography to give 52.7 mg of product – 58% yield after lyophilization. ^{1}H NMR (500 MHz, DMSO-d_6) δ 2.52 – 2.59 (m, 4H obscured by solvent peak). 3.51 – 3.59 (merged peaks 7H), 3.92 (quint, J = 6.5 Hz, 1H), 4.09 – 4.26 (m, 4H), 4.42 – 4.48 (m, 2H), 4.56 (s, 1H), 4.72 – 4.81 (m, 2H), 5.51 (br s, 1H), 5.76 – 5.91 (m, 4H), 6.97 (d, J = 9.0 Hz, 2H), 7.29 (d, J = 8.5 Hz, 2H), 9.15 (s, 1H). ^{13}C NMR (125 MHz, DMSO-d_6) δ 47.5, 48.7, 51.4, 65.9, 67.9, 70.1, 73.2, 82.4, 88.6, 107.7, 116.4, 124.8, 129.3, 132.8, 149.9, 156.7, 162.6, 163.4, 170.9 (d, J = 4.5 Hz), 171.9. MS [ESI+]: 675.0 [M^+].

Determination of Binding Affinity to eIF4E. Mouse eIF4E (obtained from Lakmal Rozumalski Ph.D.) was added to freshly prepared HEPES buffer (50 mM HEPES, 100 mM KCl, 1 mM dithiothreitol, 0.5 mM EDTA, pH 7.2) so that the final protein concentration was 50 nM in 600 μL reaction volume. The protein was allowed to equilibrate in the buffer for 30 s before adding a 5′-cap analog. The mixture was mixed by shaking and fluorescence spectra were obtained three times, 30 s apart, with mixing between each fluorescence measurement. All fluorescence spectra were obtained in triplicate at ambient temperature using a Cary Eclipse fluorescence spectrophotometer (Varian, Inc.). The fluorescence at a particular concentration of a test ligand was

corrected by subtracting the fluorescence of the ligand at that concentration from the recorded fluorescence for that particular quenching experiment. Binding affinity for all test ligands was obtained by plotting the fluorescence intensity against ligand concentration in Prism 5 graphing software.

Cell Culture and *In Vitro* T-cell Proliferation Assay. Human PBMCs were isolated by Ficoll density gradient centrifugation of buffy coats of healthy donor blood samples. Thawed hPBMCs were rested overnight in complete RPMI 1640 supplemented with 10% fetal bovine serum (FBS), 100 U mL^{-1} penicillin, 100 μg mL^{-1} streptomycin, and L-glutamine at 37 °C and 5% CO_2 in a conical tube (2 x 10^6 cells/mL) prior to use in the activation assay. hPBMCs were labeled with CellTrace Far Red (Thermo Fisher Scientific) according to the manufacturer's instructions prior to activation. For T-cell activation, hPBMCs (2 x 10^6 cells/well) were cultured in a 24-well plate in T-cell activation medium (complete RPMI 1640 supplemented with 10% FBS, 100 U mL^{-1} penicillin, 100 μg mL^{-1} streptomycin, and L-glutamine, and 40 U mL^{-1} IL-2) at 37 °C and 5% CO_2. Cells were treated with test compounds or vehicle 8 hours prior to activation with antiCD3/CD28 dynabeads according to manufacturer's instructions. Activation was over 72 hours and concentration of test compounds were supplemented every 24 hours.

Flow Cytometry Analysis. antiCD3/CD28 dynabeads were removed on a magnet and cells were pelleted by centrifugation (300 g, 5 min). Cells were washed twice with ice-cold PBS and resuspended in 1 mL FACS buffer and incubated for 15 min at 4 °C. Cells were pelleted (300 g, 5 min) and the supernatant was discarded. Cells were labeled by resuspending cells in 200 μL of mAb cocktail: FITC-conjugated anti-human CD4 (5

μL/mL, BD Biosciences), PE/Cy7-conjugated anti-human CD25 (5 μL/mL, BD Biosciences), and Ghost Red 780 viability dye (5 μL/mL, Tonbo Biosciences) in ice-cold FACS buffer. Resuspended cells were incubated in the dark at 4 °C for 45 min. Cells were washed three times with 1 mL ice-cold FACS buffer and resuspended in FACS buffer (1 mL) for analysis on an LSR II flow cytometer (BD Biosciences), and FASC data was processed with FlowJo software.

Quantification of IL-2 concentration. Prior to use, hPBMCs were rested overnight in T-cell activation medium (manufacturer) in a conical tube at a final cell density of 2 x 10^6 cells/mL. T-cell activation was performed in the same manner as already described, for 60 h. After 60 h, an aliquot of culture media was removed and diluted 20 times with assay diluent buffer (2% BSA in PBS, pH = 7.4). The ELISA was performed using BD OptEIA human IL-2 ELISA set (BD Biosciences) in a 96-well ELISA plate according to manufacturer's instructions. Concentration of IL-2 from each supernatant was determined from a concentration curve of recombinant IL-2 standards.

Molecular Modeling. All molecular docking was performed with the glide program in Schrödinger. Docked ligand was either free of constraints or was docked with two constraints – H-bond interactions between ligand and two residues of eIF4E (Glu103 and Trp102).

Bibliography

1. Kunkel, T. A.; Bebenek, K., DNA replication fidelity. *Annu Rev Biochem* **2000,** *69*, 497-529.
2. Lee, T. I.; Young, R. A., Transcription of eukaryotic protein-coding genes. *Annu Rev Genet* **2000,** *34*, 77-137.
3. Graci, J. D.; Cameron, C. E., Therapeutically targeting RNA viruses via lethal mutagenesis. *Future Virol* **2008,** *3* (6), 553-566.
4. Anderson, J. P.; Daifuku, R.; Loeb, L. A., Viral error catastrophe by mutagenic nucleosides. *Annu Rev Microbiol* **2004,** *58*, 183-205.
5. Loeb, L. A.; Mullins, J. I., Lethal mutagenesis of HIV by mutagenic ribonucleoside analogs. *AIDS Res Hum Retroviruses* **2000,** *16* (1), 1-3.
6. Crotty, S.; Cameron, C. E.; Andino, R., RNA virus error catastrophe: direct molecular test by using ribavirin. *Proc Natl Acad Sci U S A* **2001,** *98* (12), 6895-900.
7. Loeb, L. A.; Essigmann, J. M.; Kazazi, F.; Zhang, J.; Rose, K. D.; Mullins, J. I., Lethal mutagenesis of HIV with mutagenic nucleoside analogs. *Proc Natl Acad Sci U S A* **1999,** *96* (4), 1492-7.
8. Deval, J., Antimicrobial strategies: inhibition of viral polymerases by 3'-hydroxyl nucleosides. *Drugs* **2009,** *69* (2), 151-66.
9. Dulin, D.; Arnold, J. J.; van Laar, T.; Oh, H. S.; Lee, C.; Perkins, A. L.; Harki, D. A.; Depken, M.; Cameron, C. E.; Dekker, N. H., Signatures of Nucleotide Analog Incorporation by an RNA-Dependent RNA Polymerase Revealed Using High-Throughput Magnetic Tweezers. *Cell Rep* **2017,** *21* (4), 1063-1076.
10. De Clercq, E., The design of drugs for HIV and HCV. *Nat Rev Drug Discov* **2007,** *6* (12), 1001-18.
11. Johansson, N. G.; Eriksson, S., Structure-activity relationships for phosphorylation of nucleoside analogs to monophosphates by nucleoside kinases. *Acta Biochim Pol* **1996,** *43* (1), 143-60.
12. Deville-Bonne, D.; El Amri, C.; Meyer, P.; Chen, Y.; Agrofoglio, L. A.; Janin, J., Human and viral nucleoside/nucleotide kinases involved in antiviral drug activation: structural and catalytic properties. *Antiviral Res* **2010,** *86* (1), 101-20.
13. Van Rompay, A. R.; Johansson, M.; Karlsson, A., Phosphorylation of nucleosides and nucleoside analogs by mammalian nucleoside monophosphate kinases. *Pharmacol Ther* **2000,** *87* (2-3), 189-98.
14. Miller, W. H.; Miller, R. L., Phosphorylation of acyclovir (acycloguanosine) monophosphate by GMP kinase. *J Biol Chem* **1980,** *255* (15), 7204-7.
15. Garces, E.; Cleland, W. W., Kinetic studies of yeast nucleoside diphosphate kinase. *Biochemistry* **1969,** *8* (2), 633-40.
16. Krishnan, P.; Fu, Q.; Lam, W.; Liou, J. Y.; Dutschman, G.; Cheng, Y. C., Phosphorylation of pyrimidine deoxynucleoside analog diphosphates: selective

phosphorylation of L-nucleoside analog diphosphates by 3-phosphoglycerate kinase. *J Biol Chem* **2002,** *277* (7), 5453-9.
17. Jordheim, L. P.; Dumontet, C., Review of recent studies on resistance to cytotoxic deoxynucleoside analogues. *Biochim Biophys Acta* **2007,** *1776* (2), 138-59.
18. Galmarini, C. M.; Mackey, J. R.; Dumontet, C., Nucleoside analogues: mechanisms of drug resistance and reversal strategies. *Leukemia* **2001,** *15* (6), 875-90.
19. Damaraju, V. L.; Damaraju, S.; Young, J. D.; Baldwin, S. A.; Mackey, J.; Sawyer, M. B.; Cass, C. E., Nucleoside anticancer drugs: the role of nucleoside transporters in resistance to cancer chemotherapy. *Oncogene* **2003,** *22* (47), 7524-36.
20. Pastor-Anglada, M.; Cano-Soldado, P.; Molina-Arcas, M.; Lostao, M. P.; Larráyoz, I.; Martínez-Picado, J.; Casado, F. J., Cell entry and export of nucleoside analogues. *Virus Res* **2005,** *107* (2), 151-64.
21. Cano-Soldado, P.; Pastor-Anglada, M., Transporters that translocate nucleosides and structural similar drugs: structural requirements for substrate recognition. *Med Res Rev* **2012,** *32* (2), 428-57.
22. Zhang, J.; Visser, F.; King, K. M.; Baldwin, S. A.; Young, J. D.; Cass, C. E., The role of nucleoside transporters in cancer chemotherapy with nucleoside drugs. *Cancer Metastasis Rev* **2007,** *26* (1), 85-110.
23. Cano-Soldado, P.; Pastor-Anglada, M., Transporters that translocate nucleosides and structural similar drugs: structural requirements for substrate recognition. *Med. Res. Rev.* **2012,** *32* (2), 428-57.
24. Spratlin, J.; Sangha, R.; Glubrecht, D.; Dabbagh, L.; Young, J. D.; Dumontet, C.; Cass, C.; Lai, R.; Mackey, J. R., The absence of human equilibrative nucleoside transporter 1 is associated with reduced survival in patients with gemcitabine-treated pancreas adenocarcinoma. *Clin Cancer Res* **2004,** *10* (20), 6956-61.
25. Maréchal, R.; Mackey, J. R.; Lai, R.; Demetter, P.; Peeters, M.; Polus, M.; Cass, C. E.; Young, J.; Salmon, I.; Devière, J.; Van Laethem, J. L., Human equilibrative nucleoside transporter 1 and human concentrative nucleoside transporter 3 predict survival after adjuvant gemcitabine therapy in resected pancreatic adenocarcinoma. *Clin Cancer Res* **2009,** *15* (8), 2913-9.
26. Farrell, J. J.; Elsaleh, H.; Garcia, M.; Lai, R.; Ammar, A.; Regine, W. F.; Abrams, R.; Benson, A. B.; Macdonald, J.; Cass, C. E.; Dicker, A. P.; Mackey, J. R., Human equilibrative nucleoside transporter 1 levels predict response to gemcitabine in patients with pancreatic cancer. *Gastroenterology* **2009,** *136* (1), 187-95.
27. Hubeek, I.; Stam, R. W.; Peters, G. J.; Broekhuizen, R.; Meijerink, J. P.; van Wering, E. R.; Gibson, B. E.; Creutzig, U.; Zwaan, C. M.; Cloos, J.; Kuik, D. J.; Pieters, R.; Kaspers, G. J., The human equilibrative nucleoside transporter 1 mediates in vitro cytarabine sensitivity in childhood acute myeloid leukaemia. *Br J Cancer* **2005,** *93* (12), 1388-94.

28. Chang, C.; Swaan, P. W.; Ngo, L. Y.; Lum, P. Y.; Patil, S. D.; Unadkat, J. D., Molecular requirements of the human nucleoside transporters hCNT1, hCNT2, and hENT1. *Mol Pharmacol* **2004,** *65* (3), 558-70.
29. Vickers, M. F.; Zhang, J.; Visser, F.; Tackaberry, T.; Robins, M. J.; Nielsen, L. P.; Nowak, I.; Baldwin, S. A.; Young, J. D.; Cass, C. E., Uridine recognition motifs of human equilibrative nucleoside transporters 1 and 2 produced in Saccharomyces cerevisiae. *Nucleosides Nucleotides Nucleic Acids* **2004,** *23* (1-2), 361-73.
30. Zhang, J.; Visser, F.; Vickers, M. F.; Lang, T.; Robins, M. J.; Nielsen, L. P.; Nowak, I.; Baldwin, S. A.; Young, J. D.; Cass, C. E., Uridine binding motifs of human concentrative nucleoside transporters 1 and 3 produced in Saccharomyces cerevisiae. *Mol Pharmacol* **2003,** *64* (6), 1512-20.
31. Månsson, E.; Flordal, E.; Liliemark, J.; Spasokoukotskaja, T.; Elford, H.; Lagercrantz, S.; Eriksson, S.; Albertioni, F., Down-regulation of deoxycytidine kinase in human leukemic cell lines resistant to cladribine and clofarabine and increased ribonucleotide reductase activity contributes to fludarabine resistance. *Biochem Pharmacol* **2003,** *65* (2), 237-47.
32. Kazuno, H.; Sakamoto, K.; Fujioka, A.; Fukushima, M.; Matsuda, A.; Sasaki, T., Possible antitumor activity of 1-(3-C-ethynyl-beta-D-ribo-pentofuranosyl)cytosine (ECyd, TAS-106) against an established gemcitabine (dFdCyd)-resistant human pancreatic cancer cell line. *Cancer Sci* **2005,** *96* (5), 295-302.
33. Klanova, M.; Lorkova, L.; Vit, O.; Maswabi, B.; Molinsky, J.; Pospisilova, J.; Vockova, P.; Mavis, C.; Lateckova, L.; Kulvait, V.; Vejmelkova, D.; Jaksa, R.; Hernandez, F.; Trneny, M.; Vokurka, M.; Petrak, J.; Klener, P., Downregulation of deoxycytidine kinase in cytarabine-resistant mantle cell lymphoma cells confers cross-resistance to nucleoside analogs gemcitabine, fludarabine and cladribine, but not to other classes of anti-lymphoma agents. *Mol Cancer* **2014,** *13*, 159.
34. Lorkova, L.; Scigelova, M.; Arrey, T. N.; Vit, O.; Pospisilova, J.; Doktorova, E.; Klanova, M.; Alam, M.; Vockova, P.; Maswabi, B.; Klener, P.; Petrak, J., Detailed Functional and Proteomic Characterization of Fludarabine Resistance in Mantle Cell Lymphoma Cells. *PLoS One* **2015,** *10* (8), e0135314.
35. Stegmann, A. P.; Honders, W. H.; Willemze, R.; Ruiz van Haperen, V. W.; Landegent, J. E., Transfection of wild-type deoxycytidine kinase (dck) cDNA into an AraC- and DAC-resistant rat leukemic cell line of clonal origin fully restores drug sensitivity. *Blood* **1995,** *85* (5), 1188-94.
36. Hapke, D. M.; Stegmann, A. P.; Mitchell, B. S., Retroviral transfer of deoxycytidine kinase into tumor cell lines enhances nucleoside toxicity. *Cancer Res* **1996,** *56* (10), 2343-7.
37. Veuger, M. J.; Honders, M. W.; Landegent, J. E.; Willemze, R.; Barge, R. M., High incidence of alternatively spliced forms of deoxycytidine kinase in patients with resistant acute myeloid leukemia. *Blood* **2000,** *96* (4), 1517-24.

38. Owens, J. K.; Shewach, D. S.; Ullman, B.; Mitchell, B. S., Resistance to 1-beta-D-arabinofuranosylcytosine in human T-lymphoblasts mediated by mutations within the deoxycytidine kinase gene. *Cancer Res* **1992,** *52* (9), 2389-93.
39. Stammler, G.; Zintl, F.; Sauerbrey, A.; Volm, M., Deoxycytidine kinase mRNA expression in childhood acute lymphoblastic leukemia. *Anticancer Drugs* **1997,** *8* (5), 517-21.
40. Kawasaki, H.; Carrera, C. J.; Piro, L. D.; Saven, A.; Kipps, T. J.; Carson, D. A., Relationship of deoxycytidine kinase and cytoplasmic 5'-nucleotidase to the chemotherapeutic efficacy of 2-chlorodeoxyadenosine. *Blood* **1993,** *81* (3), 597-601.
41. Veuger, M. J.; Honders, M. W.; Willemze, R.; Barge, R. M., Deoxycytidine kinase expression and activity in patients with resistant versus sensitive acute myeloid leukemia. *Eur J Haematol* **2002,** *69* (3), 171-8.
42. Leiby, J. M.; Snider, K. M.; Kraut, E. H.; Metz, E. N.; Malspeis, L.; Grever, M. R., Phase II trial of 9-beta-D-arabinofuranosyl-2-fluoroadenine 5'-monophosphate in non-Hodgkin's lymphoma: prospective comparison of response with deoxycytidine kinase activity. *Cancer Res* **1987,** *47* (10), 2719-22.
43. De Clercq, E.; Holý, A.; Rosenberg, I.; Sakuma, T.; Balzarini, J.; Maudgal, P. C., A novel selective broad-spectrum anti-DNA virus agent. *Nature* **1986,** *323* (6087), 464-7.
44. Larder, B. A.; Darby, G., Virus drug-resistance: mechanisms and consequences. *Antiviral Res* **1984,** *4* (1-2), 1-42.
45. MALEY, G. F.; MALEY, F., Nucleotide interconversions in embryonic and neoplastic tissues. I. The conversion of deoxycytidylic acid to deoxyuridylic acid and thymidylic acid. *J Biol Chem* **1959,** *234*, 2975-80.
46. Laliberté, J.; Momparler, R. L., Human cytidine deaminase: purification of enzyme, cloning, and expression of its complementary DNA. *Cancer Res* **1994,** *54* (20), 5401-7.
47. Camiener, G. W.; Smith, C. G., Studies of the enzymatic deamination of cytosine arabinoside. I. Enzyme distribution and species specificity. *Biochem Pharmacol* **1965,** *14* (10), 1405-16.
48. Camiener, G. W., Studies of the enzymatic deamination of cytosine arabinoside. II. Properties of the deaminase of human liver. *Biochem Pharmacol* **1967,** *16* (9), 1681-9.
49. Ebrahem, Q.; Mahfouz, R. Z.; Ng, K. P.; Saunthararajah, Y., High cytidine deaminase expression in the liver provides sanctuary for cancer cells from decitabine treatment effects. *Oncotarget* **2012,** *3* (10), 1137-45.
50. Falk, I. J.; Fyrberg, A.; Paul, E.; Nahi, H.; Hermanson, M.; Rosenquist, R.; Höglund, M.; Palmqvist, L.; Stockelberg, D.; Wei, Y.; Gréen, H.; Lotfi, K., Decreased survival in normal karyotype AML with single-nucleotide polymorphisms in genes encoding the AraC metabolizing enzymes cytidine deaminase and 5'-nucleotidase. *Am J Hematol* **2013,** *88* (12), 1001-6.

51. Colly, L. P.; Peters, W. G.; Richel, D.; Arentsen-Honders, M. W.; Starrenburg, C. W.; Willemze, R., Deoxycytidine kinase and deoxycytidine deaminase values correspond closely to clinical response to cytosine arabinoside remission induction therapy in patients with acute myelogenous leukemia. *Semin Oncol* **1987,** *14* (2 Suppl 1), 257-61.
52. Qin, T.; Castoro, R.; El Ahdab, S.; Jelinek, J.; Wang, X.; Si, J.; Shu, J.; He, R.; Zhang, N.; Chung, W.; Kantarjian, H. M.; Issa, J. P., Mechanisms of resistance to decitabine in the myelodysplastic syndrome. *PLoS One* **2011,** *6* (8), e23372.
53. Kreis, W.; Chan, K.; Budman, D. R.; Schulman, P.; Allen, S.; Weiselberg, L.; Lichtman, S.; Henderson, V.; Freeman, J.; Deere, M., Effect of tetrahydrouridine on the clinical pharmacology of 1-beta-D-arabinofuranosylcytosine when both drugs are coinfused over three hours. *Cancer Res* **1988,** *48* (5), 1337-42.
54. Kreis, W.; Budman, D. R.; Chan, K.; Allen, S. L.; Schulman, P.; Lichtman, S.; Weiselberg, L.; Schuster, M.; Freeman, J.; Akerman, S., Therapy of refractory/relapsed acute leukemia with cytosine arabinoside plus tetrahydrouridine (an inhibitor of cytidine deaminase)--a pilot study. *Leukemia* **1991,** *5* (11), 991-8.
55. Funamizu, N.; Okamoto, A.; Kamata, Y.; Misawa, T.; Uwagawa, T.; Gocho, T.; Yanaga, K.; Manome, Y., Is the resistance of gemcitabine for pancreatic cancer settled only by overexpression of deoxycytidine kinase? *Oncol Rep* **2010,** *23* (2), 471-5.
56. Lavelle, D.; Vaitkus, K.; Ling, Y.; Ruiz, M. A.; Mahfouz, R.; Ng, K. P.; Negrotto, S.; Smith, N.; Terse, P.; Engelke, K. J.; Covey, J.; Chan, K. K.; Desimone, J.; Saunthararajah, Y., Effects of tetrahydrouridine on pharmacokinetics and pharmacodynamics of oral decitabine. *Blood* **2012,** *119* (5), 1240-7.
57. Galmarini, C. M.; Graham, K.; Thomas, X.; Calvo, F.; Rousselot, P.; El Jafaari, A.; Cros, E.; Mackey, J. R.; Dumontet, C., Expression of high Km 5'-nucleotidase in leukemic blasts is an independent prognostic factor in adults with acute myeloid leukemia. *Blood* **2001,** *98* (6), 1922-6.
58. Balzarini, J.; Naesens, L.; Aquaro, S.; Knispel, T.; Perno, C.; De Clercq, E.; Meier, C., Intracellular metabolism of CycloSaligenyl 3'-azido-2', 3'-dideoxythymidine monophosphate, a prodrug of 3'-azido-2', 3'-dideoxythymidine (zidovudine). *Mol Pharmacol* **1999,** *56* (6), 1354-61.
59. Jones, R. J.; Bischofberger, N., Minireview: nucleotide prodrugs. *Antiviral Res* **1995,** *27* (1-2), 1-17.
60. Cohen, S. S.; Plunkett, W., The utilization of nucleotides by animal cells. *Ann. N.Y. Acad. Sci.* **1975,** (255), 269-286.
61. Wagner, C. R.; Iyer, V. V.; McIntee, E. J., Pronucleotides: toward the in vivo delivery of antiviral and anticancer nucleotides. *Med Res Rev* **2000,** *20* (6), 417-51.
62. Elliott, T. S.; Slowey, A.; Ye, Y.; Conway, S. J., The use of phosphate bioisosteres in medicinal chemistry and chemical biology. *Med. Chem. Commun.* **2012,** *3*, 735-751.

63. Inglot, A. D.; Kochman, M.; Mastalerz, P., Antiviral activity of p-nitrobenzylphosphonic acid. *Nature* **1965,** *207* (998), 784-5.
64. Shipkowitz, N. L.; Bower, R. R.; Appell, R. N.; Nordeen, C. W.; Overby, L. R.; Roderick, W. R.; Schleicher, J. B.; Von Esch, A. M., Suppression of herpes simplex virus infection by phosphonoacetic acid. *Appl Microbiol* **1973,** *26* (3), 264-7.
65. Pertusati, F.; Serpi, M.; McGuigan, C., Medicinal chemistry of nucleoside phosphonate prodrugs for antiviral therapy. *Antivir Chem Chemother* **2012,** *22* (5), 181-203.
66. Holý, A., Synthesis of 5'-deoxyuridine 5'-phosphonic acid. *Tetrahedron Lett* **1967,** *10*, 881-4.
67. De Clercq, E.; Holý, A., Acyclic nucleoside phosphonates: a key class of antiviral drugs. *Nat Rev Drug Discov* **2005,** *4* (11), 928-40.
68. McGuigan, C.; Tollerfield, S. M.; Riley, P. A., Synthesis and biological evaluation of some phosphate triester derivatives of the anti-viral drug AraA. *Nucleic Acids Res* **1989,** *17* (15), 6065-75.
69. Slusarczyk, M.; Lopez, M. H.; Balzarini, J.; Mason, M.; Jiang, W. G.; Blagden, S.; Thompson, E.; Ghazaly, E.; McGuigan, C., Application of ProTide technology to gemcitabine: a successful approach to overcome the key cancer resistance mechanisms leads to a new agent (NUC-1031) in clinical development. *J Med Chem* **2014,** *57* (4), 1531-42.
70. Meier, C., Pro-Nucleotides - Recent Advances in the Design of Efficient Tools for the Delivery of Biologically Active Nucleoside Monophosphates. *Synlett* **1998,** (3), 233-242.
71. Schultz, C., Prodrugs of biologically active phosphate esters. *Bioorg Med Chem* **2003,** *11* (6), 885-98.
72. Wiemer, A. J.; Wiemer, D. F., Prodrugs of phosphonates and phosphates: crossing the membrane barrier. *Top Curr Chem* **2015,** *360*, 115-60.
73. Farquhar, D.; Srivastva, D. N.; Kattesch, N. J.; Saunders, P. P., Biologically reversible phosphate-protective groups. *J Pharm Sci* **1983,** *72* (3), 324-5.
74. Sastry, J. K.; Nehete, P. N.; Khan, S.; Nowak, B. J.; Plunkett, W.; Arlinghaus, R. B.; Farquhar, D., Membrane-permeable dideoxyuridine 5'-monophosphate analogue inhibits human immunodeficiency virus infection. *Mol Pharmacol* **1992,** *41* (3), 441-5.
75. Farquhar, D.; Khan, S.; Srivastva, D. N.; Saunders, P. P., Synthesis and antitumor evaluation of bis[(pivaloyloxy)methyl] 2'-deoxy-5-fluorouridine 5'-monophosphate (FdUMP): a strategy to introduce nucleotides into cells. *J Med Chem* **1994,** *37* (23), 3902-9.
76. Arimilli, M. N.; Kim, C. U.; Dougherty, J.; Mulato, A.; Oliyai, R.; Shaw, J. P.; Cundy, K. C.; Bischofberger, N., Synthesis, in vitro evaluation and oral bioavailability of [9-(2-phosphonylmethoxyethyl)adenine prodrugs. *Antiviral Chem. & Chemother.* **1997,** (8), 557-564.

77. Brass, E. P., Pivalate-generating prodrugs and carnitine homeostasis in man. *Pharmacol Rev* **2002,** *54* (4), 589-98.
78. Hecker, S. J.; Erion, M. D., Prodrugs of phosphates and phosphonates. *J Med Chem* **2008,** *51* (8), 2328-45.
79. McGuigan, C.; Pathirana, R. N.; Mahmood, N.; Devine, K. G.; Hay, A. J., Aryl phosphate derivatives of AZT retain activity against HIV1 in cell lines which are resistant to the action of AZT. *Antiviral Res* **1992,** *17* (4), 311-21.
80. De Lombaert, S.; Erion, M. D.; Tan, J.; Blanchard, L.; el-Chehabi, L.; Ghai, R. D.; Sakane, Y.; Berry, C.; Trapani, A. J., N-Phosphonomethyl dipeptides and their phosphonate prodrugs, a new generation of neutral endopeptidase (NEP, EC 3.4.24.11) inhibitors. *J Med Chem* **1994,** *37* (4), 498-511.
81. De Lombaert, S.; Blanchard, L.; Berry, C.; Ghai, R. D.; Trapani, A. J., Non-peptidic inhibitors and neutral endopeptidase 24.11 2. Design and Pharmacology of orally active phosphonate prodrugs. *Bioorg. Med. Chem. Lett.* **1995,** (5), 151-154.
82. Serafinowska, H. T.; Ashton, R. J.; Bailey, S.; Harnden, M. R.; Jackson, S. M.; Sutton, D., Synthesis and in vivo evaluation of prodrugs of 9-[2-(phosphonomethoxy)ethoxy]adenine. *J Med Chem* **1995,** *38* (8), 1372-9.
83. De Lombaert, S.; Singh, K.; Blanchard, L.; Soliman, V., Chemical and plasma hydrolyses of a diphenyl α-aminomethyl phosphonate prodrug inhibitor of neutral endopeptidase 24.11. *Bioorg. Med. Chem. Lett.* **1994,** (4), 899-902.
84. Mitchell, A. G.; Nicholls, D.; Walker, I.; Irwin, W. J.; Freeman, S., Prodrugs of phosphonoformate: products, kinetics and mechanisms of hydrolysis of dibenzyl(methoxycarbonyl)phosphonate. *J. Chem. Soc., Perkin Trans. 2* **1991,** (0), 1297-1303.
85. Mitchell, A. G.; Thomson, W.; Nicholls, D.; Irwin, W. J.; Freeman, S., Bioreversible protection for the phospho group: Bioactivation of the di(4-acyloxybenzyl) and mono(4-acyloxybenzyl) phosphoesters of methylphosphonate and phosphonoacetate. *J. Chem. Soc., Perkin Trans. 1* **1992,** (0), 2345-2353.
86. Freeman, S.; Irwin, W. J.; Mitchell, A. G.; Nicholls, D.; Thomson, W., Bioreversible protection for the phospho group: chemical stability and bioactivation of di(4-acetoxybenzyl) methylphosphonate with carboxyesterase. *J. Chem. Soc., Chem. Commun.* **1991**, 875-877.
87. Thomson, W.; Nicholls, D.; Irwin, W. J.; Al-Mushadani, J. S.; Freeman, S.; Karpas, A.; Petrik, J.; Mahmood, N.; Hay, A. J., Synthesis, bioactivation and anti-HIV activity of the bis(4-acyloxybenzyl) and m ono(4-acyloxybenzyl) esters of the 5'-monophosphate of AZT. *J. Chem. Soc., Perkin Trans. 1* **1993**, 1239-1245.
88. Perigaud, C.; Aubertin, A. M.; Benzaria, S.; Pelicano, H.; Girardet, J. L.; Maury, G.; Gosselin, G.; Kirn, A.; Imbach, J. L., Equal inhibition of the replication of human immunodeficiency virus in human T-cell culture by ddA bis(SATE)phosphotriester and 3'-azido-2',3'-dideoxythymidine. *Biochem Pharmacol* **1994,** *48* (1), 11-14.

89. Périgaud, C.; Gosselin, G.; Lefebvre, I.; Girardet, J.-L.; Benzaria, S.; Barber, I.; Imbach, J.-L., Rational design for cytosolic delivery of nucleoside monophosphates: "SATE" and "DTE" as enzyme-labile transient phosphate protecting groups. *Bioorg. Med. Chem. Lett.* **1993,** *3*, 2521-2526.
90. Lefebvre, I.; Périgaud, C.; Pompon, A.; Aubertin, A. M.; Girardet, J. L.; Kirn, A.; Gosselin, G.; Imbach, J. L., Mononucleoside phosphotriester derivatives with S-acyl-2-thioethyl bioreversible phosphate-protecting groups: intracellular delivery of 3'-azido-2',3'-dideoxythymidine 5'-monophosphate. *J Med Chem* **1995,** *38* (20), 3941-50.
91. Schlienger, N.; Peyrottes, S.; Kassem, T.; Imbach, J. L.; Gosselin, G.; Aubertin, A. M.; Périgaud, C., S-Acyl-2-thioethyl aryl phosphotriester derivatives as mononucleotide prodrugs. *J Med Chem* **2000,** *43* (23), 4570-4.
92. Shafiee, M.; Deferme, S.; Villard, A. L.; Egron, D.; Gosselin, G.; Imbach, J. L.; Lioux, T.; Pompon, A.; Varray, S.; Aubertin, A. M.; Van Den Mooter, G.; Kinget, R.; Périgaud, C.; Augustijns, P., New bis(SATE) prodrug of AZT 5'-monophosphate: in vitro anti-HIV activity, stability, and potential oral absorption. *J Pharm Sci* **2001,** *90* (4), 448-63.
93. Placidi, L.; Faraj, A.; Loi, A. G.; Pierra, C.; Egron, D.; Cretton-Scott, E.; Gosseli, G.; Périgaud, C.; Martin, L. T.; Schinazi, R. F.; Imbach, J. L.; el Kouni, M. H.; Bryant, M. L.; Sommadossi, J. P., Antiviral activity and intracellular metabolism of bis(tButylSATE) phosphotriester of beta-L-2',3'dideoxyadenosine, a potent inhibitor of HIV and HBV replication. *Antivir Chem Chemother* **2001,** *12* (2), 99-108.
94. Benzaria, S.; Pélicano, H.; Johnson, R.; Maury, G.; Imbach, J. L.; Aubertin, A. M.; Obert, G.; Gosselin, G., Synthesis, in vitro antiviral evaluation, and stability studies of bis(S-acyl-2-thioethyl) ester derivatives of 9-[2-(phosphonomethoxy)ethyl]adenine (PMEA) as potential PMEA prodrugs with improved oral bioavailability. *J Med Chem* **1996,** *39* (25), 4958-65.
95. Peyrottes, S.; Coussot, G.; Lefebvre, I.; Imbach, J. L.; Gosselin, G.; Aubertin, A. M.; Périgaud, C., S-acyl-2-thioethyl aryl phosphotriester derivatives of AZT: synthesis, antiviral activity, and stability study. *J Med Chem* **2003,** *46* (5), 782-93.
96. Puech, F.; Gosselin, G.; Lefebvre, I.; Pompon, A.; Aubertin, A. M.; Kirn, A.; Imbach, J. L., Intracellular delivery of nucleoside monophosphates through a reductase-mediated activation process. *Antiviral Res* **1993,** *22* (2-3), 155-74.
97. Perigaud, C.; Girardet, J.-L.; Lefebvre, I.; Xie, M.-Y.; Aubertin, A.-M.; Kirn, A.; Gosselin, G.; Imbach, J.-L.; Sommadossi, J.-P., Comparison of cytotoxicity of mononucleoside
phosphotriester derivatives bearing biolabile phosphate protecting groups in normal human bone marrow progenitor cells. *Antiviral Chem. Chemother.* **1996,** (7), 338-345.
98. Meier, C., 2-nucleos-5′-O-yl-4H-1,3,2-benzodioxaphos-phinin-2-oxides—a new concept for lipophilic, potential prodrugs of biologically active nucleoside monophosphates. *Angew. Chem. Int. Ed. Engl.* **1996,** *35* (1), 70-72.

99. Meier, C.; Lorey, M.; De Clercq, E.; Balzarini, J., cycloSal-2',3'-dideoxy-2',3'-didehydrothymidine monophosphate (cycloSal-d4TMP): synthesis and antiviral evaluation of a new d4TMP delivery system. *J Med Chem* **1998,** *41* (9), 1417-27.
100. Meier, C.; Knispel, T.; De Clercq, E.; Balzarini, J., ADA-bypass by lipophilic cycloSal-ddAMP pro-nucleotides a second example of the efficiency of the cycloSal-concept. *Bioorg. Med. Chem. Lett.* **1997,** *7* (12), 1577-1582.
101. Meier, C.; Ducho, C.; Görbig, U.; Esnouf, R.; Balzarini, J., Interaction of cycloSal-pronucleotides with cholinesterases from different origins. A structure-activity relationship. *J Med Chem* **2004,** *47* (11), 2839-52.
102. Rios Morales, E. H.; Balzarini, J.; Meier, C., Stereoselective synthesis and antiviral activity of methyl-substituted cycloSal-pronucleotides. *J Med Chem* **2012,** *55* (16), 7245-52.
103. Meier, C.; Knispel, T.; Marquez, V. E.; Siddiqui, M. A.; De Clercq, E.; Balzarini, J., cycloSal-Pronucleotides of 2'-fluoro-ara- and 2'-fluoro-ribo-2',3'-dideoxyadenosine as a strategy to bypass a metabolic blockade. *J Med Chem* **1999,** *42* (9), 1615-24.
104. Meier, C.; De Clercq, E.; Balzarin, J., Nucleotide delivery from cycloSaligenyl-3′-azido-3′-deoxythymidine monophosphates (cycloSal-AZTMP). *Eur. J. Org. Chem.* **1998**, 837-846.
105. Meier, C.; Görbig, U.; Müller, C.; Balzarini, J., cycloSal-PMEA and cycloAmb-PMEA: potentially new phosphonate prodrugs based on the cycloSal-pronucleotide approach. *J Med Chem* **2005,** *48* (25), 8079-86.
106. Meier, C.; Ruppel, M. F.; Vukadinović, D.; Balzarini, J., Second generation of cycloSal-pronucleotides with esterase-cleavable sites: the "lock-in"-concept. *Nucleosides Nucleotides Nucleic Acids* **2004,** *23* (1-2), 89-115.
107. Gisch, N.; Balzarini, J.; Meier, C., Enzymatically activated cycloSal-d4T-monophosphates: The third generation of cycloSal-pronucleotides. *J Med Chem* **2007,** *50* (7), 1658-67.
108. Erion, M. D.; Reddy, K. R.; Boyer, S. H.; Matelich, M. C.; Gomez-Galeno, J.; Lemus, R. H.; Ugarkar, B. G.; Colby, T. J.; Schanzer, J.; Van Poelje, P. D., Design, synthesis, and characterization of a series of cytochrome P(450) 3A-activated prodrugs (HepDirect prodrugs) useful for targeting phosph(on)ate-based drugs to the liver. *J Am Chem Soc* **2004,** *126* (16), 5154-63.
109. Boyer, S. H.; Sun, Z.; Jiang, H.; Esterbrook, J.; Gómez-Galeno, J. E.; Craigo, W.; Reddy, K. R.; Ugarkar, B. G.; MacKenna, D. A.; Erion, M. D., Synthesis and characterization of a novel liver-targeted prodrug of cytosine-1-beta-D-arabinofuranoside monophosphate for the treatment of hepatocellular carcinoma. *J Med Chem* **2006,** *49* (26), 7711-20.
110. Lin, C. C.; Yeh, L. T.; Vitarella, D.; Hong, Z.; Erion, M. D., Remofovir mesylate: a prodrug of PMEA with improved liver-targeting and safety in rats and monkeys. *Antivir Chem Chemother* **2004,** *15* (6), 307-17.
111. Lee, K. S.; Lim, S. G.; Chuang, W. L.; Hwang, S. G.; Cho, M.; Lai, M. Y.; Chao, Y. C.; Chang, T. T.; Han, K. H.; Lee, C. M.; Um, S. H.; Yeon, J. E.; Yang, S. S.;

Teo, E. K.; Peng, C. Y.; Lin, H. H.; Yang, S. s.; Huo, T. I.; Nguyen, T.; Chen, T. Y.; Hu, K. Q.; Xu, Y.; Sullivan-Bólyai, J. Z., Safety, tolerability and antiviral activity of pradefovir mesylate in patients with chronic hepatitis B virus infection: 48-week analysis of a phase 2 study. *J. Hepatol.* **2006,** *44 (S2)*, S274.

112. Saboulard, D.; Naesens, L.; Cahard, D.; Salgado, A.; Pathirana, R.; Velazquez, S.; McGuigan, C.; De Clercq, E.; Balzarini, J., Characterization of the activation pathway of phosphoramidate triester prodrugs of stavudine and zidovudine. *Mol Pharmacol* **1999,** *56* (4), 693-704.
113. Valette, G.; Pompon, A.; Girardet, J. L.; Cappellacci, L.; Franchetti, P.; Grifantini, M.; La Colla, P.; Loi, A. G.; Périgaud, C.; Gosselin, G.; Imbach, J. L., Decomposition pathways and in vitro HIV inhibitory effects of isoddA pronucleotides: toward a rational approach for intracellular delivery of nucleoside 5'-monophosphates. *J Med Chem* **1996,** *39* (10), 1981-90.
114. Murakami, E.; Tolstykh, T.; Bao, H.; Niu, C.; Steuer, H. M.; Bao, D.; Chang, W.; Espiritu, C.; Bansal, S.; Lam, A. M.; Otto, M. J.; Sofia, M. J.; Furman, P. A., Mechanism of activation of PSI-7851 and its diastereoisomer PSI-7977. *J Biol Chem* **2010,** *285* (45), 34337-47.
115. McGuigan, C.; Cahard, D.; Salgado, A.; De Clercq, E.; Balzarini, J., Phosphoramidates as potent prodrugs of anti-HIV nucleotides: studies in the amino region. *Antiviral Chem. Chemother.* **1996,** *7* (1), 31-36.
116. McGuigan, C.; Salgado, A.; Yarnold, C.; Harries, T. Y.; De Clercq, E.; Balzarini, J., Novel nucleoside phosphoramidates as inhibitors of HIV: studies on the stereochemical requirements of the

phosphoramidate amino acid. *Antiviral Chem. Chemother.* **1996,** *7*, 184-188.

117. McGuigan, C.; Sutton, P. W.; Cahard, D.; Turner, K.; O'Leary, G.; Wang, Y.; Gumbleton, M.; De Clercq, E.; Balzarini, J., Synthesis, anti-human immunodeficiency virus activity and esterase lability of some novel carboxylic ester-modified phosphoramidate derivatives of stavudine (d4T). *Antivir Chem Chemother* **1998,** *9* (6), 473-9.
118. McGuigan, C.; Tsang, H. W.; Sutton, P. W.; De Clercq, E.; Balzarini, J., Synthesis and anti-HIV activity of some novel chain-extended phosphoramidate derivatives of d4T (stavudine): esterase hydrolysis as a rapid predictive test for antiviral potency. *Antivir Chem Chemother* **1998,** *9* (2), 109-15.
119. Congiatu, C.; Brancale, A.; Mason, M. D.; Jiang, W. G.; McGuigan, C., Novel potential anticancer naphthyl phosphoramidates of BVdU: separation of diastereoisomers and assignment of the absolute configuration of the phosphorus center. *J. Med. Chem.* **2006,** *49* (2), 452-5.
120. Bruce, R. M.; Santodonato, J.; Neal, M. W., Summary review of the health effects associated with phenol. *Toxicol. Ind. Health* **1987,** *3* (4), 535-68.
121. den Besten, C.; Brouwer, A.; Rietjens, I. M.; van Bladeren, P. J., Biotransformation and toxicity of halogenated benzenes. *Hum. Exp. Toxicol.* **1994,** *13* (12), 866-75.

122. Peng, Y.; Yu, W.; Li, E.; Kang, J.; Wang, Y.; Yang, Q.; Liu, B.; Zhang, J.; Li, L.; Wu, J.; Jiang, J.; Wang, Q.; Chang, J., Discovery of an Orally Active and Liver-Targeted Prodrug of 5-Fluoro-2'-Deoxyuridine for the Treatment of Hepatocellular Carcinoma. *J Med Chem* **2016,** *59* (8), 3661-70.
123. McGuigan, C.; Pathirana, R. N.; Balzarini, J.; De Clercq, E., Intracellular delivery of bioactive AZT nucleotides by aryl phosphate derivatives of AZT. *J Med Chem* **1993,** *36* (8), 1048-52.
124. McGuigan, C.; Cahard, D.; Sheeka, H. M.; De Clercq, E.; Balzarini, J., Aryl phosphoramidate derivatives of d4T have improved anti-HIV efficacy in tissue culture and may act by the generation of a novel intracellular metabolite. *J Med Chem* **1996,** *39* (8), 1748-53.
125. McGuigan, C.; Harris, S. A.; Daluge, S. M.; Gudmundsson, K. S.; McLean, E. W.; Burnette, T. C.; Marr, H.; Hazen, R.; Condreay, L. D.; Johnson, L.; De Clercq, E.; Balzarini, J., Application of phosphoramidate pronucleotide technology to abacavir leads to a significant enhancement of antiviral potency. *J Med Chem* **2005,** *48* (10), 3504-15.
126. McGuigan, C.; Hassan-Abdallah, A.; Srinivasan, S.; Wang, Y.; Siddiqui, A.; Daluge, S. M.; Gudmundsson, K. S.; Zhou, H.; McLean, E. W.; Peckham, J. P.; Burnette, T. C.; Marr, H.; Hazen, R.; Condreay, L. D.; Johnson, L.; Balzarini, J., Application of phosphoramidate ProTide technology significantly improves antiviral potency of carbocyclic adenosine derivatives. *J Med Chem* **2006,** *49* (24), 7215-26.
127. Derudas, M.; Carta, D.; Brancale, A.; Vanpouille, C.; Lisco, A.; Margolis, L.; Balzarini, J.; McGuigan, C., The application of phosphoramidate protide technology to acyclovir confers anti-HIV inhibition. *J Med Chem* **2009,** *52* (17), 5520-30.
128. Sofia, M. J.; Chang, W.; Furman, P. A.; Mosley, R. T.; Ross, B. S., Nucleoside, nucleotide, and non-nucleoside inhibitors of hepatitis C virus NS5B RNA-dependent RNA-polymerase. *J Med Chem* **2012,** *55* (6), 2481-531.
129. Sofia, M. J.; Bao, D.; Chang, W.; Du, J.; Nagarathnam, D.; Rachakonda, S.; Reddy, P. G.; Ross, B. S.; Wang, P.; Zhang, H. R.; Bansal, S.; Espiritu, C.; Keilman, M.; Lam, A. M.; Steuer, H. M.; Niu, C.; Otto, M. J.; Furman, P. A., Discovery of a β-d-2'-deoxy-2'-α-fluoro-2'-β-C-methyluridine nucleotide prodrug (PSI-7977) for the treatment of hepatitis C virus. *J Med Chem* **2010,** *53* (19), 7202-18.
130. Siegel, D.; Hui, H. C.; Doerffler, E.; Clarke, M. O.; Chun, K.; Zhang, L.; Neville, S.; Carra, E.; Lew, W.; Ross, B.; Wang, Q.; Wolfe, L.; Jordan, R.; Soloveva, V.; Knox, J.; Perry, J.; Perron, M.; Stray, K. M.; Barauskas, O.; Feng, J. Y.; Xu, Y.; Lee, G.; Rheingold, A. L.; Ray, A. S.; Bannister, R.; Strickley, R.; Swaminathan, S.; Lee, W. A.; Bavari, S.; Cihlar, T.; Lo, M. K.; Warren, T. K.; Mackman, R. L., Discovery and Synthesis of a Phosphoramidate Prodrug of a Pyrrolo[2,1-f][triazin-4-amino] Adenine C-Nucleoside (GS-5734) for the Treatment of Ebola and Emerging Viruses. *J Med Chem* **2017,** *60* (5), 1648-1661.

131. McGuigan, C.; Murziani, P.; Slusarczyk, M.; Gonczy, B.; Vande Voorde, J.; Liekens, S.; Balzarini, J., Phosphoramidate ProTides of the anticancer agent FUDR successfully deliver the preformed bioactive monophosphate in cells and confer advantage over the parent nucleoside. *J Med Chem* **2011,** *54* (20), 7247-58.
132. Lackey, D. B.; Groziak, M. P.; Sergeeva, M.; Beryt, M.; Boyer, C.; Stroud, R. M.; Sayre, P.; Park, J. W.; Johnston, P.; Slamon, D.; Shepard, H. M.; Pegram, M., Enzyme-catalyzed therapeutic agent (ECTA) design: activation of the antitumor ECTA compound NB1011 by thymidylate synthase. *Biochem Pharmacol* **2001,** *61* (2), 179-89.
133. Ballatore, C.; McGuigan, C.; De Clercq, E.; Balzarini, J., Synthesis and evaluation of novel amidate prodrugs of PMEA and PMPA. *Bioorg Med Chem Lett* **2001,** *11* (8), 1053-6.
134. Lee, W. A.; He, G. X.; Eisenberg, E.; Cihlar, T.; Swaminathan, S.; Mulato, A.; Cundy, K. C., Selective intracellular activation of a novel prodrug of the human immunodeficiency virus reverse transcriptase inhibitor tenofovir leads to preferential distribution and accumulation in lymphatic tissue. *Antimicrob. Agents. Chemother.* **2005,** *49* (5), 1898-906.
135. Thornton, P. J.; Kadri, H.; Miccoli, A.; Mehellou, Y., Nucleoside Phosphate and Phosphonate Prodrug Clinical Candidates. *J Med Chem* **2016,** *59* (23), 10400-10410.
136. Wagner, C. R.; McIntee, E. J.; Schinazi, R. F.; Abraham, T. W., Aromatic amino acid phosphoramidate di- and triesters of 3′-azido-3′-deoxythymidine (AZT) are non-toxic inhibitors of HIV-1 replication. *Bioorg. Med. Chem. Lett.* **1995,** *5* (16), 1819-1824.
137. Chou, T. F.; Bieganowski, P.; Shilinski, K.; Cheng, J.; Brenner, C.; Wagner, C. R., 31P NMR and genetic analysis establish hinT as the only Escherchia coli purine nucleoside phosphoramidase and as essential for growth under high salt conditions. *J. Biol. Chem.* **2005,** *280* (15), 15356-61.
138. Chou, T. F.; Baraniak, J.; Kaczmarek, R.; Zhou, X.; Cheng, J.; Ghosh, B.; Wagner, C. R., Phosphoramidate pronucleotides: a comparison of the phosphoramidase substrate specificity of human and Escherichia coli histidine triad nucleotide binding proteins. *Mol. Pharm.* **2007,** *4* (2), 208-17.
139. Iyer, V. V.; Griesgraber, G. W.; Radmer, M. R.; McIntee, E. J.; Wagner, C. R., Synthesis, in vitro anti-breast cancer activity, and intracellular decomposition of amino acid methyl ester and alkyl amide phosphoramidate monoesters of 3'-azido-3'-deoxythymidine (AZT). *J. Med. Chem.* **2000,** *43* (11), 2266-74.
140. Chang, S.; Griesgraber, G. W.; Southern, P. J.; Wagner, C. R., Amino acid phosphoramidate monoesters of 3'-azido-3'-deoxythymidine: relationship between antiviral potency and intracellular metabolism. *J. Med. Chem.* **2001,** *44* (2), 223-31.
141. McIntee, E. J.; Remmel, R. P.; Schinazi, R. F.; Abraham, T. W.; Wagner, C. R., Probing the mechanism of action and decomposition of amino acid

phosphomonoester amidates of antiviral nucleoside prodrugs. *J Med Chem* **1997,** *40* (21), 3323-31.

142. Abraham, T. W.; Kalman, T. I.; McIntee, E. J.; Wagner, C. R., Synthesis and biological activity of aromatic amino acid phosphoramidates of 5-fluoro-2'-deoxyuridine and 1-beta-arabinofuranosylcytosine: evidence of phosphoramidase activity. *J. Med. Chem.* **1996,** *39* (23), 4569-75.
143. Song, H.; Johns, R.; Griesgraber, G. W.; Wagner, C. R.; Zimmerman, C. L., Disposition and oral bioavailability in rats of an antiviral and antitumor amino acid phosphoramidate prodrug of AZT-monophosphate. *Pharm Res* **2003,** *20* (3), 448-51.
144. Song, H.; Griesgraber, G. W.; Wagner, C. R.; Zimmerman, C. L., Pharmacokinetics of amino acid phosphoramidate monoesters of zidovudine in rats. *Antimicrob Agents Chemother* **2002,** *46* (5), 1357-63.
145. Gardelli, C.; Attenni, B.; Donghi, M.; Meppen, M.; Pacini, B.; Harper, S.; Di Marco, A.; Fiore, F.; Giuliano, C.; Pucci, V.; Laufer, R.; Gennari, N.; Marcucci, I.; Leone, J. F.; Olsen, D. B.; MacCoss, M.; Rowley, M.; Narjes, F., Phosphoramidate prodrugs of 2'-C-methylcytidine for therapy of hepatitis C virus infection. *J. Med. Chem.* **2009,** *52* (17), 5394-407.
146. Chen, E. Z.; Jacobson, B. A.; Patel, M. R.; Okon, A. M.; Li, S.; Xiong, K.; Vaidya, A. J.; Bitterman, P. B.; Wagner, C. R.; Kratzke, R. A., Small-molecule inhibition of oncogenic eukaryotic protein translation in mesothelioma cells. *Invest. New Drugs* **2014,** *32* (4), 598-603.
147. Li, S.; Jia, Y.; Jacobson, B.; McCauley, J.; Kratzke, R.; Bitterman, P. B.; Wagner, C. R., Treatment of breast and lung cancer cells with a N-7 benzyl guanosine monophosphate tryptamine phosphoramidate pronucleotide (4Ei-1) results in chemosensitization to gemcitabine and induced eIF4E proteasomal degradation. *Mol. Pharm.* **2013,** *10* (2), 523-31.
148. Smith, K. A.; Zhou, B.; Avdulov, S.; Benyumov, A.; Peterson, M.; Liu, Y.; Okon, A.; Hergert, P.; Braziunas, J.; Wagner, C. R.; Borok, Z.; Bitterman, P. B., Transforming Growth Factor-β1 Induced Epithelial Mesenchymal Transition is blocked by a chemical antagonist of translation factor eIF4E. *Sci Rep* **2015,** *5*, 18233.
149. Jones, B. C. N. M.; McGuigan, C.; O'Connor, T. J.; Jeffries, D. J.; Kinchington, D., Synthesis and anti-HIV activity of some novel phosphorodiamidate derivatives of 3′-azido-3′-deoxythymidine (AZT). *Antiviral Chem. Chemother.* **1991,** *2* (1), 35-39.
150. McGuigan, C.; Madela, K.; Aljarah, M.; Bourdin, C.; Arrica, M.; Barrett, E.; Jones, S.; Kolykhalov, A.; Bleiman, B.; Bryant, K. D.; Ganguly, B.; Gorovits, E.; Henson, G.; Hunley, D.; Hutchins, J.; Muhammad, J.; Obikhod, A.; Patti, J.; Walters, C. R.; Wang, J.; Vernachio, J.; Ramamurty, C. V.; Battina, S. K.; Chamberlain, S., Phosphorodiamidates as a promising new phosphate prodrug motif for antiviral drug discovery: application to anti-HCV agents. *J Med Chem* **2011,** *54* (24), 8632-45.

151. Hecker, S. J.; Erion, M. D., Prodrugs of phosphates and phosphonates. *J. Med. Chem.* **2008,** *51* (8), 2328-45.
152. Keith, K. A.; Hitchcock, M. J.; Lee, W. A.; Holý, A.; Kern, E. R., Evaluation of nucleoside phosphonates and their analogs and prodrugs for inhibition of orthopoxvirus replication. *Antimicrob Agents Chemother* **2003,** *47* (7), 2193-8.
153. Wolfgang, G. H.; Shibata, R.; Wang, J.; Ray, A. S.; Wu, S.; Doerrfler, E.; Reiser, H.; Lee, W. A.; Birkus, G.; Christensen, N. D.; Andrei, G.; Snoeck, R., GS-9191 is a novel topical prodrug of the nucleotide analog 9-(2-phosphonylmethoxyethyl)guanine with antiproliferative activity and possible utility in the treatment of human papillomavirus lesions. *Antimicrob Agents Chemother* **2009,** *53* (7), 2777-84.
154. Pertusati, F.; Hinsinger, K.; Flynn, Á.; Powell, N.; Tristram, A.; Balzarini, J.; McGuigan, C., PMPA and PMEA prodrugs for the treatment of HIV infections and human papillomavirus (HPV) associated neoplasia and cancer. *Eur J Med Chem* **2014,** *78*, 259-68.
155. Beltran, T.; Egron, D.; Pompon, A.; Lefebvre, I.; Périgaud, C.; Gosselin, G.; Aubertin, A.; Imbach, J., Rational design of a new series of pronucleotide. *Bioorg Med Chem Lett* **2001,** *11* (13), 1775-7.
156. Cretton-Scott, E.; Perigaud, C.; Peyrottes, S.; Licklider, L.; Camire, M.; Larsson, M.; La Colla, M.; Hildebrand, E.; Lallos, L.; Bilello, J.; McCarville, J.; Seifer, M.; Liuzzi, M.; Pierra, C.; Badaroux, E.; Gosselin, G.; Surleraux, D.; Standring, D. N., In vitro antiviral activity and pharmacology of IDX184, a novel and potent inhibitor of HCV replication. *J. Hepatol.* **2008,** *48* (Suppl. 2), S220.
157. Standring, D. N.; Lanford, R.; Cretton-Scott, E.; Licklider, L.; Larsson, M.; Pierra, C.; Gosselin, G.; Perigaud, C.; Surleraux, D.; Mayes, B.; Moussa, A.; Selden, J., Potent antiviral activity of second generation nucleoside inhibitors, IDX102 and IDX184, in HCV-infected chimpanzees. *J. Hepatol* **2008,** *48* (Suppl. 2), S30.
158. Sofia, J. M., Nucleosides and Nucleotides for the Treatment of Viral Diseases. *Annu. Rep. Med. Chem.* **2014,** *49*, 221-247.
159. Jordheim, L. P.; Durantel, D.; Zoulim, F.; Dumontet, C., Advances in the development of nucleoside and nucleotide analogues for cancer and viral diseases. *Nat Rev Drug Discov* **2013,** *12* (6), 447-64.
160. Pradere, U.; Garnier-Amblard, E. C.; Coats, S. J.; Amblard, F.; Schinazi, R. F., Synthesis of nucleoside phosphate and phosphonate prodrugs. *Chem Rev* **2014,** *114* (18), 9154-218.
161. Cho, A.; Zhang, L.; Xu, J.; Lee, R.; Butler, T.; Metobo, S.; Aktoudianakis, V.; Lew, W.; Ye, H.; Clarke, M.; Doerffler, E.; Byun, D.; Wang, T.; Babusis, D.; Carey, A. C.; German, P.; Sauer, D.; Zhong, W.; Rossi, S.; Fenaux, M.; McHutchison, J. G.; Perry, J.; Feng, J.; Ray, A. S.; Kim, C. U., Discovery of the first C-nucleoside HCV polymerase inhibitor (GS-6620) with demonstrated antiviral response in HCV infected patients. *J Med Chem* **2014,** *57* (5), 1812-25.

162. Zhou, L.; Zhang, H. W.; Tao, S.; Bassit, L.; Whitaker, T.; McBrayer, T. R.; Ehteshami, M.; Amiralaei, S.; Pradere, U.; Cho, J. H.; Amblard, F.; Bobeck, D.; Detorio, M.; Coats, S. J.; Schinazi, R. F., β-D-2'-C-Methyl-2,6-diaminopurine Ribonucleoside Phosphoramidates are Potent and Selective Inhibitors of Hepatitis C Virus (HCV) and Are Bioconverted Intracellularly to Bioactive 2,6-Diaminopurine and Guanosine 5'-Triphosphate Forms. *J Med Chem* **2015,** *58* (8), 3445-58.
163. McGuigan, C.; Gilles, A.; Madela, K.; Aljarah, M.; Holl, S.; Jones, S.; Vernachio, J.; Hutchins, J.; Ames, B.; Bryant, K. D.; Gorovits, E.; Ganguly, B.; Hunley, D.; Hall, A.; Kolykhalov, A.; Liu, Y.; Muhammad, J.; Raja, N.; Walters, R.; Wang, J.; Chamberlain, S.; Henson, G., Phosphoramidate ProTides of 2'-C-methylguanosine as highly potent inhibitors of hepatitis C virus. Study of their in vitro and in vivo properties. *J Med Chem* **2010,** *53* (13), 4949-57.
164. Wagner, C. R.; Chang, S. L.; Griesgraber, G. W.; Song, H.; McIntee, E. J.; Zimmerman, C. L., Antiviral nucleoside drug delivery via amino acid phosphoramidates. *Nucleosides Nucleotides* **1999,** *18* (4-5), 913-9.
165. Chang, S.; Griesgraber, G. W.; Southern, P. J.; Wagner, C. R., Amino acid phosphoramidate monoesters of 3'-azido-3'-deoxythymidine: relationship between antiviral potency and intracellular metabolism. *J Med Chem* **2001,** *44* (2), 223-31.
166. Li, S.; Jia, Y.; Jacobson, B.; McCauley, J.; Kratzke, R.; Bitterman, P. B.; Wagner, C. R., Treatment of breast and lung cancer cells with a N-7 benzyl guanosine monophosphate tryptamine phosphoramidate pronucleotide (4Ei-1) results in chemosensitization to gemcitabine and induced eIF4E proteasomal degradation. *Mol Pharm* **2013,** *10* (2), 523-31.
167. Wagner, C. R.; McIntee, E. J.; Schinazi, R. F.; Abraham, T. W., AROMATIC AMINO-ACID PHOSPHORAMIDATE DIESTERS AND TRIESTERS OF 3'-AZIDO-3'-DEOXYTHYMIDINE (AZT) ARE NONTOXIC INHIBITORS OF HIV-1 REPLICATION. *Bioorganic & Medicinal Chemistry Letters* **1995,** *5* (16), 1819-1824.
168. Ghosh, B.; Benyumov, A. O.; Ghosh, P.; Jia, Y.; Avdulov, S.; Dahlberg, P. S.; Peterson, M.; Smith, K.; Polunovsky, V. A.; Bitterman, P. B.; Wagner, C. R., Nontoxic chemical interdiction of the epithelial-to-mesenchymal transition by targeting cap-dependent translation. *ACS Chem Biol* **2009,** *4* (5), 367-77.
169. Chen, E. Z.; Jacobson, B. A.; Patel, M. R.; Okon, A. M.; Li, S.; Xiong, K.; Vaidya, A. J.; Bitterman, P. B.; Wagner, C. R.; Kratzke, R. A., Small-molecule inhibition of oncogenic eukaryotic protein translation in mesothelioma cells. *Invest New Drugs* **2014,** *32* (4), 598-603.
170. Abraham, T. W.; Wagner, C. R., A PHOSPHORAMIDITE-BASED SYNTHESIS OF PHOSPHORAMIDATE AMINO-ACID DIESTERS OF ANTIVIRAL NUCLEOSIDES. *Nucleosides & Nucleotides* **1994,** *13* (9), 1891-1903.
171. Bjur, E.; Larsson, O.; Yurchenko, E.; Zheng, L.; Gandin, V.; Topisirovic, I.; Li, S.; Wagner, C. R.; Sonenberg, N.; Piccirillo, C. A., Distinct translational control in CD4+ T cell subsets. *PLoS Genet* **2013,** *9* (5), e1003494.

172. Cieślak, J.; Grajkowski, A.; Livengood, V.; Beaucage, S. L., Thermolytic 4-methylthio-1-butyl group for phosphate/thiophosphate protection in solid-phase synthesis of DNA oligonucleotides. *J Org Chem* **2004,** *69* (7), 2509-15.
173. Chen, X.; Kopecky, D. J.; Mihalic, J.; Jeffries, S.; Min, X.; Heath, J.; Deignan, J.; Lai, S.; Fu, Z.; Guimaraes, C.; Shen, S.; Li, S.; Johnstone, S.; Thibault, S.; Xu, H.; Cardozo, M.; Shen, W.; Walker, N.; Kayser, F.; Wang, Z., Structure-guided design, synthesis, and evaluation of guanine-derived inhibitors of the eIF4E mRNA-cap interaction. *J Med Chem* **2012,** *55* (8), 3837-51.
174. De Benedetti, A.; Graff, J. R., eIF-4E expression and its role in malignancies and metastases. *Oncogene* **2004,** *23* (18), 3189-99.
175. Pelletier, J.; Graff, J.; Ruggero, D.; Sonenberg, N., Targeting the eIF4F translation initiation complex: a critical nexus for cancer development. *Cancer Res* **2015,** *75* (2), 250-63.
176. Jia, Y.; Polunovsky, V.; Bitterman, P. B.; Wagner, C. R., Cap-dependent translation initiation factor eIF4E: an emerging anticancer drug target. *Med Res Rev* **2012,** *32* (4), 786-814.
177. Inamdar, K. V.; Romaguera, J. E.; Drakos, E.; Knoblock, R. J.; Garcia, M.; Leventaki, V.; Medeiros, L. J.; Rassidakis, G. Z., Expression of eukaryotic initiation factor 4E predicts clinical outcome in patients with mantle cell lymphoma treated with hyper-CVAD and rituximab, alternating with rituximab, high-dose methotrexate, and cytarabine. *Cancer* **2009,** *115* (20), 4727-36.
178. Rizzieri, D. A.; Feldman, E.; Dipersio, J. F.; Gabrail, N.; Stock, W.; Strair, R.; Rivera, V. M.; Albitar, M.; Bedrosian, C. L.; Giles, F. J., A phase 2 clinical trial of deforolimus (AP23573, MK-8669), a novel mammalian target of rapamycin inhibitor, in patients with relapsed or refractory hematologic malignancies. *Clin Cancer Res* **2008,** *14* (9), 2756-62.
179. Demosthenous, C.; Han, J. J.; Stenson, M. J.; Maurer, M. J.; Wellik, L. E.; Link, B.; Hege, K.; Dogan, A.; Sotomayor, E.; Witzig, T.; Gupta, M., Translation initiation complex eIF4F is a therapeutic target for dual mTOR kinase inhibitors in non-Hodgkin lymphoma. *Oncotarget* **2015,** *6* (11), 9488-501.
180. Atherton, F. R.; Openshaw, H. T.; Todd, A. R., Studies on phosphorylation. Part II. The reaction of phosphates with polyhalogen compounds in presence of bases. A new method for the phosphorylation of amines. *J. Chem. Soc.* **1945**, 660-663.
181. BordWell, F. G.; Brannen, W. T., The Effect of the Carbonyl and Related Groups on the Reactivity of Halides in SN2 Reactions. *J. Am. Chem. Soc.* **1964,** *86* (21), 4645-4650.
182. Eliel, E. L.; Knox, D. E., Neighboring Group Participation by Sulfur Involving Four-Membered Ring Intermediates (RS-4). *J. Am. Chem. Soc.* **1985,** *107* (10), 2946-2952.
183. Hsieh, A. C.; Costa, M.; Zollo, O.; Davis, C.; Feldman, M. E.; Testa, J. R.; Meyuhas, O.; Shokat, K. M.; Ruggero, D., Genetic dissection of the oncogenic mTOR pathway reveals druggable addiction to translational control via 4EBP-eIF4E. *Cancer Cell* **2010,** *17* (3), 249-61.

184. Rosenwald, I. B.; Rhoads, D. B.; Callanan, L. D.; Isselbacher, K. J.; Schmidt, E. V., Increased expression of eukaryotic translation initiation factors eIF-4E and eIF-2 alpha in response to growth induction by c-myc. *Proc Natl Acad Sci U S A* **1993,** *90* (13), 6175-8.
185. Schmidt, E. V., The role of c-myc in cellular growth control. *Oncogene* **1999,** *18* (19), 2988-96.
186. Smith, S. M.; Anastasi, J.; Cohen, K. S.; Godley, L. A., The impact of MYC expression in lymphoma biology: beyond Burkitt lymphoma. *Blood Cells Mol Dis* **2010,** *45* (4), 317-23.
187. Ruggero, D.; Montanaro, L.; Ma, L.; Xu, W.; Londei, P.; Cordon-Cardo, C.; Pandolfi, P. P., The translation factor eIF-4E promotes tumor formation and cooperates with c-Myc in lymphomagenesis. *Nat Med* **2004,** *10* (5), 484-6.
188. Lin, C. J.; Cencic, R.; Mills, J. R.; Robert, F.; Pelletier, J., c-Myc and eIF4F are components of a feedforward loop that links transcription and translation. *Cancer Res* **2008,** *68* (13), 5326-34.
189. Gupta, M.; Maurer, M. J.; Wellik, L. E.; Law, M. E.; Han, J. J.; Ozsan, N.; Micallef, I. N.; Dogan, A.; Witzig, T. E., Expression of Myc, but not pSTAT3, is an adverse prognostic factor for diffuse large B-cell lymphoma treated with epratuzumab/R-CHOP. *Blood* **2012,** *120* (22), 4400-6.
190. Chiarle, R.; Budel, L. M.; Skolnik, J.; Frizzera, G.; Chilosi, M.; Corato, A.; Pizzolo, G.; Magidson, J.; Montagnoli, A.; Pagano, M.; Maes, B.; De Wolf-Peeters, C.; Inghirami, G., Increased proteasome degradation of cyclin-dependent kinase inhibitor p27 is associated with a decreased overall survival in mantle cell lymphoma. *Blood* **2000,** *95* (2), 619-26.
191. Quintanilla-Martinez, L.; Thieblemont, C.; Fend, F.; Kumar, S.; Pinyol, M.; Campo, E.; Jaffe, E. S.; Raffeld, M., Mantle cell lymphomas lack expression of p27Kip1, a cyclin-dependent kinase inhibitor. *Am J Pathol* **1998,** *153* (1), 175-82.
192. Chu, I. M.; Hengst, L.; Slingerland, J. M., The Cdk inhibitor p27 in human cancer: prognostic potential and relevance to anticancer therapy. *Nat Rev Cancer* **2008,** *8* (4), 253-67.
193. Bordeleau, M. E.; Robert, F.; Gerard, B.; Lindqvist, L.; Chen, S. M.; Wendel, H. G.; Brem, B.; Greger, H.; Lowe, S. W.; Porco, J. A.; Pelletier, J., Therapeutic suppression of translation initiation modulates chemosensitivity in a mouse lymphoma model. *J Clin Invest* **2008,** *118* (7), 2651-60.
194. Laane, E.; Panaretakis, T.; Pokrovskaja, K.; Buentke, E.; Corcoran, M.; Söderhäll, S.; Heyman, M.; Mazur, J.; Zhivotovsky, B.; Porwit, A.; Grandér, D., Dexamethasone-induced apoptosis in acute lymphoblastic leukemia involves differential regulation of Bcl-2 family members. *Haematologica* **2007,** *92* (11), 1460-9.
195. Saba, N. S.; Liu, D.; Herman, S. E.; Underbayev, C.; Tian, X.; Behrend, D.; Weniger, M. A.; Skarzynski, M.; Gyamfi, J.; Fontan, L.; Melnick, A.; Grant, C.; Roschewski, M.; Navarro, A.; Beà, S.; Pittaluga, S.; Dunleavy, K.; Wilson, W.

H.; Wiestner, A., Pathogenic role of B-cell receptor signaling and canonical NF-κB activation in mantle cell lymphoma. *Blood* **2016,** *128* (1), 82-92.
196. Jares, P.; Colomer, D.; Campo, E., Molecular pathogenesis of mantle cell lymphoma. *J Clin Invest* **2012,** *122* (10), 3416-23.
197. Catz, S. D.; Johnson, J. L., Transcriptional regulation of bcl-2 by nuclear factor kappa B and its significance in prostate cancer. *Oncogene* **2001,** *20* (50), 7342-51.
198. Zhang, S. Q.; Smith, S. M.; Zhang, S. Y.; Lynn Wang, Y., Mechanisms of ibrutinib resistance in chronic lymphocytic leukaemia and non-Hodgkin lymphoma. *Br J Haematol* **2015,** *170* (4), 445-56.
199. Wu, H.; Hu, C.; Wang, A.; Weisberg, E. L.; Chen, Y.; Yun, C. H.; Wang, W.; Liu, Y.; Liu, X.; Tian, B.; Wang, J.; Zhao, Z.; Liang, Y.; Li, B.; Wang, L.; Wang, B.; Chen, C.; Buhrlage, S. J.; Qi, Z.; Zou, F.; Nonami, A.; Li, Y.; Fernandes, S. M.; Adamia, S.; Stone, R. M.; Galinsky, I. A.; Wang, X.; Yang, G.; Griffin, J. D.; Brown, J. R.; Eck, M. J.; Liu, J.; Gray, N. S.; Liu, Q., Discovery of a BTK/MNK dual inhibitor for lymphoma and leukemia. *Leukemia* **2016,** *30* (1), 173-81.
200. Gupta, M.; Hendrickson, A. E.; Yun, S. S.; Han, J. J.; Schneider, P. A.; Koh, B. D.; Stenson, M. J.; Wellik, L. E.; Shing, J. C.; Peterson, K. L.; Flatten, K. S.; Hess, A. D.; Smith, B. D.; Karp, J. E.; Barr, S.; Witzig, T. E.; Kaufmann, S. H., Dual mTORC1/mTORC2 inhibition diminishes Akt activation and induces Puma-dependent apoptosis in lymphoid malignancies. *Blood* **2012,** *119* (2), 476-87.
201. Ansell, S. M.; Tang, H.; Kurtin, P. J.; Koenig, P. A.; Inwards, D. J.; Shah, K.; Ziesmer, S. C.; Feldman, A. L.; Rao, R.; Gupta, M.; Erlichman, C.; Witzig, T. E., Temsirolimus and rituximab in patients with relapsed or refractory mantle cell lymphoma: a phase 2 study. *Lancet Oncol* **2011,** *12* (4), 361-8.
202. Fadden, P.; Haystead, T. A.; Lawrence, J. C., Identification of phosphorylation sites in the translational regulator, PHAS-I, that are controlled by insulin and rapamycin in rat adipocytes. *J Biol Chem* **1997,** *272* (15), 10240-7.
203. Gingras, A. C.; Gygi, S. P.; Raught, B.; Polakiewicz, R. D.; Abraham, R. T.; Hoekstra, M. F.; Aebersold, R.; Sonenberg, N., Regulation of 4E-BP1 phosphorylation: a novel two-step mechanism. *Genes Dev* **1999,** *13* (11), 1422-37.
204. Veber, D. F.; Johnson, S. R.; Cheng, H. Y.; Smith, B. R.; Ward, K. W.; Kopple, K. D., Molecular properties that influence the oral bioavailability of drug candidates. *J Med Chem* **2002,** *45* (12), 2615-23.
205. Drontle, D. P.; Wagner, C. R., Designing a pronucleotide stratagem: lessons from amino acid phosphoramidates of anticancer and antiviral pyrimidines. *Mini Rev Med Chem* **2004,** *4* (4), 409-19.
206. Hipp, S.; Ringshausen, I.; Oelsner, M.; Bogner, C.; Peschel, C.; Decker, T., Inhibition of the mammalian target of rapamycin and the induction of cell cycle arrest in mantle cell lymphoma cells. *Haematologica* **2005,** *90* (10), 1433-4.
207. Jia, Y.; Chiu, T. L.; Amin, E. A.; Polunovsky, V.; Bitterman, P. B.; Wagner, C. R., Design, synthesis and evaluation of analogs of initiation factor 4E (eIF4E) cap-binding antagonist Bn7-GMP. *Eur J Med Chem* **2010,** *45* (4), 1304-13.

208. Teitelbaum, A. M.; Meissner, A.; Harding, R. A.; Wong, C. A.; Aldrich, C. C.; Remmel, R. P., Synthesis, pH-dependent, and plasma stability of meropenem prodrugs for potential use against drug-resistant tuberculosis. *Bioorg Med Chem* **2013,** *21* (17), 5605-17.
209. Kore, A. R.; Xiao, Z.; Li, M., Synthesis and biological validation of N^7-(4-chlorophenoxyethyl) substituted dinucleotide cap analogs for mRNA translation. *Bioorg Med Chem* **2013,** *21* (15), 4570-4.
210. Gupta, M.; Ansell, S. M.; Novak, A. J.; Kumar, S.; Kaufmann, S. H.; Witzig, T. E., Inhibition of histone deacetylase overcomes rapamycin-mediated resistance in diffuse large B-cell lymphoma by inhibiting Akt signaling through mTORC2. *Blood* **2009,** *114* (14), 2926-35.
211. Hu, G.; Lou, Z.; Gupta, M., The long non-coding RNA GAS5 cooperates with the eukaryotic translation initiation factor 4E to regulate c-Myc translation. *PLoS One* **2014,** *9* (9), e107016.
212. Chen, Y. L.; Yokokawa, F.; Shi, P. Y., The search for nucleoside/nucleotide analog inhibitors of dengue virus. *Antiviral Res* **2015,** *122*, 12-9.
213. Yeo, K. L.; Chen, Y. L.; Xu, H. Y.; Dong, H.; Wang, Q. Y.; Yokokawa, F.; Shi, P. Y., Synergistic suppression of dengue virus replication using a combination of nucleoside analogs and nucleoside synthesis inhibitors. *Antimicrob Agents Chemother* **2015,** *59* (4), 2086-93.
214. Olsen, D. B.; Eldrup, A. B.; Bartholomew, L.; Bhat, B.; Bosserman, M. R.; Ceccacci, A.; Colwell, L. F.; Fay, J. F.; Flores, O. A.; Getty, K. L.; Grobler, J. A.; LaFemina, R. L.; Markel, E. J.; Migliaccio, G.; Prhavc, M.; Stahlhut, M. W.; Tomassini, J. E.; MacCoss, M.; Hazuda, D. J.; Carroll, S. S., A 7-deaza-adenosine analog is a potent and selective inhibitor of hepatitis C virus replication with excellent pharmacokinetic properties. *Antimicrob Agents Chemother* **2004,** *48* (10), 3944-53.
215. Behnam, M. A.; Nitsche, C.; Boldescu, V.; Klein, C. D., The Medicinal Chemistry of Dengue Virus. *J Med Chem* **2016,** *59* (12), 5622-49.
216. Lim, S. P.; Noble, C. G.; Shi, P. Y., The dengue virus NS5 protein as a target for drug discovery. *Antiviral Res* **2015,** *119*, 57-67.
217. Koonin, E. V.; Dolja, V. V., Evolution and taxonomy of positive-strand RNA viruses: implications of comparative analysis of amino acid sequences. *Crit Rev Biochem Mol Biol* **1993,** *28* (5), 375-430.
218. Ng, K. K.; Arnold, J. J.; Cameron, C. E., Structure-function relationships among RNA-dependent RNA polymerases. *Curr Top Microbiol Immunol* **2008,** *320*, 137-56.
219. Migliaccio, G.; Tomassini, J. E.; Carroll, S. S.; Tomei, L.; Altamura, S.; Bhat, B.; Bartholomew, L.; Bosserman, M. R.; Ceccacci, A.; Colwell, L. F.; Cortese, R.; De Francesco, R.; Eldrup, A. B.; Getty, K. L.; Hou, X. S.; LaFemina, R. L.; Ludmerer, S. W.; MacCoss, M.; McMasters, D. R.; Stahlhut, M. W.; Olsen, D. B.; Hazuda, D. J.; Flores, O. A., Characterization of resistance to non-obligate chain-

terminating ribonucleoside analogs that inhibit hepatitis C virus replication in vitro. *J Biol Chem* **2003,** *278* (49), 49164-70.
220. Cho, A.; Saunders, O. L.; Butler, T.; Zhang, L.; Xu, J.; Vela, J. E.; Feng, J. Y.; Ray, A. S.; Kim, C. U., Synthesis and antiviral activity of a series of 1'-substituted 4-aza-7,9-dideazaadenosine C-nucleosides. *Bioorg Med Chem Lett* **2012,** *22* (8), 2705-7.
221. Wagner, C. R., Iyer, V. V., and McIntee, E. J., Pronucleotides: toward the in vivo delivery of antiviral and anticancer nucleotides. *Med. Res. Rev.* **2000,** *20* (6), 417-451.
222. Hecker, S. J.; Erion, M. D., Prodrugs of phosphates and phosphonates. *Journal of Medicinal Chemistry* **2008,** *51* (8), 2328-2345.
223. Mehellou, Y., The ProTides Boom. *Chemmedchem* **2016,** *11* (11), 1114-1116.
224. Summers, B. B.; Beavers, J. W. F.; Klibanov, O. M., Sofosbuvir, a novel nucleotide analogue inhibitor used for the treatment of hepatitis C virus. *Journal of Pharmacy and Pharmacology* **2014,** *66* (12), 1653-1666.
225. McGuigan, C.; Perrone, P.; Madela, K.; Neyts, J., The phosphoramidate ProTide approach greatly enhances the activity of beta-2'-C-methylguanosine against hepatitis C virus. *Bioorg Med Chem Lett* **2009,** *19* (15), 4316-20.
226. Farquhar, D.; Chen, R.; S., K., 5'-[4-(Pivaloyloxy)-1,3,2-dioxaphosphorinan-2-yl]-2 0-deoxy-5-¯uorouridine: A membrane-permeating prodrug of 5-¯uoro-20-deoxyuridylic acid(FdUMP). *J. Med. Chem.* **1995,** *38*, 488-495.
227. Girardet, J.-L.; Perigaud, C.; Aubertin, A. M.; Gosselin, G.; Kirn, A.; Imbach, J.-L., Increase of the anti-HIV activity of d4T in human T-cell culture by the use of the SATE pronucleotide approach. *Bioorg. Med. Chem. Lett.* **1995,** *5*, 2981-2984.
228. Borch, R. F.; Canute, G. W., Synthesis and antitumor properties of activated cyclophosphamide analogues. *J. Med. Chem.* **1991,** *34*, 3044-3052.
229. Meier, C.; Knispel, T.; De Clercq, E.; Balzarini, J., CycloSal-pronucleotides of 20,3 0-dideoxyadenosine and
20,3 0-dideoxy-2 0,3 0-didehydroadenosine: synthesis and antiviral evaluation of a highly ef®cient
nucleotide delivery system. *J. Med. Chem.* **1999,** *42*, 1604-1614.
230. Pradere, U.; Garnier-Amblard, E. C.; Coats, S. J.; Amblard, F.; Schinazi, R. F., Synthesis of Nucleoside Phosphate and Phosphonate Prodrugs. *Chemical Reviews* **2014,** *114* (18), 9154-9218.
231. Gardelli, C.; Attenni, B.; Donghi, M.; Meppen, M.; Pacini, B.; Harper, S.; Di Marco, A.; Fiore, F.; Giuliano, C.; Pucci, V.; Laufer, R.; Gennari, N.; Marcucci, I.; Leone, J. F.; Olsen, D. B.; MacCoss, M.; Rowley, M.; Narjes, F., Phosphoramidate prodrugs of 2'-C-methylcytidine for therapy of hepatitis C virus infection. *J Med Chem* **2009,** *52* (17), 5394-407.
232. Minagawa, T.; Kohno, Y.; Suwa, T.; Tsuji, A., Species differences in hydrolysis of isocarbacyclin methyl ester (TEI-9090) by blood esterases. *Biochem Pharmacol* **1995,** *49* (10), 1361-5.

233. Rudakova, E. V.; Boltneva, N. P.; Makhaeva, G. F., Comparative analysis of esterase activities of human, mouse, and rat blood. *Bull Exp Biol Med* **2011,** *152* (1), 73-5.
234. Garzón, J.; Herrero-Labrador, R.; Rodríguez-Muñoz, M.; Shah, R.; Vicente-Sánchez, A.; Wagner, C. R.; Sánchez-Blázquez, P., HINT1 protein: a new therapeutic target to enhance opioid antinociception and block mechanical allodynia. *Neuropharmacology* **2015,** *89*, 412-23.
235. Kawana, M.; Kuzuhara, H., General method for the synthesis of 2′-azido-2′,3′-dideoxynucleosides by the use of [1,2]-hydride shift and β-elimination reactions. *J. Chem. Soc. Perkin Trans. I* **1992,** *4*, 469 - 478.
236. Surleraux, D. Compounds and pharmaceutical compositions for the treatment of viral infections. US2012/251487, March 30, 2012.
237. Johnson, B. W.; Russell, B. J.; Lanciotti, R. S., Serotype-specific detection of dengue viruses in a fourplex real-time reverse transcriptase PCR assay. *J Clin Microbiol* **2005,** *43* (10), 4977-83.
238. Jordheim, L. P.; Durantel, D.; Zoulim, F.; Dumontet, C., Advances in the development of nucleoside and nucleotide analogues for cancer and viral diseases. *Nat. Rev. Drug Discov.* **2013,** *12* (6), 447-64.
239. Jordheim, L. P.; Dumontet, C., Review of recent studies on resistance to cytotoxic deoxynucleoside analogues. *Biochim. Biophys. Acta.* **2007,** *1776* (2), 138-59.
240. Deville-Bonne, D.; El Amri, C.; Meyer, P.; Chen, Y.; Agrofoglio, L. A.; Janin, J., Human and viral nucleoside/nucleotide kinases involved in antiviral drug activation: structural and catalytic properties. *Antiviral Res.* **2010,** *86* (1), 101-20.
241. Ghosh, B.; Benyumov, A. O.; Ghosh, P.; Jia, Y.; Avdulov, S.; Dahlberg, P. S.; Peterson, M.; Smith, K.; Polunovsky, V. A.; Bitterman, P. B.; Wagner, C. R., Nontoxic chemical interdiction of the epithelial-to-mesenchymal transition by targeting cap-dependent translation. *ACS. Chem. Biol.* **2009,** *4* (5), 367-77.
242. Peng, Y.; Yu, W.; Li, E.; Kang, J.; Wang, Y.; Yang, Q.; Liu, B.; Zhang, J.; Li, L.; Wu, J.; Jiang, J.; Wang, Q.; Chang, J., Discovery of an Orally Active and Liver-Targeted Prodrug of 5-Fluoro-2'-Deoxyuridine for the Treatment of Hepatocellular Carcinoma. *J. Med. Chem.* **2016,** *59* (8), 3661-70.
243. Okon, A.; Han, J.; Dawadi, S.; Demosthenous, C.; Aldrich, C. C.; Gupta, M.; Wagner, C. R., Anchimerically Activated ProTides as Inhibitors of Cap-Dependent Translation and Inducers of Chemosensitization in Mantle Cell Lymphoma. *J Med Chem* **2017,** *60* (19), 8131-8144.
244. Reid, G.; Wielinga, P.; Zelcer, N.; De Haas, M.; Van Deemter, L.; Wijnholds, J.; Balzarini, J.; Borst, P., Characterization of the transport of nucleoside analog drugs by the human multidrug resistance proteins MRP4 and MRP5. *Mol Pharmacol* **2003,** *63* (5), 1094-103.
245. Singh, A.; Thornton, E. R.; Westheimer, F. H., The photolysis of diazoacetylchymotrypsin. *J Biol Chem* **1962,** *237*, 3006-8.
246. Brunner, J., New photolabeling and crosslinking methods. *Annu Rev Biochem* **1993,** *62*, 483-514.

247. Geurink, P. P.; Prely, L. M.; van der Marel, G. A.; Bischoff, R.; Overkleeft, H. S., Photoaffinity labeling in activity-based protein profiling. *Top Curr Chem* **2012,** *324*, 85-113.
248. Pham, N. D.; Parker, R. B.; Kohler, J. J., Photocrosslinking approaches to interactome mapping. *Curr Opin Chem Biol* **2013,** *17* (1), 90-101.
249. Murale, D. P.; Hong, S. C.; Haque, M. M.; Lee, J. S., Photo-affinity labeling (PAL) in chemical proteomics: a handy tool to investigate protein-protein interactions (PPIs). *Proteome Sci* **2016,** *15*, 14.
250. Dolot, R.; Ozga, M.; Włodarczyk, A.; Krakowiak, A.; Nawrot, B., A new crystal form of human histidine triad nucleotide-binding protein 1 (hHINT1) in complex with adenosine 5'-monophosphate at 1.38 Å resolution. *Acta Crystallogr Sect F Struct Biol Cryst Commun* **2012,** *68* (Pt 8), 883-8.
251. Xia, Y.; Peng, L., Photoactivatable lipid probes for studying biomembranes by photoaffinity labeling. *Chem Rev* **2013,** *113* (10), 7880-929.
252. Schrock, A. K.; Schuster, G. B., Photochemistry of Phenyl Azide: Chemical Properties of the Transient Intermediates. *J. Am. Chem. Soc.* **1984,** *106*, 5228-5234.
253. Friedrich, A.; Bräse, S.; O'Connor, S. E., Synthesis of 4-, 5-, 6-, and 7-Azidotryptamines. *Tetrahedron Lett* **2009,** *50* (1), 75-76.
254. Lee, K.; Ren, T.; Côté, M.; Gholamreza, B.; Misasi, J.; Bruchez, A.; Cunningham, J., Inhibition of Ebola Virus Infection: Identification of Niemann-Pick C1 as the Target by Optimization of a Chemical Probe. *ACS Med Chem Lett* **2013,** *4* (2), 239-243.
255. Okon, A.; Matos de Souza, M. R.; Shah, R.; Amorim, R.; da Costa, L. J.; Wagner, C. R., Anchimerically Activatable Antiviral ProTides. *ACS Med Chem Lett* **2017,** *8* (9), 958-962.
256. Nakashima, H.; Hashimoto, M.; Sadakane, Y.; Tomohiro, T.; Hatanaka, Y., Simple and versatile method for tagging phenyldiazirine photophores. *J Am Chem Soc* **2006,** *128* (47), 15092-3.
257. Beigelman, L.; Haeberli, P.; Sweedler, D.; Karpeisky, A., Improved Synthetic Approaches Toward 2′-O-Methyl-Adenosine and Guanosine and Their N-Acyl Derivatives. *Tetrahedron* **2000,** *56* (8), 1047-1056.
258. Pujari, S. S.; Leonard, P.; Seela, F., Oligonucleotides with "clickable" sugar residues: synthesis, duplex stability, and terminal versus central interstrand cross-linking of 2'-O-propargylated 2-aminoadenosine with a bifunctional azide. *J Org Chem* **2014,** *79* (10), 4423-37.
259. Rostovtsev, V. V.; Green, L. G.; Fokin, V. V.; Sharpless, K. B., A stepwise huisgen cycloaddition process: copper(I)-catalyzed regioselective "ligation" of azides and terminal alkynes. *Angew Chem Int Ed Engl* **2002,** *41* (14), 2596-9.
260. Speers, A. E.; Adam, G. C.; Cravatt, B. F., Activity-based protein profiling in vivo using a copper(i)-catalyzed azide-alkyne [3 + 2] cycloaddition. *J Am Chem Soc* **2003,** *125* (16), 4686-7.

261. Trinkle-Mulcahy, L.; Boulon, S.; Lam, Y. W.; Urcia, R.; Boisvert, F. M.; Vandermoere, F.; Morrice, N. A.; Swift, S.; Rothbauer, U.; Leonhardt, H.; Lamond, A., Identifying specific protein interaction partners using quantitative mass spectrometry and bead proteomes. *J Cell Biol* **2008,** *183* (2), 223-39.
262. Park, J.; Koh, M.; Koo, J. Y.; Lee, S.; Park, S. B., Investigation of Specific Binding Proteins to Photoaffinity Linkers for Efficient Deconvolution of Target Protein. *ACS Chem Biol* **2016,** *11* (1), 44-52.
263. Mellacheruvu, D.; Wright, Z.; Couzens, A. L.; Lambert, J. P.; St-Denis, N. A.; Li, T.; Miteva, Y. V.; Hauri, S.; Sardiu, M. E.; Low, T. Y.; Halim, V. A.; Bagshaw, R. D.; Hubner, N. C.; Al-Hakim, A.; Bouchard, A.; Faubert, D.; Fermin, D.; Dunham, W. H.; Goudreault, M.; Lin, Z. Y.; Badillo, B. G.; Pawson, T.; Durocher, D.; Coulombe, B.; Aebersold, R.; Superti-Furga, G.; Colinge, J.; Heck, A. J.; Choi, H.; Gstaiger, M.; Mohammed, S.; Cristea, I. M.; Bennett, K. L.; Washburn, M. P.; Raught, B.; Ewing, R. M.; Gingras, A. C.; Nesvizhskii, A. I., The CRAPome: a contaminant repository for affinity purification-mass spectrometry data. *Nat Methods* **2013,** *10* (8), 730-6.
264. Shah, R.; Maize, K. M.; Zhou, X.; Finzel, B. C.; Wagner, C. R., Caught before Released: Structural Mapping of the Reaction Trajectory for the Sofosbuvir Activating Enzyme, Human Histidine Triad Nucleotide Binding Protein 1 (hHint1). *Biochemistry* **2017,** *56* (28), 3559-3570.
265. Trmčić, M.; Hodgson, D. R., Synthesis of thiophosphoramidates in water: click chemistry for phosphates. *Chem Commun (Camb)* **2011,** *47* (21), 6156-8.
266. Ishihama, Y.; Oda, Y.; Tabata, T.; Sato, T.; Nagasu, T.; Rappsilber, J.; Mann, M., Exponentially modified protein abundance index (emPAI) for estimation of absolute protein amount in proteomics by the number of sequenced peptides per protein. *Mol Cell Proteomics* **2005,** *4* (9), 1265-72.
267. Colotti, G.; Poser, E.; Fiorillo, A.; Genovese, I.; Chiarini, V.; Ilari, A., Sorcin, a calcium binding protein involved in the multidrug resistance mechanisms in cancer cells. *Molecules* **2014,** *19* (9), 13976-89.
268. Lokuta, A. J.; Meyers, M. B.; Sander, P. R.; Fishman, G. I.; Valdivia, H. H., Modulation of cardiac ryanodine receptors by sorcin. *J Biol Chem* **1997,** *272* (40), 25333-8.
269. Qu, Y.; Yang, Y.; Liu, B.; Xiao, W., Comparative proteomic profiling identified sorcin being associated with gemcitabine resistance in non-small cell lung cancer. *Med Oncol* **2010,** *27* (4), 1303-8.
270. Yang, Y. X.; Chen, Z. C.; Zhang, G. Y.; Yi, H.; Xiao, Z. Q., A subcelluar proteomic investigation into vincristine-resistant gastric cancer cell line. *J Cell Biochem* **2008,** *104* (3), 1010-21.
271. Montgomery, D. C.; Sorum, A. W.; Meier, J. L., Chemoproteomic profiling of lysine acetyltransferases highlights an expanded landscape of catalytic acetylation. *J Am Chem Soc* **2014,** *136* (24), 8669-76.
272. Kulkarni, R. A.; Worth, A. J.; Zengeya, T. T.; Shrimp, J. H.; Garlick, J. M.; Roberts, A. M.; Montgomery, D. C.; Sourbier, C.; Gibbs, B. K.; Mesaros, C.;

Tsai, Y. C.; Das, S.; Chan, K. C.; Zhou, M.; Andresson, T.; Weissman, A. M.; Linehan, W. M.; Blair, I. A.; Snyder, N. W.; Meier, J. L., Discovering Targets of Non-enzymatic Acylation by Thioester Reactivity Profiling. *Cell Chem Biol* **2017,** *24* (2), 231-242.
273. Rappsilber, J.; Mann, M.; Ishihama, Y., Protocol for micro-purification, enrichment, pre-fractionation and storage of peptides for proteomics using StageTips. *Nat Protoc* **2007,** *2* (8), 1896-906.
274. Hanahan, D.; Weinberg, R. A., The hallmarks of cancer. *Cell* **2000,** *100* (1), 57-70.
275. Hanahan, D.; Weinberg, R. A., Hallmarks of cancer: the next generation. *Cell* **2011,** *144* (5), 646-74.
276. Sonenberg, N.; Hinnebusch, A. G., Regulation of translation initiation in eukaryotes: mechanisms and biological targets. *Cell* **2009,** *136* (4), 731-45.
277. von der Haar, T.; Gross, J. D.; Wagner, G.; McCarthy, J. E., The mRNA cap-binding protein eIF4E in post-transcriptional gene expression. *Nat Struct Mol Biol* **2004,** *11* (6), 503-11.
278. Jackson, R. J.; Hellen, C. U.; Pestova, T. V., The mechanism of eukaryotic translation initiation and principles of its regulation. *Nat Rev Mol Cell Biol* **2010,** *11* (2), 113-27.
279. Duncan, R.; Milburn, S. C.; Hershey, J. W., Regulated phosphorylation and low abundance of HeLa cell initiation factor eIF-4F suggest a role in translational control. Heat shock effects on eIF-4F. *J. Biol. Chem.* **1987,** *262* (1), 380-8.
280. Hiremath, L. S.; Webb, N. R.; Rhoads, R. E., Immunological detection of the messenger RNA cap-binding protein. *J. Biol. Chem.* **1985,** *260* (13), 7843-9.
281. Silvera, D.; Formenti, S. C.; Schneider, R. J., Translational control in cancer. *Nat Rev Cancer* **2010,** *10* (4), 254-66.
282. Bhat, M.; Robichaud, N.; Hulea, L.; Sonenberg, N.; Pelletier, J.; Topisirovic, I., Targeting the translation machinery in cancer. *Nat Rev Drug Discov* **2015,** *14* (4), 261-78.
283. Hsieh, A. C.; Ruggero, D., Targeting eukaryotic translation initiation factor 4E (eIF4E) in cancer. *Clin Cancer Res* **2010,** *16* (20), 4914-20.
284. Khoutorsky, A.; Bonin, R. P.; Sorge, R. E.; Gkogkas, C. G.; Pawlowski, S. A.; Jafarnejad, S. M.; Pitcher, M. H.; Alain, T.; Perez-Sanchez, J.; Salter, E. W.; Martin, L.; Ribeiro-da-Silva, A.; De Koninck, Y.; Cervero, F.; Mogil, J. S.; Sonenberg, N., Translational control of nociception via 4E-binding protein 1. *Elife* **2015,** *4*.
285. Mao, X.; Green, J. M.; Safer, B.; Lindsten, T.; Frederickson, R. M.; Miyamoto, S.; Sonenberg, N.; Thompson, C. B., Regulation of translation initiation factor gene expression during human T cell activation. *J Biol Chem* **1992,** *267* (28), 20444-50.
286. Chen, X.; Kopecky, D. J.; Mihalic, J.; Jeffries, S.; Min, X.; Heath, J.; Deignan, J.; Lai, S.; Fu, Z.; Guimaraes, C.; Shen, S.; Li, S.; Johnstone, S.; Thibault, S.; Xu, H.; Cardozo, M.; Shen, W.; Walker, N.; Kayser, F.; Wang, Z., Structure-guided

design, synthesis, and evaluation of guanine-derived inhibitors of the eIF4E mRNA-cap interaction. *J. Med. Chem.* **2012,** *55* (8), 3837-51.
287. Jia, Y.; Chiu, T. L.; Amin, E. A.; Polunovsky, V.; Bitterman, P. B.; Wagner, C. R., Design, synthesis and evaluation of analogs of initiation factor 4E (eIF4E) cap-binding antagonist Bn7-GMP. *Eur. J. Med. Chem.* **2010,** *45* (4), 1304-13.
288. Soukarieh, F.; Nowicki, M. W.; Bastide, A.; Pöyry, T.; Jones, C.; Dudek, K.; Patwardhan, G.; Meullenet, F.; Oldham, N. J.; Walkinshaw, M. D.; Willis, A. E.; Fischer, P. M., Design of nucleotide-mimetic and non-nucleotide inhibitors of the translation initiation factor eIF4E: Synthesis, structural and functional characterisation. *Eur J Med Chem* **2016,** *124*, 200-217.
289. Niedzwiecka, A.; Marcotrigiano, J.; Stepinski, J.; Jankowska-Anyszka, M.; Wyslouch-Cieszynska, A.; Dadlez, M.; Gingras, A. C.; Mak, P.; Darzynkiewicz, E.; Sonenberg, N.; Burley, S. K.; Stolarski, R., Biophysical studies of eIF4E cap-binding protein: recognition of mRNA 5' cap structure and synthetic fragments of eIF4G and 4E-BP1 proteins. *J Mol Biol* **2002,** *319* (3), 615-35.
290. Roos, D.; Loos, J. A., Changes in the carbohydrate metabolism of mitogenically stimulated human peripheral lymphocytes. II. Relative importance of glycolysis and oxidative phosphorylation on phytohaemagglutinin stimulation. *Exp Cell Res* **1973,** *77* (1), 127-35.
291. Jones, R. G.; Thompson, C. B., Revving the engine: signal transduction fuels T cell activation. *Immunity* **2007,** *27* (2), 173-8.
292. So, L.; Lee, J.; Palafox, M.; Mallya, S.; Woxland, C. G.; Arguello, M.; Truitt, M. L.; Sonenberg, N.; Ruggero, D.; Fruman, D. A., The 4E-BP-eIF4E axis promotes rapamycin-sensitive growth and proliferation in lymphocytes. *Sci Signal* **2016,** *9* (430), ra57.
293. Ohno, M.; Kobayashi, S.; Iimori, T.; Wang, Y.-F.; Izawa, T., Synthesis of (S)- and (R)-4[(methoxycarbonyl)methyl]-2-azetidinone by chemicoenzymic approach. *J. Am. Chem. Soc.* **1981,** *103* (9), 2405-2406.
294. Pandiyan, P.; Zheng, L.; Ishihara, S.; Reed, J.; Lenardo, M. J., CD4+CD25+Foxp3+ regulatory T cells induce cytokine deprivation-mediated apoptosis of effector CD4+ T cells. *Nat Immunol* **2007,** *8* (12), 1353-62.
295. Boyman, O.; Sprent, J., The role of interleukin-2 during homeostasis and activation of the immune system. *Nat Rev Immunol* **2012,** *12* (3), 180-90.
296. Bjur, E.; Larsson, O.; Yurchenko, E.; Zheng, L.; Gandin, V.; Topisirovic, I.; Li, S.; Wagner, C. R.; Sonenberg, N.; Piccirillo, C. A., Distinct translational control in CD4+ T cell subsets. *PLoS Genet.* **2013,** *9* (5), e1003494.
297. Ichikawa, Y.; Hirata, K.; Ohbayashi, M.; Isobe, M., Total synthesis of (+)-blasticidin s. *Chemistry* **2004,** *10* (13), 3241-51.
298. Cushman, M.; Insaf, S.; Paul, G.; Ruell, J. A.; De Clercq, E.; Schols, D.; Pannecouque, C.; Witvrouw, M.; Schaeffer, C. A.; Turpin, J. A.; Williamson, K.; Rice, W. G., Extension of the polyanionic cosalane pharmacophore as a strategy for increasing anti-HIV potency. *J Med Chem* **1999,** *42* (10), 1767-77.

299. Turcotte, S.; Bouayad-Gervais, S. H.; Lubell, W. D., N-Aminosulfamide peptide mimic synthesis by alkylation of aza-sulfurylglycinyl peptides. *Org Lett* **2012,** *14* (5), 1318-21.

Appendix

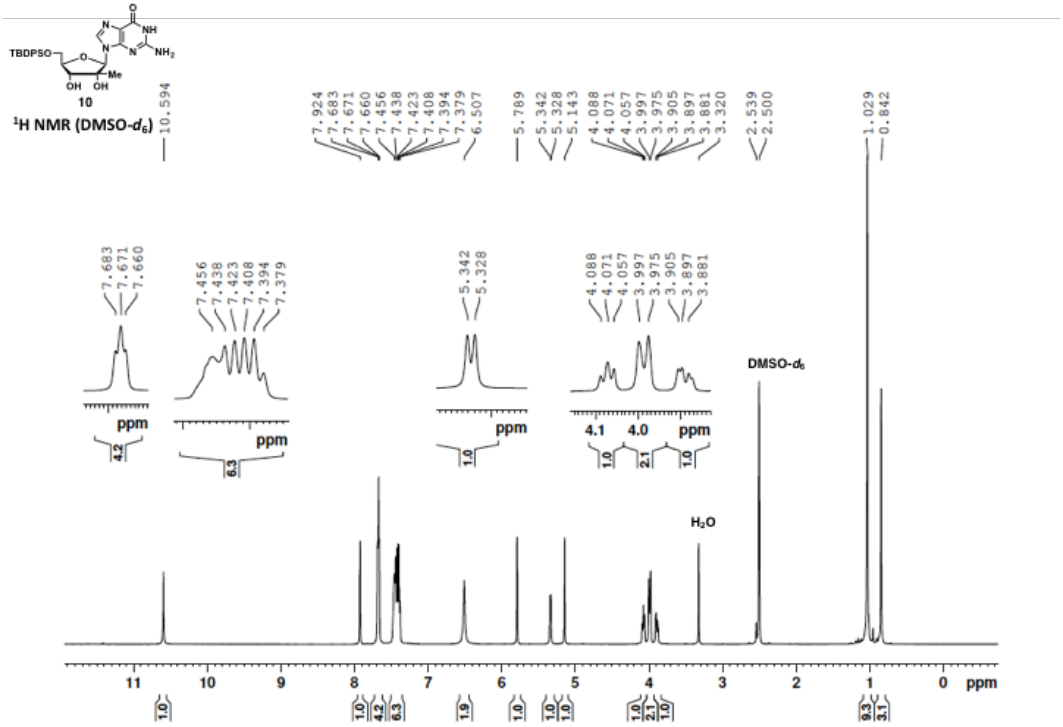
TBDPSO
Me
OH OH
10
^{1}H NMR (DMSO-d_6)
DMSO-d_6
H_2O
ppm

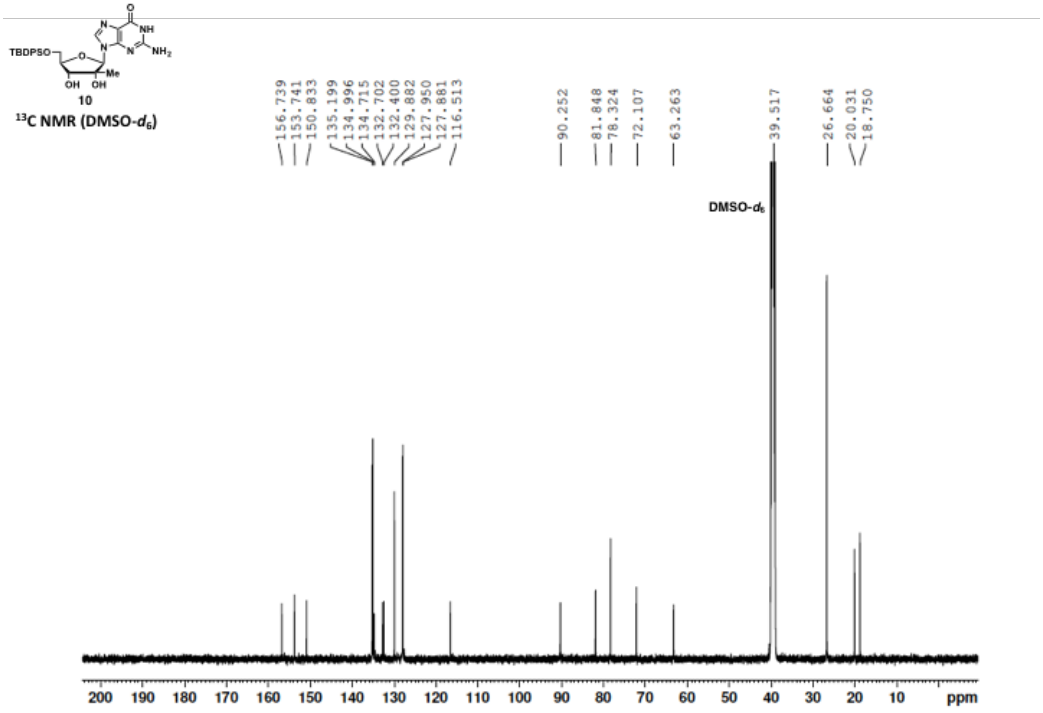
TBDPSO
Me
OH OH
10
^{13}C NMR (DMSO-d_6)
DMSO-d_6
ppm

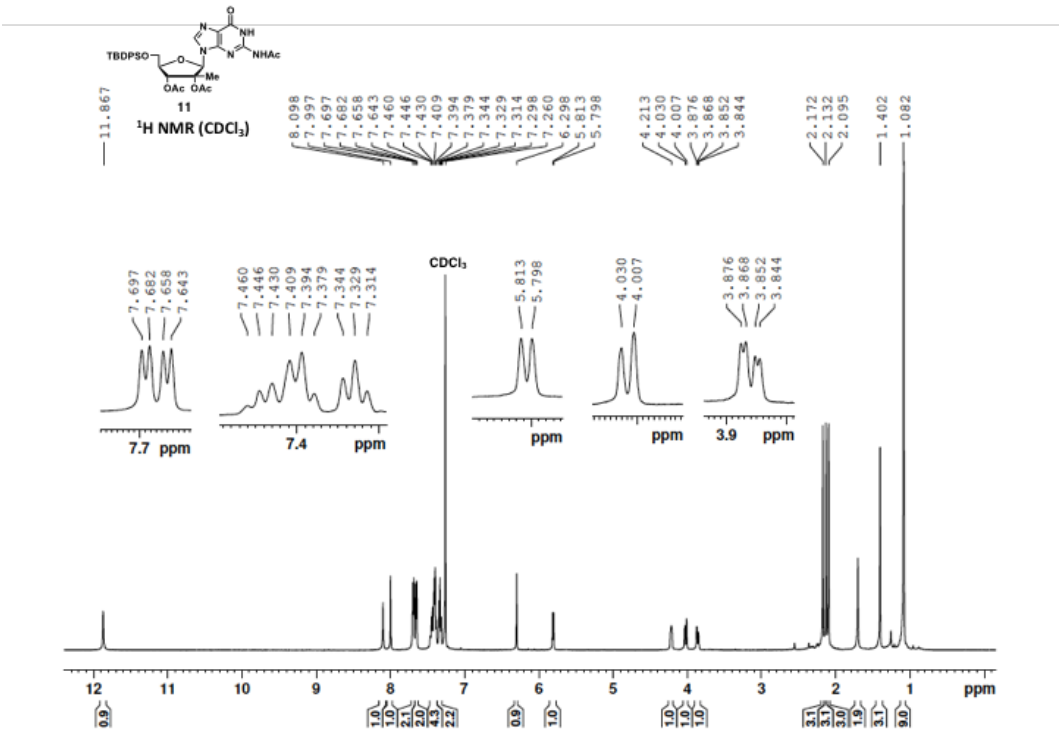
TBDPSO
NHAc
OAc OAc
Me
11
^{1}H NMR ($CDCl_3$)
CDCl₃
ppm

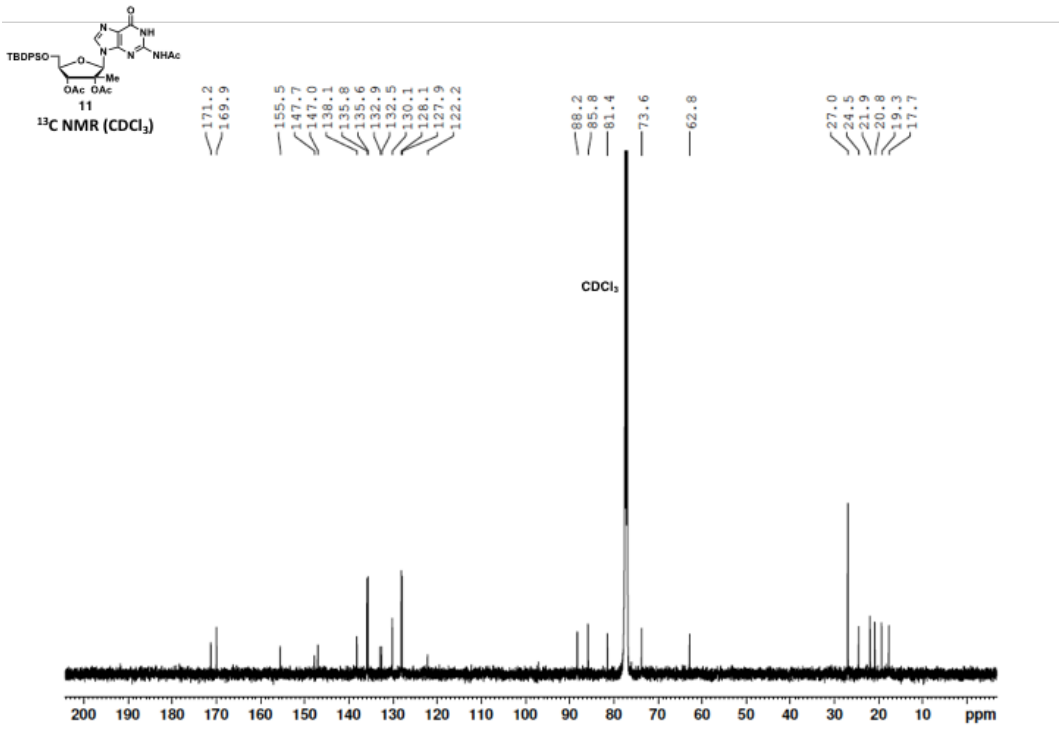
TBDPSO
NHAc
OAc OAc
Me
11
^{13}C NMR ($CDCl_3$)
CDCl₃
ppm

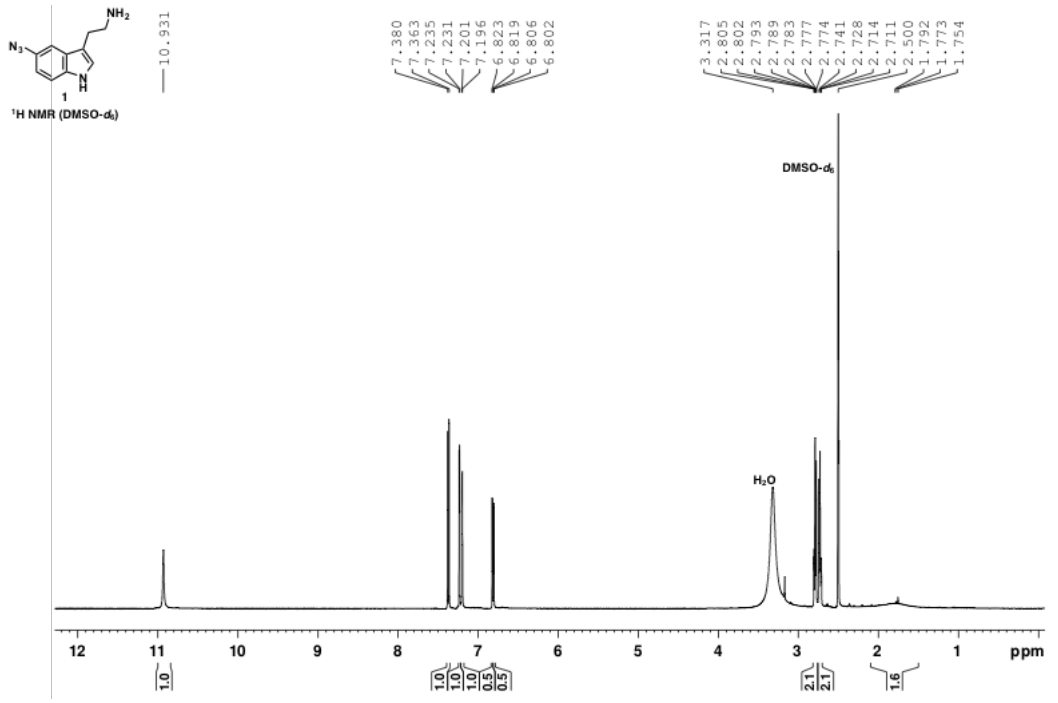
1
^{1}H NMR (DMSO-d_6)
10.931
7.380
7.363
7.235
7.231
7.201
7.196
6.823
6.819
6.806
6.802
3.317
2.805
2.802
2.793
2.789
2.783
2.777
2.774
2.741
2.728
2.714
2.711
2.500
1.792
1.773
1.754
DMSO-d_6
H_2O
12
11
10
9
8
7
6
5
4
3
2
1
ppm
1.0
1.0
1.0
1.0
0.5
0.5
2.1
2.1
1.6

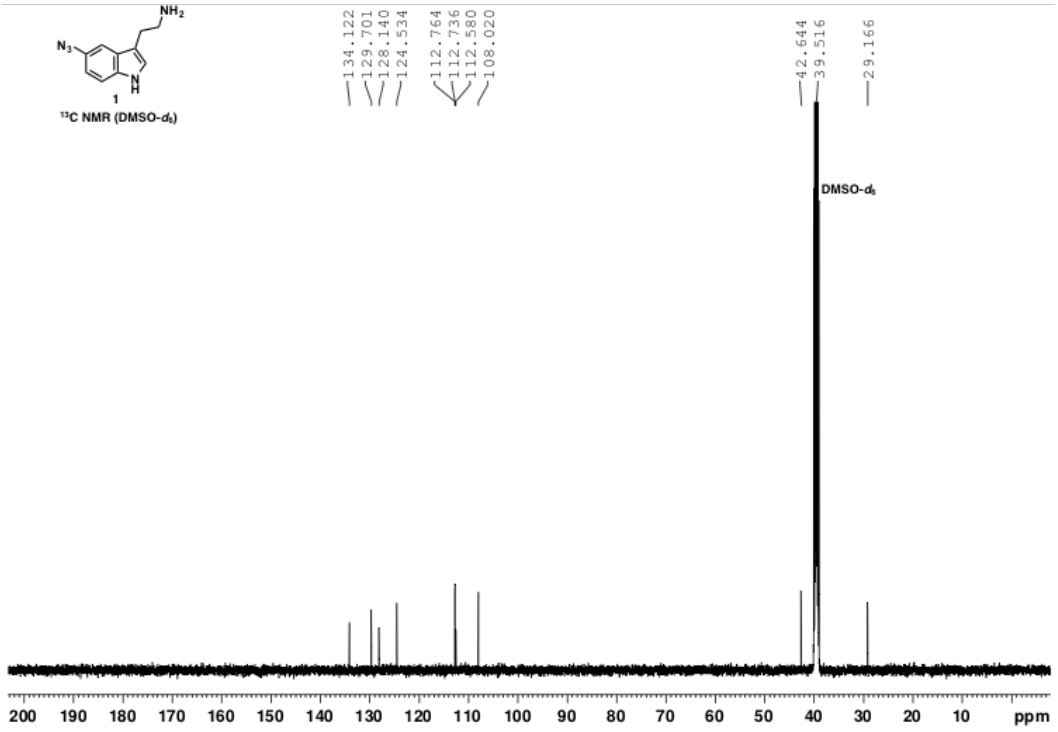
1
^{13}C NMR (DMSO-d_6)
134.122
129.701
128.140
124.534
112.764
112.736
112.580
108.020
42.644
39.516
29.166
DMSO-d_6
200
190
180
170
160
150
140
130
120
110
100
90
80
70
60
50
40
30
20
10
ppm

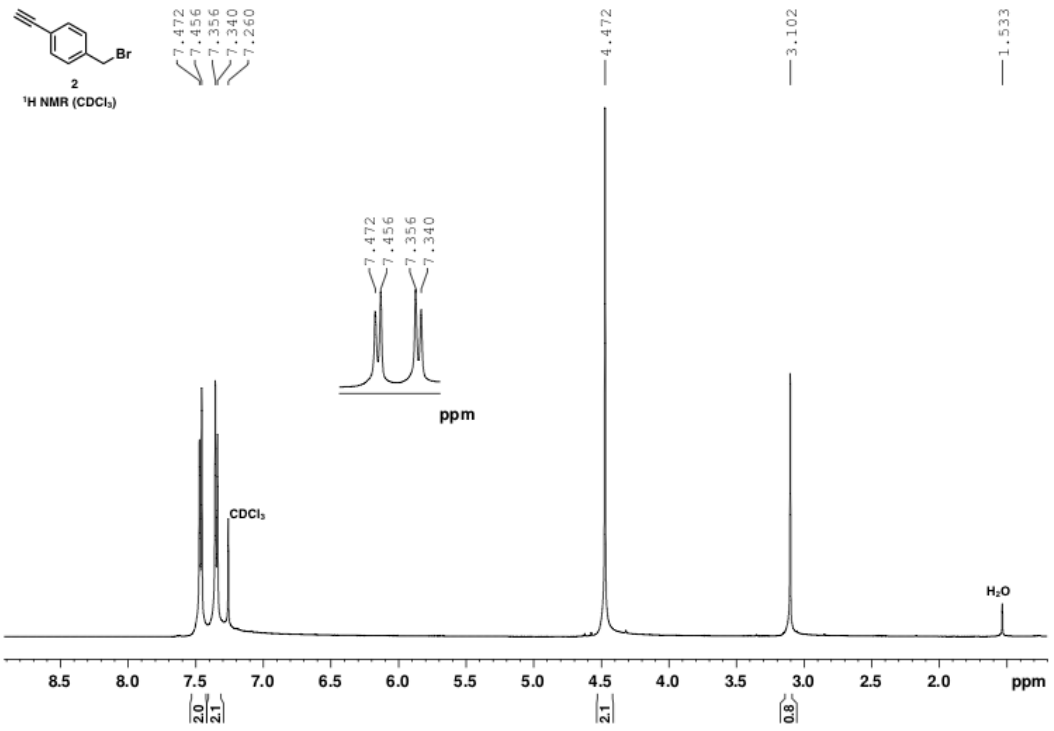
Br
2
¹H NMR (CDCl₃)
7.472
7.456
7.356
7.340
7.260
4.472
3.102
1.533
ppm
CDCl₃
H₂O
8.5
8.0
7.5
7.0
6.5
6.0
5.5
5.0
4.5
4.0
3.5
3.0
2.5
2.0
ppm
2.0
2.1
2.1
0.8

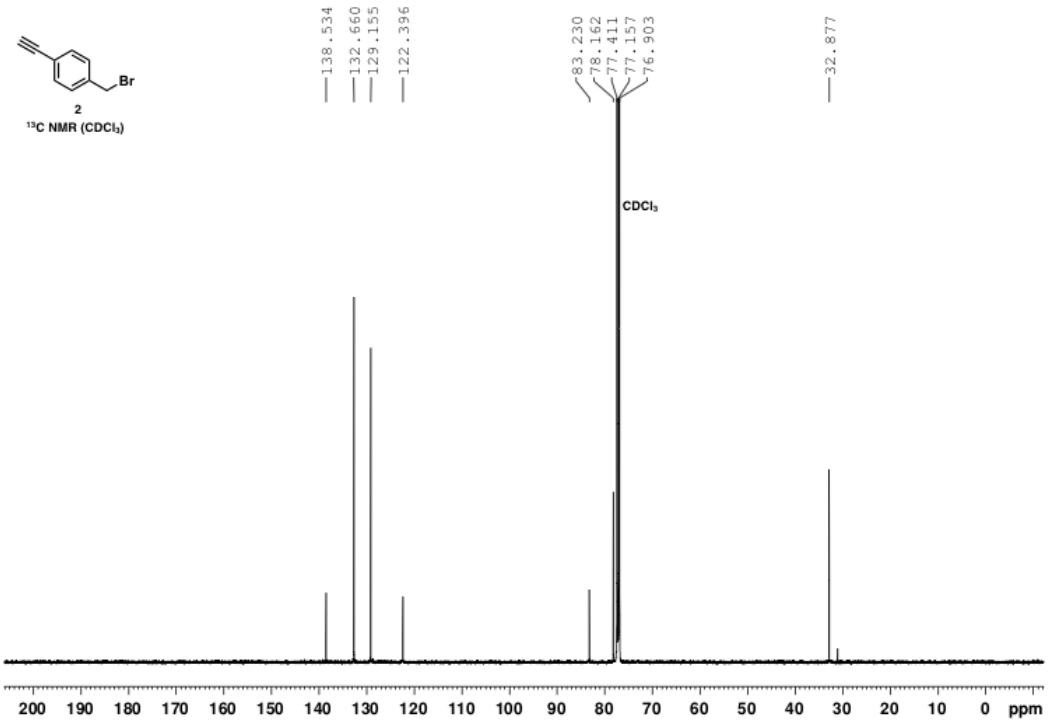
Br
2
¹³C NMR (CDCl₃)
138.534
132.660
129.155
122.396
83.230
78.162
77.411
77.157
76.903
32.877
CDCl₃
200
190
180
170
160
150
140
130
120
110
100
90
80
70
60
50
40
30
20
10
0
ppm

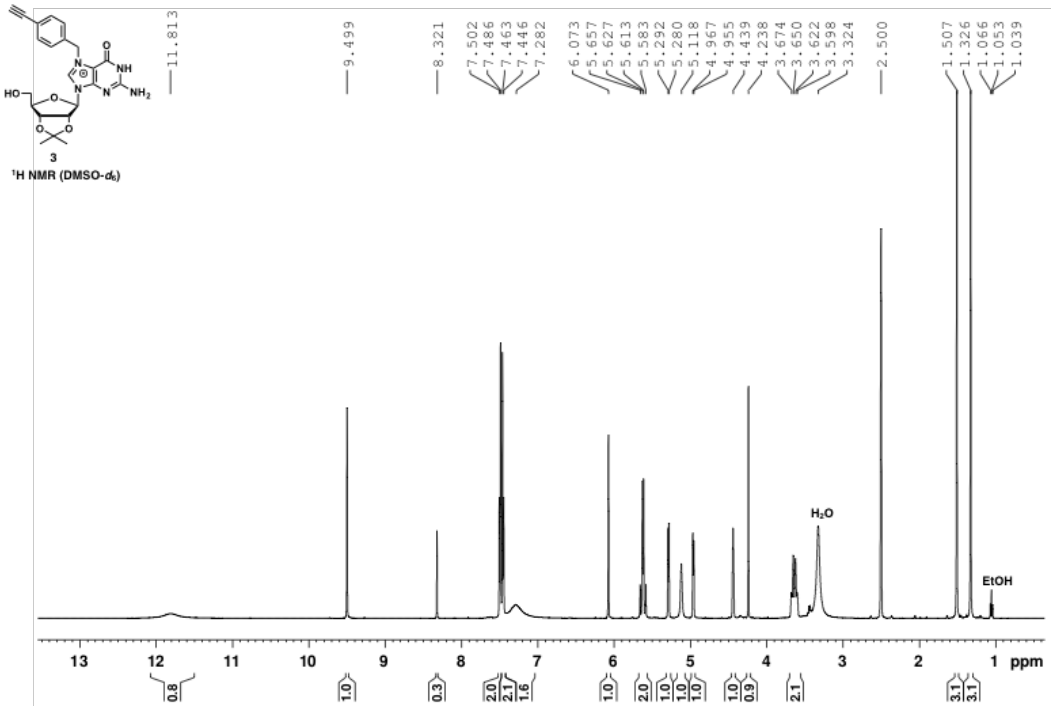
3
^{1}H NMR (DMSO-d_6)
11.813
9.499
8.321
7.502
7.486
7.463
7.446
7.282
6.073
5.657
5.627
5.613
5.583
5.292
5.280
5.118
4.967
4.955
4.439
4.238
3.674
3.650
3.622
3.598
3.324
2.500
1.507
1.326
1.066
1.053
1.039
H2O
EtOH
13 12 11 10 9 8 7 6 5 4 3 2 1 ppm
0.8 1.0 0.3 2.0 2.1 1.6 1.0 2.0 1.0 1.0 1.0 1.0 0.9 2.1 3.1 3.1

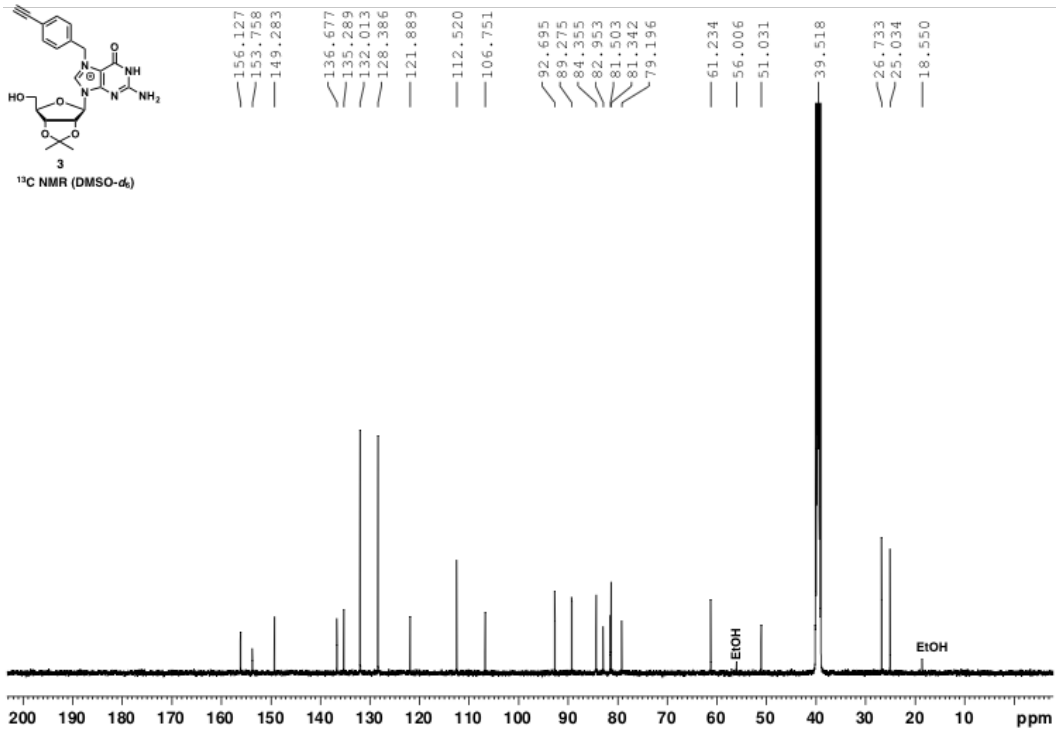
3
^{13}C NMR (DMSO-d_6)
156.127
153.758
149.283
136.677
135.289
132.013
128.386
121.889
112.520
106.751
92.695
89.275
84.355
82.953
81.503
81.342
79.196
61.234
56.006
51.031
39.518
26.733
25.034
18.550
EtOH
EtOH
200 190 180 170 160 150 140 130 120 110 100 90 80 70 60 50 40 30 20 10 ppm

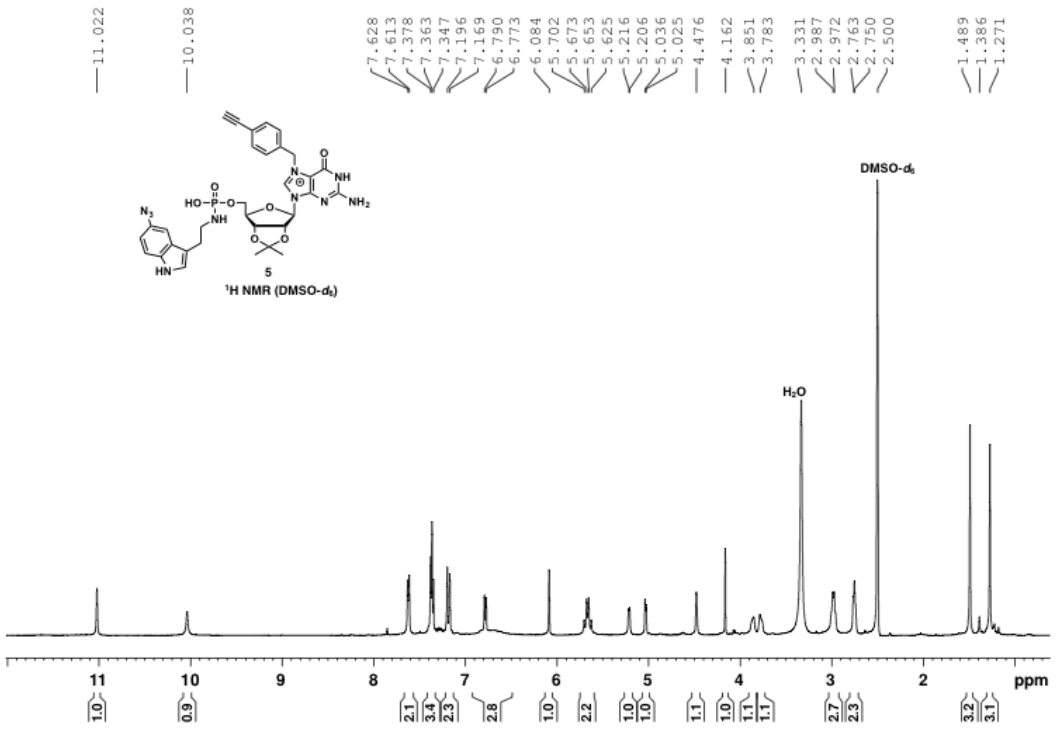
11.022
10.038
7.628
7.613
7.378
7.363
7.347
7.196
7.169
6.790
6.773
6.084
5.702
5.673
5.653
5.625
5.216
5.206
5.036
5.025
4.476
4.162
3.851
3.783
3.331
2.987
2.972
2.763
2.750
2.500
1.489
1.386
1.271
DMSO-d_6
H_2O
5
^{1}H NMR (DMSO-d_6)
11 10 9 8 7 6 5 4 3 2 ppm
1.0 0.9 2.1 3.4 2.3 2.8 1.0 2.2 1.0 1.0 1.1 1.0 1.1 1.1 2.7 2.3 3.2 3.1

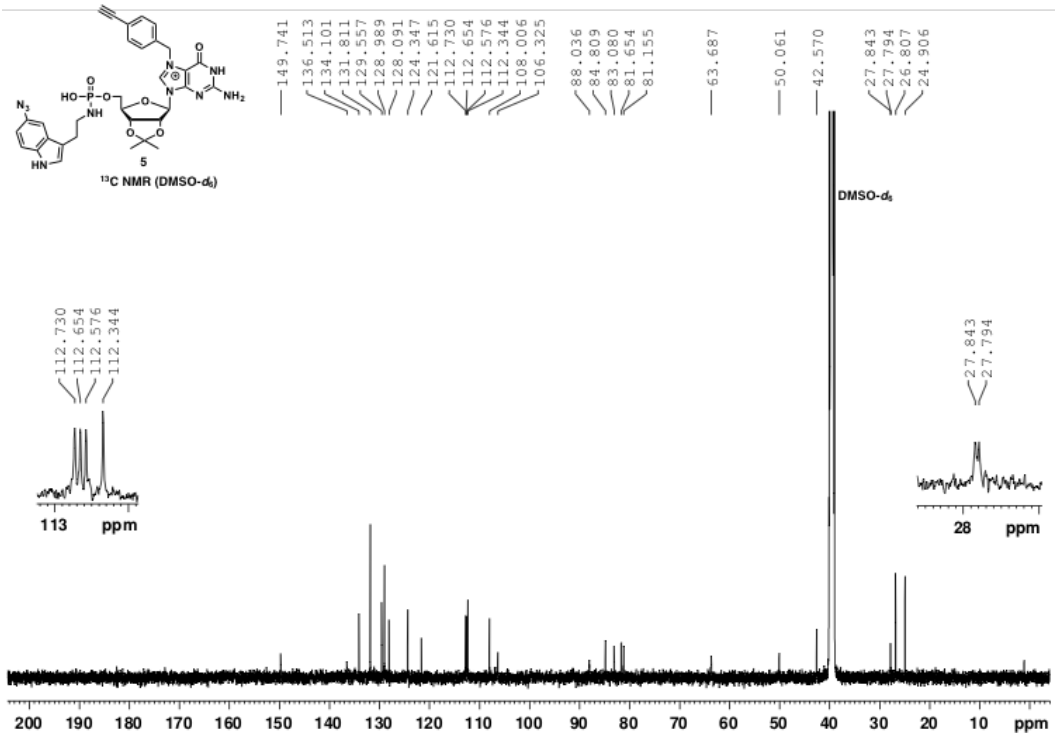
149.741
136.513
134.101
131.811
129.557
128.989
128.091
124.347
121.615
112.730
112.654
112.576
112.344
108.006
106.325
88.036
84.809
83.080
81.654
81.155
63.687
50.061
42.570
27.843
27.794
26.807
24.906
DMSO-d_6
5
^{13}C NMR (DMSO-d_6)
112.730
112.654
112.576
112.344
113 ppm
27.843
27.794
28 ppm
200 190 180 170 160 150 140 130 120 110 100 90 80 70 60 50 40 30 20 10 ppm

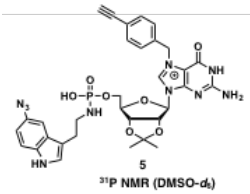

5

^{31}P NMR (DMSO-d_6)

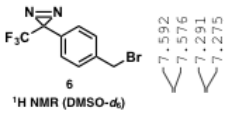

6

^{1}H NMR (DMSO-d_6)

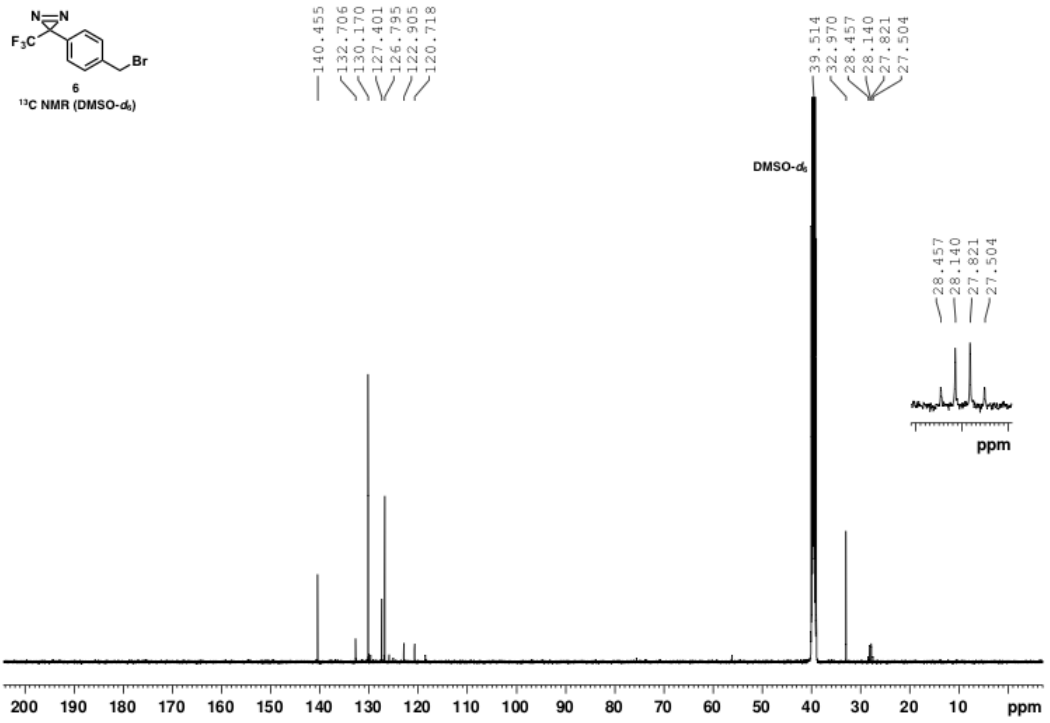
6
13C NMR (DMSO-d6)
140.455
132.706
130.170
127.401
126.795
122.905
120.718
39.514
32.970
28.457
28.140
27.821
27.504
DMSO-d6
28.457
28.140
27.821
27.504
ppm
200 190 180 170 160 150 140 130 120 110 100 90 80 70 60 50 40 30 20 10 ppm

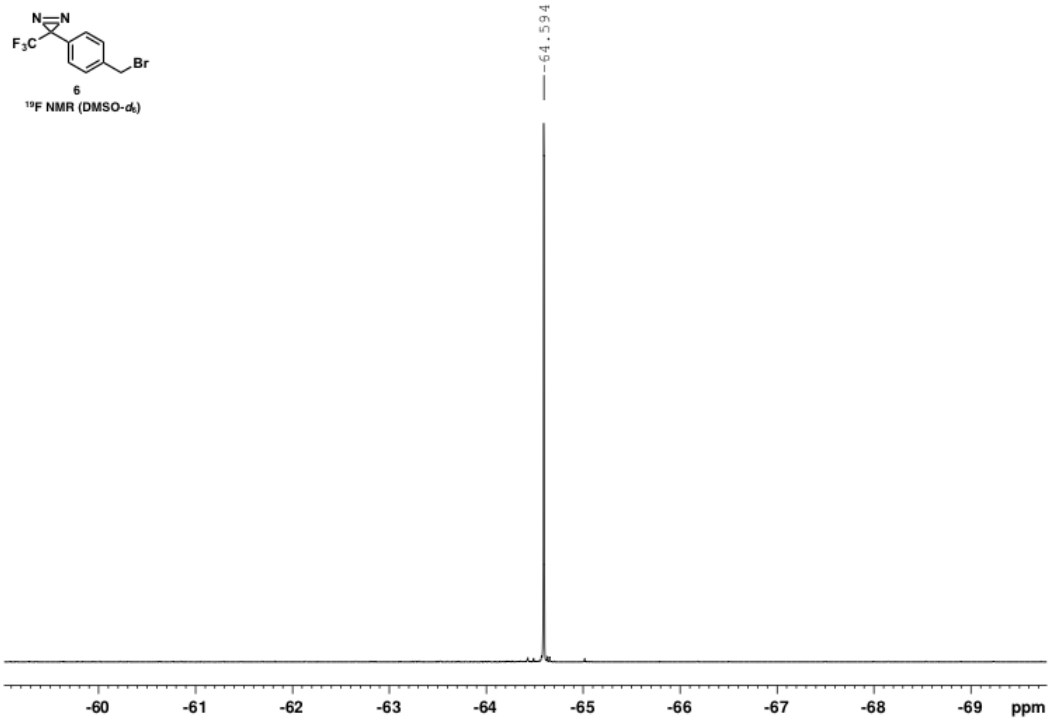
6
19F NMR (DMSO-d6)
-64.594
-60 -61 -62 -63 -64 -65 -66 -67 -68 -69 ppm

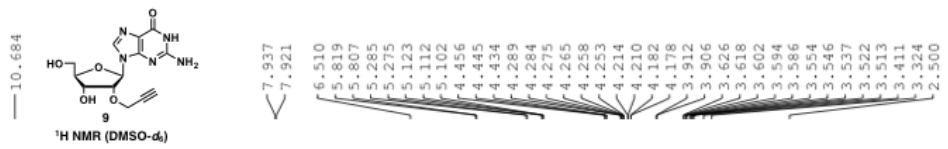
10.684
7.937
7.921
6.510
5.819
5.807
5.285
5.275
5.123
5.112
5.102
4.456
4.445
4.434
4.289
4.284
4.275
4.265
4.258
4.253
4.214
4.210
4.182
4.178
3.912
3.906
3.626
3.618
3.602
3.594
3.586
3.554
3.546
3.537
3.522
3.513
3.411
3.324
2.500
9
^{1}H NMR (DMSO-d_6)

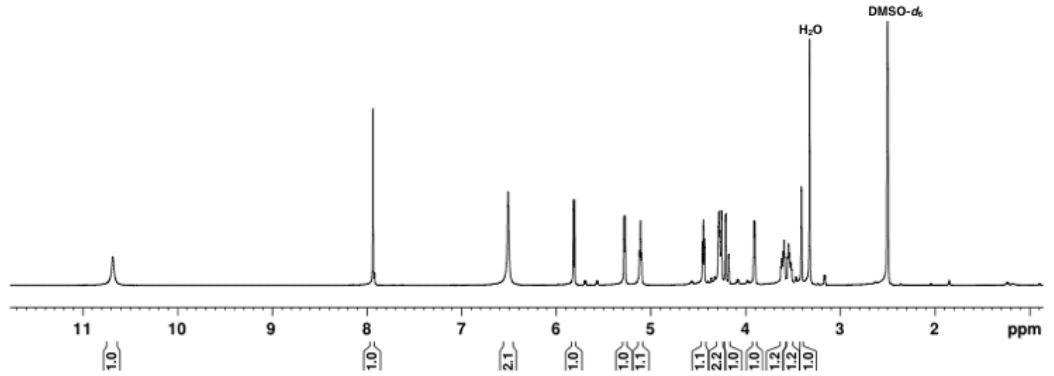
H$_2$O
DMSO-d_6
11
10
9
8
7
6
5
4
3
2
ppm
1.0
1.0
2.1
1.0
1.0
1.1
1.1
2.2
1.0
1.0
1.2
1.2
1.0

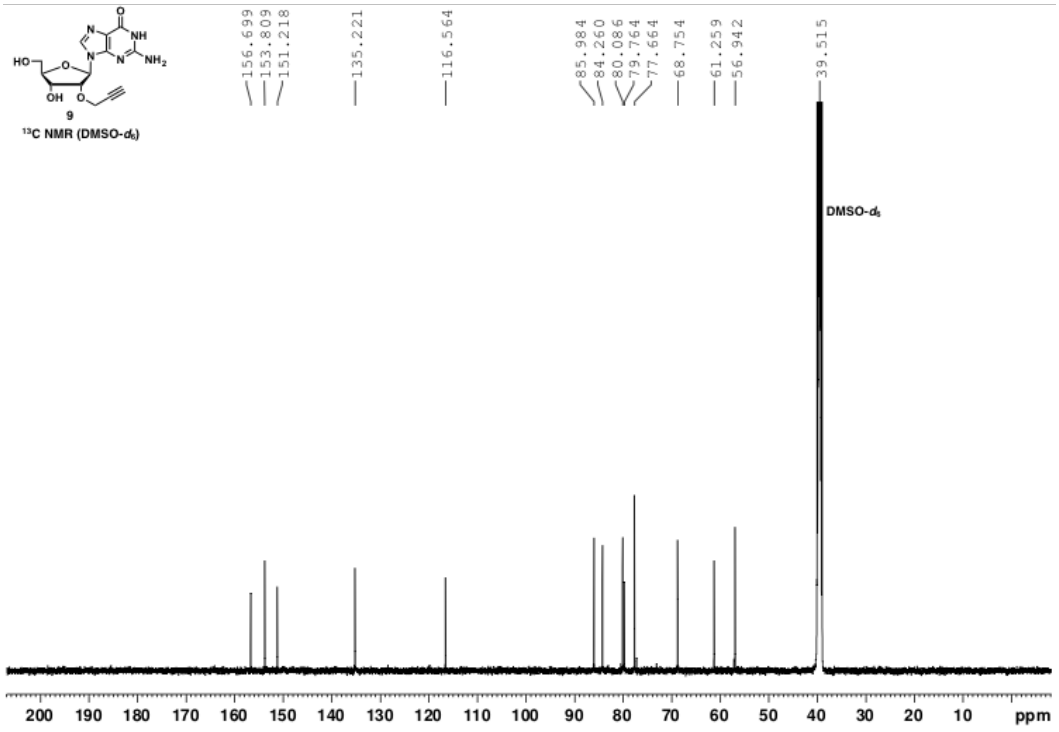
156.699
153.809
151.218
135.221
116.564
85.984
84.260
80.086
79.764
77.664
68.754
61.259
56.942
39.515
9
^{13}C NMR (DMSO-d_6)
DMSO-d_6
200
190
180
170
160
150
140
130
120
110
100
90
80
70
60
50
40
30
20
10
ppm

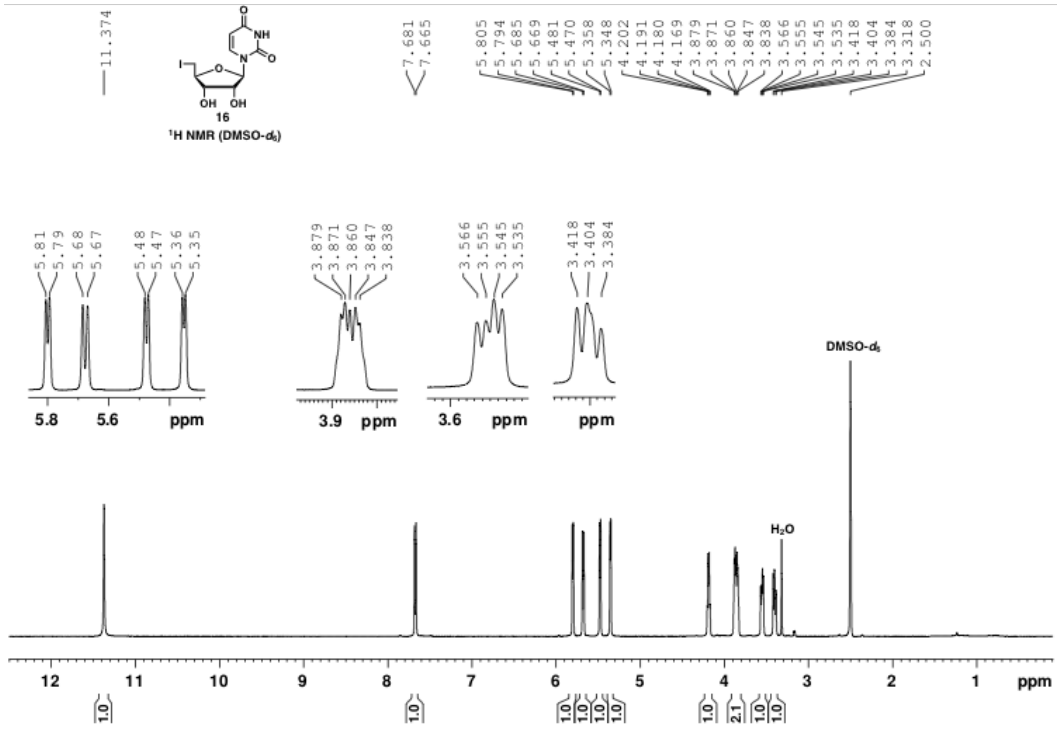
11.374
7.681
7.665
5.805
5.794
5.685
5.669
5.481
5.470
5.358
5.348
4.202
4.191
4.180
4.169
3.879
3.871
3.860
3.847
3.838
3.566
3.555
3.545
3.535
3.418
3.404
3.384
3.318
2.500
OH OH
16
¹H NMR (DMSO-d₆)
5.81
5.79
5.68
5.67
5.48
5.47
5.36
5.35
5.8
5.6
ppm
3.879
3.871
3.860
3.847
3.838
3.9
ppm
3.566
3.555
3.545
3.535
3.6
ppm
3.418
3.404
3.384
ppm
DMSO-d₆
H₂O
12
11
10
9
8
7
6
5
4
3
2
1
ppm
1.0
1.0
1.0
1.0
1.0
1.0
2.1
1.0
1.0

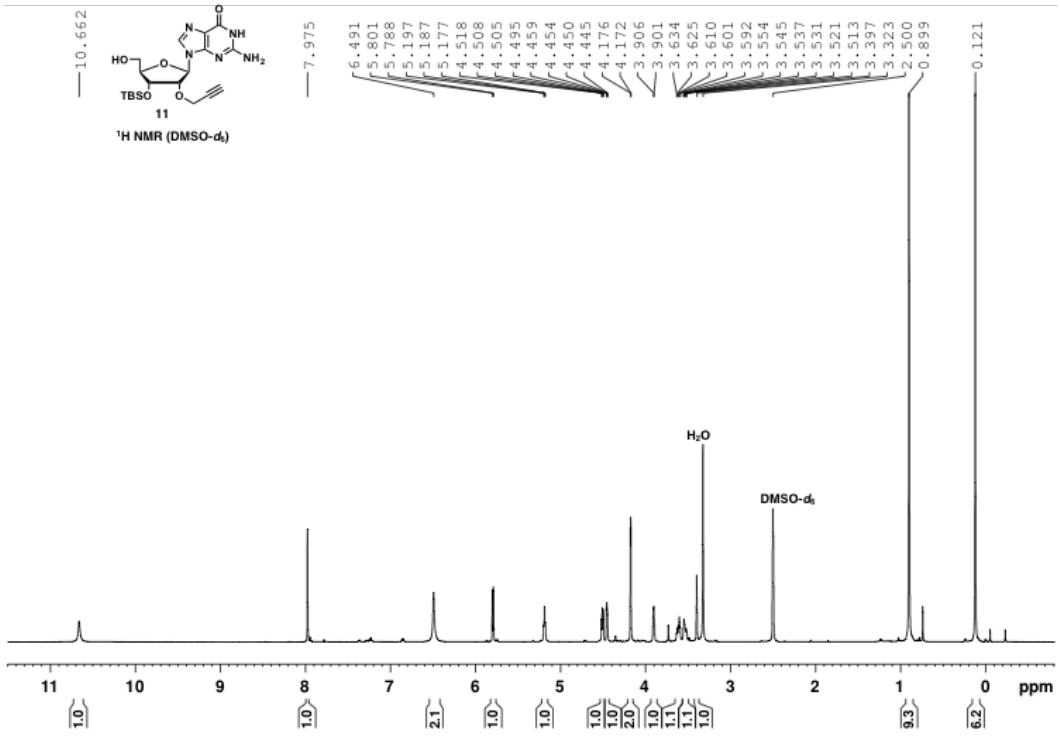
10.662
7.975
6.491
5.801
5.788
5.197
5.187
5.177
4.518
4.508
4.505
4.495
4.459
4.454
4.450
4.445
4.176
4.172
3.906
3.901
3.634
3.625
3.610
3.601
3.592
3.554
3.545
3.537
3.531
3.521
3.513
3.397
3.323
2.500
0.899
0.121
HO
TBSO
11
¹H NMR (DMSO-d₆)
H₂O
DMSO-d₆
11
10
9
8
7
6
5
4
3
2
1
0
ppm
1.0
1.0
2.1
1.0
1.0
1.0
1.0
2.0
1.0
1.1
1.1
1.0
9.3
6.2

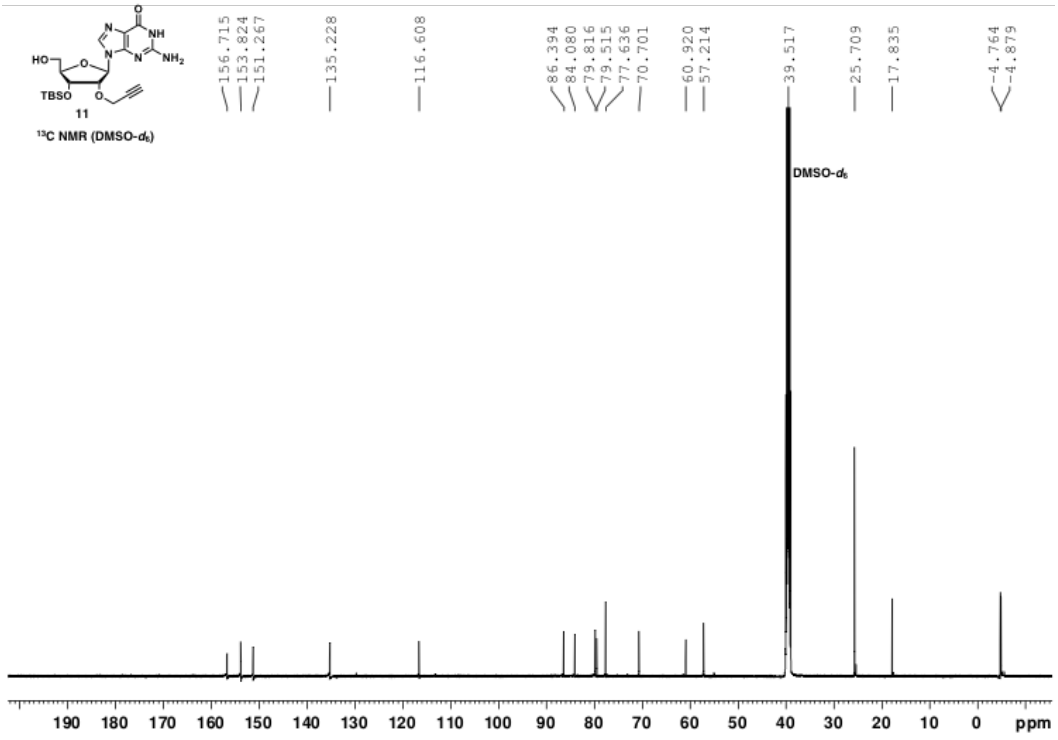
11
^{13}C NMR (DMSO-d_6)
156.715
153.824
151.267
135.228
116.608
86.394
84.080
79.816
79.515
77.636
70.701
60.920
57.214
39.517
25.709
17.835
-4.764
-4.879
DMSO-d_6
190 180 170 160 150 140 130 120 110 100 90 80 70 60 50 40 30 20 10 0 ppm

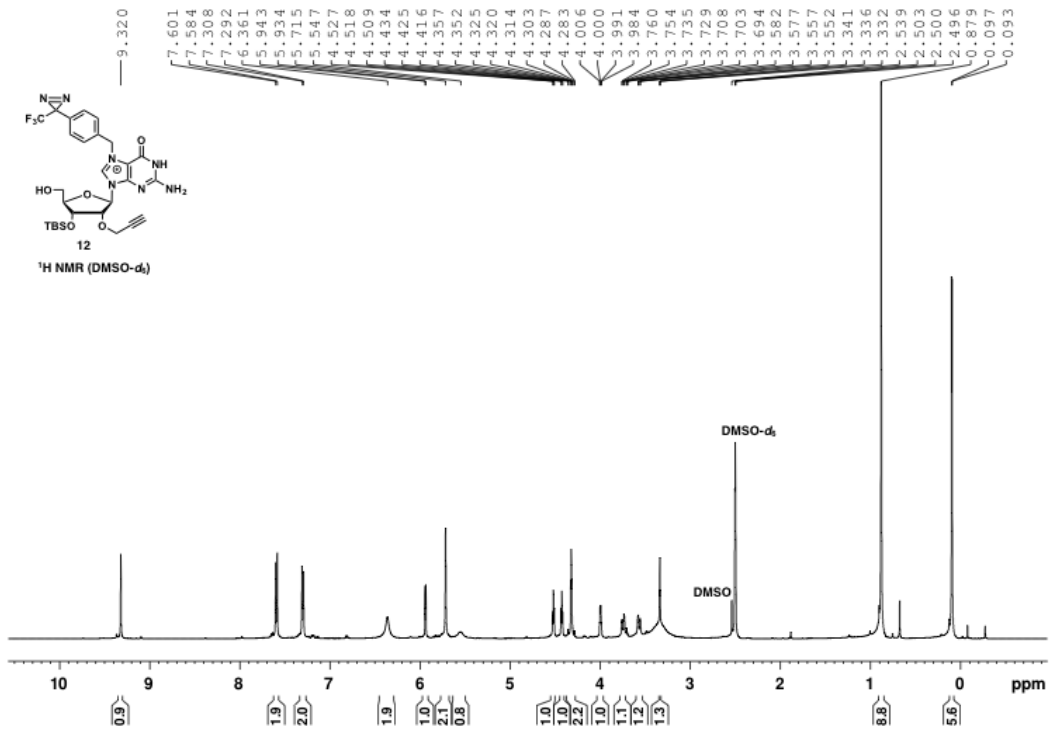
12
^{1}H NMR (DMSO-d_6)
9.320
7.601
7.584
7.308
7.292
6.361
5.943
5.934
5.715
5.547
4.527
4.518
4.509
4.434
4.425
4.416
4.357
4.352
4.325
4.320
4.314
4.303
4.287
4.283
4.006
4.000
3.991
3.984
3.760
3.754
3.735
3.729
3.708
3.703
3.694
3.582
3.577
3.557
3.552
3.341
3.336
3.332
2.539
2.503
2.500
2.496
0.879
0.097
0.093
DMSO-d_5
DMSO
10 9 8 7 6 5 4 3 2 1 0 ppm
0.9 1.9 2.0 1.9 1.0 2.1 0.8 1.0 1.0 2.2 1.0 1.1 1.2 1.3 8.8 5.6

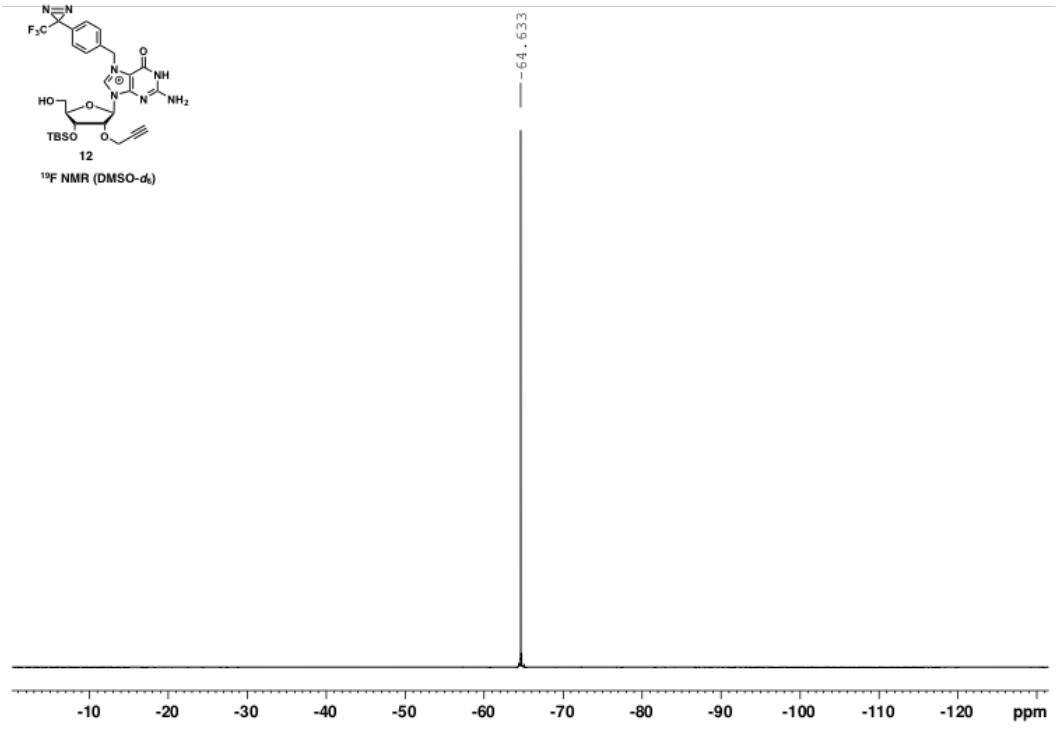
12
^{19}F NMR (DMSO-d_6)
-64.633
-10 -20 -30 -40 -50 -60 -70 -80 -90 -100 -110 -120 ppm

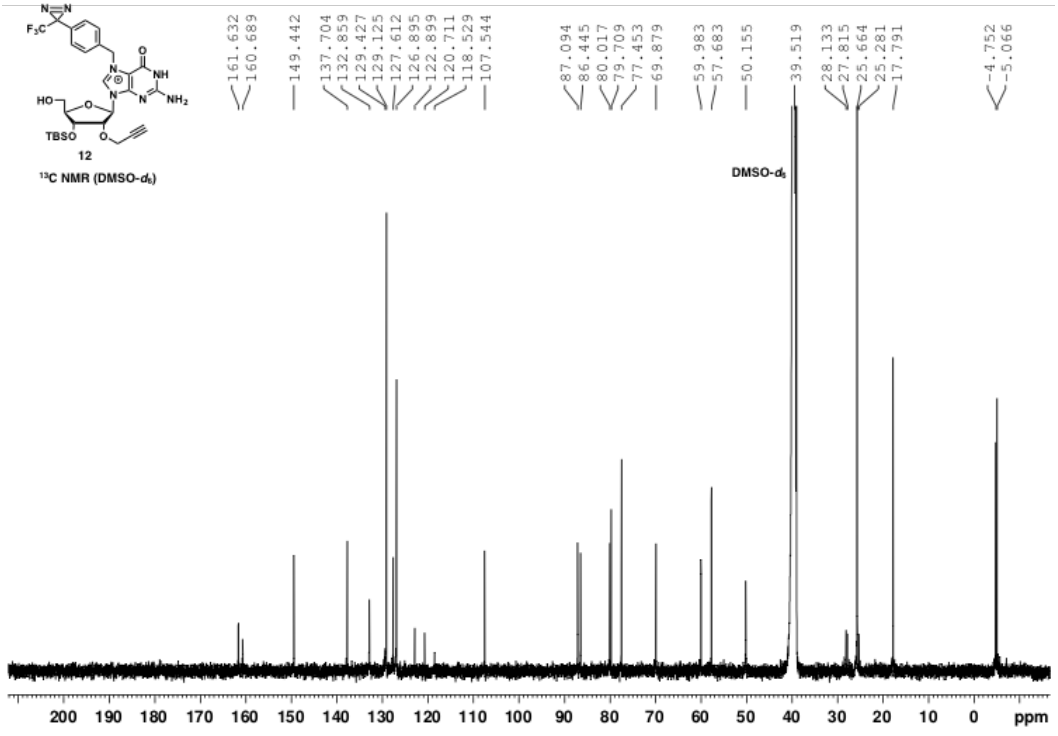
12
^{13}C NMR (DMSO-d_6)
161.632
160.689
149.442
137.704
132.859
129.427
129.125
127.612
126.895
122.899
120.711
118.529
107.544
87.094
86.445
80.017
79.709
77.453
69.879
59.983
57.683
50.155
39.519
28.133
27.815
25.664
25.281
17.791
-4.752
-5.066
DMSO-d_5
200 190 180 170 160 150 140 130 120 110 100 90 80 70 60 50 40 30 20 10 0 ppm

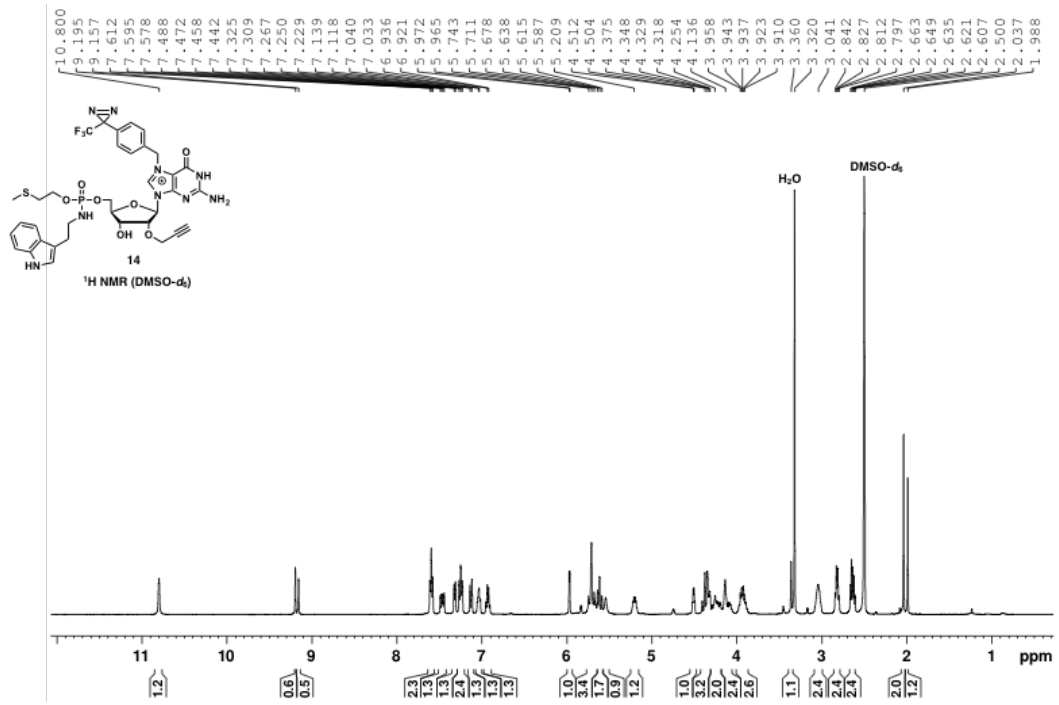
14
^{1}H NMR (DMSO-d_6)
H_2O
DMSO-d_6
ppm

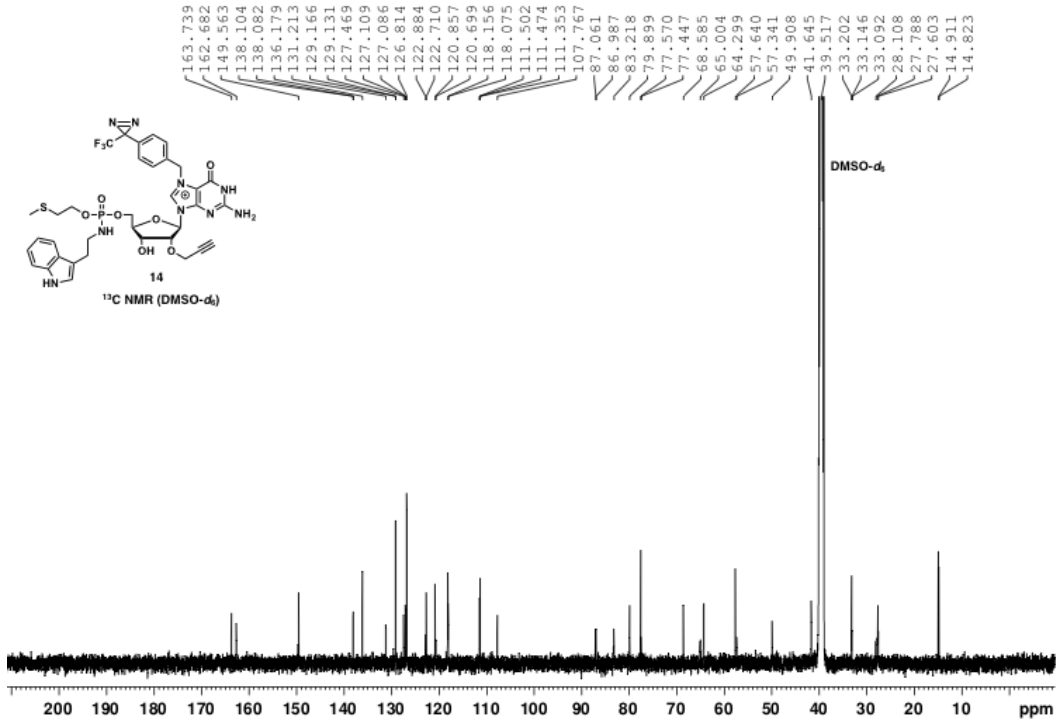
14
^{13}C NMR (DMSO-d_6)
DMSO-d_6
ppm

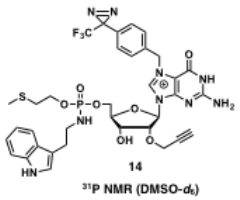

14

^{31}P NMR (DMSO-d_6)

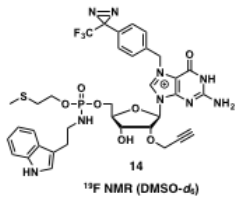

14

^{19}F NMR (DMSO-d_6)

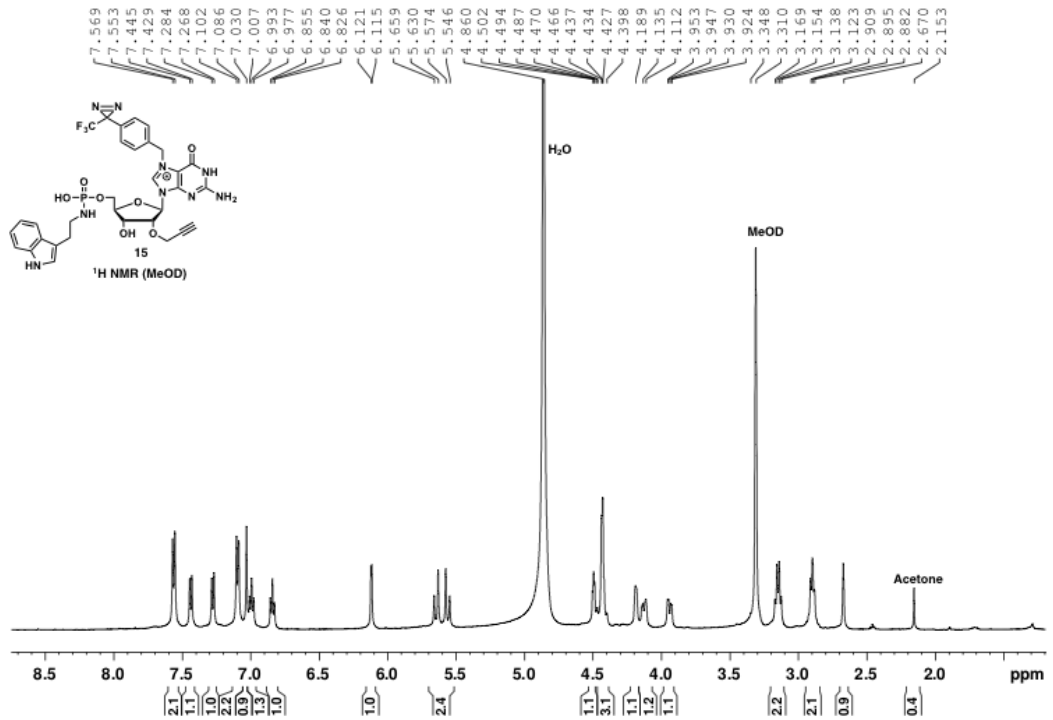
7.569
7.553
7.445
7.429
7.284
7.268
7.102
7.086
7.030
7.007
6.993
6.977
6.855
6.840
6.826
6.121
6.115
5.659
5.630
5.574
5.546
4.860
4.502
4.494
4.487
4.470
4.466
4.437
4.434
4.427
4.398
4.189
4.135
4.112
3.953
3.947
3.930
3.924
3.348
3.310
3.169
3.154
3.138
3.123
2.909
2.895
2.882
2.670
2.153
H2O
MeOD
Acetone
15
1H NMR (MeOD)
8.5
8.0
7.5
7.0
6.5
6.0
5.5
5.0
4.5
4.0
3.5
3.0
2.5
2.0
ppm

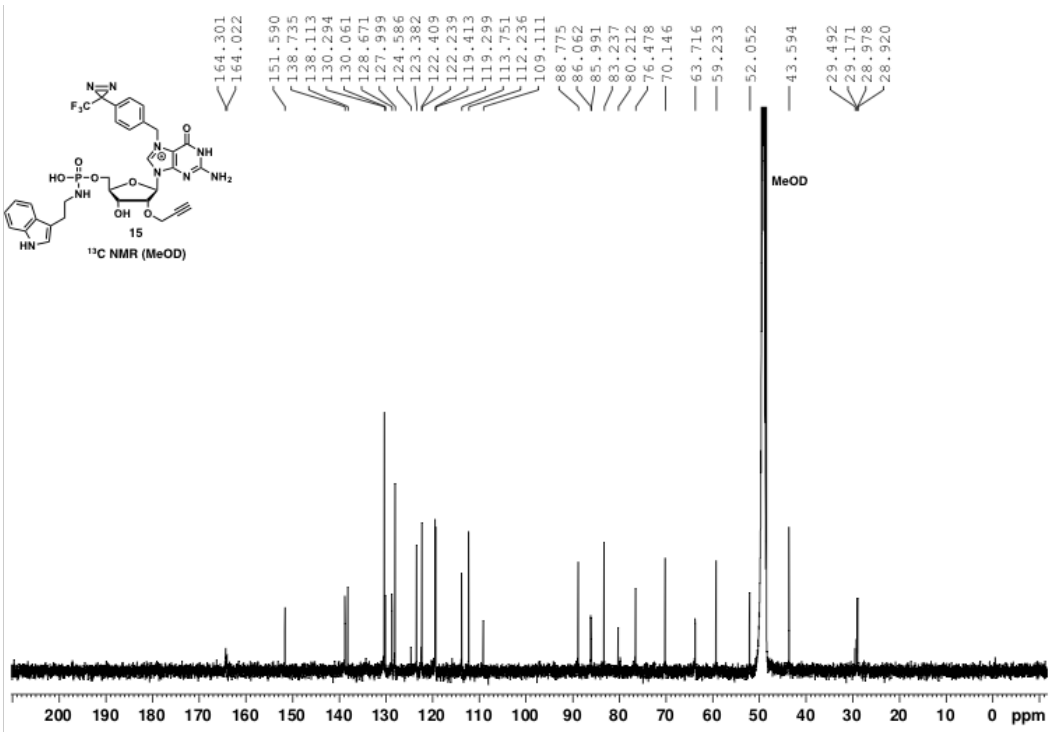
164.301
164.022
151.590
138.735
138.113
130.294
130.061
128.671
127.999
124.586
123.382
122.409
122.239
119.413
119.299
113.751
112.236
109.111
88.775
86.062
85.991
83.237
80.212
76.478
70.146
63.716
59.233
52.052
43.594
29.492
29.171
28.978
28.920
MeOD
15
13C NMR (MeOD)
200
190
180
170
160
150
140
130
120
110
100
90
80
70
60
50
40
30
20
10
0
ppm

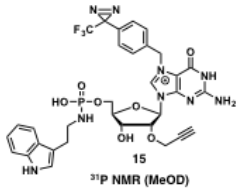

15

^{31}P NMR (MeOD)

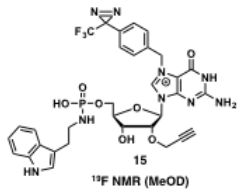

15

^{19}F NMR (MeOD)

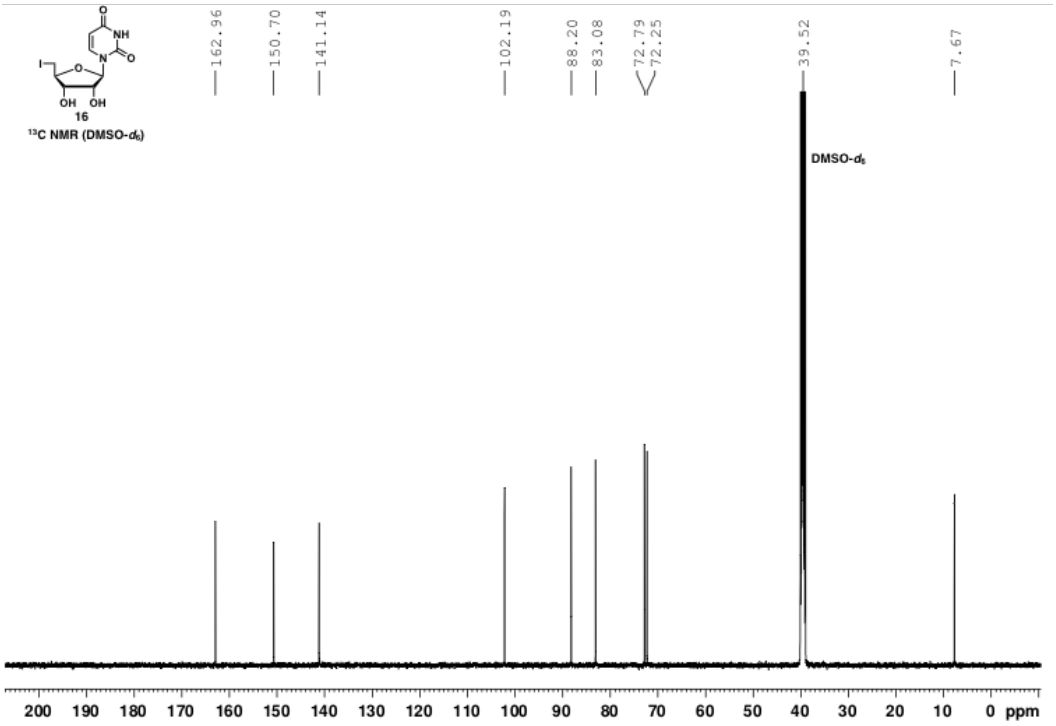
16
^{13}C NMR (DMSO-d_6)
162.96
150.70
141.14
102.19
88.20
83.08
72.79
72.25
39.52
7.67
DMSO-d_6
200 190 180 170 160 150 140 130 120 110 100 90 80 70 60 50 40 30 20 10 0 ppm

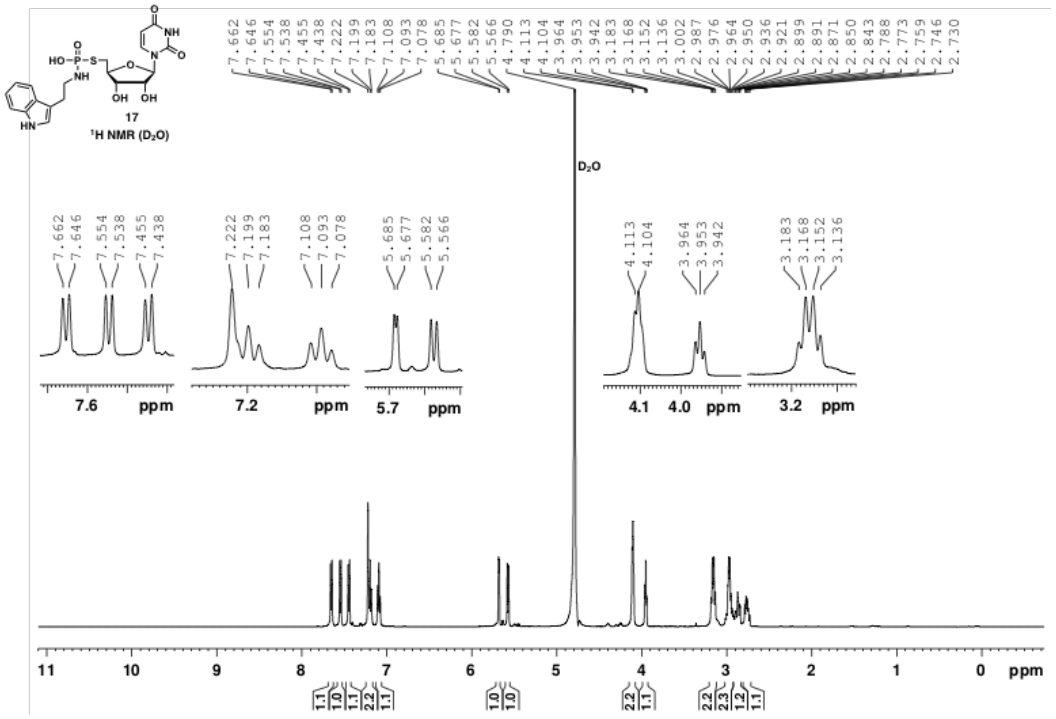
17
^{1}H NMR (D_2O)
D_2O
7.6 ppm
7.2 ppm
5.7 ppm
4.1 4.0 ppm
3.2 ppm
11 10 9 8 7 6 5 4 3 2 1 0 ppm

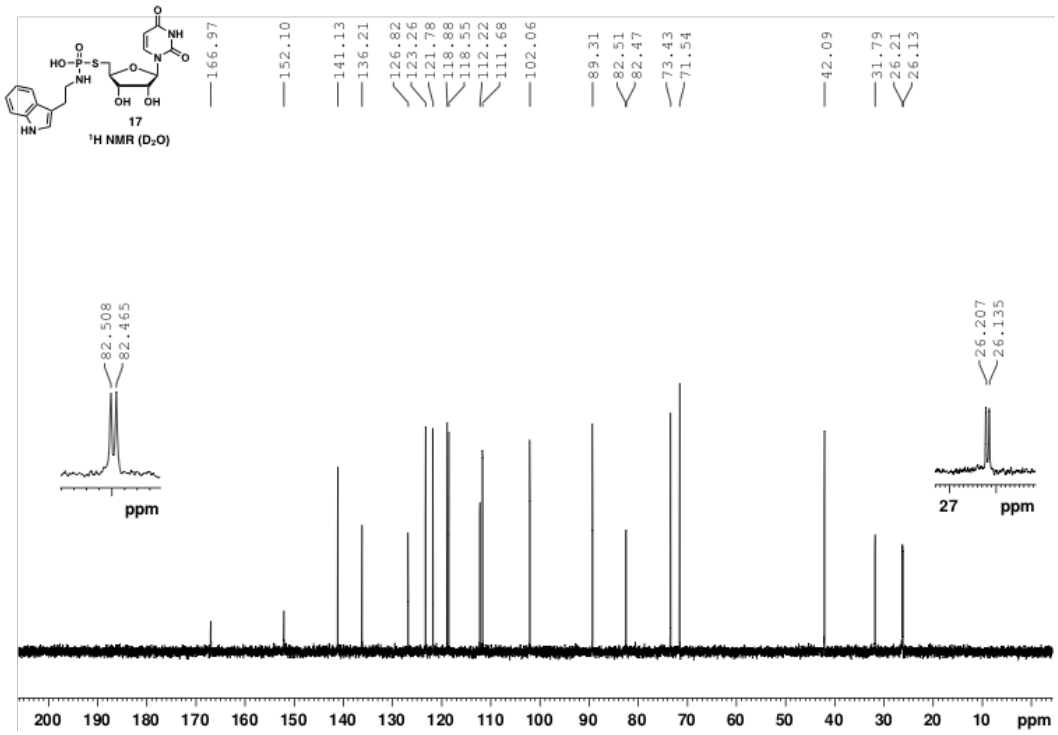
17
^{1}H NMR (D_2O)
166.97
152.10
141.13
136.21
126.82
123.26
121.78
118.88
118.55
112.22
111.68
102.06
89.31
82.51
82.47
73.43
71.54
42.09
31.79
26.21
26.13
82.508
82.465
ppm
26.207
26.135
27
ppm
200 190 180 170 160 150 140 130 120 110 100 90 80 70 60 50 40 30 20 10 ppm

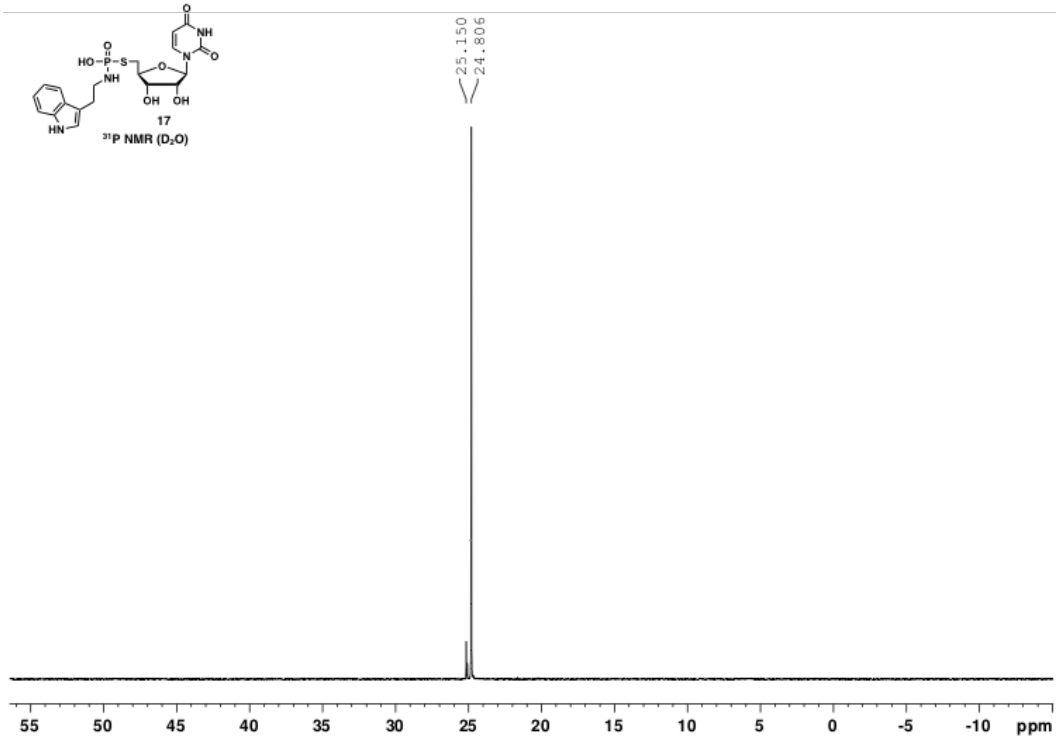
17
^{31}P NMR (D_2O)
25.150
24.806
55 50 45 40 35 30 25 20 15 10 5 0 -5 -10 ppm

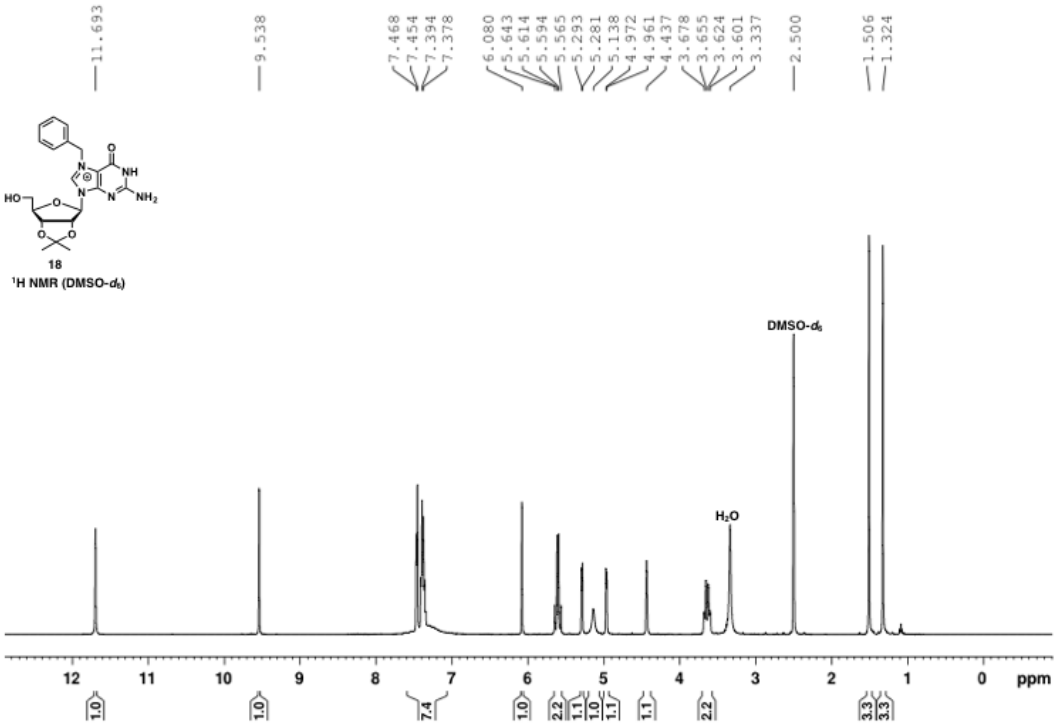
11.693
9.538
7.468
7.454
7.394
7.378
6.080
5.643
5.614
5.594
5.565
5.293
5.281
5.138
4.972
4.961
4.437
3.678
3.655
3.624
3.601
3.337
2.500
1.506
1.324
18
^{1}H NMR (DMSO-d_6)
DMSO-d_6
H_2O
ppm

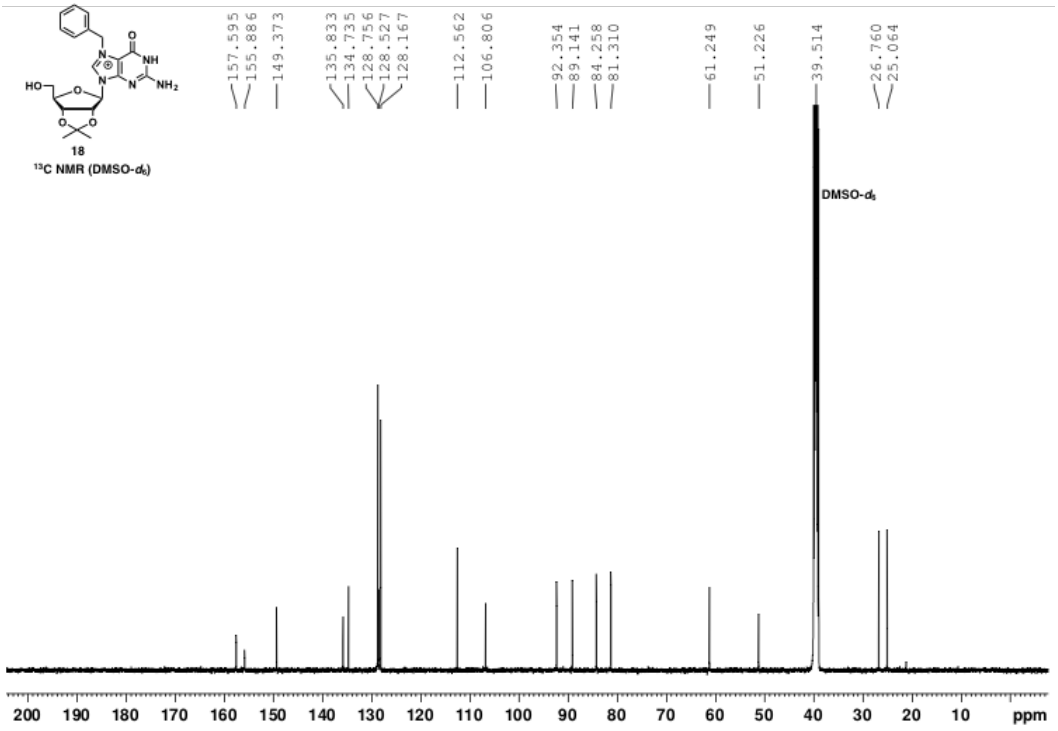
157.595
155.886
149.373
135.833
134.735
128.756
128.527
128.167
112.562
106.806
92.354
89.141
84.258
81.310
61.249
51.226
39.514
26.760
25.064
18
^{13}C NMR (DMSO-d_6)
DMSO-d_6
ppm

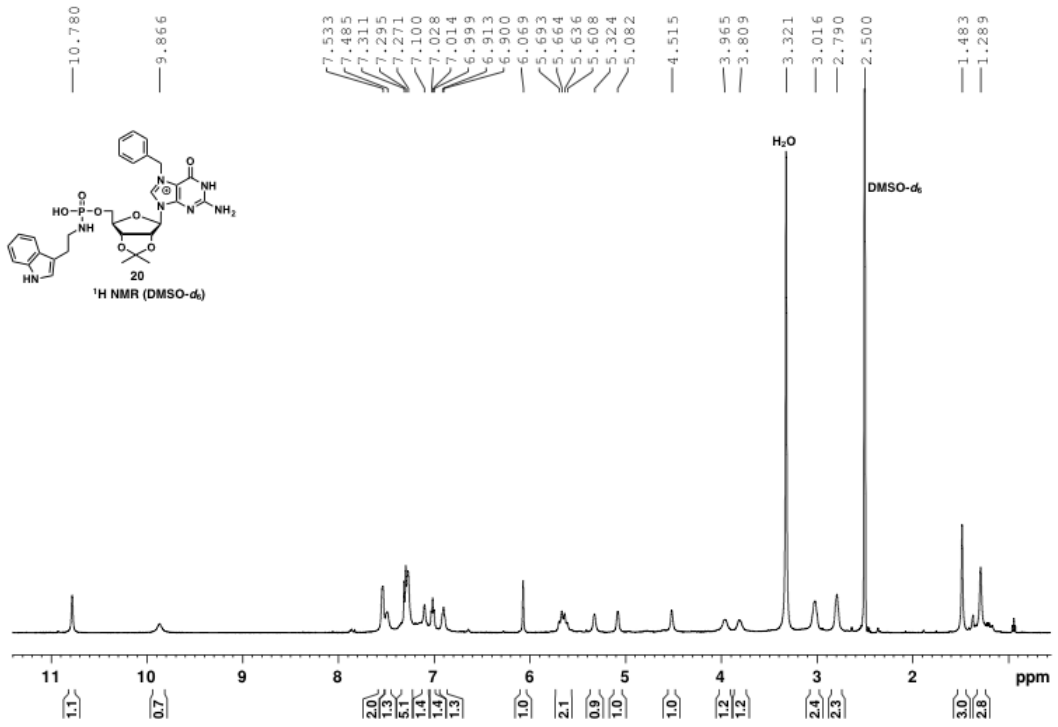
10.780
9.866
7.533
7.485
7.311
7.295
7.271
7.100
7.028
7.014
6.999
6.913
6.900
6.069
5.693
5.664
5.636
5.608
5.324
5.082
4.515
3.965
3.809
3.321
3.016
2.790
2.500
1.483
1.289
H2O
DMSO-d6
20
1H NMR (DMSO-d6)
11
10
9
8
7
6
5
4
3
2
ppm
1.1
0.7
2.0
1.3
5.1
1.4
1.4
1.3
1.0
2.1
0.9
1.0
1.0
1.2
1.2
2.4
2.3
3.0
2.8

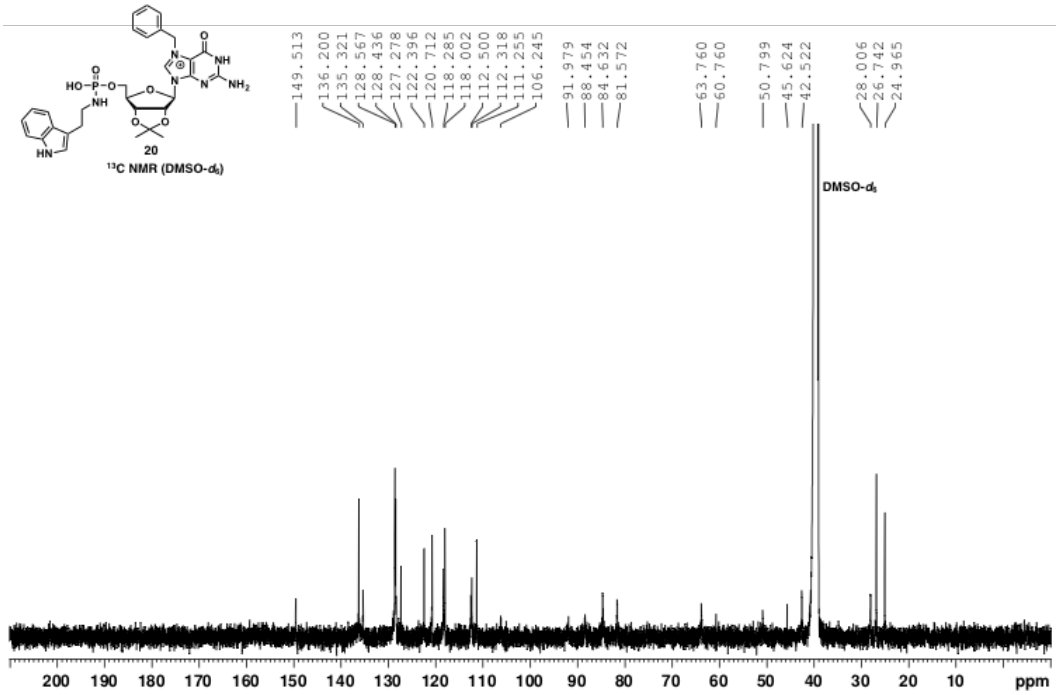
149.513
136.200
135.321
128.567
128.436
127.278
122.396
120.712
118.285
118.002
112.500
112.318
111.255
106.245
91.979
88.454
84.632
81.572
63.760
60.760
50.799
45.624
42.522
28.006
26.742
24.965
DMSO-d6
20
13C NMR (DMSO-d6)
200
190
180
170
160
150
140
130
120
110
100
90
80
70
60
50
40
30
20
10
ppm

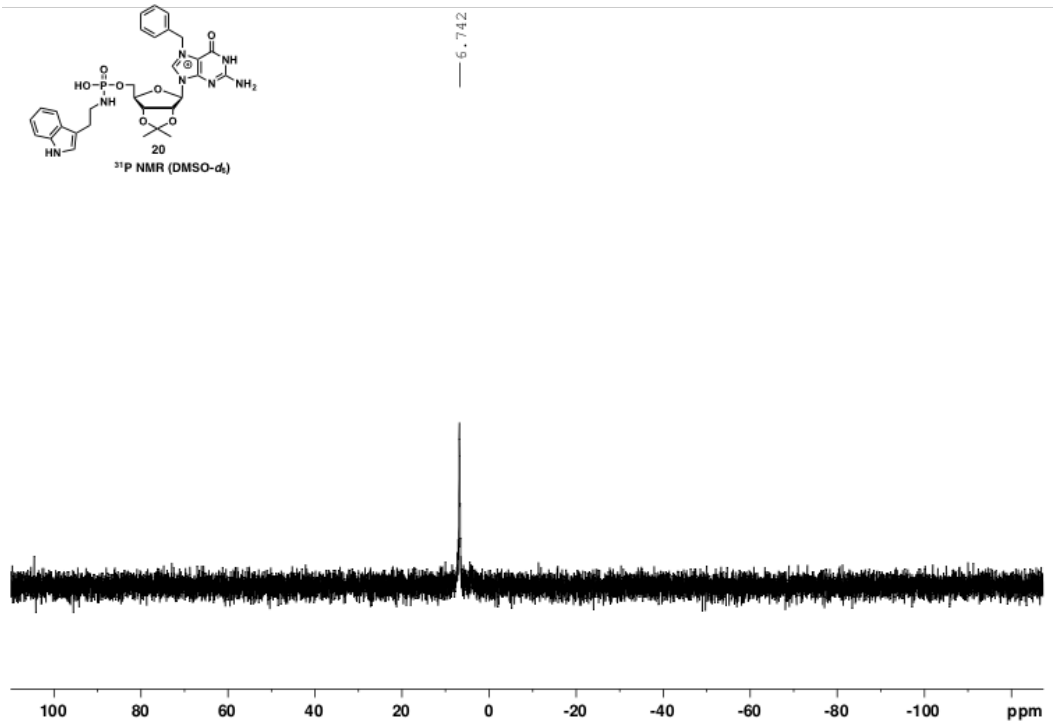
20
31P NMR (DMSO-d6)
6.742
100
80
60
40
20
0
-20
-40
-60
-80
-100
ppm

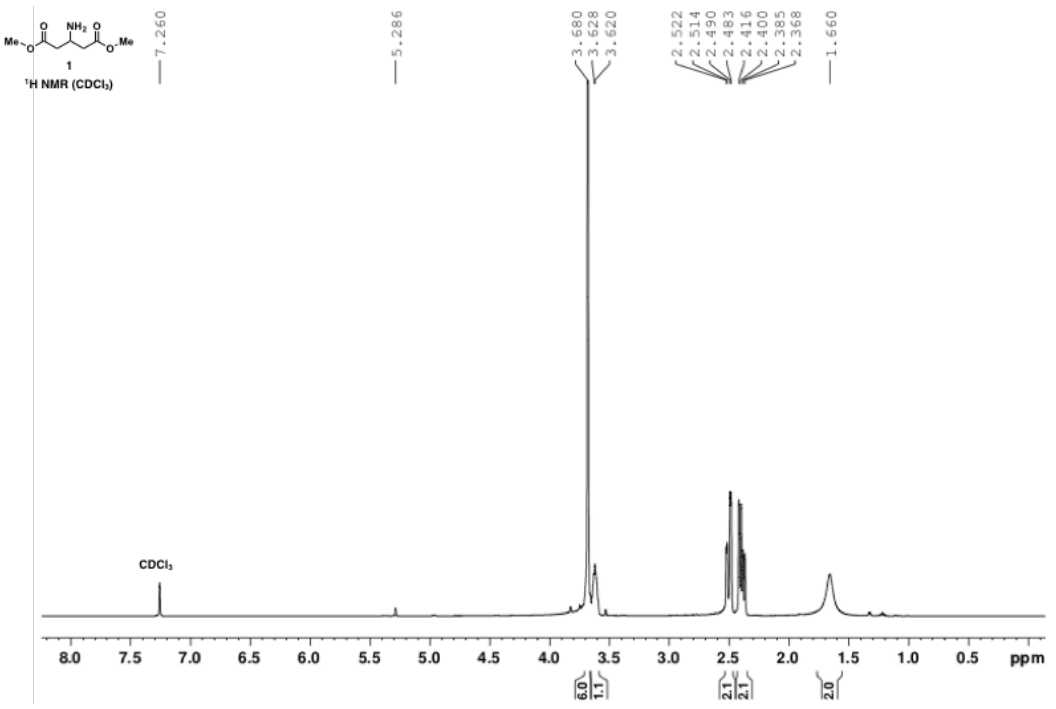
1
1H NMR (CDCl3)
7.260
5.286
3.680
3.628
3.620
2.522
2.514
2.490
2.483
2.416
2.400
2.385
2.368
1.660
CDCl3
8.0
7.5
7.0
6.5
6.0
5.5
5.0
4.5
4.0
3.5
3.0
2.5
2.0
1.5
1.0
0.5
ppm
6.0
1.1
2.1
2.1
2.0

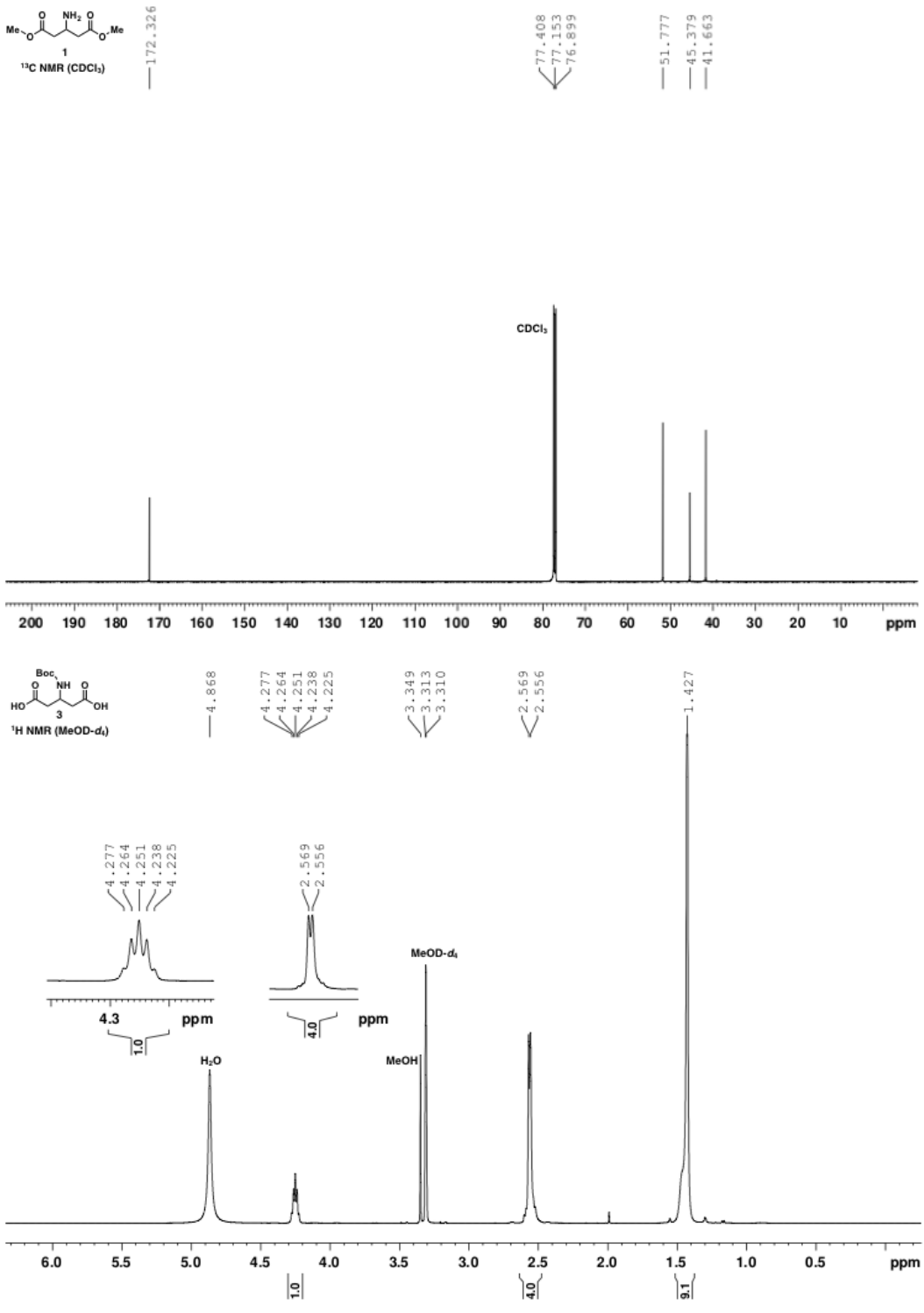
1
13C NMR (CDCl3)
172.326
77.408
77.153
76.899
51.777
45.379
41.663
CDCl3
200 190 180 170 160 150 140 130 120 110 100 90 80 70 60 50 40 30 20 10 ppm
3
1H NMR (MeOD-d4)
4.868
4.277
4.264
4.251
4.238
4.225
3.349
3.313
3.310
2.569
2.556
1.427
4.3 ppm
1.0
ppm
4.0
MeOD-d4
H2O
MeOH
6.0 5.5 5.0 4.5 4.0 3.5 3.0 2.5 2.0 1.5 1.0 0.5 ppm
1.0
4.0
9.1

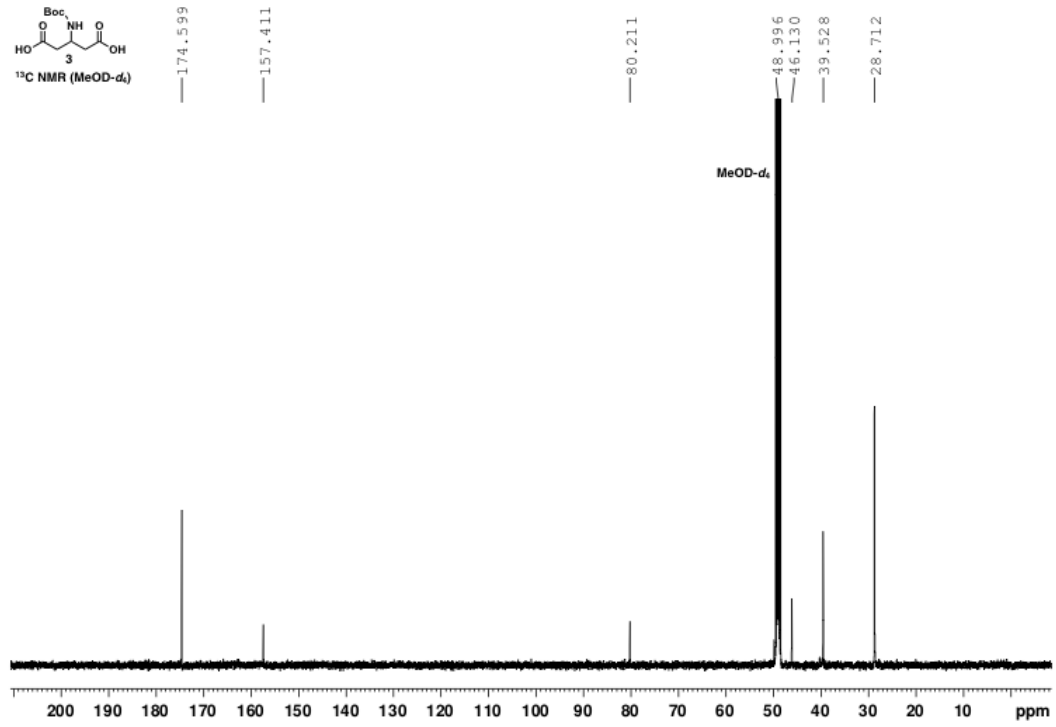
Boc
NH
HO
OH
3
^{13}C NMR (MeOD-d_4)
174.599
157.411
80.211
48.996
46.130
39.528
28.712
MeOD-d_4
200 190 180 170 160 150 140 130 120 110 100 90 80 70 60 50 40 30 20 10 ppm

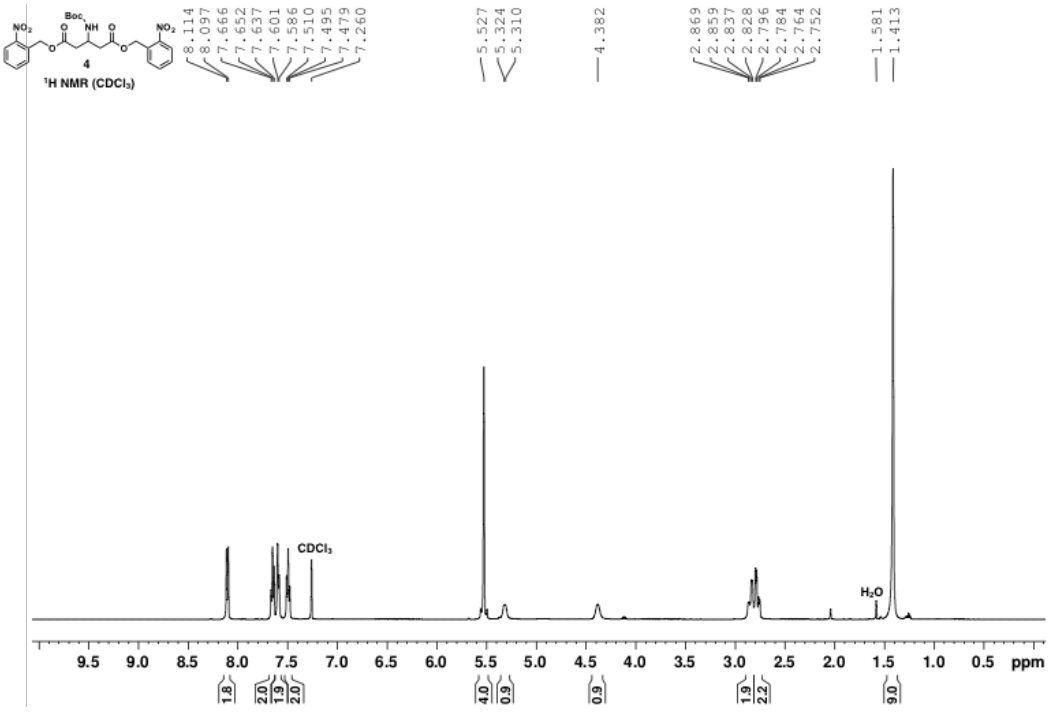
Boc
NH
NO_2
NO_2
4
^{1}H NMR ($CDCl_3$)
8.114
8.097
7.666
7.652
7.637
7.601
7.586
7.510
7.495
7.479
7.260
5.527
5.324
5.310
4.382
2.859
2.859
2.837
2.828
2.796
2.784
2.764
2.752
1.581
1.413
$CDCl_3$
H_2O
9.5 9.0 8.5 8.0 7.5 7.0 6.5 6.0 5.5 5.0 4.5 4.0 3.5 3.0 2.5 2.0 1.5 1.0 0.5 ppm
1.8
2.0
1.9
2.0
4.0
0.9
0.9
1.9
2.2
9.0

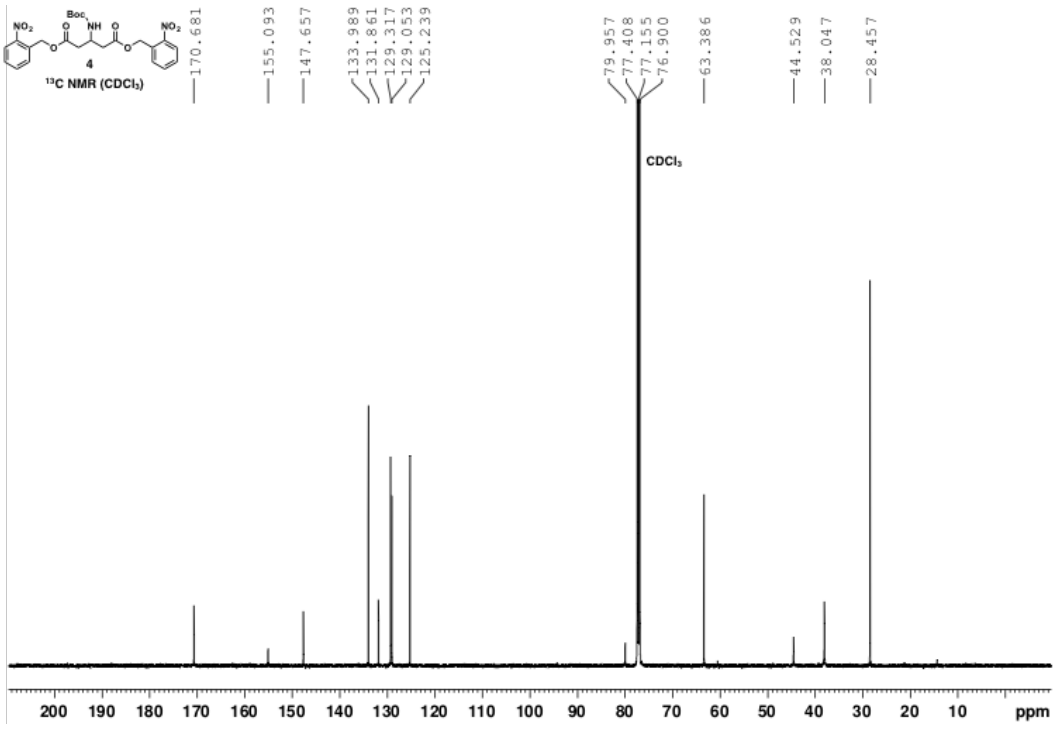
4
^{13}C NMR ($CDCl_3$)
170.681
155.093
147.657
133.989
131.861
129.317
129.053
125.239
79.957
77.408
77.155
76.900
63.386
44.529
38.047
28.457
$CDCl_3$
200 190 180 170 160 150 140 130 120 110 100 90 80 70 60 50 40 30 20 10 ppm

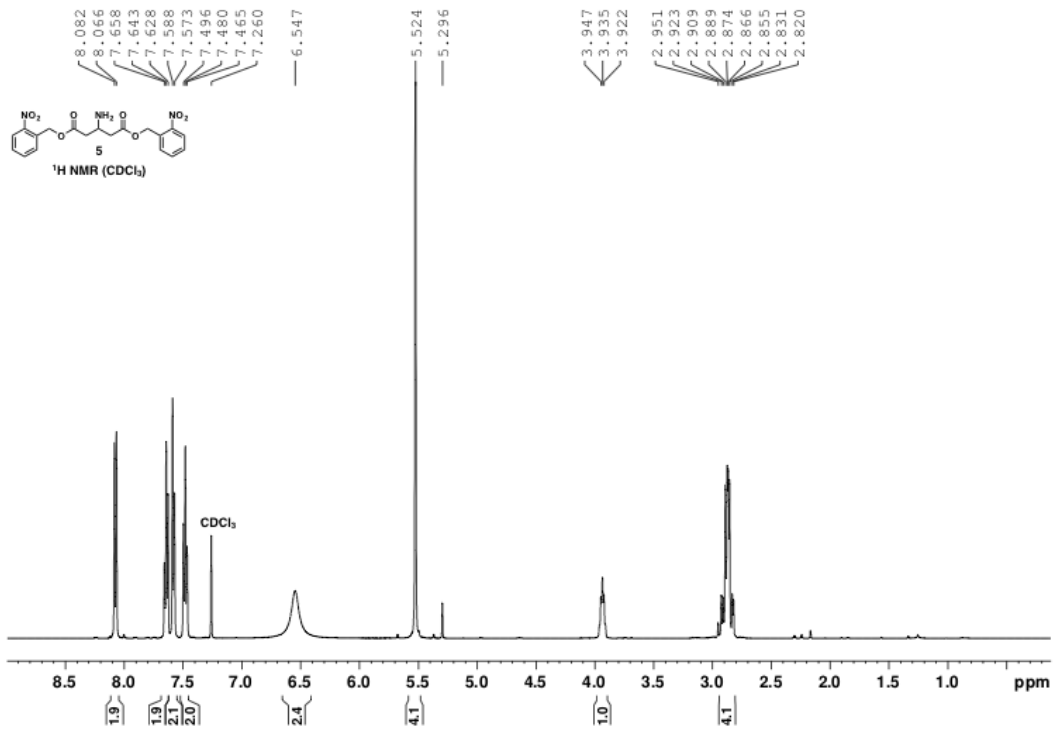
8.082
8.066
7.658
7.643
7.628
7.588
7.573
7.496
7.480
7.465
7.260
6.547
5.524
5.296
3.947
3.935
3.922
2.951
2.923
2.909
2.889
2.874
2.866
2.855
2.831
2.820
5
^{1}H NMR ($CDCl_3$)
$CDCl_3$
8.5 8.0 7.5 7.0 6.5 6.0 5.5 5.0 4.5 4.0 3.5 3.0 2.5 2.0 1.5 1.0 ppm
1.9
1.9
2.1
2.0
2.4
4.1
1.0
4.1

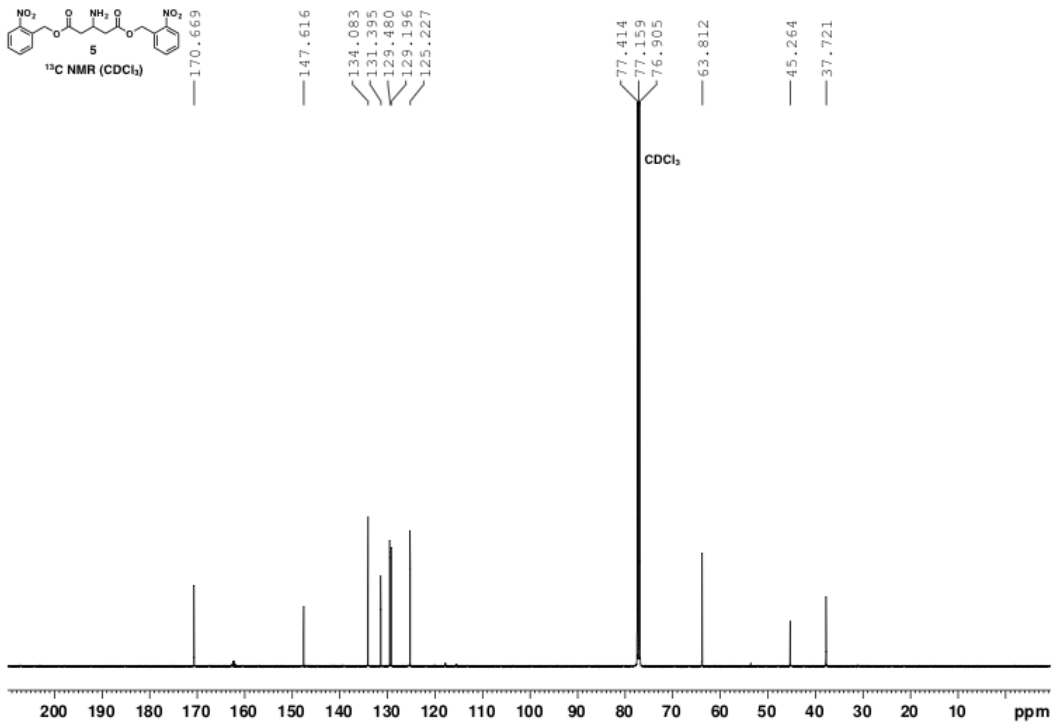
5
^{13}C NMR ($CDCl_3$)
170.669
147.616
134.083
131.395
129.480
129.196
125.227
77.414
77.159
76.905
63.812
45.264
37.721
$CDCl_3$
200 190 180 170 160 150 140 130 120 110 100 90 80 70 60 50 40 30 20 10 ppm

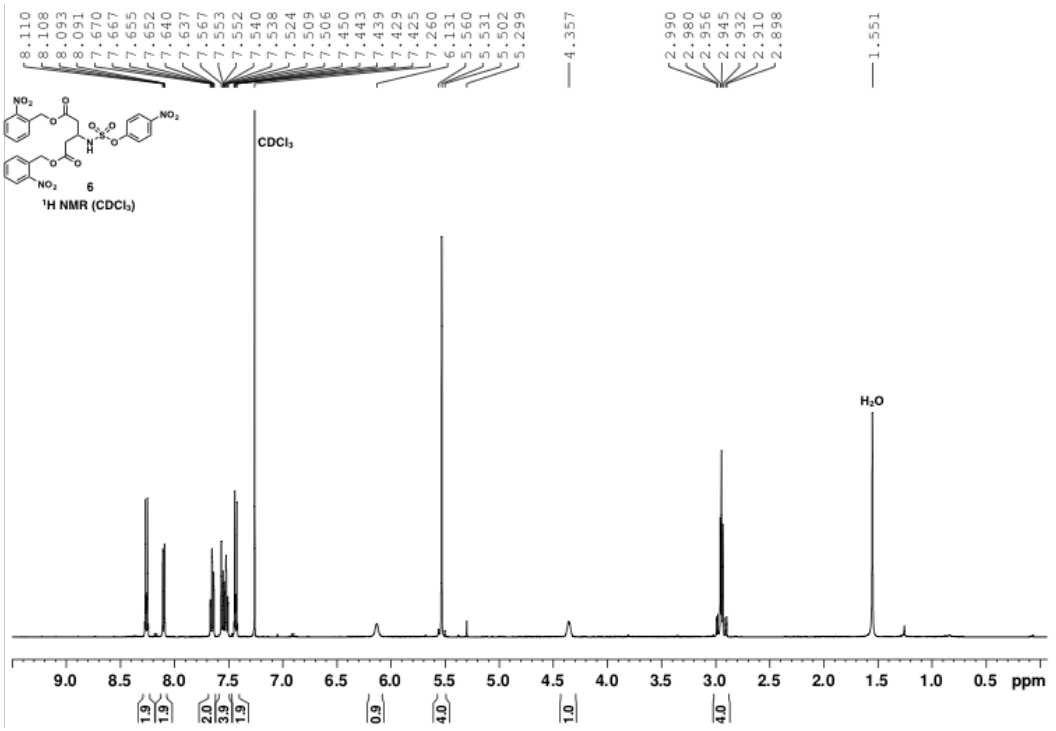
8.110
8.108
8.093
8.091
7.670
7.667
7.655
7.652
7.640
7.637
7.567
7.553
7.552
7.540
7.538
7.524
7.509
7.506
7.450
7.443
7.439
7.429
7.425
7.260
6.131
5.560
5.531
5.502
5.299
4.357
2.990
2.980
2.956
2.945
2.932
2.910
2.898
1.551
6
^{1}H NMR ($CDCl_3$)
$CDCl_3$
H_2O
9.0 8.5 8.0 7.5 7.0 6.5 6.0 5.5 5.0 4.5 4.0 3.5 3.0 2.5 2.0 1.5 1.0 0.5 ppm
1.9
1.9
2.0
3.9
1.9
0.9
4.0
1.0
4.0

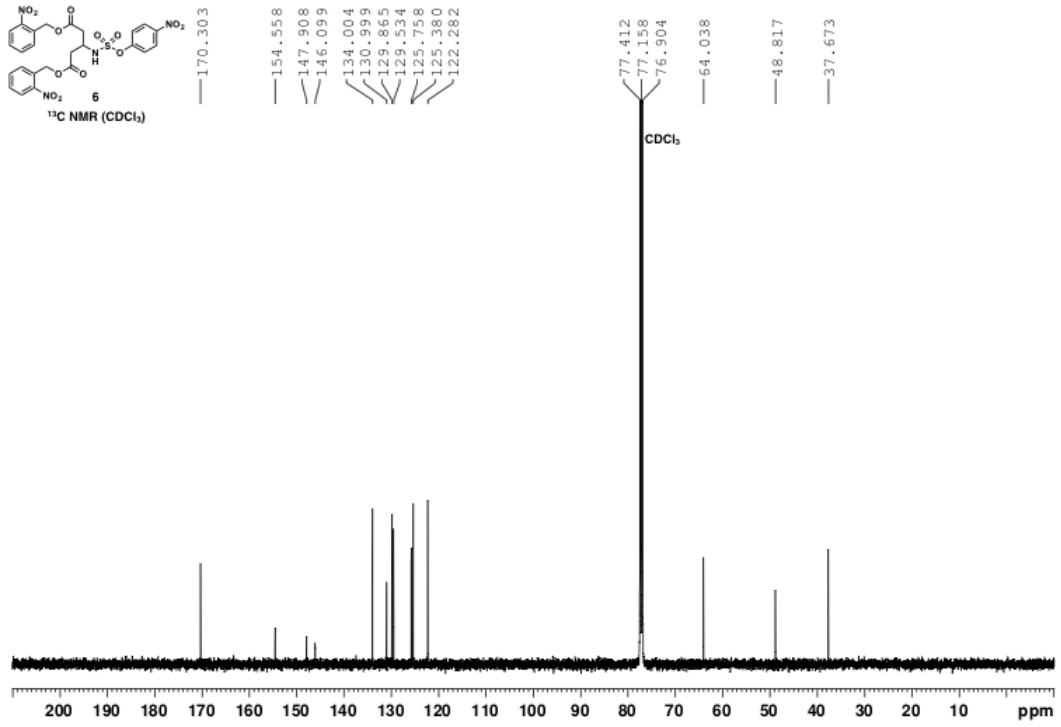
6
^{13}C NMR ($CDCl_3$)
170.303
154.558
147.908
146.099
134.004
130.999
129.865
129.534
125.758
125.380
122.282
77.412
77.158
76.904
64.038
48.817
37.673
$CDCl_3$
200 190 180 170 160 150 140 130 120 110 100 90 80 70 60 50 40 30 20 10 ppm

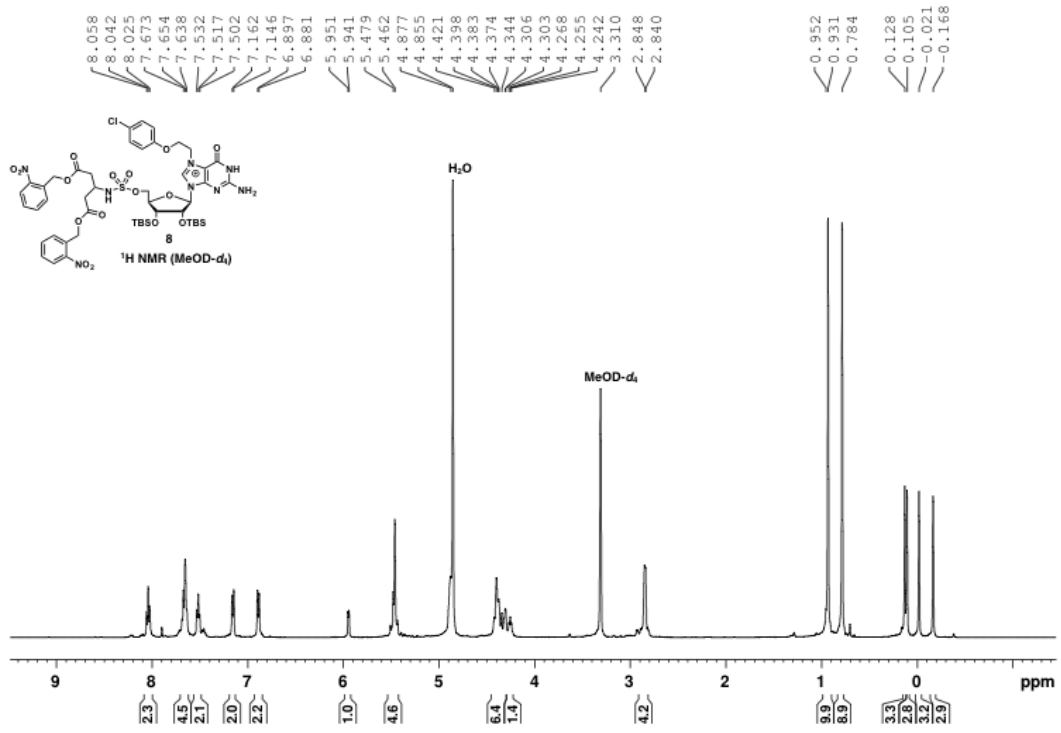
8.058
8.042
8.025
7.673
7.654
7.638
7.532
7.517
7.502
7.162
7.146
6.897
6.881
5.951
5.941
5.479
5.462
4.877
4.855
4.421
4.398
4.383
4.374
4.344
4.306
4.303
4.268
4.255
4.242
3.310
2.848
2.840
0.952
0.931
0.784
0.128
0.105
-0.021
-0.168
TBSO
OTBS
8
^{1}H NMR (MeOD-d_4)
H_2O
MeOD-d_4
9 8 7 6 5 4 3 2 1 0 ppm
2.3
4.5
2.1
2.0
2.2
1.0
4.6
6.4
1.4
4.2
9.9
8.9
3.3
2.8
3.2
2.9

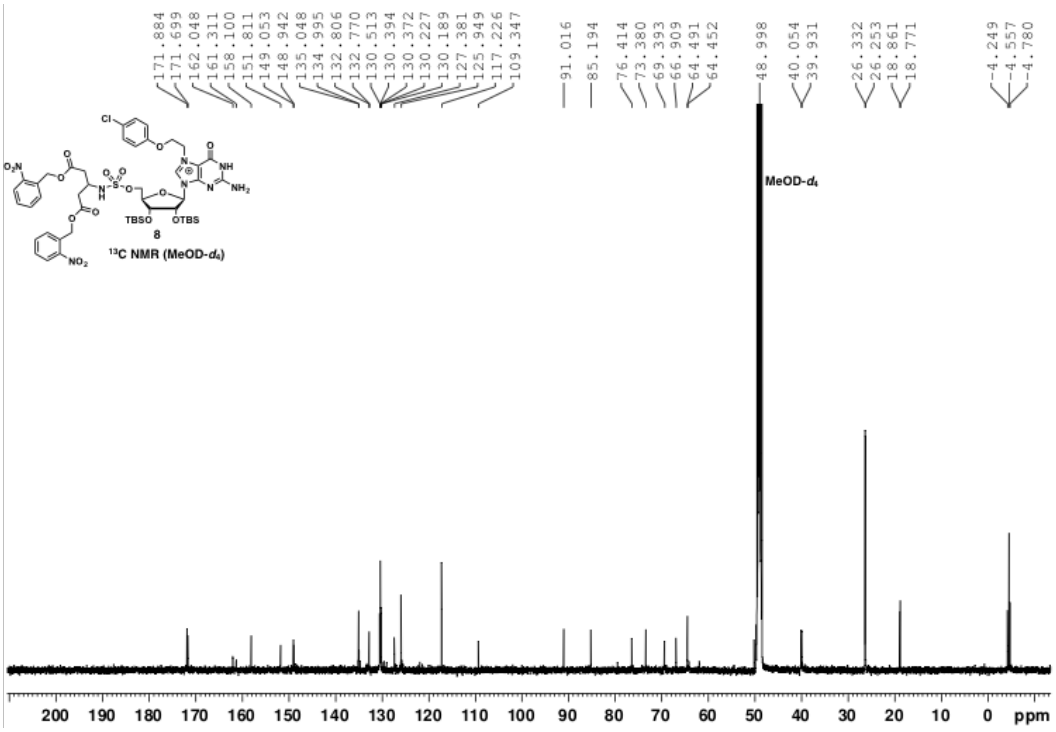
171.884
171.699
162.048
161.311
158.100
151.811
149.053
148.942
135.048
134.995
132.806
132.770
130.513
130.394
130.372
130.227
130.189
127.381
125.949
117.226
109.347
91.016
85.194
76.414
73.380
69.393
66.909
64.491
64.452
48.998
40.054
39.931
26.332
26.253
18.861
18.771
-4.249
-4.557
-4.780
MeOD-d4
8
13C NMR (MeOD-d4)
200 190 180 170 160 150 140 130 120 110 100 90 80 70 60 50 40 30 20 10 0 ppm

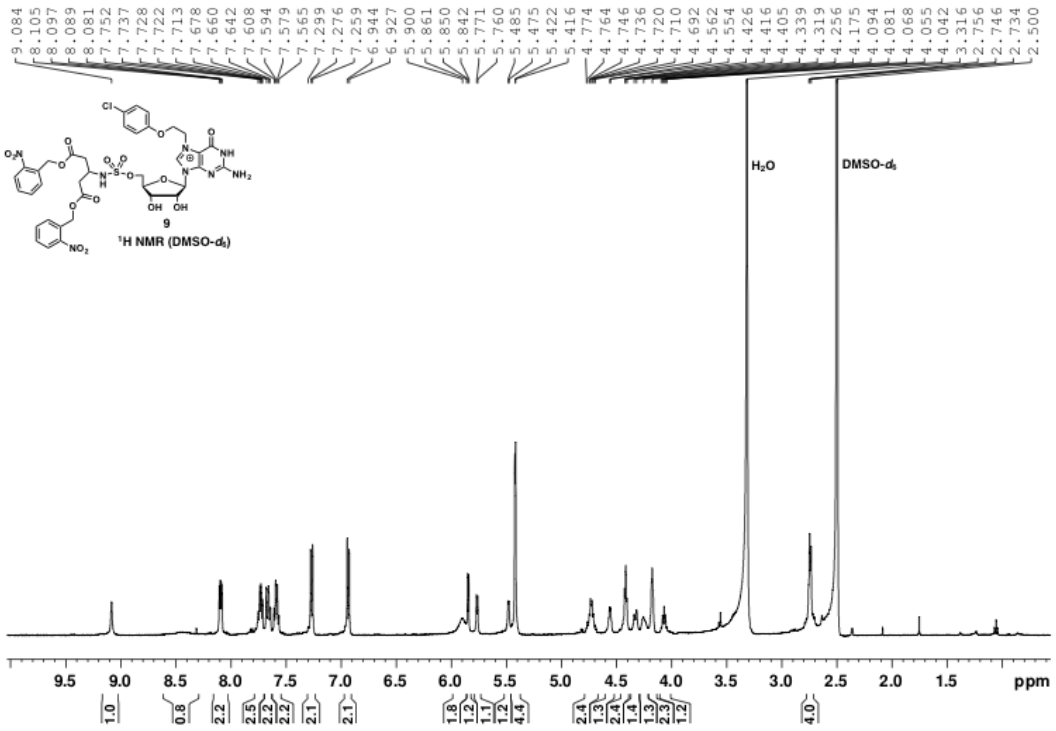
9.084
8.105
8.097
8.089
8.081
7.752
7.737
7.728
7.722
7.713
7.678
7.660
7.642
7.608
7.594
7.579
7.565
7.299
7.276
7.259
6.944
6.927
5.900
5.861
5.850
5.842
5.771
5.760
5.485
5.475
5.422
5.416
4.774
4.764
4.746
4.736
4.720
4.710
4.692
4.562
4.554
4.426
4.416
4.405
4.339
4.319
4.256
4.175
4.094
4.081
4.068
4.055
4.042
3.316
2.756
2.746
2.734
2.500
H2O
DMSO-d5
9
1H NMR (DMSO-d6)
9.5 9.0 8.5 8.0 7.5 7.0 6.5 6.0 5.5 5.0 4.5 4.0 3.5 3.0 2.5 2.0 1.5 ppm
1.0 0.8 2.2 2.5 2.2 2.2 2.1 2.1 1.8 1.2 1.1 1.2 4.4 2.4 1.3 2.4 1.4 1.3 2.3 1.2 4.0

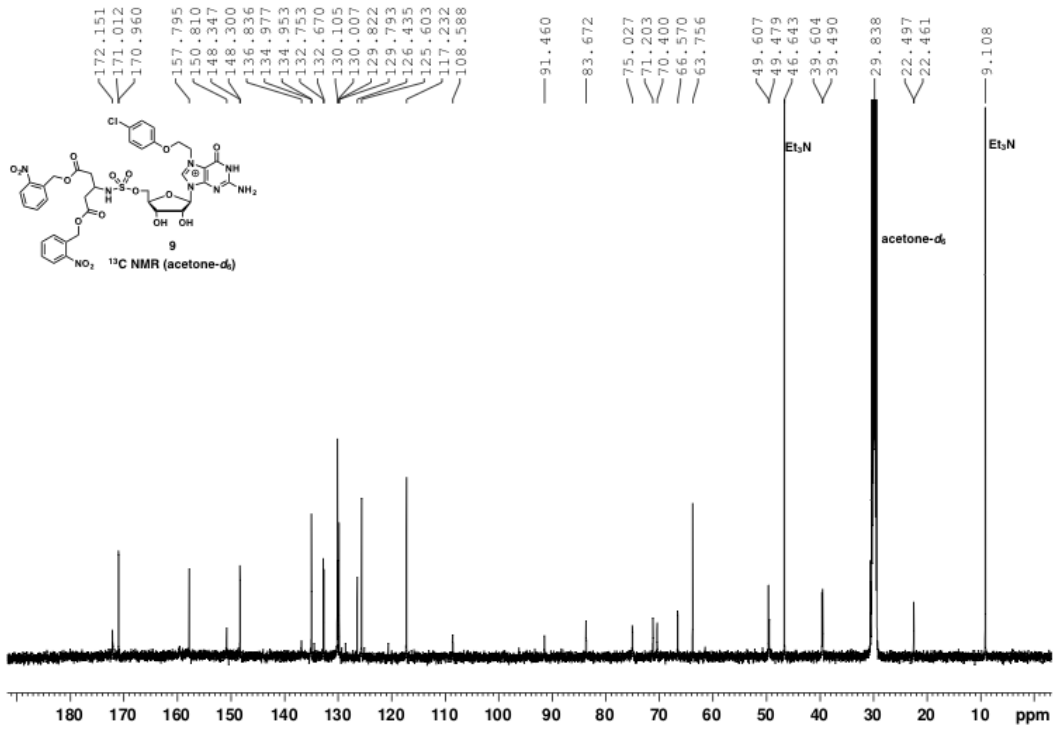
172.151
171.012
170.960
157.795
150.810
148.347
148.300
136.836
134.977
134.953
132.753
132.670
130.105
130.007
129.822
129.793
126.435
125.603
117.232
108.588
91.460
83.672
75.027
71.203
70.400
66.570
63.756
49.607
49.479
46.643
39.604
39.490
29.838
22.497
22.461
9.108
Et3N
Et3N
acetone-d6
9
13C NMR (acetone-d6)
180 170 160 150 140 130 120 110 100 90 80 70 60 50 40 30 20 10 ppm

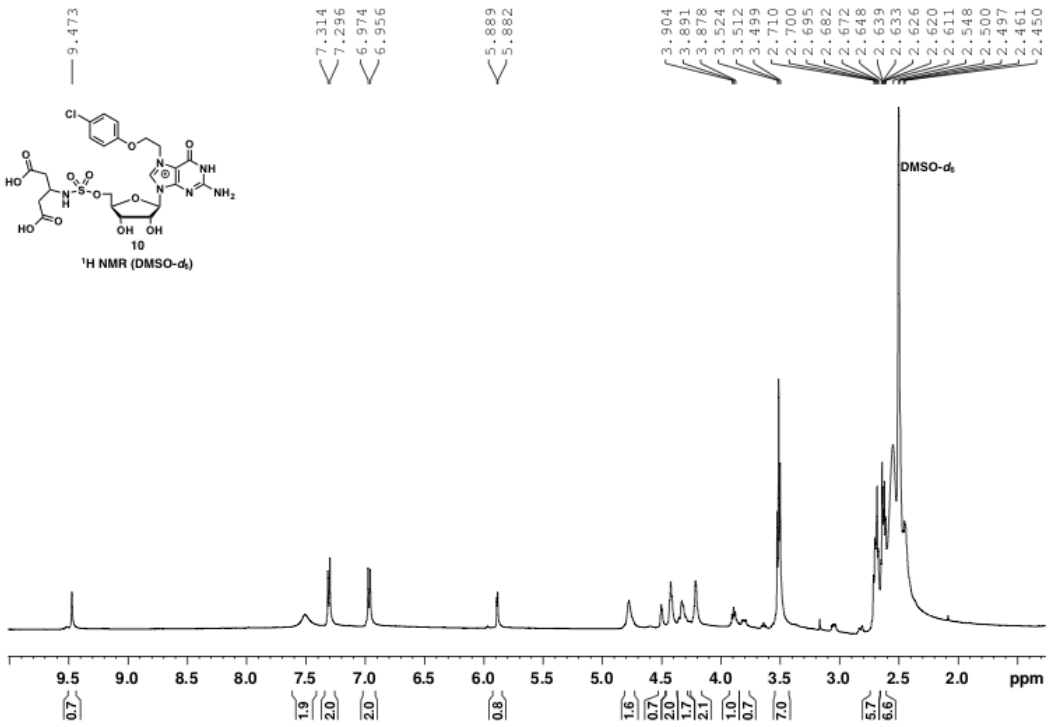
9.473
7.314
7.296
6.974
6.956
5.889
5.882
3.904
3.891
3.878
3.524
3.512
3.499
2.710
2.700
2.695
2.682
2.672
2.648
2.639
2.633
2.626
2.620
2.611
2.548
2.500
2.497
2.461
2.450
DMSO-d6
10
1H NMR (DMSO-d6)
9.5 9.0 8.5 8.0 7.5 7.0 6.5 6.0 5.5 5.0 4.5 4.0 3.5 3.0 2.5 2.0 ppm
0.7
1.9
2.0
2.0
0.8
1.6
0.7
2.0
1.7
2.1
1.0
0.7
7.0
5.7
6.6

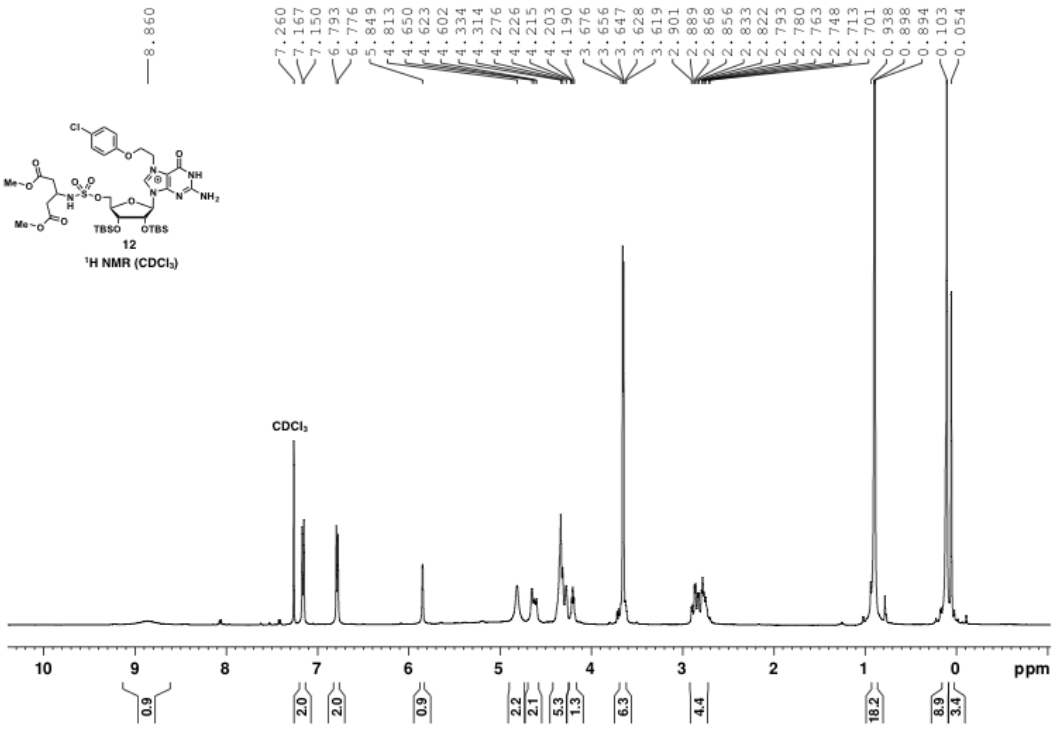
8.860
7.260
7.167
7.150
6.793
6.776
5.849
4.813
4.650
4.623
4.602
4.334
4.314
4.276
4.226
4.215
4.203
4.190
3.676
3.656
3.647
3.628
3.619
2.901
2.889
2.868
2.856
2.833
2.822
2.793
2.780
2.763
2.748
2.713
2.701
0.938
0.898
0.894
0.103
0.054
CDCl3
12
1H NMR (CDCl3)
10
9
8
7
6
5
4
3
2
1
0
ppm
0.9
2.0
2.0
0.9
2.2
2.1
5.3
1.3
6.3
4.4
18.2
8.9
3.4

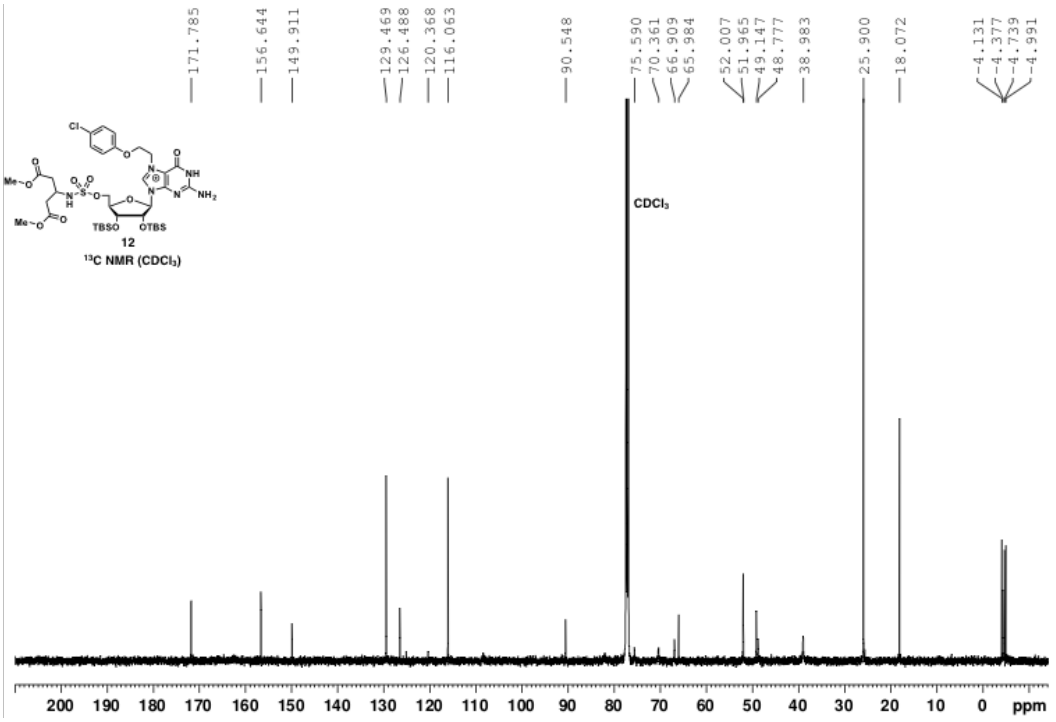
171.785
156.644
149.911
129.469
126.488
120.368
116.063
90.548
75.590
70.361
66.909
65.984
52.007
51.965
49.147
48.777
38.983
25.900
18.072
-4.131
-4.377
-4.739
-4.991
CDCl3
12
13C NMR (CDCl3)
200
190
180
170
160
150
140
130
120
110
100
90
80
70
60
50
40
30
20
10
0
ppm

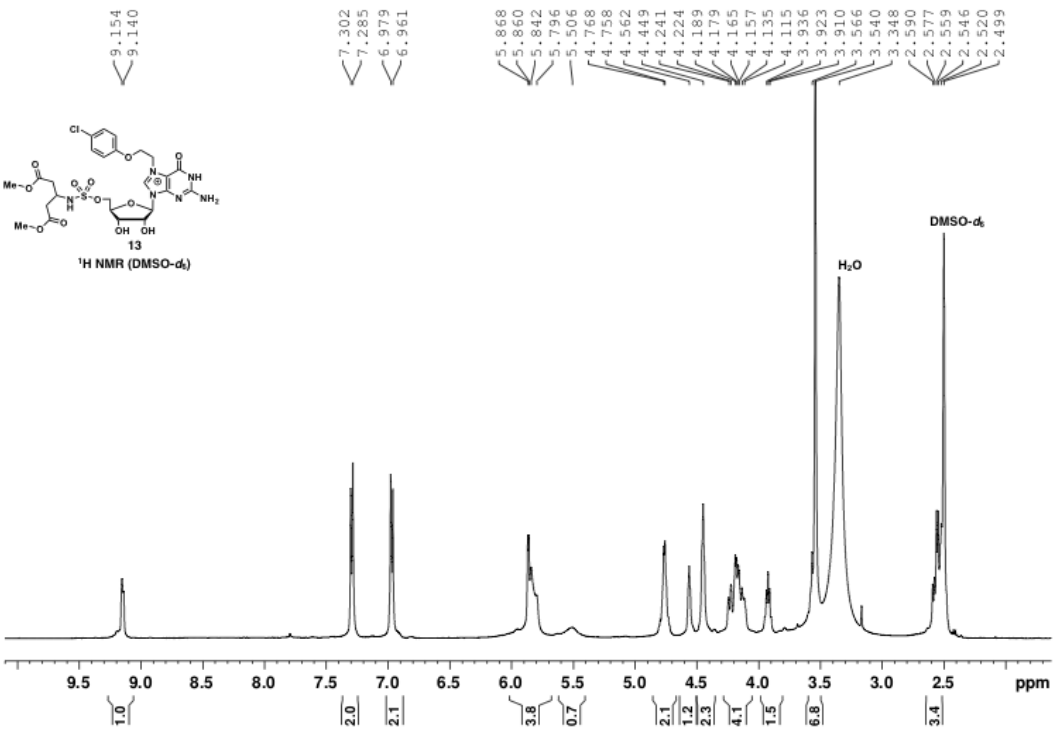
9.154
9.140
7.302
7.285
6.979
6.961
5.868
5.860
5.842
5.796
5.506
4.768
4.758
4.562
4.449
4.241
4.224
4.189
4.179
4.165
4.157
4.135
4.115
3.936
3.923
3.910
3.566
3.540
3.348
2.590
2.577
2.559
2.546
2.520
2.499
DMSO-d_6
H_2O
13
^{1}H NMR (DMSO-d_6)
9.5 9.0 8.5 8.0 7.5 7.0 6.5 6.0 5.5 5.0 4.5 4.0 3.5 3.0 2.5 ppm
1.0 2.0 2.1 3.8 0.7 2.1 1.2 2.3 4.1 1.5 6.8 3.4

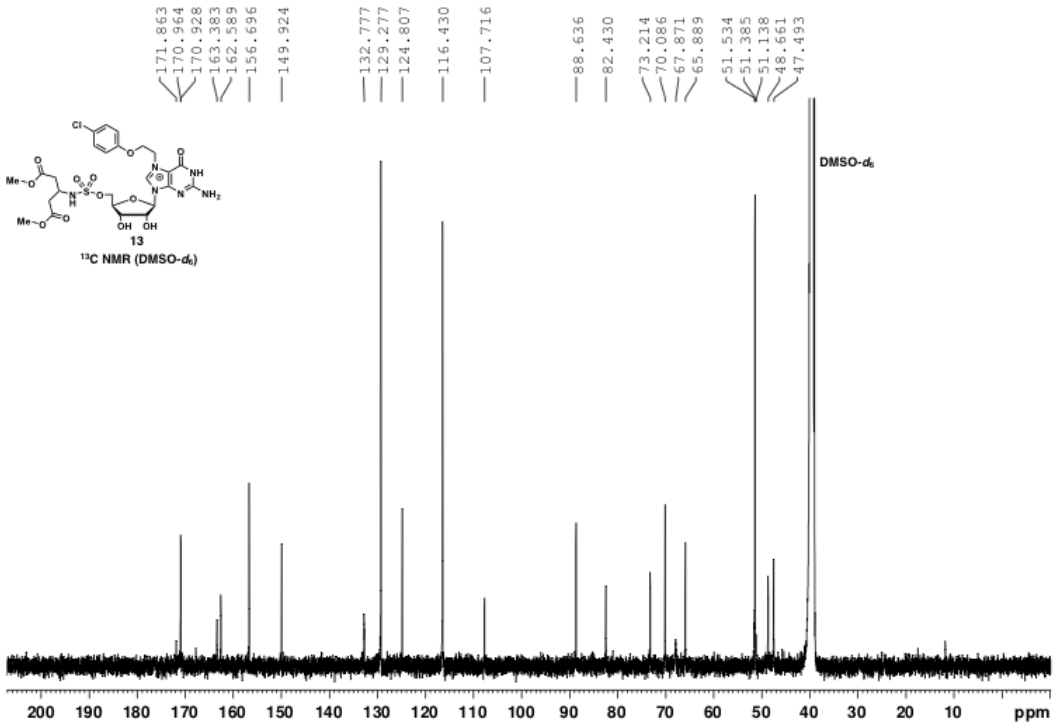
171.863
170.964
170.928
163.383
162.589
156.696
149.924
132.777
129.277
124.807
116.430
107.716
88.636
82.430
73.214
70.086
67.871
65.889
51.534
51.385
51.138
48.661
47.493
DMSO-d_6
13
^{13}C NMR (DMSO-d_6)
200 190 180 170 160 150 140 130 120 110 100 90 80 70 60 50 40 30 20 10 ppm

List of Proteins Identified after LC-MS/MS Proteomics with Probe B With no Competition.

Gene Name	Protein Name
SEC31A	Protein Transport protein
AASDHPPT	L-aminoadipate-semialdehyde dehydrogenase-phosphopantetheinyl transferase
ACAT2	Acetyl-CoA acetyltransferase, cytosolic
ADI1	1,2-dihydroxy-3-keto-5-methylthiopentene dioxygenase
ADSS	Adenylosuccinate synthetase isozyme 2
AKR1B1	Aldose reductase
ANP32A	Acidic leucine-rich nuclear phosphoprotein 32 family member A
ANP32B	Acidic leucine-rich nuclear phosphoprotein 32 family member B
ARFIP2	Arfaptin-2
ARMC6	Armadillo repeat-containing protein 6
ASNA1	ATPase ASNA1
ATIC	Bifunctional purine biosynthesis protein PURH
BANF1	Barrier-to-autointegration factor
BAX	Apoptosis regulator BAX
BID	BH3-interacting domain death agonist
BLMH	Bleomycin hydrolase
BLOC1S2	Biogenesis of lysosome-related organelles complex 1 subunit 2
BZW1	Basic leucine zipper and W2 domain-containing protein 1
BZW2	Basic leucine zipper and W2 domain-containing protein 2
C12orf57	Protein C10
C5orf51	UPF0600 protein C5orf51
CALU	Calumenin
CAPNS1	Calpain small subunit 1
CDKN2A	Cyclin-dependent kinase inhibitor 2A
CMPK1	UMP-CMP kinase
COPE	Coatomer subunit epsilon
COPS8	COP9 signalosome complex subunit 8
CSTB	Cystatin-B
DNAAF5	Dynein assembly factor 5, axonemal
EIF2B1	Translation initiation factor eIF-2B subunit alpha
ERP29	Endoplasmic reticulum resident protein 29

FAH	Fumarylacetoacetase
FAM49B	Protein FAM49B
GLA	Alpha-galactosidase A
GLRX3	Glutaredoxin-3
GNPDA1	Glucosamine-6-phosphate isomerase 1
GOT1	Aspartate aminotransferase, cytoplasmic
GOT2	Aspartate aminotransferase, mitochondrial
GPI	Glucose-6-phosphate isomerase
GSS	Glutathione synthetase
GSTK1	Glutathione S-transferase kappa 1
HEATR3	HEAT repeat-containing protein 3
HMBS	Porphobilinogen deaminase
HPRT1	Hypoxanthine-guanine phosphoribosyltransferase
HSD17B4	Peroxisomal multifunctional enzyme type 2
IPO8	Importin-8
KCTD12	BTB/POZ domain-containing protein KCTD12
LTA4H	Leukotriene A-4 hydrolase
MIF	Macrophage migration inhibitory factor
MPI	Mannose-6-phosphate isomerase
MRI1	Methylthioribose-1-phosphate isomerase
MTAP	S-methyl-5'-thioadenosine phosphorylase
NAPA	Alpha-soluble NSF attachment protein
NIF3L1	NIF3-like protein 1
NQO2	Ribosyldihydronicotinamide dehydrogenase [quinone]
NUCB2	Nucleobindin-2
NUTF2	Nuclear transport factor 2
PAFAH1B2	Platelet-activating factor acetylhydrolase IB subunit beta
PEBP1	Phosphatidylethanolamine-binding protein 1
PEPD	Xaa-Pro dipeptidase
PEX19	Peroxisomal biogenesis factor 19
PITPNB	Phosphatidylinositol transfer protein beta isoform
POLE3	DNA polymerase epsilon subunit 3
PPP2R4	Serine/threonine-protein phosphatase 2A activator
PPP5C	Serine/threonine-protein phosphatase 5
PRPSAP2	Phosphoribosyl pyrophosphate synthase-associated protein 2
PSAT1	Phosphoserine aminotransferase

PTGES2	Prostaglandin E synthase 2
PYGB	Glycogen phosphorylase, brain form
RAD23B	UV excision repair protein RAD23 homolog B
RAP1GDS1	Rap1 GTPase-GDP dissociation stimulator 1
RBM3	RNA-binding protein 3
RCN1	Reticulocalbin-1
RCN2	Reticulocalbin-2
RNPEP	Aminopeptidase B
RRM1	Ribonucleoside-diphosphate reductase large subunit
SARS	Serine--tRNA ligase, cytoplasmic
SCP2	Non-specific lipid-transfer protein
SEPHS1	Selenide, water dikinase 1
SERPINB6	Serpin B6
SGTA	Small glutamine-rich tetratricopeptide repeat-containing protein alpha
SH3GLB1	Endophilin-B1
SRI	Sorcin
SRM	Spermidine synthase
TFG	Protein TFG
TKFC	Triokinase/FMN cyclase
TNPO2	Transportin-2
TRAPPC3	Trafficking protein particle complex subunit 3
TTC9C	Tetratricopeptide repeat protein 9C
TTI1	TELO2-interacting protein 1 homolog
TXNDC5	Thioredoxin domain-containing protein 5
TXNRD1	Thioredoxin reductase 1, cytoplasmic
TYMS	Thymidylate synthase
UAP1	UDP-N-acetylhexosamine pyrophosphorylase
UBE2C	Ubiquitin-conjugating enzyme E2 C
UBL4A	Ubiquitin-like protein 4A
UBQLN2	Ubiquilin-2
UBQLN4	Ubiquilin-4
UCHL3	Ubiquitin carboxyl-terminal hydrolase isozyme L3
UCHL5	Ubiquitin carboxyl-terminal hydrolase isozyme L5
UMPS	Uridine 5'-monophosphate synthase
VAT1	Synaptic vesicle membrane protein VAT-1 homolog
VPS26A	Vacuolar protein sorting-associated protein 26A

VPS35	Vacuolar protein sorting-associated protein 35

Putative Protein Binding Partners of Probe B identified after In-Cell Protein Labeling and LC-MS/MS Proteomics.

Gene Name	Protein Name	Function	Compartment
APRT	Adenine phosphoribosyltransferase	Nucleotide salvage	cytosol
CALU	Calumenin	Calcium binding	cytosol - ER
XPO5	Exportin 5	mRNA binding/nuclear export	Nucleus and cytosol
GPI	Glucose-6-phosphate isomerase	Glucose metabolism	cytosol
HBA2	Hemoglobin subunit alpha	Heme and iron ion binding	cytosol
MDH1	Malate dehydrogenase 1	Glucose metabolism	cytosol
SLC16A1	Monocarboxylate transporter 1	Transport of small molecules	Plasma membrane
PSAT1	Phosphoserine aminotransferase	Amino acid metabolism	cytosol
CPVL	Probable serine carboxypeptidase	Serine-type carboxypeptidase activity	Extracellular region or secreted
RCN1	Reticulocalbin-1	Calcium ion binding	ER
VAT1	Synaptic vesicle membrane protein VAT-1	Oxireductase activity	Mitochondrion outer membrane
TMX1	Thioredoxin-related transmembrane protein 1	Disulfide oxireductase/isomerase activity	ER
TFRC	Transferrin receptor protein 1	Transport of small molecules	Plasma membrane
TNPO1	Transportin-1	RNA metabolism	Nucleus and cytosol

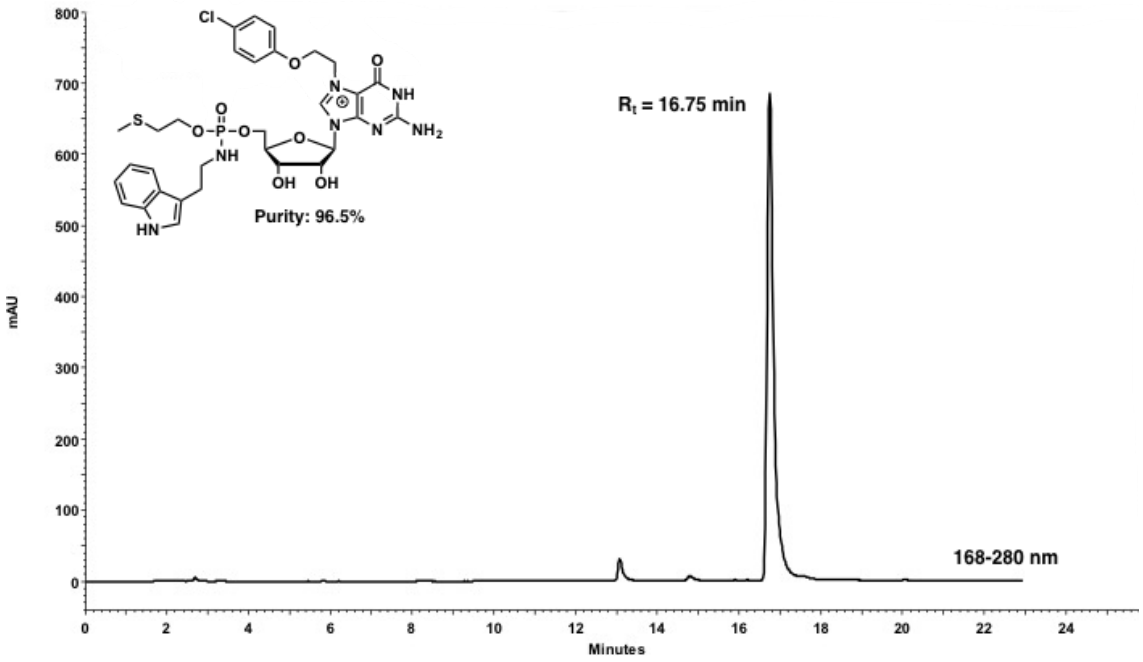
Purity: 96.5%
R_t = 16.75 min
168-280 nm
mAU
Minutes

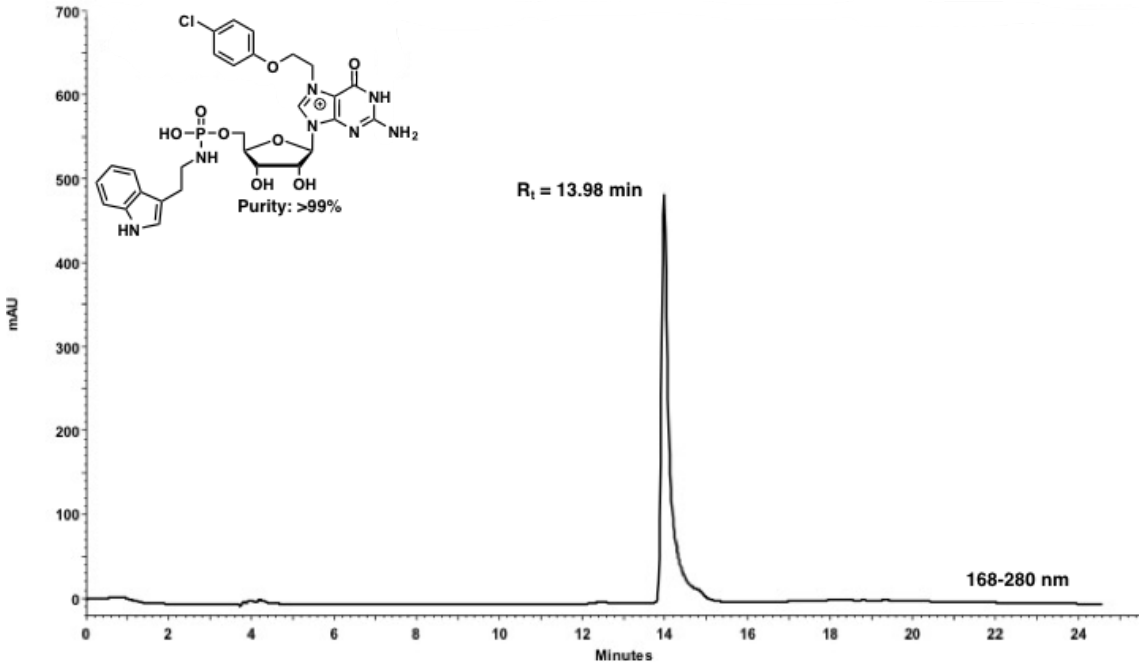
Purity: >99%
R_t = 13.98 min
168-280 nm
mAU
Minutes

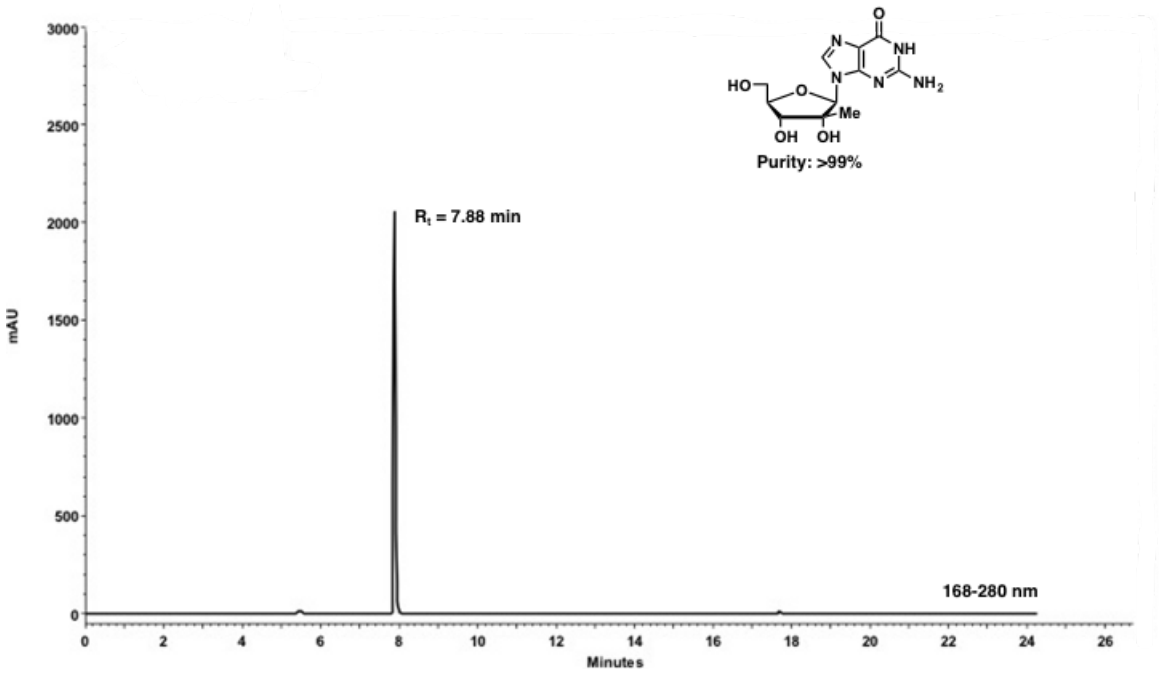
Purity: >99%
R_t = 7.88 min
168-280 nm
mAU
Minutes

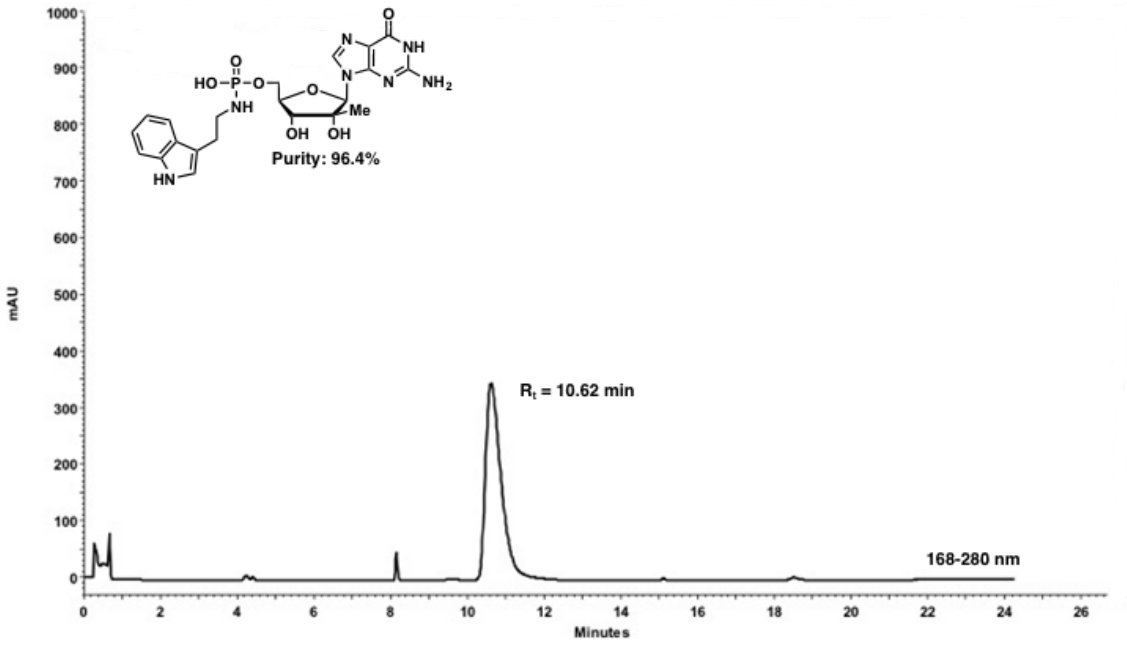
Purity: 96.4%
R_t = 10.62 min
168-280 nm
mAU
Minutes

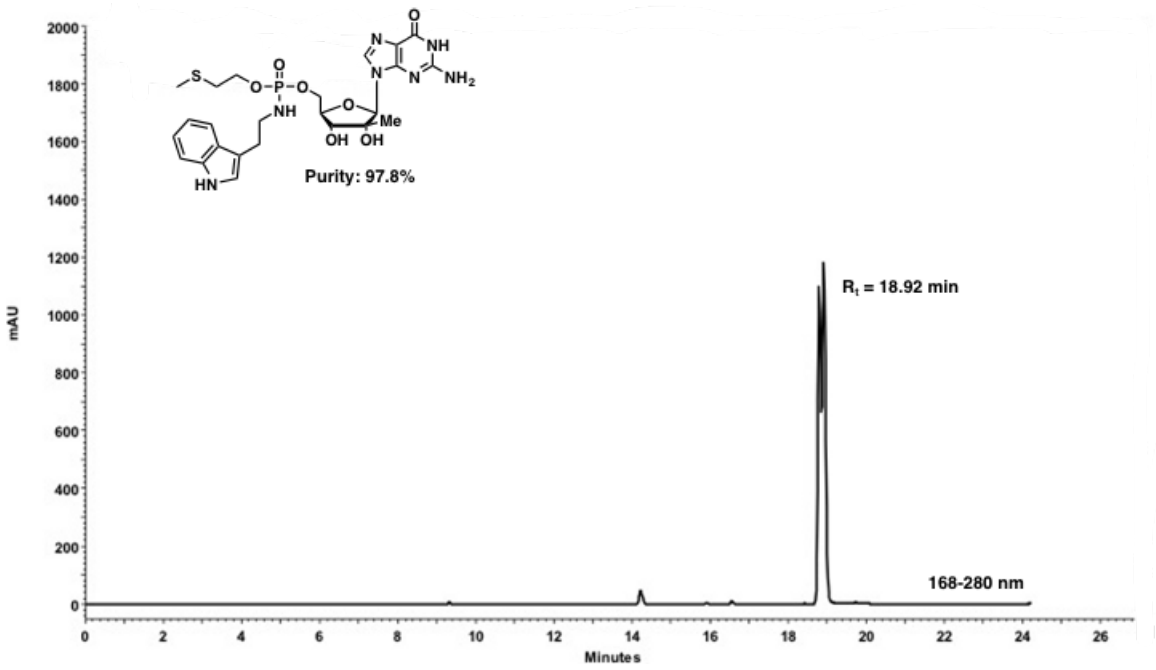
Purity: 97.8%
R_t = 18.92 min
168-280 nm
mAU
Minutes

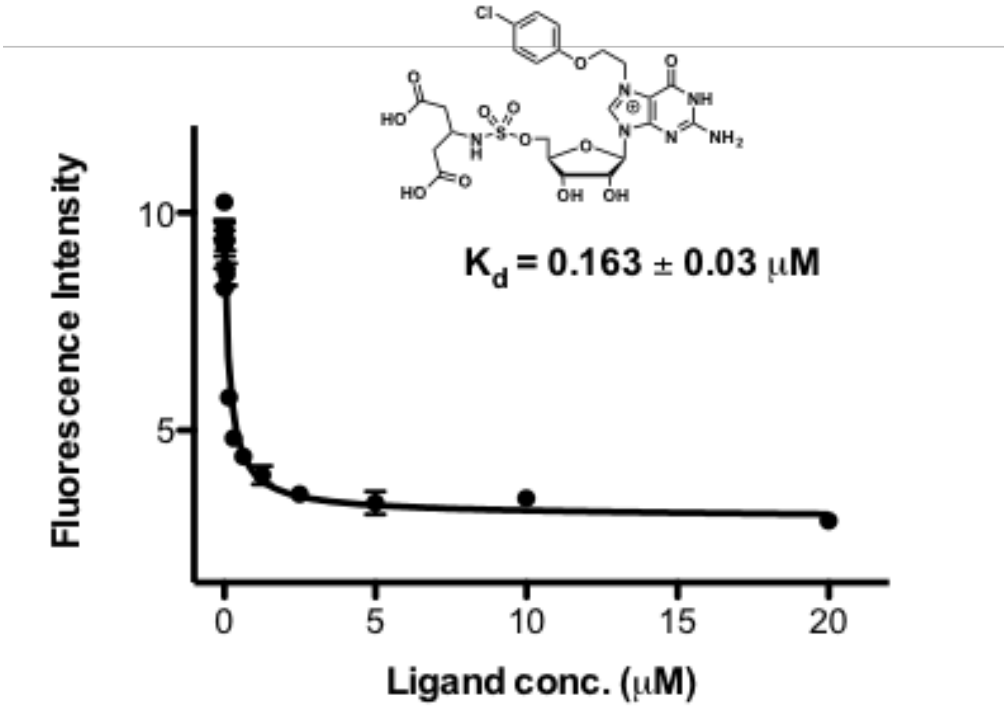
K_d = 0.163 ± 0.03 μM
Fluorescence Intensity
Ligand conc. (μM)

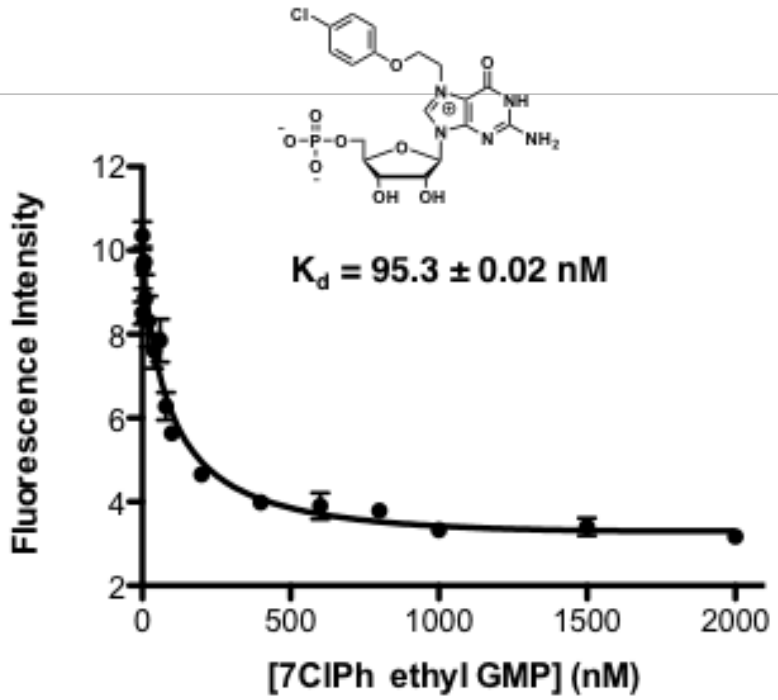
Cl
O
NH
N
NH2
O
P
O
OH
OH
K_d = 95.3 ± 0.02 nM
Fluorescence Intensity
12
10
8
6
4
2
0
500
1000
1500
2000
[7ClPh ethyl GMP] (nM)

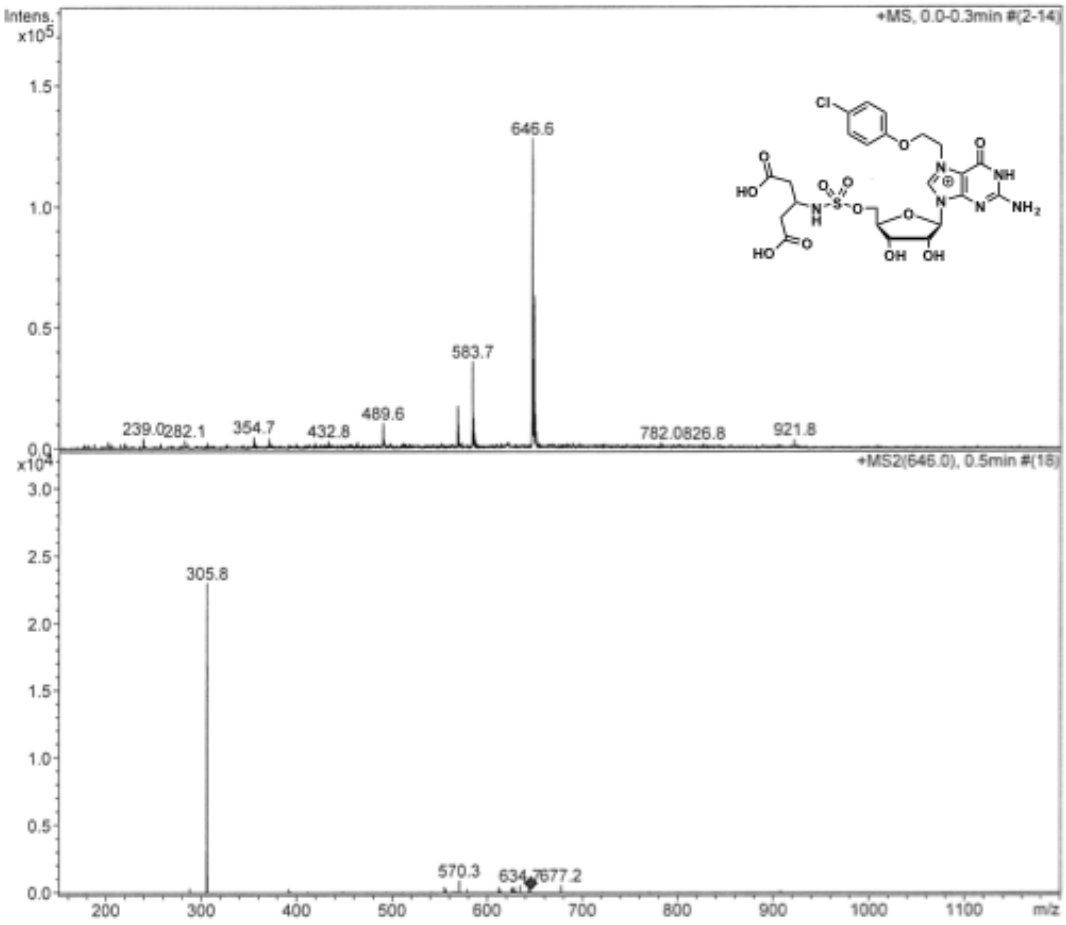
Intens.
x10^5
+MS, 0.0-0.3min #(2-14)
646.6
583.7
489.6
239.0
282.1
354.7
432.8
782.0
826.8
921.8
x10^4
+MS2(646.0), 0.5min #(18)
305.8
570.3
634.7
677.2
m/z